# The Determination of Dyers' Perceived Components of Colour Difference (Depth, Brightness and Hue) between two similar Colours from their Spectral Reflectance Values

A thesis submitted by

**Salma Farooq**

In Fulfilment of the Requirements

For the Degree of Doctor of Philosophy

At Heriot-Watt University, Edinburgh, United Kingdom

**School of Textiles and Design** **March 2011**

# ABSTRACT

An algorithm, called the WSF algorithm, was developed which could predict the dyers' attributes of colour difference (depth, $\Delta D$, brightness, $\Delta B$, and hue, $\Delta H^*$) from the reflectance values of a pair of dyeings, enabling the dyer to take full advantage of colorimetric analysis. The algorithm was based on extensive experimental work to map surfaces of constant visual depth throughout the colour space and the thesis describes the methodology and the necessary calculations to determine the $\Delta D$, $\Delta B$ and $\Delta H$ values of a pair of dyed samples. This algorithm was compared to other existing algorithms (the DBH and the Sato models) using two data sets with 49 dyed pairs for data set 1 and 117 dyed pairs for data set 2 respectively. The correlation of the values of $\Delta D$, $\Delta B$ and $\Delta H$ determined using the WSF algorithm with the DBH and the Sato models showed an excellent relationship between these three algorithms for both the data sets. Qualitative comparison of the visual assessments of data set 2 with the WSF algorithm was encouraging but the quantitative comparison of the visual assessment for data set 1 was disappointing.

The pre-requisite of the WSF algorithm is the six equi-depth surfaces which have been defined numerically in the CIELAB colour space and previously reported as WSI depth surfaces. The first stage of this algorithm was to generate, using the WSI algorithm, the equi-depth line in the $L^*$ $C^*$ plane that passes through the $L^*$ $C^*$ coordinates of the standard. The K/S values of the batch were then iterated, until its depth became equal to that of the standard. At this point, the precise location of the batch on the equi-depth surface might be different from that of the standard. The linear distances between the batch and the standard, gave the differences in depth and brightness between the standard and the batch. A new approach was investigated for the hue correction of dyed pairs, where the hue of the batch was different from that of the standard. Real data of highest possible chroma values from Munsell colour atlas were used to create maximum chroma boundaries which were found necessary for the hue correction of the batch. It was noted that the DBH and the Sato models also incorporated hue correction of the batch.

The WSF algorithm described in Chapter 4 contained an iterative stage which created an additional complexity in programming. Therefore an alternative version of the WSF algorithm was developed, called the linear WSF model, which avoided the need for iteration and yielded the same results. This linear WSF algorithm strongly correlated with the WSF (iterative) model and also to other empirical models as well.

# ACKNOWLEDGEMENT

Firstly, I would like to give my deepest gratitude to my supervisor, Professor Roger H Wardman, whose encouragement, guidance and continuous support were the invaluable contribution to this thesis.

I would like to give my heartily thanks to Professor K J Smith for his important suggestions, and for sharing his experience in a very friendly way. Here I would also like to thank my co-supervisor, Professor Bob Christie for his encouragement throughout the thesis.

My thanks to the visual assessors for conducting the visual assessments, which is an important part of this thesis.

I would like to thank all the technical staff who have help along the way, especially Ann Hardie and Maggie Robson for their support. My special thank to Peter Sandison, library manager for various assistance throughout the years. In addition, I would like to thank computer services staff for their co-operation

I am extremely thankful to my husband, kids and my parents for their love, continuous moral support and encouragement.

I would like to thank NED University of Engineering and Technology for the scholarship to pursue my PhD studies.

Finally, I thank almighty Allah for blessing me to achieve my endeavor nicely.

# CONTENTS

# LIST OF TABLES

# LIST OF FIGURES

# LIST OF APPENDICES

## PUBLICATIONS

Conference proceeding

Salma Farooq, Roger H Wardman and K J Smith, "Development of an algorithm to convert Colorimetric variables of ΔL*, ΔC* ΔH* to Dyers' variables of differences in Depth, Brightness and Hue," Proceeding of 22nd IFATCC Congress-Stresa (Italy), May 5th -7th, 2010.

Journal Article

Roger H Wardman, Salma Farooq and K J Smith, "The Determination of Dyers' Perceived Components of Colour Difference (Depth, Brightness and Hue) Between Two Similar Colours from their Spectral Reflectance Values," Paper submitted to Colouration Technology, January 2011.

# CHAPTER 1: INTRODUCTION

## 1.1 Background

Colour is ultimately a sensation in our mind, associated with light striking our eyes; the light that is reflected, refracted or transmitted by an object [1]. For all the industries related to colour manufacturing and colour application it is always desirable to measure physically the colour in order to record and reproduce it. In order to control the colour it is necessary that a perceived difference in colour between a standard and the batch should be known. This quantification of the colour difference is achieved by using a colour difference formula. A colour difference formula provides a prediction of perceived colour differences based on stimulus differences between coloured materials (reflectance function differences) and thereby provides a tool for quality control purposes.

The development of colour difference formulae can be divided into two distinct periods, according to their performance. These are before and during 1976. Formulae developed after CIELAB (1976), are referred to as advanced colour difference formulae. ANLAB was the most successful formula, developed by Adams and Nickerson in1944. CMC, CIE94, and CIEDE2000 are the most successful ones after 1976 [2]. In the textile industry the CMC (l:c) colour difference formula is used as an international standard [3]. In 2001, the International Commission on Illumination (CIE) recommended the CIEDE2000 formula, replacing the CIE94. A common feature of all these was that the colour difference was expressed in terms of differences in the colorimetric variables of lightness, chroma and hue.

It is often desirable to identify the component of the colour difference responsible for making a batch an unacceptable match to the standard. It will help to set the working directions to make a batch acceptable. From the $L^*a^*b^*C^*h°_{ab}$ coordinates of a standard and batch, it is possible to split total colour difference into its three components; $L^*a^*$ $b^*$ and $L^*C^*$ $h°_{ab}$ methods of splitting are widely used for this purpose [4].

Though these numeric systems are advantageous in settling many colour matching disputes, dyers prefer to use their own terms in judging a batch against a standard. They use the DBH method of splitting, in which only hue is common to $L^*C^*$ $h°_{ab}$, where D stands for depth, and B stands for brightness. The reason for this is that most colourists have been trained since the start of their career, to recognize the effect on appearance of

increasing or decreasing the amount of colourant present. The second component which colourists have been trained to recognize is the effect of adding a trace of a grey or black to a chromatic dyeing or paint [5,6, 7, 8]. It is known that observers vary in their opinion to judge the colour difference of a dyed pair. An experienced dyer is more consistent and accurate than a less experienced dyer, especially in reporting the nature of the colour difference [9, 10]. Therefore an objective method is required which may predict the dyers' variables derived from colorimetric colour difference variables to reduce the mistakes made by inexperienced dyers in reporting the nature of colour differences.

Colour physics software is an integral part of the quality control of a colour in the colour manufacturing and application industries, but it is not an ideal solution to re-educate the dyer to make use of the colour physics system thus preventing them from using their own familiar way. It is important to note here that dyer's depth is still an important and decisive factor to determine the fastness properties of different colourants under comparable conditions and the application properties of different colourants in colouration processes [11]. The Hilfstypen samples, which are a set of 18 woollen dyed samples of equal depth, are still used for comparison of fastness properties of a dyed material at a same depth level [12, 13]. Therefore the utility of the dyer's variables cannot be obviated. If a dyer does not use a colorimetric system at all no benefits of the colour physics can be exploited by him. Accordingly, there is a need for an algorithm which can predict/determine the dyer's output from the colour physics system. This is only possible if the uniform standard depth planes at different level of depths with good agreement to visual assessments are defined and mapped into the CIE $L^*C^*$ $h°_{ab}$ colour space. The depth level of the standard can be found using these depth surfaces and finally the difference in depth and brightness of a batch from the standard can be found. The WSI algorithm [14, 15] has defined the six depth surfaces from a large number of visual assessments and currently under round-robin trial to be accepted as an ISO standard to determine the depth of a dyed fabric.

In view of above an algorithm has been developed in this study which can compute dyers' colour difference components in terms of difference in depth, brightness and hue ($\Delta D$, $\Delta B$, $\Delta H$) from the reflectance values of the standard and the batch using the WSI surfaces of uniform visual depths in the $L^*$ $C^*$ $h°_{ab}$ colour space.

## 1.2 Aim of the thesis

The output of colour physics software is usually the colour differences in terms of $\Delta L^*$, $\Delta a^*$, $\Delta b^*$, $\Delta C^*$, $\Delta H^*$ which has limited use to dyer. The overall aim of the project was to develop an algorithm which computes the dyers' variables of $\Delta D$, $\Delta B$ and $\Delta H$ from the spectral reflectance values of a pair of dyeings. This algorithm was designed to give information in dyers' terms and thus facilitate the dyer to perform his routine tasks in an efficient and confident way. The algorithm also intends to reduce the percentage disagreement in reporting the colour errors between an experienced and an inexperienced dyer. This algorithm was named the WSF (Wardman-Smith-Farooq) algorithm.

In order to achieve this aim it was necessary to extend the WSI algorithm for all those samples lying in between the six defined WSI equal depth surfaces. Following this stage the position of the batch on the equi-depth line passing through the standard was found by varying the K/S values of the batch and hence the difference in depth, brightness and hue between a standard and batch.

It was considered appropriate to develop a method which could eliminate the iterative step of the WSF algorithm and yield the same position of the batch on the standard depth line as that determined by the iterative method, so that the accurate difference in depth and brightness could be calculated in a simple and easy way.

## 1.3 Thesis outline

Chapter 1 outlines the aim and objectives set and achieved for the given project. Background includes the developmental stages of the algorithm, methodology adopted and the findings supporting the basic idea/spirit of the project is also a part of this chapter.

Chapter 2 establishes the concrete base of the project. It includes detailed study of colour attributes and the various colour specifying systems. It also enlightens the importance of colour difference evaluation and various attempts made to get an acceptable colour difference formula. The final portion of the chapter describes the colour splitting methods and the importance of the dyers terms in evaluating the colour difference.

Chapter 3 explains different methods which were derived in the past to evaluate one of the important dyers' term, "depth" and a brief comparison of the various depth evaluation techniques. A detailed discussion on the WSI algorithm including its

development and its correlation to the visual assessment is also an integral part of this chapter

Chapter 4 discuss the methodologies followed to develop an algorithm (the WSF algorithm) which can predict the differences in dyers' variables of depth, brightness and hue ($\Delta D$, $\Delta B$ and $\Delta H$) from the reflectance values of a dyed pair. It includes various stages involved to develop the model and the hue correction strategy for all those dyed pairs where the hue angle of a batch is different from the standard. It also describes the plan to verify the WSF algorithm. Extension of the WSI algorithm at higher chroma values is also discussed in this chapter.

Chapter 5 gives a comprehensive comparison of the results obtained from the WSF algorithms with the existing models which include DBH and Sato algorithms. It also shows the performance of the WSF algorithm with the visual assessments.

Chapter 6 describes the methodology and the developmental stages for the linear WSF algorithm. This linear WSF model use $L^*C^*$ $h°_{ab}$ values of a dyed pair as input than reflectance values instead. It also includes a comparison of this linear model with the WSF iterative model, the DBH and the Sato models as well. This chapter also describe the advantages of this linear model over the iterative WSF algorithm.

Finally the last chapter (Chapter 7) gives the conclusions and future directions, highlighting the limitations and usefulness of the WSF algorithm.

# CHAPTER 2: COLOUR DIFFERENCE EVALUATION

## 2.1 Colour Attributes

Defining a colour is not easy and straightforward. Although, colour perception is similar for almost all the humans, however, its communication varies from person to person. Colour, being three dimensional in nature, usually best specified in term of its three perceptual attributes which are hue, colourfulness and brightness [16, 17, 18]

**Hue:** The property of colours by which they can be perceived as ranging from red through yellow, green, and blue, as determined by the dominant wavelength of the light. Hue is also one of the three dimensions in some colour-spaces along with the saturation, and lightness.

**Colourfulness:** Colourfulness is the attribute of the visual sensation according to which an area appears to exhibit more or less of its hue

**Brightness:** Brightness is an attribute of visual sensation according to which an area appears to exhibit more or less light.

Colour cannot be fully understood without describing the relative perceptual attributes of the colour which are; chroma and lightness.

**Chroma:** Chroma is the colourfulness of an area judged in proportion to the brightness of a similarly illuminated area that appears to be white or highly transmitting.

**Lightness:** the brightness of an area judged relative to the brightness of a similarly illuminated area that appears to be white. The Munsell value is an example of a lightness scale.

**Saturation:** it can be defined as the colourfulness of an area judged in proportion to its brightness

Human visual system is complex and depends upon various factors which include the nature of substrate, viewing conditions and the age and experience of an observer. These attributes are necessary to express a colour in a systematic and logical way so that even in the absence of a physical sample the right colour can be communicated to the others at anywhere.

Colour can be expressed using colour order systems which employ physical samples or numerically using colorimetric principles. These approaches are dealt in Section 2.2 and 2.3 respectively.

**2.2 Colour order systems**

A colour order system is a rational method of ordering and specifying all object colours by means of a set of material standards, selected and displayed so as to represent adequately the whole set of object colours under consideration. There are certain advantages as well as limitations which limits their widespread application in day to day colour communication [16, 17].

The advantages claimed for colour order systems are:

- An easy concept to understand.
- They can be used in visual experiments. It is possible for a person to colour match with a standard and a trial side by side, without the need for complex instruction or complex instrumentation.
- Colour order systems are widely used in art and design. Colour communication becomes simple with the use of colour order systems
- They are important tool in educating students about colour and its various attributes.

However the disadvantages are issues such as:

- There are only a limited number of samples in an atlas. This leads to large differences between the colours of neighbouring samples.
- The colour of the samples may change with time and with use.
- The accuracy of colour specification depends on the level of agreement between the colours of the samples in the atlases.
- The colour gamut available to the designer or to the colour mixer may not be fully represented in the atlas.
- The colours in the atlas are not specified mathematically in relation to physically measureable values.
- Visual comparison between the colours and the samples is valid for only one set of viewing data.

- There is not just one colour space in use, and there is no simple means of transferring a colour specification in one atlas to a specification in another.
- They are expensive

All colour order systems fall broadly into three major groups. Those in the first group are based primarily on the principle of additive mixtures of colour stimuli. The arrangements based on colourant behaviour provide the basis for colour order systems of the second group. In some industries, such as the paint and printing ink industries, it is common practice to produce a wide variety of coloured samples by a systematic mixing of a relatively few high chroma colourants with one another and with white, black and grey. This system is widely used for house paint producers, industrial and automotive finish makers and for the plastic colourant suppliers. Pantone is one of the popular examples in this group [16, 17, 18]

The third group of colour order systems is based on principles of colour perception. Material standards are selected to represent scales of constant hue, chroma and lightness, each one spaced uniformly in accordance with the perception of an observer with normal colour vision. Colour order systems of this group are sometimes called colour appearance systems [17, 18]. Examples include:

- The Munsell Colour Systems
- The Optical Society America- Uniform Colour Scales System (OSA-UCS)
- The Natural Colour Systems (NCS)
- The German Standardization Institute System (DIN)
- The Coloroid System

A separate type of colour order system which also specifies colours but does not include any physical samples, rather it specifies the colours mathematically/numerically is the CIE system of colour measurement. The CIE system is widely used in colour measurement nowadays.

### *2.2.1 The Munsell Colour Order System*

One of the most widely used colour order systems is the Munsell system, originated by the artist A.H. Munsell in 1905 [19, 20, 21]. Colour in the Munsell system is specified by the three variables:

- Munsell Hue

- Munsell Value
- Munsell Chroma

The hue circle in the Munsell system is divided into five principle hues (purple, blue, green, yellow and red) denoted as 5P, 5B, 5G, 5Y, and 5R respectively and is designed to divide the hue circle into five equal perceptual intervals. Five intermediate hues are also designated in the Munsell system as 5PB, 5BG, 5GY, 5YR, and 5RP, giving a total of 10 hue names. For each of the ten hues there are ten integral hues with notations as illustrated by the range between 5P and 5PB and consisting of 5P, 6P, 7P, 8P, 9P, 10P, 1PB, 2PB, 3PB and 4PB. In practice pages are shown at the intervals 2.5, 5, 7.5 and 10.

There are ten main steps in the Munsell value scale with white given a notation of 10, black 0, and intermediate greys given notations ranging between 0 and 10. The design of the Munsell value scale is such that an intermediate grey with a Munsell value of 5 is perceptually half way between an ideal white and an ideal black. Lightness perception falling in-between two Munsell value steps are denoted with decimals.

The third attribute of the Munsell system is Chroma. The Chroma scale is designed to have equal visual increments from zero for neutral samples to increasing values for samples with stronger hue content. There is no set maximum for the chroma scale. The highest chroma achievable depends upon the hue and the Munsell value of the samples and on the colourants used to produce them.

An important feature of the Munsell system is that the colours are arranged so that, for each perceptual attribute of Hue, Value and Chroma, as nearly as possible the perceptual difference between any two neighbouring samples is constant. Equal spacing of value and chroma can be maintained throughout, but in a cylindrical system, the spacing of the hue varies with the chroma.

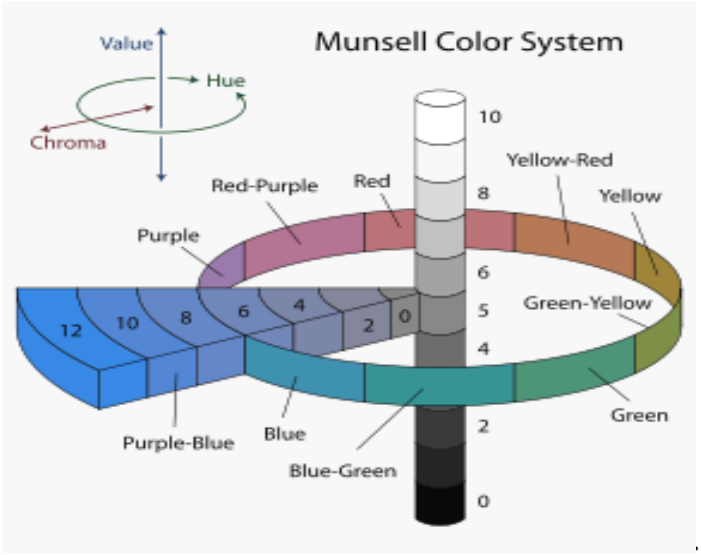


Figure 2.1: Munsell colour order system [75]

The Munsell system is used to denote a specific coloured stimulus using Munsell Hue, Value and Chroma designations in a triplet, arranged with the hue designation followed by the Value, a forward slash and then the Chroma, sometimes known as HV/C.

Various additions have been made to improve the visual scaling of the Munsell colour order system. In 1943 a careful study of the tristimulus values of the Munsell colour book was made by the Optical Society of America [19, 22]. Some irregularities were observed in the tristimulus values from one sample to the next. These irregularities were corrected by this OSA committee, in what became known as Munsell Renotation System. Since 1957 all the Munsell colour books/atlases are based on this Munsell Renotation System.

### *2.2.2 DIN colour order system*

The DIN system was developed by M. Richter and his co-workers in Germany. The basic principle of the DIN system is equality of visual spacing for series of colours in which single colour attributes are varied. Colours are specified by the three variables; hue (T), saturation (S), and darkness (D). The system uses standard daylight, D65, and CIE X, Y, Z tristimulus values to define the attributes of a colour [23].

Colours of constant dominant wavelength are regarded as being of constant hue. There are 24 principles hues, having values of T=1 for a yellow, proceeding via Red, Purples, Blues, to a Yellow Green of T=24 and back from T=25 to T=1.

The second of the three variables, saturation, S, is a function of the distance from the point representing the reference white on the chromaticity diagram and with the same luminance factor as the colour being specified. Equal saturation represents equal perceptual differences from the grey of the same luminance factor.

The measure of brightness adopted for the DIN system is unique, following Ostwald who emphasized that equally saturated colours of complementary hues are not recognized as equivalent if they have equal luminous reflectance Y and saturation degree. It was assumed that this condition might be achieved if equal luminance factors were used. These are defined as the ratios $Y / Y_0$, where $Y_0$ is the maximum possible luminance reflectance of a surface colour and is shown in Figure 2.2 This third variable is related to the darkness degree, D, rather than to lightness, ranging from 0, for perfect white and colours with $Y = Y_0$, to 10 for perfect black, according to equation 2.1;

$$D = 10 - 6.1723 \log [ 40.7 (Y / Y_0) + 1 ] \qquad \text{Equation 2.1}$$

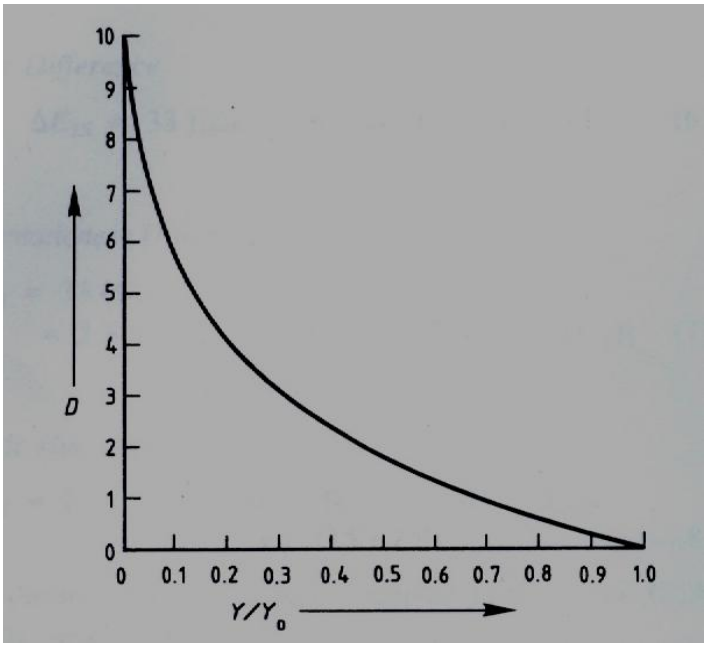


Figure 2.2: Darkness degree D as function of relative luminance factor $Y / Y_0$ [23]

The DIN colour space is formed by having the grey scale as a vertical axis, with white at the top, for which D=0, and black at the bottom, for which D=10. The top surface of the solid is then a portion of a sphere having the black point at the centre, as shown in Figure 2.3; this surface represents the optimal colours. Optimal colours are the colours of the imaginary objects which reflect perfectly in some parts of the spectrum and absorb completely in the remainder, so that everywhere, either R = 100 or R = 0.

Different hues, T, are then situated in 24 different planes with one edge coincident with the grey scale axis and the same angle 15, between adjacent planes. DIN darkness D is represented by distance down from the top surface towards the black point. DIN saturation, S, is represented by the angular distance out from the grey scale axis, and evaluated from the black point.

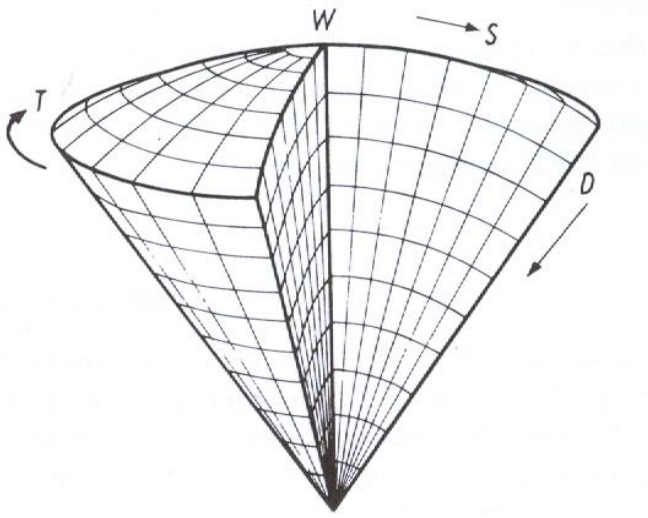


Figure 2.3: Sphere sector colour solid of the DIN colour system [23]

### *2.2.3 Natural Colour System (NCS)*

Natural colour order system was developed in 1981 in Sweden. NCS is based upon Hering's opponent colours theory [24]. The system starts from six elementary colours which are perceived by human beings as being pure. There are four elementary chromatic colours Yellow, Green, Blue and Red and two non chromatic colours Black and White. The three variables used to define in the NCS colour order system are hue, chromaticness and blackness. The hue variable is defined in terms of resemblance of the test colour to the two nearest chromatic elementary colours.

The second variable, chromaticness, can be defined as the resemblance of the test colour to the colour of the same hue having the maximum possible chromatic content. The third variable, blackness, is the resemblance of the test colour to the perfect black. Chromaticness and blackness can be illustrated by means of an equilateral triangle, the three corners of which represent the colour of maximal blackness, S, (100%), whiteness, W,(100%) and the chromaticness, C,(100%) . For any stimulus, values of S, W, and C must sum to 100.

$$W + S + C = 100 \qquad \text{Equation 2.2}$$

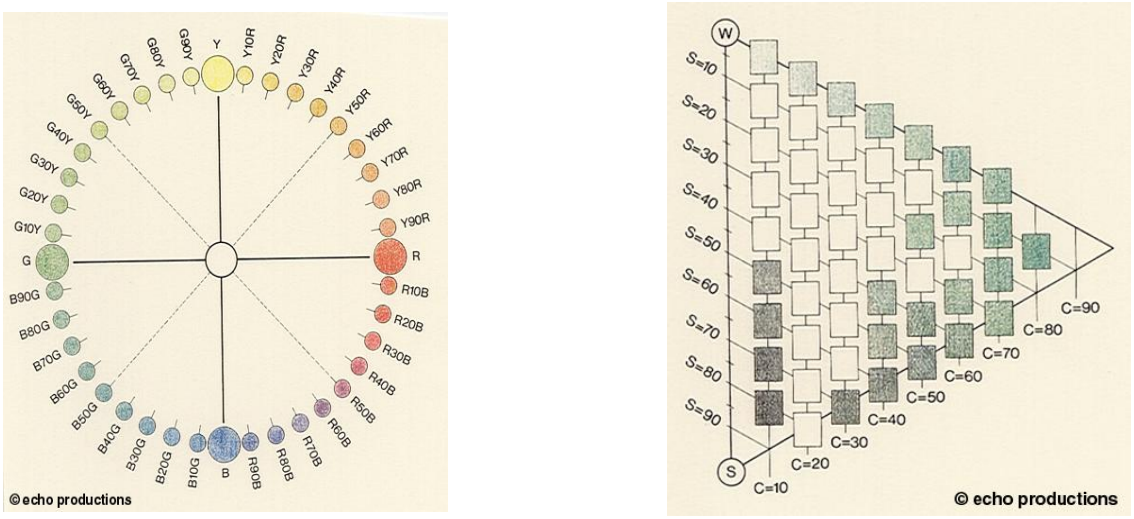


Figure 2.4: (a) The NCS hue circle. (b) the chromaticness and blackness of NCS colour system [74]

### *2.2.4 OSA-UCS Colour order system*

The OSA-UCS system was initiated in 1947 and ended in 1977, in which the leading part was taken by Judd [25]. The basic guiding principle of the OSA committee was to achieve the best possible uniform visual spacing of colours. An OSA-UCS specification consists of three numbers. The first represents the lightness L. When L = 0 the colour has the same lightness as a medium grey of 30% reflectance. Uniform steps of lightness above L = 0 are specified progressively as positive levels (L = 1, 2, 3…..) steps; below L = 0 are specified as negative (L = -1, -2, -3…). Values of L range from about -7 to +5.

The second number in an OSA specification, j, represents the yellowness-blueness of the colour; j is positive for yellowish colours and negative for bluish colours. Values of j range from about -6 to +11. The third number, g, represent the greenness-redness of the colour; g is positive for greenish colours and negative for reddish colours. Values of g range from about -10 to +6.

A rhombohedral lattice is used to achieve equal perceptual spacing. The basic geometric figure used to describe the rhombohedral lattice of the OSA-UCS system is the cubo-octahedron, formed by removing the 8 corners of a cube [26]. A sample located at the centre of the cubo-octahedron has 12 nearest neighbours, at the twelve corner points of a solid. These twelve points are all equidistant from the point lying at the centre of the original cube.

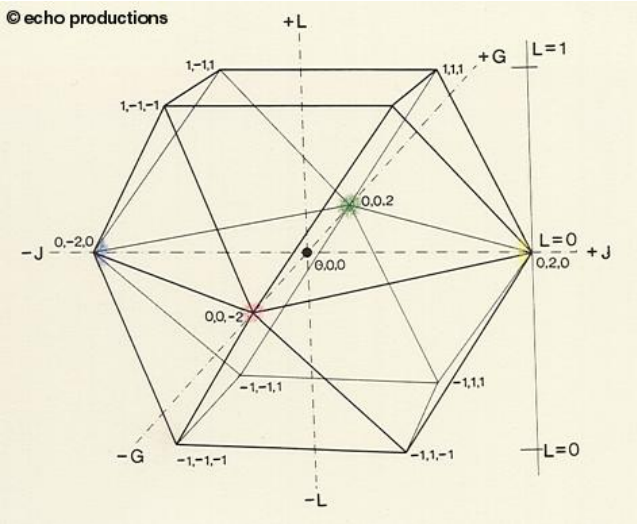


Figure 2.5: OSA-UCS Colour order system [74]

### *2.2.5 The Coloroid Colour System*

The colouriod colour space was developed between 1962 and 1980 by Prof. Antal Nemcsics at the Budapest University of Technology and Economics [27]. The objective of this arrangement was to provide both a technical and artistic aid to architects involved in coloured environmental design. Uniform aesthetic spacing was chosen as the guiding principle behind this construction with perceived differences ranking in second place.

Colours in the Coloroid colour space are fundamentally specified according to the perceptual attributes of "luminosity" (luminance factor, V), "saturation" (excitation purity, T) and hue (the matching or dominant spectral wavelength, A).

The colours of the spectrum and the purple line are distributed around the axis as shown in the Figure 2.6. To be more exact, they are located around an approximately elliptical, inclined section through the three-dimensional construction. They represent the so-called Coloroid limit-colours. Each limit-colour in the Coloroid system is linked to white and black by a so-called limit-curve. A closed colour-space is thus created which contains all sensations of colour within an arrangement corresponding to the perceived characteristic values of the system. A (smaller) Coloroid colour-solid containing colours of lesser brightness and saturation is located within this Coloroid-space. The extremes of red (beyond 700 nm) and violet (beyond 450 nm) are not included in its colour-hues. With the outer solid, brightness increases along the scale from black towards white in

100 uniform gradations which are more accurately defined by the system's authors as the square root of luminosity. Saturation, also divided into 100 units, is defined by analysis of the test colour as an additive mixture of the spectral colours (or purple). The saturation of a colour is stated as being the percentage content of the spectral colour (or purple) existing within the mixture.

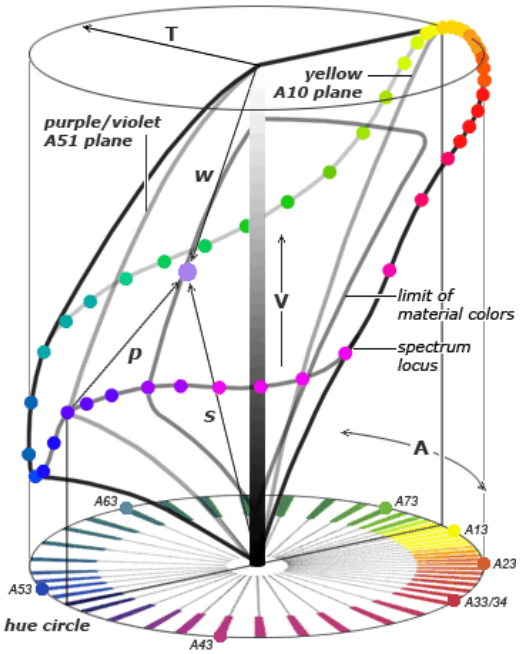


Figure 2.6: The Coloroid Colour System [74]

## 2.3 The CIE system and Colorimerty

Colorimerty is the science of measuring and specifying colour. The basis for colorimerty was established by the CIE in 1931, based on visual experiments. Almost all modern colour measurement is based on the CIE system of colour specification. The initials come from the French title, (Commission Internationale de l' Eclairage) an international committee on illumination. It is essentially, an empirical system, based on experimental observations rather than on theories of colour vision [28, 29, 30].

The CIE specification for the visual appearance of colours takes the additive mixture of red, blue and green coloured lights as its starting point. These three lights can be regarded as real primaries and may be imagined to occupy the corners of an equilateral triangle. It is assumed that at the corner of the triangle, the amount of a particular primary colour is 100%. All colours located within the triangle can be matched by positive quantities of the red, green and blue primaries. It is not possible always to

match certain colours with positive amounts of these primaries especially spectral colours which means that they fall outside the triangle as can be observed in Figure 2.7.

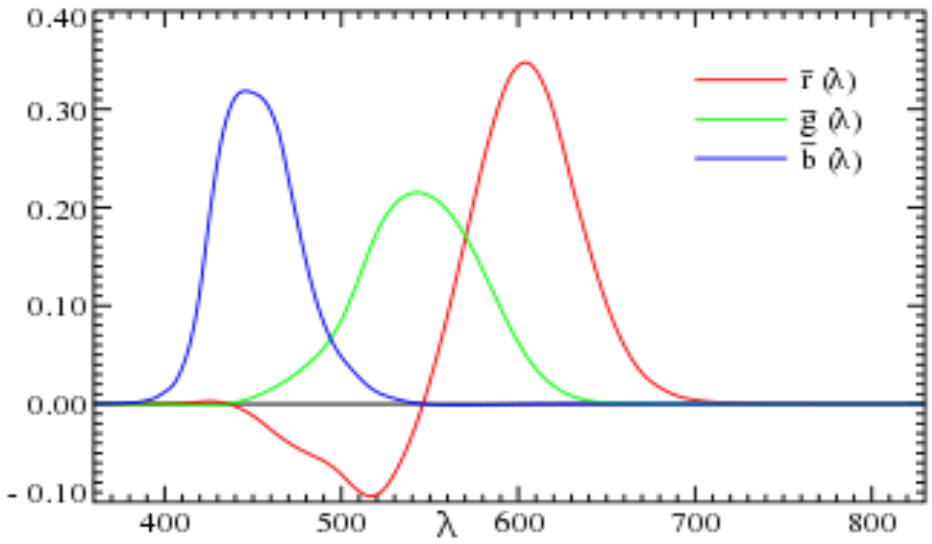


Figure 2.7: CIE 1931 $\bar{r}, \bar{g}, \bar{b}$ colour matching functions [75]

The CIE system adopted three imaginary reference primaries which are theoretical in conception, in that they are conceived as having greater saturation than pure spectral primary colours, and consequently fall right outside the spectrum locus. Thus the use of negative values when matching very pure colours can be avoided. This is shown in Figure 2.8.

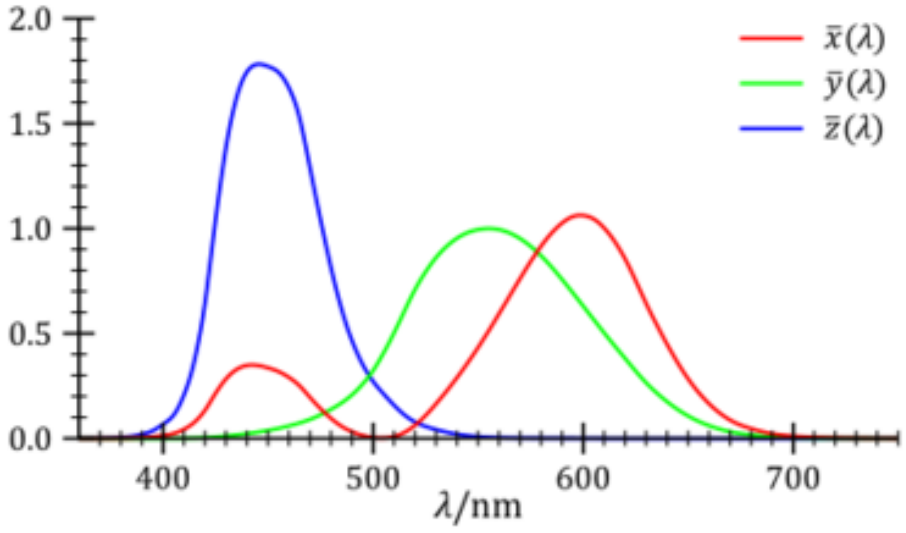


Figure 2.8: CIE 1964 $\bar{x}, \bar{y}, \bar{z}$ colour matching functions [75]

Since these three theoretical primaries cannot be produced, nor appreciated by the eye, they are always referred to as imaginary stimuli. These three reference stimuli are called [X], [Y], and [Z] and they are defined in terms of real spectral primaries [R], [G], [B] so that the spectral colours can be matched by the positive amounts of these three primaries.

By projecting the tristimulus values onto the unit plane (X+ Y+ Z = 1), colour can be expressed in a two dimensional plane, such a unit plane is known as the chromaticity diagram [28, 29, 30, 31, 32] and is shown in Figure 2.9.

$$x = \frac{X}{X + Y + Z}$$

$$y = \frac{Y}{X + Y + Z} \qquad \text{Equation 2.3}$$

$$z = \frac{Z}{X + Y + Z}$$

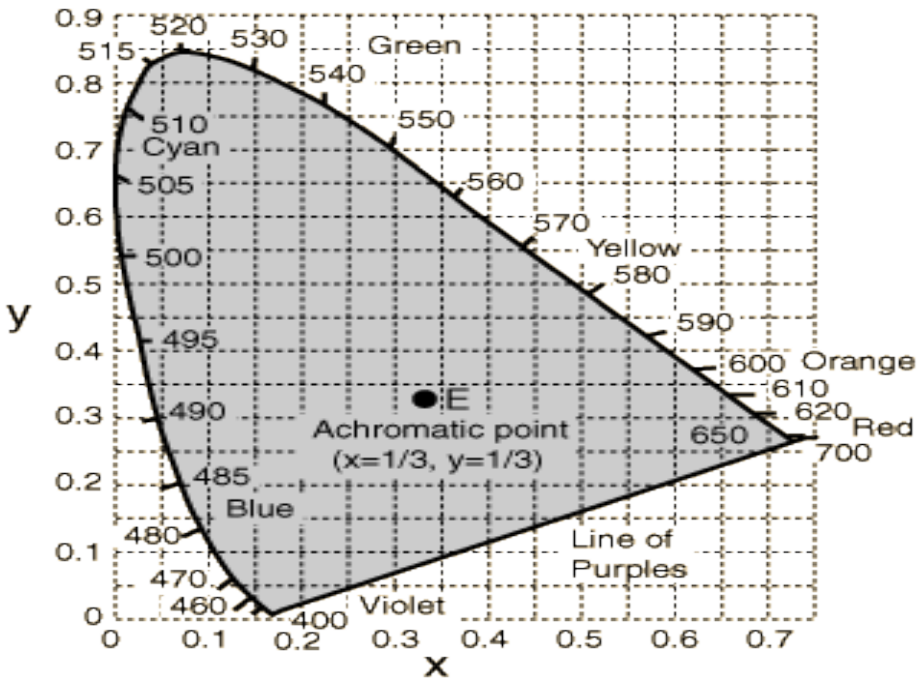


Figure 2.9: CIE Chromaticity Diagram [76]

If two specimens have identical X, Y, Z. values, they are a perfect match under one illuminant to the particular observer chosen: the distance between the positions of these specimens in X Y Z space is therefore zero.

The quantities X, Y and Z are termed tristimulus values. These tristimulus values depend upon the observer's field of view. The CIE in 1931 established the $2^{\circ}$ standard observer

which was defined as the chromatic response of the average human viewing at a 2 degree field of view, as it was believed at that time that the colour-sensitive cones resided within a 2° arc of the fovea. In 1964 the standard observer at a 10 degree field of view was introduced which was recommended for viewing at angles of more than 4 degrees.

In addition to the standard observer, the CIE has also defined various illuminants. The standard illuminants as described by CIE are given in Table 2.1

Table 2.1: Standard illuminants and their representation

| Illuminant | Representation |
|---|---|
| A | average incandescent light at CCT 2856K |
| B | direct sunlight at CCT 4874K |
| C | average daylight at CCT 6774K |
| D | phases of daylight at various CCTs |
| E | equal-energy illuminant |
| F | fluorescent lamps of various composition |

Illuminants B and C are no longer recommended and have been replaced by the D series. The CIE recommends D65 as the standard daylight illuminant. Illuminant D65 is a part of the D series, corresponds roughly to a mid-day sun in Western Europe / Northern Europe, hence it is also called a daylight illuminant.

Illuminant E is an equal-energy radiator; it has a constant spectral power distribution in the visible spectrum and is roughly isothermal with D55. Illuminant E is not a black body, so it does not have a colour temperature, but it can be approximated by a D series illuminant with a correlated colour temperature of 5455 K.

The F series of illuminants represent various types of fluorescent lighting.

The tristimulus values X, Y, Z are the amounts of the imaginary primaries [X], [Y], and [Z] required by the standard observer to match a colour, illuminated by a standard illuminant.

The tristimulus values of the textile fabric can be calculated from the amount of light reflected at each wavelength throughout the visible region. If $R_{\lambda}$ is the fraction of light reflected at each wavelength by the fabric and $E_{\lambda}$ is the relative amount of light emitted

by the light source at each wavelength, then the amount reflected at each wavelength will be: $E_\lambda * R_\lambda$ [33,34, 35, 36, 37].The total amount of energy reflected over the visible spectrum is the sum of the amount reflected at each wavelength:

$$X = \int_{380}^{760} E_\lambda * R_\lambda \bar{x} d\lambda$$
$$Y = \int_{380}^{780} E_\lambda * R_\lambda \bar{y} d\lambda \qquad \text{Equation 2.4}$$
$$Z = \int_{380}^{780} E_\lambda * R_\lambda \bar{z} d\lambda$$

The amount of the light reflected from coloured surface can be matched by:

$$\int_{380}^{760} E_\lambda * R_{\lambda *} \bar{x} d\lambda + \int_{380}^{760} E_\lambda * R_\lambda * \bar{y} d\lambda + \int_{380}^{760} E_\lambda * R_\lambda * \bar{z} d\lambda \qquad \text{Equation 2.5}$$

These are the tristimulus values (X + Y + Z), in which $\bar{x}, \bar{y}, \bar{z}$ are the colour matching functions of the CIE standard observer.

The product in equation 2.5 must be carried out at every wavelength, which is tedious process. Most often an approximation method is used typically the weighted ordinate method (Equation 2.6)

$$X = \sum W_\lambda * R_\lambda \Delta\lambda$$
$$Y = \sum W_\lambda * R_\lambda \Delta\lambda \qquad \text{Equation 2.6}$$
$$Z = \sum W_\lambda * R\Delta\lambda_{\lambda\lambda}$$

Where

$$W_\lambda = E_\lambda * \bar{x}_\lambda (or \bar{y}_\lambda or \bar{z}_\lambda)$$

Where, $R_\lambda$ is the reflectance of the substrate, $E_\lambda$ is the relative amount of light emitted by the source at each wavelength and $\bar{x}_\lambda, \bar{y}_\lambda, \bar{z}_\lambda$ are the colour matching functions of the standard observer. Tables for the $E_\lambda \bar{x}_\lambda, E_\lambda \bar{y}_\lambda, E_\lambda \bar{z}_\lambda$, weighted for different wavelength intervals, have been published by the CIE [38].

## 2.4 Colour difference formulae

Colour difference formulae are important tools in the production of coloured goods. They provide a prediction of perceived colour differences based on stimulus differences between coloured materials (reflectance function differences) and thereby represent a tool for quality control purposes.

Many colour difference equations have been proposed since the introduction of the CIE system in 1931. The accuracy of the equation can be assessed by producing a series of colour differences, measuring the required tristimulus values and calculating the ΔE values for any particular equation. These ΔE values are then compared with some form of visual assessments of the corresponding differences, usually involving a number of observers. The ideal formula would allow for a pass/fail decision based on a single number colour difference value from the standard, regardless of the colour of the standard [28, 39].

Of all those developed, no one equation has proven to be uniform throughout colour space with respect to average visual observation of sample pairs when such pairs exhibit small to medium colour difference. Lack of agreement between the objective and subjective methods of evaluation is caused by any one, or a combination, of the following [18]:

- The accuracy of the measurement
- The accuracy of the visual assessment
- The accuracy of the colour difference equation

### *2.4.1 The Adams-Nickerson Colour Difference Formula*

The ANLAB colour difference formula is based on the Adams UCS diagram at constant lightness, which is different from the x, y, Y chromaticity diagram, in which plots of colours of constant chroma are very irregular [40].The Adam UCS diagram is based upon the opponent colour theory of colour vision that results in an AB diagram. It was observed that the Y tristimulus value for any series of surface colours is not linearly related to the perceived lightness as shown for greys in Figure 2.10. The curve represents the response of the green sensitive cones in the XYZ system of colour measurement.

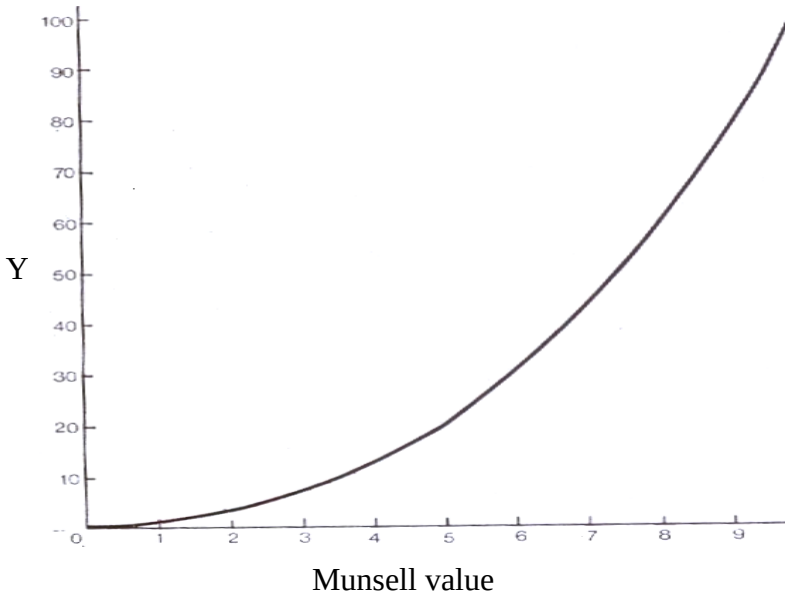


Figure 2.10: Relationship between perceived lightness and tristimulus value Y [40]

A fifth order polynomial function was devised by Judd to express the Y tristimulus value in relation to the Munsell value scale:

$$I_0 = 1.2219V_I - 0.23111V_I^{\,2} + 0.23951V_I^{\,3} - 0.021009V_I^{\,4} + 0.00084045V_I^{\,5} \qquad \text{Equation 2.7}$$

Where $I_0$ corresponds to the Y tristimulus value and ranges from 0 to 100. Adams believed that the visual sensations from the excitation of only red cones or only the blue sensitive cones have the same relation to the X and Z tristimulus values and represented as $V_x$ and $V_z$ respectively. Tables relating $V_x$, $V_y$ and $V_z$ to X, Y, Z have been published by the CIE [40].

Adams didn't extend his UCS diagram into a three dimensional uniform colour space. This extension was made by Dorothy Nickerson. The appropriate uniform lightness scale for combining with the Adams UCS diagram was the Munsell value $V_y$ multiplied by a scale factor so that a unit difference in $V_y$ was approximately perceptually the same as unit differences in $V_x$ and $V_y$.

The co ordinates of Adams Nickerson uniform colour space are therefore:

$$L = 42 * 0.23V_y \qquad \text{The lightness axis}$$

$$A = 42(V_x - V_y) \qquad \text{The redness-greenness axis} \qquad \text{Equation 2.8}$$

$$B = 16.8(V_y - V_z) \qquad \text{The yellowness-blueness axis}$$

In the ANLAB colour space the colour difference (ΔE) between a sample and the standard is computed by applying the Pythagoras theorem in the three dimensions: L, A and B,

$$\Delta E = [(0.23V_y)^2 + (\Delta(V_x - V_y))^2 + 0.4(\Delta(V_y - V_z))^2]^{1/2} \qquad \text{Equation 2.9}$$

The above equation is usually written as**:**

$$\Delta E = \sqrt{(\Delta L)^2 + (\Delta A)^2 + (\Delta B)^2} \qquad \text{Equation 2.10}$$

ANLAB colour space, one of the most uniform at the time of its publication, was not suitable for single number shade passing [4]. Single number shade passing requires that, once the closeness of match has been specified, the same pass/ fail value of ΔE can be used successfully irrespective of the colour of the standard or of the nature of the colour difference. While the formula was satisfactory for quantifying colour differences around a standard in a particular area of colour space, it was generally found that different numerical tolerance values were required for different parts of colour space.

### *2.4.2 CIELAB Colour Difference Formula*

The ANLAB formula is simplified by using a cube root approximation of the fifth degree polynomial (Equation 2.8) established by Adams, which was adopted in the CIELAB colour difference formula [41, 42]. The formula was approved by the CIE in 1976 and is known as the CIE 1976 ($L^*$ $a^*$ $b^*$) formula. The CIELAB colour space is generated by plotting in rectangular coordinates as shown in Figure 2.11, the quantities L*, a*, and b*, defined by the rectangular co-ordinates:

$$L^* = 116\left(\frac{Y}{Y_0}\right)^{1/3} - 16 \qquad X/X_\circ, Y/Y_\circ, Z/Z_\circ > 0.00885$$

$$a^* = 500[(X/X_0)^{1/3} - (Y/Y_0)^{1/3}] \qquad \text{Equation 2.11}$$

$$b^* = 200[(Y/Y_0)^{1/3} - (Z/Z_0)^{1/3}]$$

Where X, Y and Z are the tristimulus values of the surface colour and $X_0$, $Y_0$ and $Z_0$ are the tristimulus values of the illuminant, ($Y_0$=100).

When either $X/X_0$ or $Y/Y_0$ or $Z/Z_0$ is less than 0.00885 the relavent cube root functions in equations 2.12, 2.13 and 2.14 must be replaced by a linear re-weighting. A rescaling constant 7.787 that is common to all three dimensions is used and the other re-scaling constants, 116, 500, and 200 (for L* a* and b*) are retained unaltered. Thus the value $(Y/Y_0)^{1/3}$ is replaced by 7.787 $(Y/Y_0)$ etc.

Alternatively the space can be defined by the polar co-ordinates, known as CIE $L^*$,$C^*$, $h°_{ab}$, in which chroma, $C^*$, represents how far from grey an object is when compared to neutral grey of equal lightness, and hue angle, $h°_{ab}$ varies from 0 - $360^0$. The equations for calculating hue and chroma are:

$$C^* = \sqrt{(a^{*2} + b^{*2})} \qquad \text{Equation 2.12}$$

$$h = \tan^{-1}(b^* / a^*) \qquad \text{Equation 2.13}$$

The total difference $\Delta E^*_{ab}$ between two colours, each specified in terms of L*a*b* rectangular co-ordinates, is calculated using equation 2.17:

$$\Delta E^* = [(\Delta L^*)^2 + (\Delta a^*)^2 + (\Delta b^*)^2]^{1/2} \qquad \text{Equation 2.14}$$

Alternatively the colour difference can be computed using polar co-ordinates from equation 2.18

$$\Delta E^* = [(\Delta L^*)^2 + (\Delta C^*)^2 + (\Delta H^*)^2]^{1/2} \qquad \text{Equation 2.15}$$

Where

$$\Delta H^* = [(\Delta E^*)^2 - (\Delta C^*)^2 - (\Delta L^*)^2]^{1/2} \qquad \text{Equation 2.16}$$

It should be noted that the CIELAB equation does not give an appreciably better correlation with visual data than that given by ANLAB and it is still be necessary to establish different pass/fail values according to the colour involved and the nature of the colour difference.

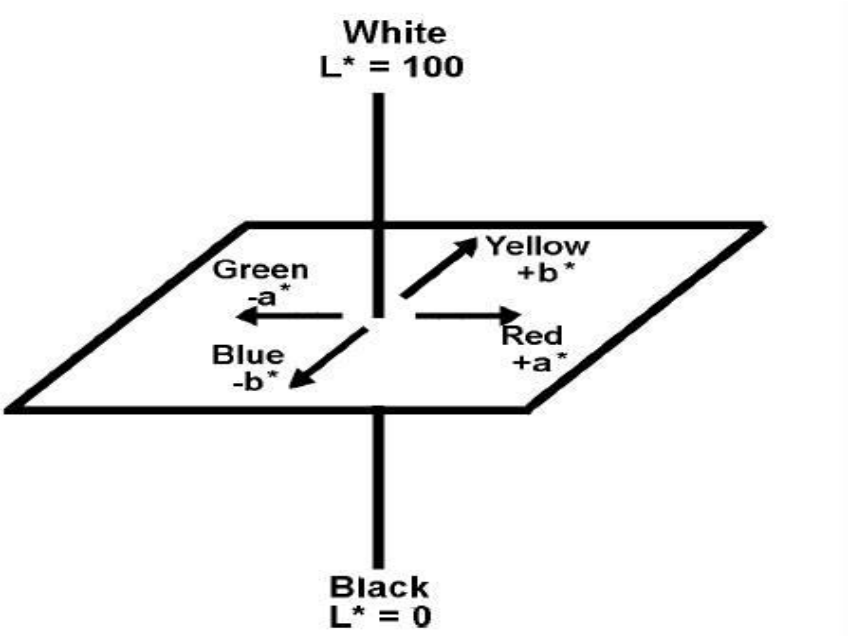


Figure 2.11 :CIE L* a*b* Colour space

### *2.4.3 JPC 79 Formula*

The early colour difference formulas were mainly derived to fit the Munsell data but the Munsell samples are much smaller than those on which judgments are typically made. Also, in the Munsell system, an adjacent pair along each of the H, V, and C scales has 5-10 CIELAB colour difference units, which is about 10 times larger than the difference common in typical industrial applications.

Since 1976 most of the experimental sets on colour discrimination have been produced using surface samples viewed under typical industrial viewing conditions. An extensive set of visual acceptability data was produced by McDonald, at the company J&P Coats Ltd, who produced over 600 coloured polyester thread pairs, surrounding 55 colour standards [43, 44, 45, 46].

The formula developed by McDonald is

$$\Delta E_{JPC79} = [(\Delta L^* / \Delta L^*_t)^2 + (\Delta C^* / \Delta C^*_t)^2 + (\Delta H^* / \Delta H^*_t)^2]^{1/2} \qquad \text{Equation 2.17}$$

Where ΔL*, ΔC*, and ΔH* are respectively the ANLAB lightness, chroma and hue difference between batch and standard. The values of $L_t$, $C_t$ and $H_t$ are computed for the particular location of the standard in the colour space and the equations below are used to calculate them:

$$L_t = 0.08195L^*_S / 1 + 0.01765L^*_S$$

$$C_t = 0.638 + 0.0638C^*_S / 1 + 0.0131C^*_S \qquad \text{Equation 2.18}$$

$$H_t = C_t * T$$

$$T = 1 \qquad \text{If} \quad C^*_S < 0.638 \quad \text{otherwise}$$

$$T = k_1 + [k_2 \cos(h_s + k_3)] \qquad \text{if} \qquad C^*_S \geq 0.638$$

$$k_1 = 0.36, k_2 = 0.4, k_3 = 35 \quad \text{if} \quad h_s \geq 345 \quad \text{or} \quad h_s \leq 164$$

$$k_1 = 0.56, k_2 = 0.2, k_3 = 168 \quad \text{if} \quad 164 \langle h_s \langle 345$$

$L^*_S$, $C^*_S$, and $h_S$ are respectively the AN (43.909) lightness, chroma and hue angle of the standard.

JPC79 has two anomalies

i. A discontinuity of chromatic differences for samples close to the achromatic axis
ii. An over-prediction of lightness differences for samples close to black

In 1984 the JPC79 formula was modified by Colour Measurement Committee (CMC) of the Society of Dyers and Colourists (SDC). Modifications were introduced to correct these two anomalies:

**i. Lightness differences for very dark colours**

For very dark colours as $L^*$ approaches zero $L_t$ also approaches zero and hence $\Delta L/L_t$ can be extremely large. The CMC suggested that this can be avoided if, for $L^*$ values below 16, $L_t$ is taken to be 1.022.

**ii. Anomalies with near neutral samples**

All the shades near neutral axes are all essentially grey (or white or black)). The hue discrimination does not depend upon the hue angle of a standard if it is lying near the neutral axes and its magnitude remains same as that of chroma discrimination. Therefore, for all the colours with $C^* < 0.638$, the JPC formula sets $H^*_t = C^*_t$.

### *2.4.4 CMC (l: c) formula*

It was decided in a CMC meeting that the formula should be further modified to allow for the possibility of different lightness or chroma weightings being required for different circumstances (that is perceptibility rather than acceptability, or for acceptability judgments of different substrates such as paints , textiles and leather) [47]. It was observed that different weighing factors are required for different industrial sectors, the JPC formula gave worse results than CIELAB for the assessment of plastic samples visually but when the lightness difference component was doubled, the formula was significantly better. It was decided that the unit weightings should be used for perceptibility data, and it was found necessary to divide the *l* values by the factor 2 for acceptability judgments

The terms $L_T$, $C_T$ and $H_T$ of the JPC formula were replaced by $S_L$, $S_C$ and $S_H$ (indicating the length of the half axes of the ellipsoid defining unit ΔE), and the formula was named CMC (l: c), where l and c are the relative tolerances required for the particular application. Thus for the perceptibility data the formula would be named CMC (1:1) and for acceptability data CMC (2:1).The final specification of the formula is

$$\Delta E_{CMC(l.c)} = [(\Delta L^* / lS_L)^2 + (\Delta C^* / cS_C)^2 + (\Delta H^* / S_H)^2]^{1/2} \quad \text{Equation 2.19}$$

$$S_L = 0.040975 L^*_1 / (1 + 0.01765 L^*_1) \quad \text{if } L^*_1 \geq 16$$

$$\text{But } S_L = 0.511 \quad \text{if } L^*_1 < 16$$

$$S_C = (0.0638 C^*_1) / (1 + 0.0131 C^*_1) + 0.638$$

$$S_H = S_C (Tf + 1 - f) \quad \text{Equation 2.20}$$

$$f = [(C^*_1)^4 / ((C^*_1)^4 + 1900]^{1/2}$$

$$T = 0.36 + [0.4 \cos(h_1 + 35)]$$

Unless $h_1$ is between $164^0$ and $345^0$ when

$$T = 0.56 + [0.2 \cos(h_1 + 168)] \quad \text{Equation 2.21}$$

$L^*_1$, $C^*_1$ and $h_1$ refer to the standard of a pair of the samples, and the values ΔL*, ΔC* and ΔH* are calculated from the CIELAB formula.

### *2.4.5 BFD colour difference formula*

Luo and Rigg in 1987[48, 49] pointed out that the tolerance ellipses fitted to the visual results and the CMC (*l*: c) formula ellipses were not in good agreement. For example the ellipses fitted to visual data did not all point toward the neutral point, especially in the saturated blue region of the colour space, as predicted by the CMC (*l*: c) formula. Therefore, it was considered necessary to modify the CMC (*l*: c) formula to eliminate this discrepancy.

Luo and Rigg combined various acceptability data sets into one set and similarly various perceptibility data in another set from previously published work. These new data sets were then used to modify the CMC (*l*: c) colour difference formula. The newly developed colour difference formula was termed BFD (*l*: c) formula, which was obtained by optimizing the constants in the formula to fit all visual data when combined together.

The BFD (*l*:c) colour difference formula is different from the CMC (*l*:c) formula as a new lightness scale was introduced and hue correction was made by tilting the ellipsoids relative to the chromaticity plane in different regions of the colour space. This was achieved by introducing a new term which was a rotational factor.

The BFD (*l*: c) colour difference formula is given in equation 2.22;

$$\Delta E(BFD) = \{[\sqrt{\Delta L(BFD)/l)^2 + [\Delta C^*/(cD_C)]^2 + (\Delta H^*/D_H)^2 + R_T(\Delta C^*/D_C)(\Delta H^*/D_H)]}\}$$

Equation 2.22

$$D_C = 0.035\overline{C}^*/(1 + 0.00365\overline{C}^*) + 0.521$$
$$D_H = D_C(GT' + 1 - G)$$
$$G = \{(\overline{C}^*)^4/[(\overline{C}^*)^4 + 14000]\}^{1/2}$$
$$T' = 0.627 + 0.055\cos(h - 254^0) - 0.040\cos(2h - 136^0) +$$
$$0.070\cos(3h - 32^0) + 0.049\cos(4h + 114^0) - 0.015\cos(5h - 103^0)$$
$$R_T = R_H R_C$$
$$R_H = -0.260\cos(h - 308^0) - 0.379\cos(2h - 160^0) - 0.636\cos(3h + 254^0) +$$
$$0.226\cos(4h + 140^0) - 0.194\cos(5h + 280^0)$$
$$R_C = \{(\overline{C}^*)^6/[(\overline{C}^*)^6 + 7 \times 10^7]\}^{1/2}$$

Equation 2.23

The terms $\overline{C}^*$ and *h* refer to the mean of the *C** and h values for the standard and sample. The values Δ*C** and ΔH* are calculated from the CIE L* a* b* formula, and *l* and c represent the tolerance limits applied to lightness and chroma respectively.

### *2.4.6 CIE 94 ($K_l$:$K_c$:$K_h$) Colour Difference Formula*

The CIE established a technical committee in 1989, with the remit to study existing metrics used in industry to evaluate colour difference between object colours in daylight illumination, and to develop a recommendation on this subject [50]. It resulted in a different formula, the full title of which is the CIE 1994 ($D_L$, $D_{C,AB}$, $D_{H,AB}$) colour difference model, with the official abbreviation CIE94 and the colour difference symbol DE94. There are many factors that affect visual assessments, such as the nature of the specimens and the conditions under which they are viewed. Reference conditions are set to those pertaining in industrial colour difference assessment. The new formula performs better in these conditions. The conditions are:

- The specimens are homogenous in colour;
- The colour difference between them is such that DE ≤5;
- They are placed in direct edge contact;
- Each specimen subtends an angle greater than 4 $^0$ to the assessor, whose colour vision is normal;
- They are illuminated at 1000 lux and viewed in object mode against a uniform gray background of L = 50 under illumination simulating D65.

The new formula is based on CIELAB colour space. The CIE94 formula includes a new term ΔV, which is the visually perceived magnitude of a colour difference:

$$\Delta V = k_E{}^{-1}\Delta E94 \qquad \text{Equation 2.24}$$

Where $k_E$ is an overall visual sensitivity factor, set to unity and therefore making $\Delta V=\Delta E_{94}$ under the conditions specified above. The CIE94 colour difference formula is:

$$\Delta E^*_{94} = [(\Delta L^* / K_L S_L)^2 + (\Delta C^* / K_C S_C)^2 + (\Delta H^* / K_H S_H)^2]^{1/2} \qquad \text{Equation 2.25}$$

The purpose of the variables $K_L$, $K_C$ and $K_H$ is the same as that of l and c in the CMC

(*l*: c) formula. In the CIE94 formula however, they are called parametric factors. Under reference conditions $k_L = k_C = k_H = 1$. A reduction in lightness sensitivity is well established for assessing textile samples so for the textile assessment:

$$k_L = 2, k_C = k_H = 1$$

The lengths of the ellipsoid semi-axes ($S_L$, $S_C$ and $S_H$), termed 'weighing functions' in CIE94, allow adjustment of their respective components according to the location of the standard in CIELAB colour space, but they are defined differently from those in the CMC (l: c) formula:

$$\begin{aligned} S_L &= 1 \\ S_C &= 1 + 0.045C^*_{ab,X} \\ S_H &= 1 + 0.015C^*_{ab,X} \end{aligned} \qquad \text{Equation 2.26}$$

The following differences exist between the CMC (*l*: c) and CIE94 formulae:

- No change in $S_L$ with $L^*_S$, whereas in CMC $S_L$ increases with $L^*_S$
- Linear expansion of $S_C$ and $S_H$ with $C_{abs}$ whereas there is a nonlinear expansion in the CMC(*l*:c) formula
- No dependence of $S_H$ on $h_{abs}$ whereas there is a systematic variation in the CMC (*l*:c) formula

### *2.4.7 CIEDE2000 ($K_l$:$K_c$:$K_h$) Colour Difference Formula*

After the development of the CIE94 formula, two separate colour difference equations were recommended by different organizations, i.e. CMC (*l*: c) by ISO and CIE94 by the CIE. However these formulae were derived from two main data sets: Luo and Rigg, and Ritt-DuPont respectively. If theCIELAB formula agrees perfectly with the experimental results, all ellipses should be circles of constant radii [51, 52]. Hence the pattern of ellipses in the a* b* diagram shows poor performance by CIELAB. It can be seen that the pattern of the ellipses from the two sets are quite similar e.g. very small ellipses for neutral colours, an increase in the size of the ellipse sizes as chroma increases, and all ellipses for the blue region pointing away from neutral. Ellipses from all other colour regions generally point towards the neutral point.

Both of the formulas fit badly to the experimental results in the blue region. It has been observed that there is a large discrepancy in predicting lightness difference, and both have errors in predicting colour difference in the grey and the blue regions. With this in mind, a CIE technical committee (TC 1-47) on hue and lightness dependent correction to industrial colour difference evaluation was formed in 1998, and a formula named CIEDE2000 was published.

$$\Delta E^{\bullet}_{00} = \left[ \left( \frac{\Delta L'}{K_L S_L} \right)^2 + \left( \frac{\Delta C'}{K_C S_C} \right)^2 + \left( \frac{\Delta H'}{K_H S_H} \right)^2 + R_T \left( \frac{\Delta C'}{K_C S_C} \right) \left( \frac{\Delta H'}{K_H S_H} \right) \right]^{1/2}$$

Equation 2.27

Where

$$S_L = 1 + \frac{(0.015\bar{L}' - 50)^2}{\sqrt{20 + (\bar{L}' - 50)^2}}$$

$$S_C = 1 + 0.045\bar{C}'$$

$$S_H = 1 + 0.015\bar{C}'T$$

$$T = 1 - 0.17\cos(\bar{h}' - 30) + 0.24\cos(2\bar{h}') + 0.32\cos(3\bar{h}' + 6°) - 0.20\cos(4\bar{h}' - 63°)$$

$$R_T = -\sin(2\Delta\theta)R_C$$

Equation 2.28

$$\Delta\theta = 30\exp\left[ -\left[ \frac{(\bar{H}' - 275°)}{25} \right]^2 \right]$$

$$R_C = 2\left[ \sqrt{\frac{\bar{C}'^7}{\bar{C}'^7 + 25^7}} \right]$$

$$L' = L^*$$

$$a' = (1 + G)a^*$$

$$b' = b^*$$

$$C' = \sqrt{a'^2 + b'^2}$$

$$h' = \tan^{-1}(b'/a')$$

$$G = 1 - \frac{\sqrt{\frac{\bar{C}^{*7}}{\bar{C}^{*7} + 25^7}}}{2}$$

Equation 2.29

CIEDE2000 formula includes five corrections to CIELAB

- A lightness weighting function ($S_L$).
- A chroma weighting function ($S_c$).
- A hue weighting function ($S_H$).

- An interactive term ($R_T$) between chroma and hue difference for improving the performance for blue colours.
- A factor [1+G] for rescaling the CIELAB a scale for improving the performance for grey colours.

**2.5 Colour Difference partitioning**

It is often desirable to identify the component of the colour difference responsible for making a batch an unacceptable match to the standard. It will help to set the working directions to make a batch acceptable.

Three methods of colour splitting were reported by K. McLaren in 1981[4]:

- $L^* a^* b^*$ the rectangular co-ordinate colour difference component splitting
- $L^* C^* h^\circ_{ab}$ the polar co-ordinate colour difference component splitting
- H B S the dyers' colour difference component partitioning

The total difference $\Delta E^*_{ab}$ between two colours, each specified in terms of $L^*a^*b^*$ rectangular co-ordinates is calculated using:

$$\Delta E^* = [(\Delta L^*)^2 + (\Delta a^*)^2 + (\Delta b^*)^2]^{1/2}$$

From the $L^*a^*b^*$ coordinates of standard and batch, it is possible to split any colour difference into its three components. The three dimensions of difference are:

$$\Delta L^* = L^*_{sample} - L^*_{std}$$
$$\Delta a^* = a^*_{sample} - a^*_{std} \qquad \text{Equation 2.30}$$
$$\Delta b^* = b^*_{sample} - b^*_{std}$$

If $\Delta L^*$ ($L^*_{batch}$-$L^*_{standard}$) is positive the batch is lighter than standard and darker if $\Delta L^*$ is negative. Similarly, a positive $\Delta a^*$ and $\Delta b^*$ indicates that batch is redder and yellower and a negative sign to $\Delta a^*$ and $\Delta b^*$ show that batch is greener and bluer respectively. However in certain circumstances these simple interpretations can be highly misleading. In terms of the cylindrical components the colour differences are computed using

$$\Delta E^* = [(\Delta L^*)^2 + (\Delta C^*)^2 + (\Delta H^*)^2]^{1/2}$$

From the $L^*C^* h^\circ_{ab}$ coordinates of standard and batch, colour difference components splitting will be computed as follows;

$$\Delta L^* = L^*_{sample} - L^*_{std}$$ Equation 2.31

$$\Delta C^* = C^*_{sample} - C^*_{std}$$

Where

$C^*_{sample} = (a^*_{sample}{}^2 + b^*_{sample}{}^2)^{1/2}$, and

$C^*_{standard} = (a^*_{standard}{}^2 + b^*_{standard}{}^2)^{1/2}$

$$\Delta H^* = [(\Delta E^*)^2 - (\Delta C^*)^2 - (\Delta L^*)^2]^{1/2}$$ Equation 2.32

Equation 2.32 quantifies the hue difference component but does not indicate the nature of the hue difference [53]. In order to overcome this problem it was recommended by the CIE that a sign must be given to ΔH* based on the difference in CIELAB hue angles.

McLaren and Taylor pointed out that this differentiation is only helpful to indicate the direction of the batch relative to the standard in the $a^*$ $b^*$ plane [53]. They suggested a method to rotate the standard either clockwise or anti-clockwise (whichever gives minimum angular rotation) until it passes through the position of the batch and cuts one of the four $a^*$ $b^*$ axes. Four terms were suggested to show the nature of colour difference: redder, yellower, greener and bluer. The single hue term to the ΔH* values out of these four is then used depending upon the axis cut by the standard. This method gives some erroneous hue difference indication. A new method dual term approach, was explored which was reliable and simple. In dual term approach every hue difference is described by two comparatives: redder/yellower, yellower/greener, greener/bluer, or bluer/redder. The method adopted to determine the hue difference term is same as stated above with one addition of continuing the rotation of the standard since it cuts the second axis as well. The hue difference term of this second axis is the second comparative term of this dual term approach.

The $L^*$ $a^*$ $b^*$ and $L^*$ $C^*$ $h^\circ_{ab}$ are computed from the reflectance values of a sample which is measured on the modern instruments and hence used to compute the total colour difference. Though these numeric systems are advantageous in settling many colour matching disputes, dyers prefer to use their own terms in judging a batch against standard. Whenever a dyer or a colourist is asked to describe the perceived colour difference he responds in terms of strength (S), brightness (B) and the hue, known as the HBS method of splitting, in which only hue is common to $L^*C^*$ $h^\circ_{ab}$. This system is qualitative in nature which use different terms to describe the change in strength and brightness.

The reason why the colourists prefer the HBS system might be their training, since the start of their career, they have come to recognize the effect on appearance of increasing or decreasing the amount of colourant present, and to recognize the effect of adding a trace of a grey or black to a chromatic dyeing or paint [4, 5, 6].

# CHAPTER 3: DYERS' COLOUR DIFFERENCE COMPONENTS AND THEIR DETERMINATION

## 3.1 Dyers colour difference components

Depth and brightness are important terms to dyers. Depth is related to the amount of dye taken up by a textile material and brightness is that component of colour difference that is neither depth nor hue. Dullness is related to the amount of neutral grey present in the colour and brightness is best defined as the opposite of dullness [1]. Dyers associate various terms with differences in depth and brightness. Commonly, a dyeing that has less depth (less amount of dye) than another is described as "thinner"; one that has greater depth as "fuller". In the case of brightness, a dyeing with more grey content is said to be "flatter"; other with less grey as "brighter" [8].

The relationship between colorimetric variables and the dyers variables was reported firstly by Waters in terms of chromaticity coordinates. A number of colourists [6, 9, 10] reported dyers' variables in terms of dominant hue, excitation purity, and lightness. They found that a change in the strength and dullness of a colour resulted in a simultaneous change of both purity and lightness. Further, it was found that the differences in strength of dyeings which do not differ in hue can be estimated visually with confidence, while the situation is worse with dyeings differing in hue. The strength of dyeing changes with change in concentration and the extent of this change depends upon the dye itself [9]. For a blue dye, where the effect of change in concentration is easy to judge, strength is easy to evaluate, but for a yellow dye, where the effect of change in concentration is not easy to perceive, depth is harder to evaluate. An important development at this stage was to identify how inexperienced and experienced colourists varied in perceiving and reporting colour difference.

Variation in depth and brightness of dyeings were investigated systematically in ANLAB colour space by Cooper and Mclaren [5, 7]. They studied the behaviour of increasing the dye concentration in the lightness-chroma plane and found that an increase in strength normally results in an increase in chroma and decrease in lightness, until a point of maximum chroma is reached, as shown in Figure 3.1.

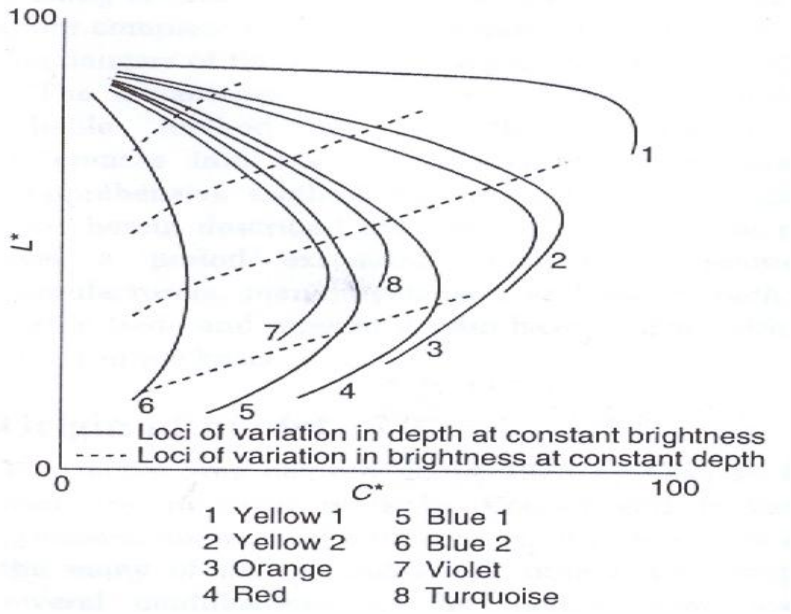


Figure 3.1: Depth and Brightness loci of typical dyes on textile substrate [5]

The maximum chroma point is the point in depth loci after which addition of any more dye to the fibre would result in a decrease in chroma and lightness. Again, an exception is yellow dye where the increase in strength increases the chroma without a maximum being reached. It is because the absorption band of yellow is sharper, giving steeper reflectance curves than dyes of other hues. Cooper and McLaren stressed that the maximum chroma is not necessarily the point at which the maximum perceived depth of the colour is achieved.

McLaren [5] pointed out that in the case of two dyeings of the same hue and perceived equal strength but which still do not a match, the difference is probably due to a difference in the third dyers' variable, which is brightness. The difference in brightness cannot be eliminated by changing the concentration of the dyeing but the addition of neutral grey in a small amount to the brighter dyeing may fix the problem. It was further emphasized that an increase in dullness will always cause a decrease in both lightness and chroma and the extent of this change is dependent upon the hue angle of the dyed sample. However, increase in dullness does not change the strength of the dye.

It can be concluded from the above discussion that the change in brightness or change in depth is always accompanied by changes in both lightness and chroma, but their relative weighting varies through the colour space. Therefore the partitioning of colour-differences into $\Delta L^*$, $\Delta C^*$ and $\Delta H^*$ is not directly equivalent to the dyer's method of partitioning.

### 3.2 Standard depth and its importance

The depth of a colour is a very important parameter in dyeing [11, 28, 54]. The evaluation of depth is necessary not only to describe the nature of the colour difference for a standard-batch pair by the dyer but also for:

- Determination of fastness properties of different colourants under comparable conditions. The Hilfstypen samples, which are a set of 18 woollen dyed samples of equal depth, are still used for comparison of fastness properties of a dyed material at the same depth level. It is termed as 1/1 standard depth [12, 13]. Depths at 1/3, 1/6, 1/12, 1/25 (all weaker) and 2/1(stronger) are also available.
- Determination of application properties of different colourants
- The estimation of the relative cost effectiveness of different colourants in colouration.

### 3.3 Methods to determine depth

Visual assessments of relative depths are not always repeatable or reproducible.

Visual colour matching and colourant standardising are iterative processes in which the aim is an overall colour difference, and hence a difference in any component, that is approximately zero. Instrumental methods are much more repeatable and reproducible. The principle difficulty has always been that of finding a colorimetric method which gives results in a sufficiently good agreement with visual assessments. Colorimetric methods may be divided into three types:

i. Single Wavelength Methods
ii. K/S Summation Methods
iii. Methods based in Colour Order Systems and Colour Spaces

#### *3.3.1 Single Wavelength Methods*

These methods use the absorption spectrum to measure the relative strength of a dye in solution. The relative strength is measured routinely for the standardization and quality control of dye by dye manufacturers [55, 56, 57]. The method is easy to perform but it has a limitation that the dye should be completely soluble in the solvent. Further, as this

method is based upon the wavelength of maximum absorption, neglecting the behaviour at the other wavelengths, this method is suitable only for similar colourants. Depth of the dye from this method is determined by the formula given in equation 3.1

$$D_S = kA_{\lambda(R.\min)} \qquad \text{Equation 3.1}$$

Where $A_\lambda$ is the absorbance at $\lambda_{max}$ and k is a scaling constant.

Absorption is directly proportional to the concentration of the dye in the solution. For dyed fabric, the Kubelka Munk function can be used to determine the depth. The K/S function of reflectance provides a linear relationship with the concentration of the dye on a fibre. The simplest application of the $(K/S)_\lambda$ function is to assume depth ($D_{K/S}$) is proportional to

$(K/S)_{\lambda(R\min)}$ and is given by equation 3.2 :

$$(K/S)_\lambda = \frac{(1-R_\lambda)^2}{2R_\lambda} \qquad \text{Equation 3.2}$$

$$D_{K/S} = k(K/S)_{\lambda(R\min)} \qquad \text{Equation 3.3}$$

This method is also restricted to comparing the depth of similar colourants. In order to take into account dissimilar colours the whole of the visible spectrum should be taken into account and a summation method is used.

### *3.3.2 (K/S) Summation Methods*

In order to compare dissimilar dyes it is necessary to take whole visible spectrum into account. In the simplest way depth based on the summation method can be evaluated as the sum of $(K/S)_\lambda$ values and is given in equation 3.4:

$$D_{\sum(K/S)} = k\sum_{400}^{700}(K/S)_\lambda \qquad \text{Equation 3.4}$$

This summation method does not include the possible variations caused by the observer and the light source. It only considers the reflectance of the dyed material.

Garland introduced the concept of Complementary Tristimulus Colorimerty [58]. This Colorimetry provided a method to determine numerically the concentrations of

colourants in solution by calculating their tristimulus values in absorbance mode. Complementary tristimulus values for this system are defined by:

$$X' = \sum_{400}^{700} FE_c \bar{x} \Delta\lambda$$

$$Y' = \sum_{400}^{700} FE_c \bar{y} \Delta\lambda \qquad \text{Equation 3.5}$$

$$Z' = \sum FE_c \bar{z} \Delta\lambda$$

F is the photometric function based on measured absorbance values. Absorbance value is that amount of light which is not transmitted. It varies from 0 -2. If A =0 no light is absorbed and with A =2 almost 99% of the light is being absorbed. $E_c$ is the spectral energy distribution of illuminant, $\bar{x}, \bar{y}, \bar{z}$ are the colour matching functions and $\Delta\lambda$ is a 5nm wavelength interval over the visible spectrum from 380-770nm. The complementary tristimulus values are used as decimal fractions where Y'=1.00.
Since X', Y', Z' are determined from absorbance measurements, they are proportional to the concentration of the dye in solution and so also is their sum. This sum can be used to determine the Pseudo-absorptivity according to the equation 3.6:

$$A_{vis} = (X' + Y' + Z') \,/\, bc \qquad \text{Equation 3.6}$$

Where $A_{vis}$ is the absorptivity across the visible spectrum, b is the path length of the sample in centimetres and c is the colourant concentration in g/l.

the chromaticity co-ordinates of the sample are shown in equation 3.7:

$$x' = X' \,/\, (X' + Y' + Z')$$

$$y' = Y' \,/\, (X' + Y' + Z') \qquad \text{Equation 3.7}$$

Shade and strength of the dye can be measured in a complementary colour space with three dimensions x' ,y' and $A_{vis}$ . The purity or percent active ingredient (%AI) of a sample is determined by:

$$\%\,AI = A_{vis.sample} \times 100 / A_{vis.100\,\%} \qquad \text{Equation 3.8}$$

The brightness–dullness influence on $A_{vis}$ can easily be put to use as an index of brightness. This index of brightness factor ($B_t$), is obtained by dividing $A_{max}$ by $A_{vis}$ . $A_{max}$ is the absorbance at the point of maximum absorption. Since B is independent of concentration, it can be determined as:

$$B = A_{max} / A_{vis} = A / (X' + Y' + Z') \qquad \text{Equation 3.9}$$

B values range from 0.33 for a neutral black to about 2.00 for a very bright dye.
Garland suggested that the complementary tristimulus values can be calculated by using a Kubelka-Munk type functions, and that the sum of these three values is proportional to the depth of dyeing. This suggestion was adopted by Derbyshire and Marshall [59] which resulted in a new formula to determine depth of a dyeing known as Integ, which is an integration of the weighted function of a measured reflectance values of a dyeing throughout the range of the visible wavelengths and is given in equation 3.10:

$$INTEG = \sum_{400}^{700} I_\lambda . F_\lambda . (\bar{x}_\lambda + \bar{y}_\lambda + \bar{z}_\lambda) \qquad \text{Equation 3.10}$$

Where

$$F_\lambda = \frac{[1-(R_\lambda - R_\circ)]^2}{2(R_\lambda - R_\circ)} - \frac{[1-(R_S - R_\circ)]^2}{2(R_S - R_\circ)} \qquad \text{Equation 3.11}$$

$R_\lambda$ is the fractional reflectance of the dyeing at wavelength λ, $R_s$ is the fractional reflectance of the un-dyed substrate at that wavelength and $R_o$ is a small constant.
$I_\lambda$ is the spectral energy distribution of illuminant C and $\bar{x}_\lambda, \bar{y}_\lambda, \bar{z}_\lambda$ are the colour matching functions based on $2^o$ standard observer. This Integ value is proportional to the depth of the dyeing. It provides a very convenient and quantitative comparison for evaluating depth, even when colours differ very widely.

Another Integ method has been adopted by six of the major Western European dyestuff manufacturers [60]. It is based on reflectance measurements on textile dyeings produced under prescribed conditions. Colour strength values are calculated using the Kubelka-Munk equation, as shown in equation 3.12, which defines the relationship between measured reflectance values, R, and dye concentration:

$$K/S = \frac{(1-R)^2}{2R} = Ac \qquad \text{Equation 3.12}$$

A = proportionality factor

Colour strength is taken as the sum of the weighted K/S values in the visible region of the spectrum. It is calculated as

$$f_k = \sum_{400}^{700} (K/S)_\lambda (\bar{x}_{10\lambda} + \bar{y}_{10\lambda} + \bar{z}_{10\lambda}) \qquad \text{Equation 3.13}$$

In this case illuminant weighing is omitted.

In this thesis, equation 3.13 has been used, but with the weighting for illuminant D65 included.

### *3.3.3 Methods based on Colour Order Systems and Colour Spaces*

One of these methods is to determine the colour difference between the Hilfstypen colours and the white plane in the equal depth space. Since all of the Hilfstypen colours have equal visual depth, they should all yield the same colour difference values. Godlove [61] devised a formula based on the above concept to calculate the depth value, A, of 18 samples of the 1/1 standard depth series,i.e.,

$$A = S + 0.025C(\Delta H_{10PB}) \qquad \text{Equation 3.14}$$

Where

$$S = (16V^2 + C^2)^{1/2} \qquad \text{Equation 3.15}$$

V=10-V, where V is the Munsell value and C is the Munsell chroma. $\Delta H_{10PB}$ is the least number of hue steps on the Munsell 100 hue scale by which the hue differs from 10PB. The formula does not produce very uniform results for 1/1 standard depth series and is unable to perform consistently in other areas of depth.

Rabe & Koch in 1957 proposed a colour difference formula based upon the DIN colour order system [62]. The work was focussed on the 1/1SD surfaces and used three

parameters; hue (T), saturation (S) and darkness (d). Darkness and depth were defined by the equations 3.16 and 3.17:

$$d = [10 - 6.1723\log_{10}(40.7\ Y/Y_o + 1)] \quad \text{Equation 3.16}$$

$$D_{RK} = S\ (10 - 1.2d) / 9 + 1.06d \quad \text{Equation 3.17}$$

'S' is a function of the distance of the specimen from the achromatic point in the CIE chromaticity diagram, Y is the CIE Y value of the specimen and $Y_o$ that of the optical colour stimulus of the same hue (T). This formula was used in developing the ratios of SD other than 1/1.

Gall & Riedel pointed out that the Rabe and Koch formula does not perform well for visually equal depth colours of the lower DIN-S than the majority of those in the 1/1SD series [63]. They proposed another formula to calculate depth (DGR) based on the visual assessment data of lacquered specimens. This is given in equation 3.18:

$$D_{GR} = Y^{½}\ (10 - sa_{\Phi}) \quad \text{Equation 3.18}$$

Where Y is the CIE Y and's' is calculated as

$$s = 10\ [(x - x_n)^2 + (y - y_n)^2]^{1/2} \quad \text{Equation 3.19}$$

The terms x and y are the CIE chromaticity co-ordinates of the specimen under the given illuminant and observer, and $x_n$ and $y_n$ are the achromatic points.

In 1985, Christ devised an algorithm based on CIE L*, C*, h coordinates to define 1/1 standard depth [64] and is given in equation 3.20:

$$L_{SD} = 20.4 + C^*_{ab,B} P + 6^{-C^* ab, p^{P/6}} \quad \text{Equation 3.20}$$

$$P = \sum_{m=0}^{3} K_{n,m} (h_{ab,B} - h_n)^m \quad \text{Equation 3.21}$$

Where C* is the chroma, h is the hue, $h_n \leq h_{ab,B} \leq h_{n+1}$. The values of $K_{n,m}$ are obtained, for each limiting $h_n$, from Table 3.1.

Table 3.1: Limiting angles ($h_0$) and coefficient (Km,n) of the polynomial P

| n | $h_n$ | $K_{n,0}$ | $K_{n,1}$ | $K_{n,2}$ | $K_{n,3}$ |
|---|---|---|---|---|---|
| 1 | 0 | $3.27*10^{-1}$ | $1.73*10^{-3}$ | $-2.13*10^{-5}$ | $8.68*10^{-7}$ |
| 2 | 52 | $4.81*10^{-1}$ | $6.57*10^{-3}$ | $1.14*10^{-4}$ | $-3.49*10^{-6}$ |
| 3 | 79 | $6.73*10^{-1}$ | $5.08*10^{-3}$ | $-1.69*10^{-4}$ | $1.06*10^{-6}$ |
| 4 | 135 | $6.14*10^{-1}$ | $-3.83*10^{-3}$ | $1.02*10^{-5}$ | $6.40*10^{-8}$ |
| 5 | 203 | $4.21*10^{-1}$ | $-1.56*10^{-3}$ | $2.32*10^{-5}$ | $-4.82*10^{-7}$ |
| 6 | 267 | $2.90*10^{-1}$ | $-4.51*10^{-3}$ | $-6.93*10^{-5}$ | $2.42*10^{-6}$ |
| 7 | 302 | $1.51*10^{-1}$ | $-4.40*10^{-4}$ | $1.85*10^{-4}$ | $-2.29*10^{-6}$ |
| 8 | 340 | $2.76*10^{-1}$ | $3.69*10^{-3}$ | $-7.66*10^{-5}$ | $9.22*10^{-7}$ |

The ISO adopted the Christ formula in 1995 into ISO 105 AO6, "A method for the instrumental determination of 1/1 standard depth" [12, 13]. It defines 1/1 standard depth numerically, but its error is significantly more than 10%. Further the algorithm does not apply to other levels of depth.

Sato in 1995 proposed a numerical method of computing the dyers depth and brightness from CIEL*C*h values of a coloured sample [65, 66]. He proposed equations 3.22 and 3.23 to compute the depth and brightness of the dyed sample:

$$D = (100 - L^*) + (0.1 + \Delta h_{290}/360)(1 - \Delta h_{290}/360)C^* \qquad \text{Equation 3.22}$$

$$B_D = 2000C^*(1 - \Delta h_{290}/360)/(L^*(100 - L^*)) \qquad \text{Equation 3.23}$$

Where,

- D and $B_D$ are the Sato depth and brightness
- $L^*$ and $C^*$ are CIELAB metric lightness and chroma respectively
- $\Delta h_{290}$ is the hue angle difference from h = 290.

Hawkyard and Kelly in 2000 proposed a method of assessing the standard depth of the dyed sample by calculating the lightness of the dyed material by the following relationship [ 67, 68]

$$Y = (4.480E - 18x^9) - (7.778E - 15x^8) + (5.616E - 12x^7) - (2.166e - 9x^6) + (4.792E - 7x^5) - (6.042E - 5x^4) + 0.00402x^3 - 0.11794x^2 + 1.284x + 46.132$$

Equation 3.24

Where Y = L* at the position of $C^*_{max}$ and x = $h^\circ_{ab}$

They found that the lightness of a dyed sample is independent of chroma but depends upon hue of the dyed sample at $C^*_{max}$ . However, the Hawkyard method for assessment of standard depth was not verified by any visual assessments and also the established fact that lightness and chroma vary with varying concentration of the colourant was not taken into account.

Smith [54, 69] reported a method of partitioning colour differences, in terms of dyers' depth, brightness and hue variables, developed initially by Cooper. This is the DBH model, and is based on the parabolic modeling of the depth locus of dyeings in the $L^*C^*$ plane, with three distinct points: standard or batch, vertex and the white point. This DBH model used $L^*$, $C^*$ and $h^\circ_{ab}$ of the standard and the batch to compute the differences in depth, brightness and hue of a batch from the standard and expressed as $\Delta D$, $\Delta B$, and $\Delta H$.

### 3.4 The WSI Algorithm

The aim of the WSI algorithm was to define numerically in CIELAB space the standard depth surfaces. The algorithm was based on mapping in the CIELAB colour space planes of equal depth surfaces derived from visual assessments. These equi-depth surfaces were defined by the variation of lightness with hue and chroma. The overall mapping revealed that surfaces of equal visual depth, established in the CIELAB colour space are not regular in shape [14, 15, 70, 71]. The higher the depth (2/1) the less the samples of the same visual depth vary in their lightness, so the flatter the surface in the L*C* plane. Conversely the lower the depth (1/25) the more curved is the surface. Also the surface tends to be more curved in the yellow hues.

The algorithm was developed to indicate whether the particular dyed sample, of given L* C* h values, corresponded to one of the six standard depths, 2/1, 1/1, 1/3, 1/6, 1/12, and 1/25. The conic formula as shown in equation 3.25 was found to be most suitable to define the equi - depth surfaces numerically. The developed algorithm had two components:

- A mathematical function which computes the $L^*$ values as a function of the chroma
- A mathematical function which allows the conic constants to be determined in computing the L* values for any hue angle

The conic equation which fits best is given in equation 3.25:

$$k_1 L^{*2} + k_2 C^{*2} + k_3 L^* + k_4 L^* C^* + k_5 C^* + k_6 = 0 \qquad \text{Equation 3.25}$$

Where $k_1$ to $k_6$ are the conic constants and $L^*$ & $C^*$ are the CIELAB metric lightness and chroma respectively. This equation was converted to the quadratic form for the ease of solving it:

$$L^*_{SD} = \frac{-b \pm \sqrt{b^2 - 4ac}}{2a} \qquad \text{Equation 3.26}$$

where

$$a = k_1$$
$$b = k_3 + k_4 C^*$$
$$c = k_2 C^{*2} + k_5 C^* + k_6$$

In order to apply equation 3.25, it was firstly necessary to determine the values of the conic constants $k_{1\text{-}6}$ to use. The values of these constants depend on the standard depth of interest, and also on hue angle of sample. The general cosine formula (equation 3.27) was applied to compute the conic constants against any hue angle.

$$k_i = l_1\cos(h+m_1)+l_2\cos(h+m_2)+l_3\cos(h+m_3)\ l_4\cos(h+m_4)\ l_5\cos(h+m_5) \qquad \text{Equation 3.27}$$

Where i = 1 to 6. The formulae used to compute the conic constants at various depth levels are shown in Table 3.2:

Table 3.2: Formulae to determine the conic constants by WSI method

**2/1**

$k_1 = 0.043$

$k_2 = -0.002+0.0017\cos(2\,h^\circ_{ab} +19) +0.0001\cos(4\,h^\circ_{ab})$

$k_3 = -1$

$k_4 = -0.008\cos(h^\circ_{ab} -87)-0.003\cos(3\,h^\circ_{ab} -82)$

$k_5 = 0.1435\cos(h^\circ_{ab} -79) +0.0662\cos(3\,h^\circ_{ab} -83)$

$k_6 = 1.151$

**1/1**

$k_1 = 0.03$

$k_2 = -0.0044+0.0018\cos(2\,h^\circ_{ab} +45)$

$k_3 = -1$

$k_4 = -0.0079\cos(h^\circ_{ab} -95)-0.0025\cos(3\,h^\circ_{ab} -49)$

$k_5 = 0.1485\cos(h^\circ_{ab} - 72) + 0.0914\cos(3\,h^\circ_{ab} - 62)$

$k_6 = 2.907$

**1/3**

$k_1 = 0.0195$

$k_2 = -0.0049 + 0.0011\cos(2\,h^\circ_{ab} + 68)$

$k_3 = -1$

$k_4 = -0.0072\cos(h^\circ_{ab} - 87) - 0.0023\cos(3\,h^\circ_{ab} - 31)$

$k_5 = 0.2234\cos(h^\circ_{ab} - 77) + 0.1218\cos(3\,h^\circ_{ab} - 29)$

$k_6 = 4.892$

**1/6**

$k_1 = 0.0167$

$k_2 = -0.006 + 0.0015\cos(2\,h^\circ_{ab} + 121) + 0.0002\cos(4\,h^\circ_{ab})$

$k_3 = -1$

$k_4 = -0.0068\cos(h^\circ_{ab} - 84) - 0.0029\cos(3\,h^\circ_{ab} - 12)$

$k_5 = 0.2735\cos(h^\circ_{ab} - 75) + 0.1611\cos(3\,h^\circ_{ab} - 14)$

$k_6 = 5.691$

**1/12**

$k_1 = 0.0142$

$k_2 = -0.0091 + 0.009\cos(2\,h^\circ_{ab} + 124) - 0.0004\cos(4\,h^\circ_{ab})$

$k_3 = -1$

$k_4 = -0.0068\cos(h^\circ_{ab} - 81) - 0.0033\cos(3\,h^\circ_{ab} + 4)$

$k_5 = 0.3424\cos(h^\circ_{ab} - 70) + 0.2203\cos(3\,h^\circ_{ab} + 2)$

$k_6 = 7.166$

**1/25**

$k_1 = 0.0128$

$k_2 = -0.013 + 0.0029\cos(2\,h^\circ_{ab} + 149) - 0.0005\cos(4\,h^\circ_{ab})$

$k_3 = -1$

$k_4 = -0.0063\cos(h^\circ_{ab} - 78) - 0.0039\cos(3\,h^\circ_{ab} + 6)$

$k_5 = 0.3716\cos(h^\circ_{ab} - 69) + 0.2727\cos(3\,h^\circ_{ab} + 9)$

$k_6 = 8.136$

The resulting algorithm is structured so that it determines the $L^*$ value that a colour of any given hue and chroma should possess for it to correspond to one of the levels of standard depth. It is assumed that the colour can be said to be of the standard depth selected if the L* of the dyed sample and $L^*_{SD}$ as calculated from the proposed formula are sensibly close. The WSI algorithm and Christ formula has a good agreement for 1/1 standard depth. This algorithm is currently the subject of a round-robin trial as a pre-curser to being adopted as an ISO standard.

# CHAPTER 4: METHODOLOGIES AND CALCULATIONS

The conversion of the colorimetric variables of colour difference ($\Delta L^*$, $\Delta C^*$, $\Delta H^*$) to dyers' variables of colour difference is not straightforward. The Hilfstyphen samples do not define standard depth surfaces numerically and they are not exactly uniform in depth. Further, the Christ formula, which is a current standard for defining 1/1 standard depth surface numerically, is limited to one surface only. Six such equi-depth surfaces, mapped into the CIELAB colour space, have been reported as WSI depth surfaces [15]. The WSI depth algorithm was in reasonably good agreement to the Christ formula for 1/1 depth level, except for yellow and orange samples, for which it is generally accepted that the Hilfstyphen samples are erroneous. These six WSI depth surfaces were the milestones for the development of an algorithm to convert colorimetric colour differences expressed as $\Delta L^*$, $\Delta C^*$, $\Delta H^*$ into dyer's colour differences expressed as $\Delta D$, $\Delta B$, & $\Delta H$.

Two cases were identified to develop an algorithm, called the WSF algorithm, to predict the dyers' variables of differences in depth, brightness and hue from the spectral reflectance values of a dyed pair. These are:

- Determination of difference in depth and brightness between a batch and a standard having the same hue;
- Determination of the difference in depth and brightness between a batch and a standard having different hues.

## 4.1 Methodology for determination of difference in depth and brightness between the standard and the batch having the same hue

This applies to the rare situation where the standard and the batch have exactly the same hue. The methodology adopted to develop this algorithm was to generate, using the WSI algorithm, the equi depth line in the $L^*$ $C^*$ plane that passes through the $L^*$ $C^*$ coordinates of the standard. The %R of the batch was measured and converted to K/S values. These K/S values of the batch are then either increased or decreased by changing the concentration of the dye, until its depth becomes equal to that of standard (see Section 4.3.2). The linear distances between the batch and the standard were calculated; shown in Figure 4.1, to give the differences in depth and brightness between the standard and the batch.

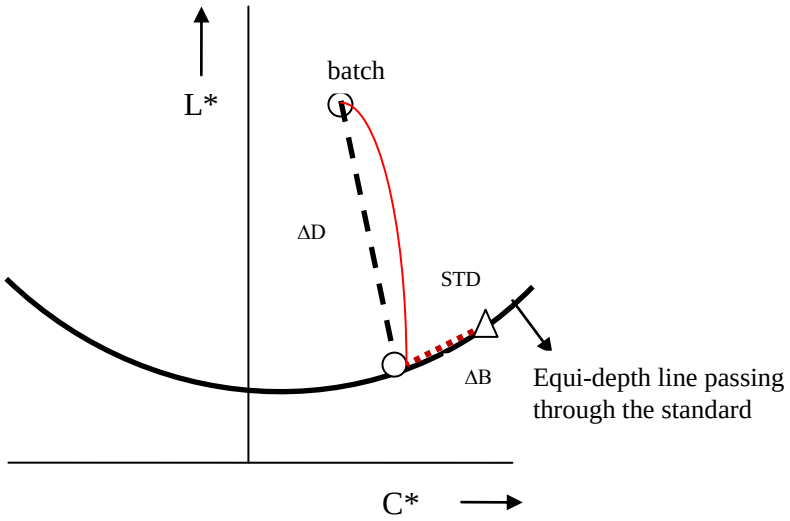


Figur 4.1: Graphical representation of difference in depth and brightness from the $L^*$ $C^*$ coordinates of the standard and the batch

## 4.2 Methodology for the determination of the difference in depth and brightness between a batch and a standard having different hues

Most often the hue angle of the batch is not the same as that of the standard. It is not possible in these situations to project the batch to the standard plane as the dyer's concept of brightness varies with the hue angle. The methodology adopted to develop the algorithm for the pair of dyeings with no hue difference was applied in a similar way with the exception of hue correction to the batch. This hue correction of the batch was performed after increasing or decreasing the K/S values of the batch until its depth becomes equal to that of standard. The build-up behaviour of the dyestuff upto the maximum chroma possible round the hue circle has to be taken into account for this purpose. The chroma of the batch was adjusted by using this chroma boundary, as shown in Figure 4.2:

Adjusted $C^*_{batch}$ = (g/h) * $C^*_1$ Equation 4.1

g = $C^*_{max}$ of the batch for the given hue angle of the batch

h = $C^*_{max}$ of the standard for the given hue angle of the standard

$C^*_1$= chroma of the batch when it intersect the standard depth surface

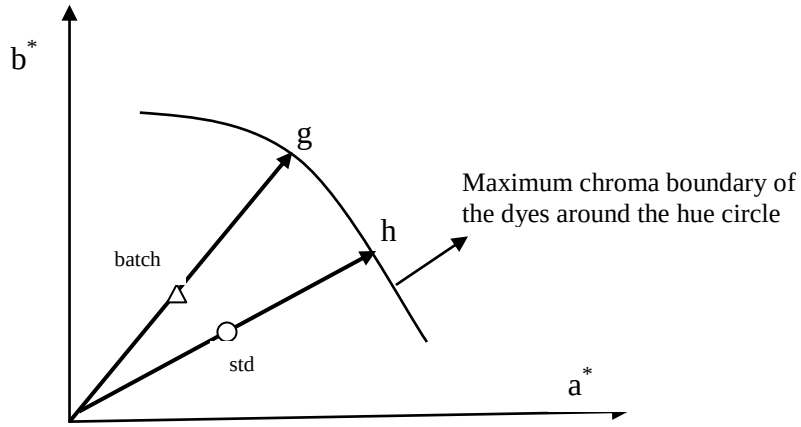


Figur 4.2: Maximum chroma boundary and hue correction of the batch

The linear distances between the batch and the standard, shown in Figure 4.1, give the differences in depth and brightness between the standard and the batch in a similar way as for case (A).

### 4.3 Developmental stages of the WSF algorithm

The following three stages were involved in the development of the WSF algorithm:

1) Generation of an equi-depth line for the standard
2) Determination of the strength of the batch to intersect the equi-depth line of the standard
3) Determination of differences in depth, brightness and hue between the standard and the batch

Each of the three stages required careful consideration and an explanation of the procedures adopted is described below.

#### *4.3.1Generation of an equi-depth line for the standard*

The pre-requisite of this WSF algorithm is the six depth surfaces defined by the WSI algorithm [15]. If the standard happens to lie on one of the defined surfaces, equation for that surface will serve as equi-depth line of the standard. However it is most unlikely that the standard of a pair of colours will lie on one of these six defined standard depth surfaces. It is most likely to lie either between two of the established surfaces, or above or below the 1/25 or 2/1 depth levels respectively.

In such cases it is necessary to generate the equation of the equi-depth line which passes through the standard, as shown in Figure 4.3. In order to generate this equi-depth line, the $L^*$, $a^*$, $b^*$, $C^*$, and $h^\circ_{ab}$ values of the standard are calculated from the measured reflectance values and the standard depth surfaces lying immediately above and below the standard are then found. The weighted conic constants ($k_1$ to $k_6$) are determined by interpolation from the values of the constants for these two surfaces to generate the equi-depth line passing through the standard.

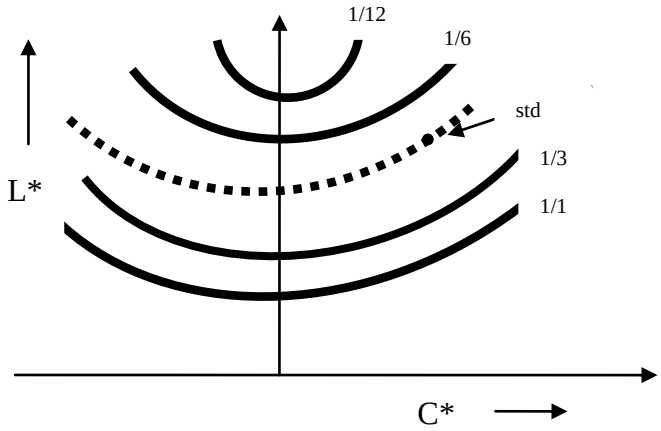


Figure 4.3: Equi depth line passing through the standard, enclosed by two pre-defined standard depth surfaces

The conic constants of the equation necessary to generate the equi-depth line are calculated by determining the Integ of the surfaces lying immediately above and below the standard, and from the Integ of the standard. The average Integ values of the Hilfstyphen samples at different levels of depth are shown in Table 4.1**.** The average Integ values of surfaces lying immediately above and below the standard are found from this table:

Table 4.1: Average Integ values of Hilfstyphen samples

| Standard depth surface | Average Integ |
|---|---|
| 2/1 | 39.42 |
| 1/1 | 22.01 |
| 1/3 | 8.1 |
| 1/6 | 4.42 |
| 1/12 | 2.46 |
| 1/25 | 1.48 |

The Integ of the standard is determined from the equation 3.10:

$$INTEG = \sum_{400}^{700} E_\lambda .(K/S)_\lambda .(\bar{x}_\lambda + \bar{y}_\lambda + \bar{z}_\lambda)$$ Equation 3.10

Where:

$$K/S = \frac{(1-R_\lambda)^2}{2R_\lambda}$$ Equation 3.11

$E_\lambda$ = Relative energy of the illuminant (D65)

$R_\lambda$ is the fractional reflectance of the dyeing at wavelength λ,

The weighted conic constants are calculated by the equation 4.2:

$$k_{std} = k_{close\ to\ std} + ((B/A)* (k_{below} - k_{above}))$$ Equation 4.2

Where

A = difference in the Integ values of the depth surfaces lying immediately above and below the standard

B = difference in the Integ values of the standard to the depth surface lying closer to the standard

While working with Integ it was observed that ΔL > 0.5 in most of the cases. ΔL is the difference between the lightness of the standard as measured on the spectrophotometer and the lightness predicted from the WSI equation of the standard depth line. It was realized that instead of basing the interpolation on Integ, it is better to use lightness, to determine the weighted conic constants. The methodology adopted to calculate the weighted conic constants using lightness of the standard is described below:

The lightness of the standard at all the six established surfaces for the hue and chroma of the standard is calculated. These lightness values are closely examined to find which two depth surfaces lie immediately above and below the standard. This can be better understood by considering an example; let the $L^*$, $a^*$, $b^*$, $C^*$ and $h^\circ_{ab}$ of the standard be 55, 0, 25, 25, $90^0$ respectively, as computed from the reflectance values of the standard measured on a spectrophotometer. The C* and $h^\circ_{ab}$ values of the standard are entered to the WSI algorithm and the lightness values for all the six depth levels (2/1, 1/1, 1/3, 1/6, 1/12, 1/25) are calculated to be 22, 33, 48, 60, 68, 75 respectively. It is clear that standard's lightness value "55" lies between 48 and 60, derived from 1/3 and 1/6 standard depth surfaces respectively. This means the standard depth surfaces lying immediately below and above the standard are 1/3 and 1/6. The conic constants of the line passing through the standard are then calculated using Equation 4.3:

$k_{1,std} = k_{1,below} + \Delta k_1$

$\Delta k_1 = \Delta L_1/\Delta L_t \times \Delta k_t$ Equation 4.3

$\Delta k_t = k_{above} - k_{below}$

$\Delta L_t = L_{above} - L_{below}$

$\Delta L_1 = L_{std} - L_{below}$

$\Delta k_1$ is the factor by which the conic constant $k_1$, of the standard depth surface lying below the standard is adjusted to give the $k_1$ conic constant for the depth surface passing through the standard. The same procedure is used for calculating all of the conic constants ($k_1$ to $k_6$) for the standard.

### *4.3.2 Determination of strength of a batch to intersect the equi-depth line of a standard*

The %R values of the batch are measured and converted to the corresponding K/S values using equation 3.11. Assuming a nominal concentration of the batch of 1%, its concentration is adjusted by a factor as shown in Equation 4.4:

$(K/S)_{batch,adj} = (K/S)_{batch,initial} \times$ conc factor Equation 4.4

$(K/S)_{batch,initial}$ is the K/S at the nominal concentration. The $(K/S)_{batch,adj}$ values are converted to %R values and thence to XYZ and $L^*_{batch,adj}$, $a^*_{batch,adj}$, $C^*_{batch,adj}$, $h_{batch,adj}$ values. The concentration factor is gradually altered until the intersection point on the equi-depth line for the standard is reached. Matlab *software for engineers* was used for this iteration. The Matlab iterative programs are given in Appendices A1 & A2. This iterative procedure is performed with the condition that the difference between the lightness of the batch and the lightness predicted by the equation of the standard depth line is less than 0.1 ($\Delta L^* \leq 0.1$), as shown in Figure 4.1. During this iteration, the $C^*$ value of the batch, as well as the $L^*$ value, changes with concentration. It is therefore necessary to determine the $L^*$ of the equi-depth line at each $C^*$ value of the batch, to determine whether the batch has intersected with the equi-depth line of the standard. For this purpose the WSI algorithm is used as given in (Equation 3.26):

$\Delta L^* = (L^*_{WSI} - L^*_{batch}) < 0.1$

$$L^*_{WSI} = \frac{-b \pm \sqrt{b^2 - 4ac}}{2a}$$ Equation 3.26

Where:

$a = k_1$

$b = k_3 + k_4C^*$

$c = k_2C^{*2} + k_5C^* + k_6$

$L^*_{batch}$ is the lightness of the batch calculated from K/S at different concentrations. $L^*_{WSI}$ is the lightness on the equi-depth line corresponding to the C* of the batch, calculated through the WSI algorithm for every change in concentration. $k_1$- $k_6$ are the conic constants for the equi-depth line for a standard, which can be calculated by the procedure described above.

### *4.3.3 Determination of difference in depth, brightness and hue of standard and batch & its verbal description*

The difference in depth between the standard and the batch is calculated as the linear distance from the initial position of a batch to the position at which it intersects the equi-depth line for the standard as illustrated in Figure 4.1. The batch is stronger if the concentration of the batch has to be lowered from nominal concentration (1.00%) to move it towards the equi-depth surface of the standard in which case a positive sign is assigned to ΔD, and vice versa:

$$\Delta D = \sqrt{(C^*_{batch,final} - C^*_{batch,initial})^2 + (L^*_{batch,final} - L^*_{batch,initial})^2} \qquad \text{Equation 4.5}$$

The difference in brightness is calculated as the linear distance between the location of the batch where it intersects the equi-depth line and the location of the standard (Figure 4.1). The batch is brighter if its chroma on the equi depth line of the standard is higher than the chroma of the standard in which case a positive sign is assigned to ΔB, and vice versa:

$$\Delta B = \sqrt{(C^*_{batch,final} - C^*_{std})^2 + (L^*_{batch,final} - L^*_{std})^2} \qquad \text{Equation 4.6}$$

These value ΔD and ΔB are scaled so the Pythagorean sum of the difference in brightness and depth become equal to the Pythagorean sum of the difference in lightness and chroma between the standard and the batch. Scaling is done by multiplying the ΔD and ΔB values with a scaling factor which can be calculated from Equation 4.7:

$$k = \sqrt{((L^*_{batch} - L^*_{std})^2 + (C^*_{batch} - C^*_{std})^2) \Big/ ((\Delta D)^2 + (\Delta B)^2)}$$

Equation 4.7

$$\Delta D_1 = k \times \Delta D$$
$$\Delta B_1 = k \times \Delta B$$

Equation 4.8

The resulting $\Delta D_1$ & $\Delta B_1$ values are the scaled differences in depth and brightness of a coloured pair. The difference in metric hue between the standard and the batch ($\Delta H^*$) as computed from the CIE colorimetric system is assumed to be same as that of the dyers' colour difference component in hue.

### 4.4 Strategy and Calculation for Hue correction of the batch

The standard and the batch do not necessarily need to be of same hue angle. In those situations it is always better to adjust the chroma of the batch by either increasing or decreasing the chroma of the batch, after carrying out any iteration to determine the intersection point of the batch on the equi-depth line of the standard. The effects of difference in hue between a batch and a standard become more prominent as the dyeings become closer to the maximum $C^*$ values (the pure colours). The build-up behaviour of a dyestuff towards the maximum chroma possible is different at different lightness levels and it also varies with hue. A complete dyestuff database of $C^*_{max}$ values throughout the colour space is therefore required at each lightness level for every hue.

For non-fluorescent colours the theoretical upper limit to $C^*$(chroma) can be determined by optimal colour stimuli [28]. Optimal colours are the colours of the imaginary objects which reflect perfectly in some parts of the spectrum and absorb completely in the remainder, so that everywhere, either R = 100 or R = 0.

The I.C.I (x, y) equivalents of the theoretical pigment maxima for 40 hues on nine Munsell value levels were published by OSA in its final report on Munsell renotation system [22] were taken as the starting point for determining the maximum chroma boundary of a colour. These values are given in Appendix B.

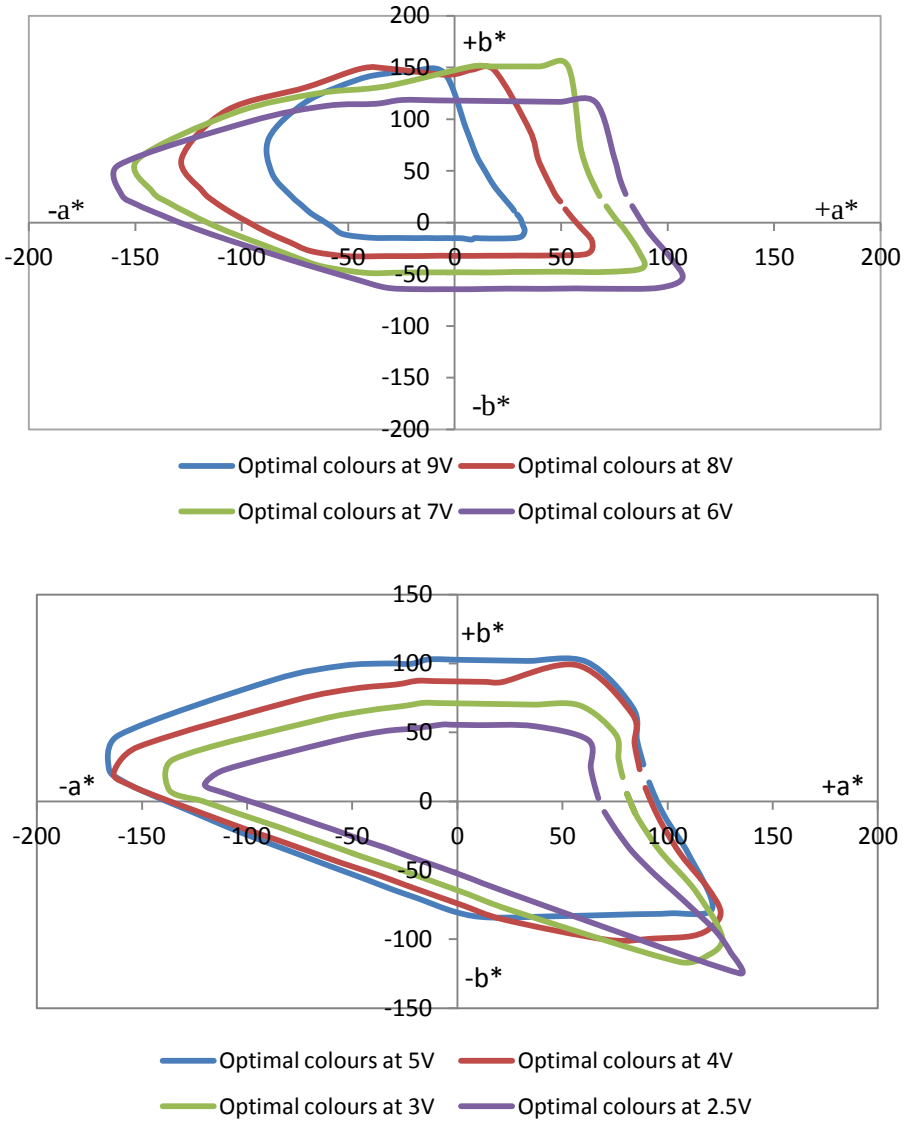


Figure 4.4: Maximum chroma values of the optimal colours at different Munsell values

These I.C.I (x, y) theoretical pigment maxima values were converted to $L^*$, $a^*$, $b^*$, $C^*$ and $h^\circ_{ab}$ values and are given in Appendices C1 – C8. These values are plotted in Figure 4.4 where it is clear that the yellow gives the highest chroma value at high Munsell value levels but low chroma at low Munsell value levels. Generally magenta colour does not give high chroma values than yellow for surface colours but in Figure 4.4 it is not the case at low Munsell value levels. This does not happen with the dyestuffs used to dye textiles. Green colours appeared as extremely pure in comparison to other colours at Munsell 7V and lower value levels, which is also not true for a green dye. It was therefore concluded that the optimal colour approach led to the results which were difficult to use. Also the data were based on illuminant C and the $2^o$ observer, so this approach was disregarded.

It was decided to use real colour data rather than imaginary colour data to build the maximum chroma boundary ($C^*_{max}$). The $C^*$ values of the Munsell coloured chips of the highest chroma, at the various Value levels were measured [72]. The chips of highest chroma for the purple region at different Munsell values are shown in Figure 4.5. However, it was found that the $C^*$ values of the chips of highest chroma do not vary uniformly around the hue circle.

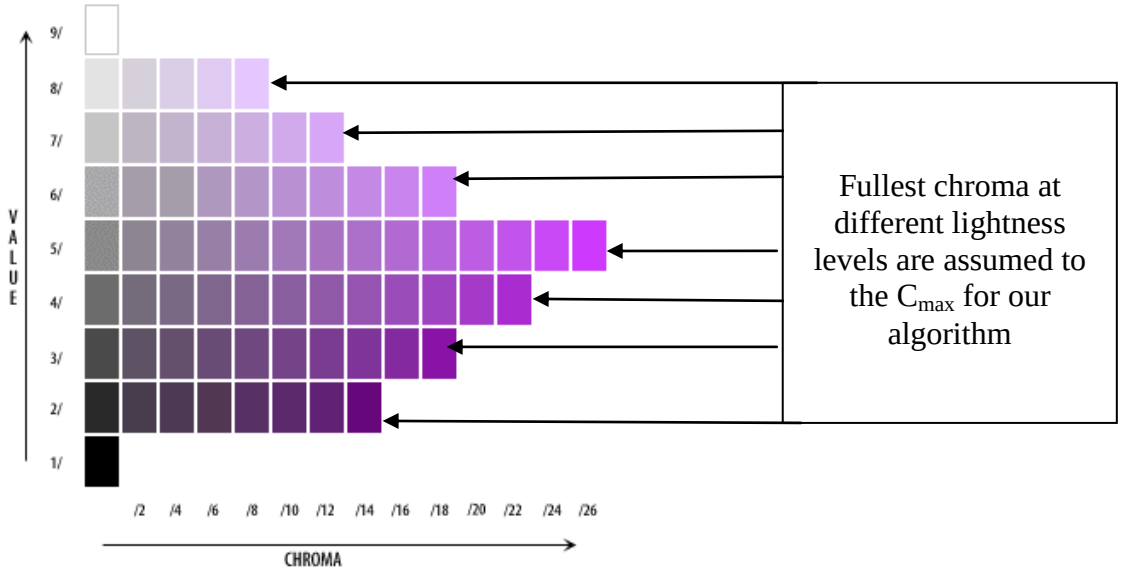


Figure 4.5: Highest Munsell Chroma for Purple region at different Munsell Values

The computed $L^*$, $a^*$, $b^*$, $C^*$, and $h^\circ_{ab}$ values of Munsell chips with highest chroma at different lightness levels around the hue circle are given in Appendices D1 – D6. These are regarded as the $C^*_{max}$ boundary and are shown in Figure 4.6.

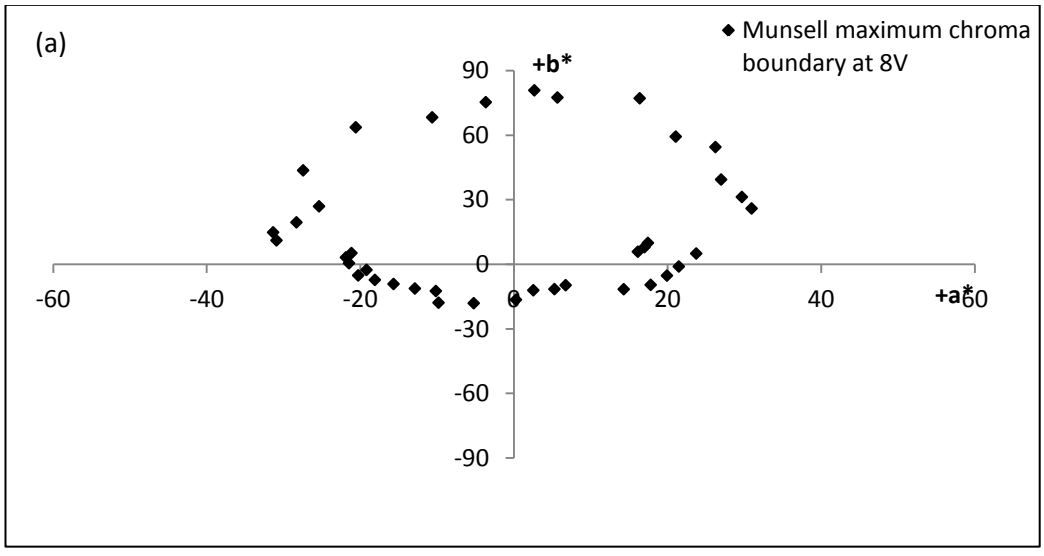

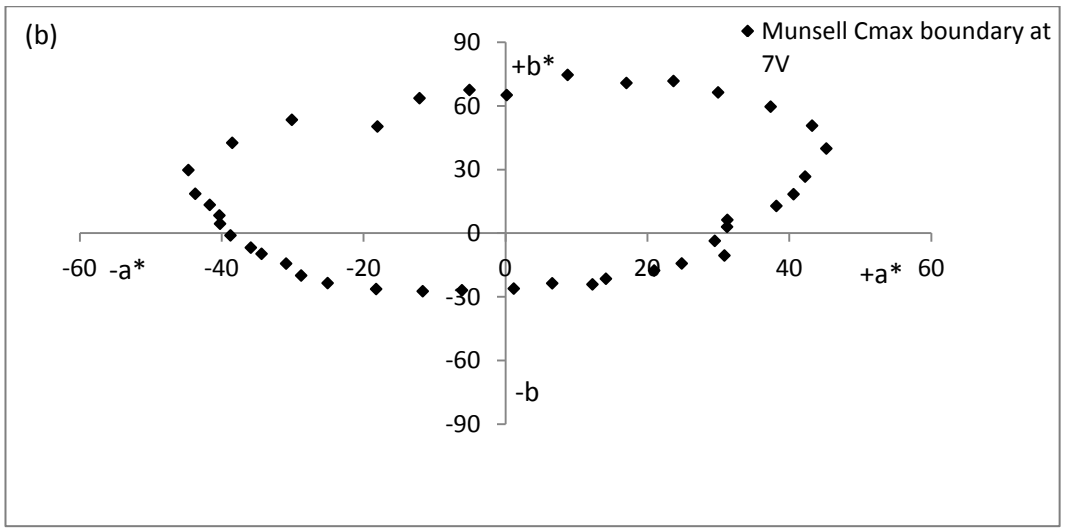
(b)
Munsell Cmax boundary at 7V
90
+b*
60
30
0
-60
-a*
-40
-20
0
20
40
+a*
60
-30
-60
-b
-90

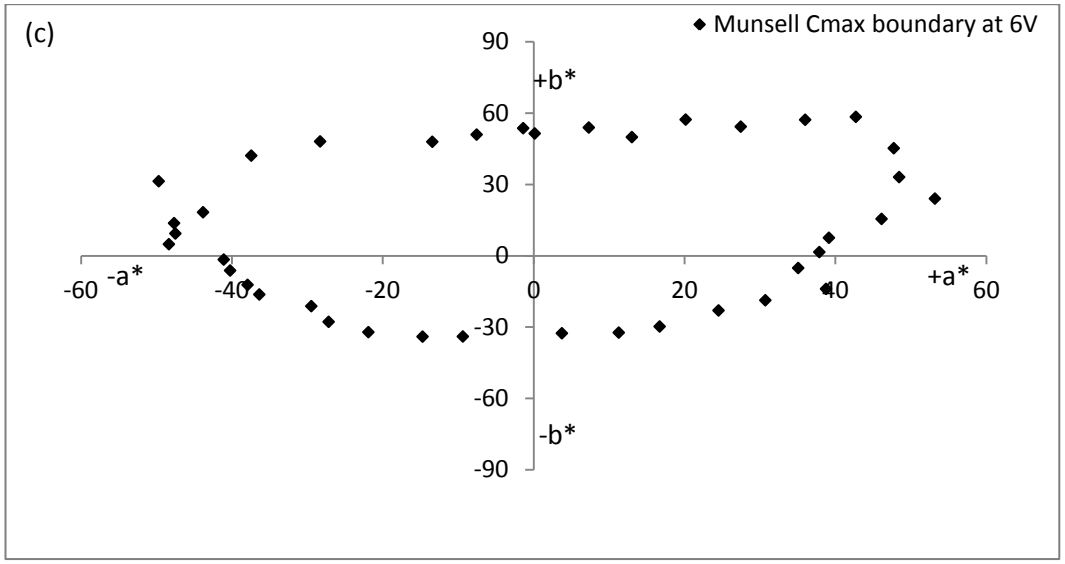
(c)
Munsell Cmax boundary at 6V
90
+b*
60
30
0
-60
-a*
-40
-20
0
20
40
+a*
60
-30
-60
-b*
-90

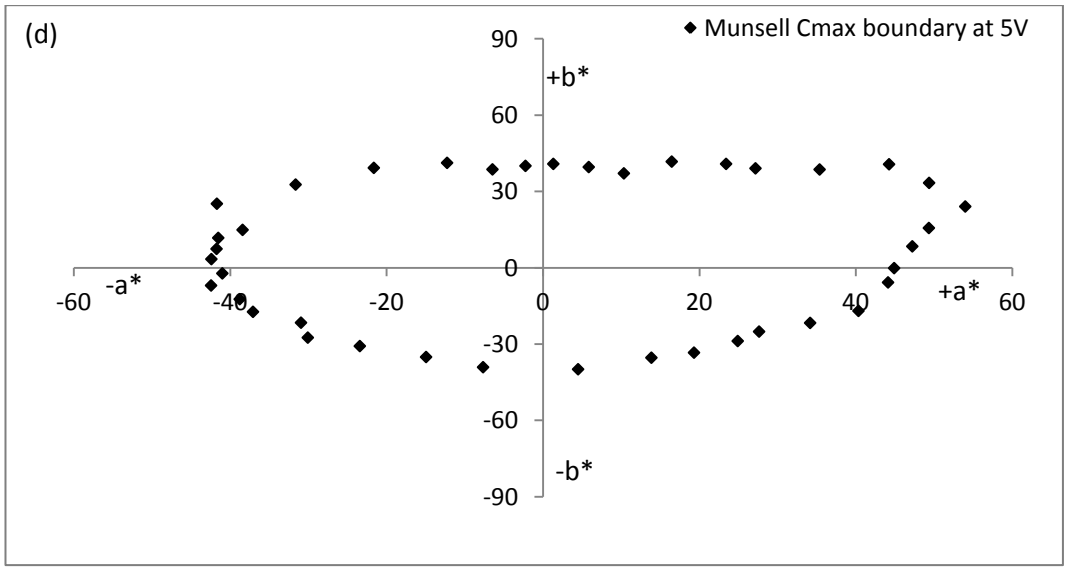
(d)
Munsell Cmax boundary at 5V
90
+b*
60
30
0
-60
-a*
-40
-20
0
20
40
+a*
60
-30
-60
-b*
-90

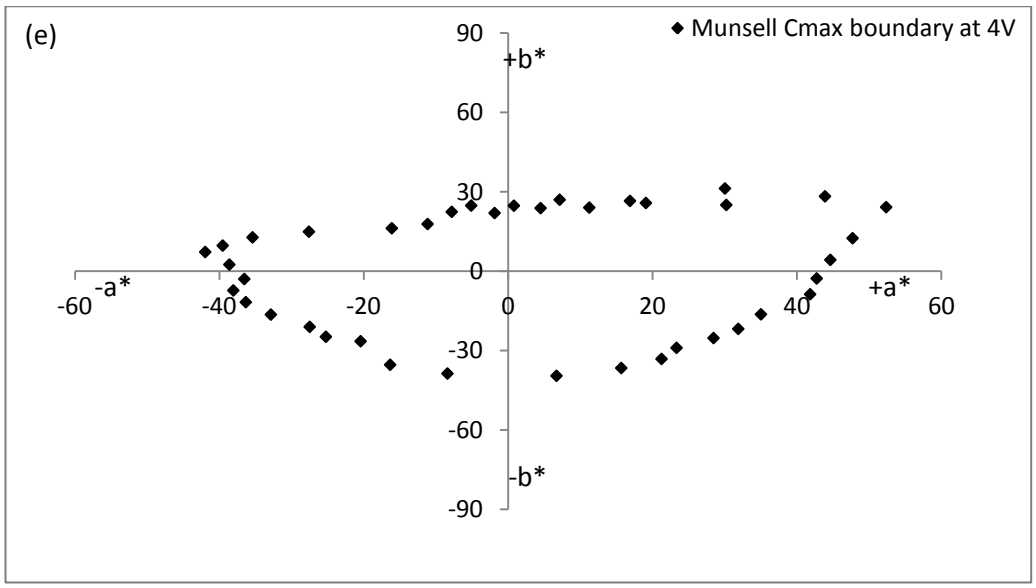


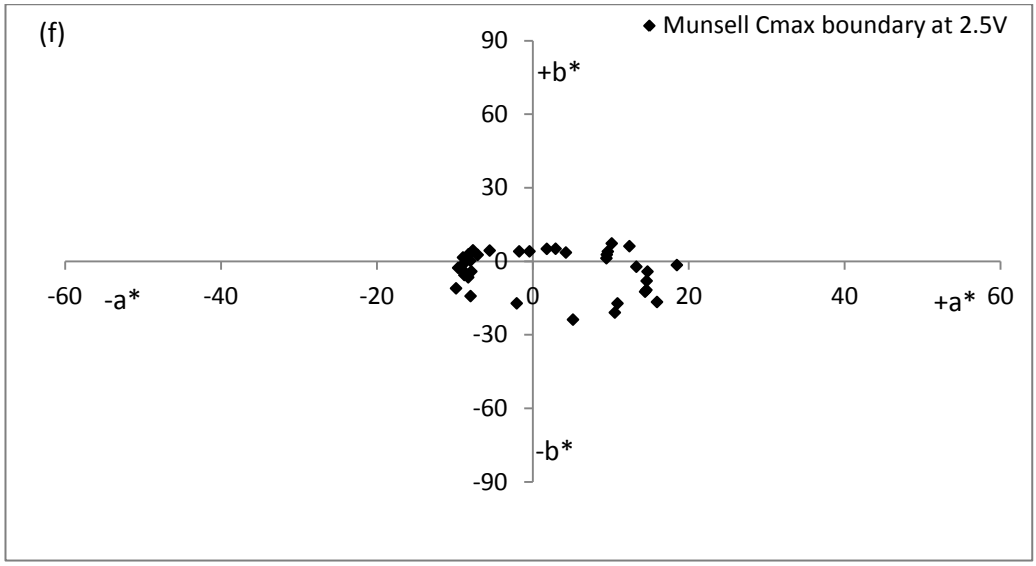


Figure 4.6 (a-f)**:** $C^*_{max}$ boundary with highest possible Munsell chroma at six different Munsell value scales

The chroma of the batch is adjusted by increasing or decreasing it by the factor calculated from Equation 4.9, after carrying out iteration to determine the strength of the batch to intersect the equi-depth line of the standard.

Adjusted factor = (g/h) Equation 4.9

Adjusted $C_{batch}$ = (g/h) * $C^*_{batch}$ Equation 4.10

g = $C^*_{max}$ of the batch for the given hue angle of the batch

h = $C^*_{max}$ of the standard for the given hue angle of the standard

Here it is worth noting that the hue at which the fullest chroma occurs varies with Munsell Value as shown in Figure 4.7 (a-f). There is a gradual shifting of the $C^*_{max}$ peak from yellow to red and a rise in $C^*_{max}$ values for green to red-purple region with a consistent trend, at all the Munsell Value scales except for 2.5V. The Munsell data at 2.5V is odd in the sense that there is an immediate shift of the $C^*_{max}$ peak from red ($10^{\circ}$) to the magenta ($325^{\circ}$) with a least $C^*_{max}$ for red to yellow green region ($20^{\circ}$-$120^{\circ}$).

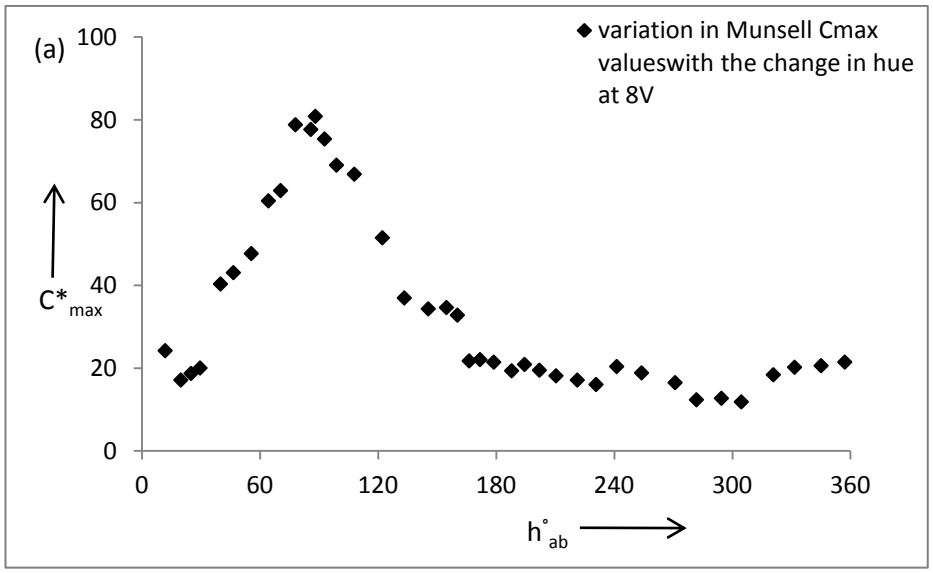


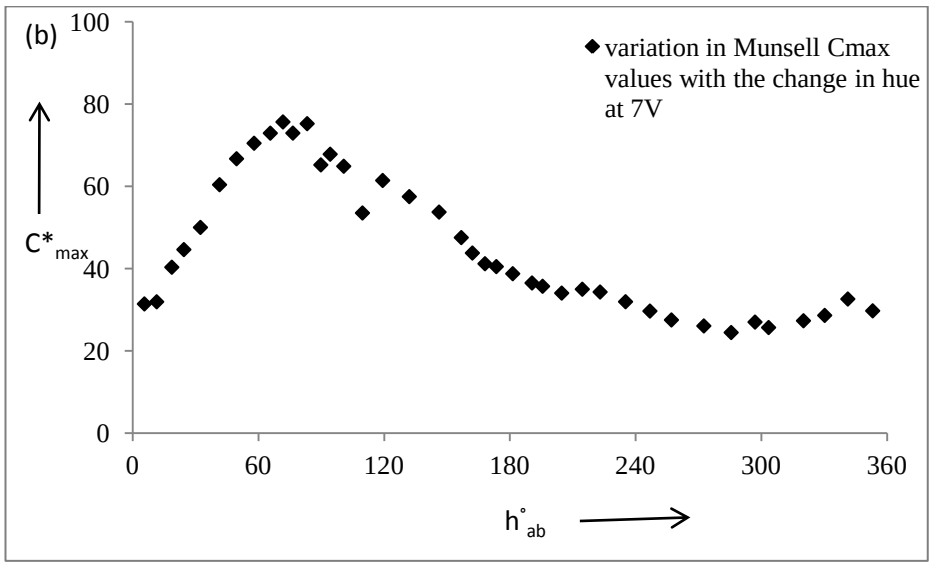

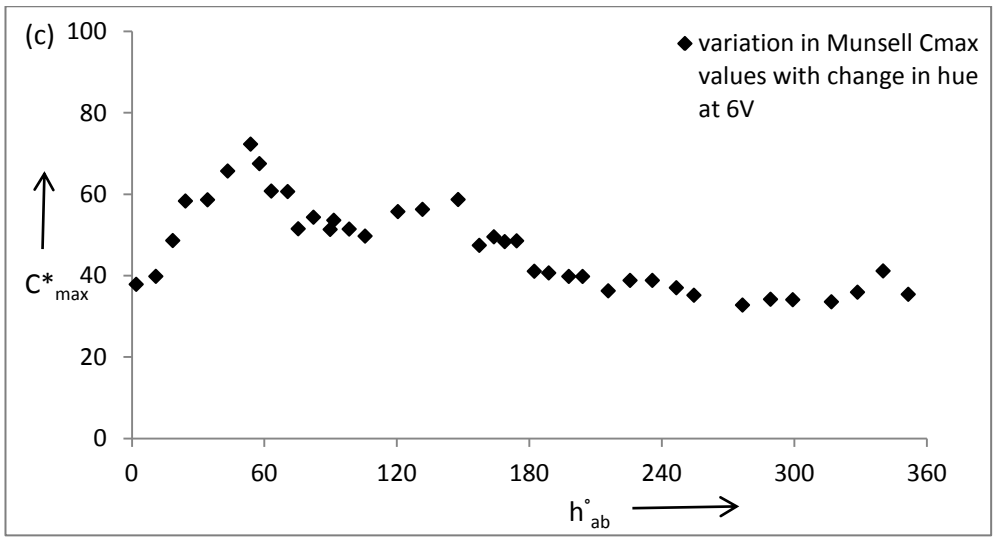
(c)
100
80
60
40
20
0
C*max
0
60
120
180
240
300
360
h°ab
variation in Munsell Cmax values with change in hue at 6V

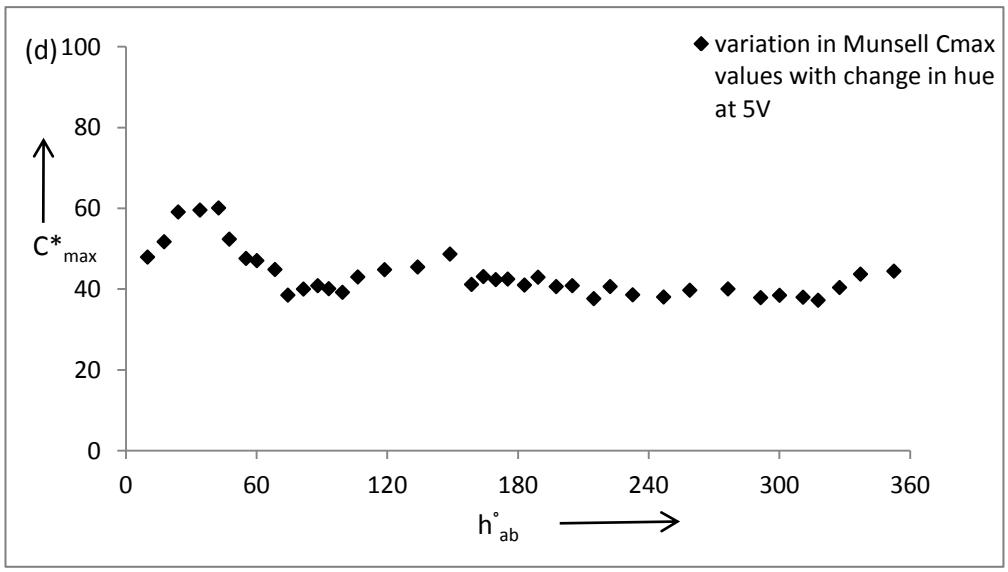
(d)
100
80
60
40
20
0
C*max
0
60
120
180
240
300
360
h°ab
variation in Munsell Cmax values with change in hue at 5V

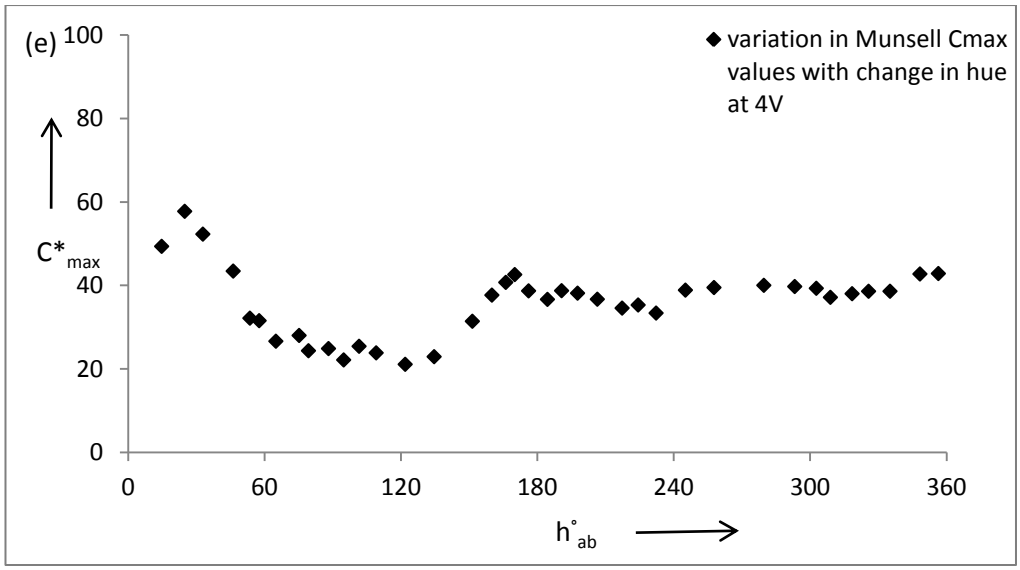
(e)
100
80
60
40
20
0
C*max
0
60
120
180
240
300
360
h°ab
variation in Munsell Cmax values with change in hue at 4V

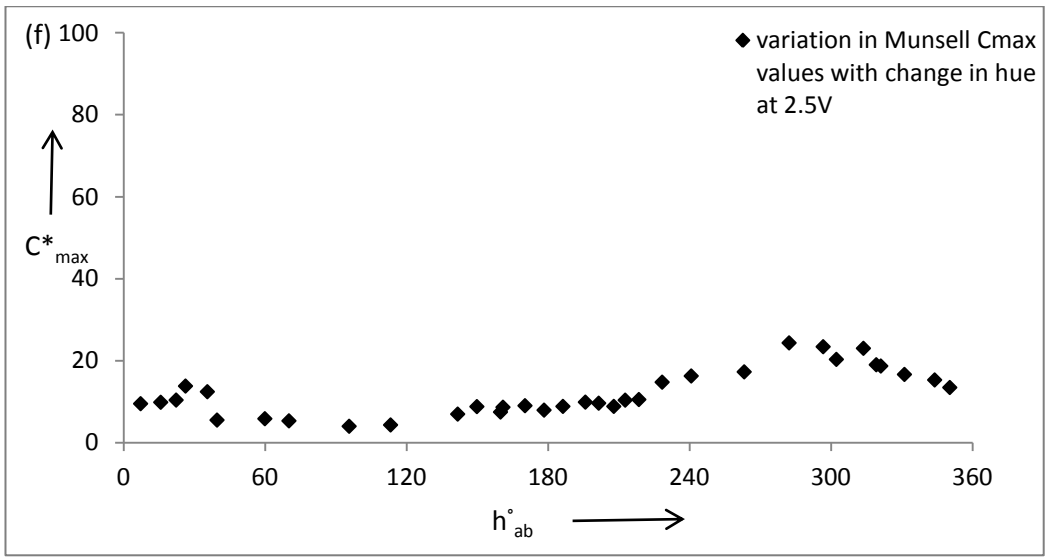


Figure 4.7 (a-f): Variation in Munsell $C^*_{max}$ values with change in hue at different Munsell values

There is a need to establish a relationship between the fullest chroma and the hue at every Munsell value. It is necessary to determine these $C^*_{max}$ values around the hue circle by any suitable method, initially for the lightness levels for which these $C^*_{max}$ have been derived, and then for the values in between these levels. One method is to fit a cosine formula of the form given in Equation 4.11 to the data at each lightness level. Microsoft excel solver is used to fit the cosine function to the Munsell values. The corresponding $a^*$, $b^*$ values derived from the $C^*_{max}$ serve as the boundary around the hue circle:

$$C^*_{max} = m_1 + m_2 \cos(h+n_1) + m_3 \cos(2h+n_2) + m_4 \cos(3h+n_3) + m_5 \cos(4h+n_4)$$

Equation 4.11

The constants $m_{1\text{-}5}$ and $n_{1\text{-}4}$ that were fitted to Equation 4.11 to fit the curves shown in Figure 4.7 (a to f) are tabulated in Table 4.2:

Table 4.2: The cosine equation constants for the given Munsell values

| Munsell value scale | $m_1$ | $m_2$ | $m_3$ | $m_4$ | $m_5$ | $n_1$ | $n_2$ | $n_3$ |
|---|---|---|---|---|---|---|---|---|
| 8V | 30.93 | -23.12 | -13.00 | 8.00 | 5.50 | 7.85 | -0.10 | 7.82 |
| 7V | 43.00 | -18.50 | -5.20 | 0.60 | -1.75 | 7.80 | 0.50 | 8.50 |
| 6V | 46.50 | -14.00 | -1.50 | -3.00 | -2.25 | 7.90 | 0.60 | 8.00 |
| 5V | 44.00 | -8.00 | 2.50 | -4.00 | -0.48 | 8.40 | 0.18 | 7.95 |
| 4V | 37.50 | -3.50 | 5.50 | -4.50 | 0.75 | 10.2 | -0.70 | 7.66 |
| 2.5V | 11.87 | 6.50 | 2.76 | 1.58 | -1.20 | 13.8 | -3.70 | 4.50 |

The cosine relation did not give a completely satisfactorily fit to the Munsell data which might be due to the nature of data, as shown in Figure 4.8 (a-f).

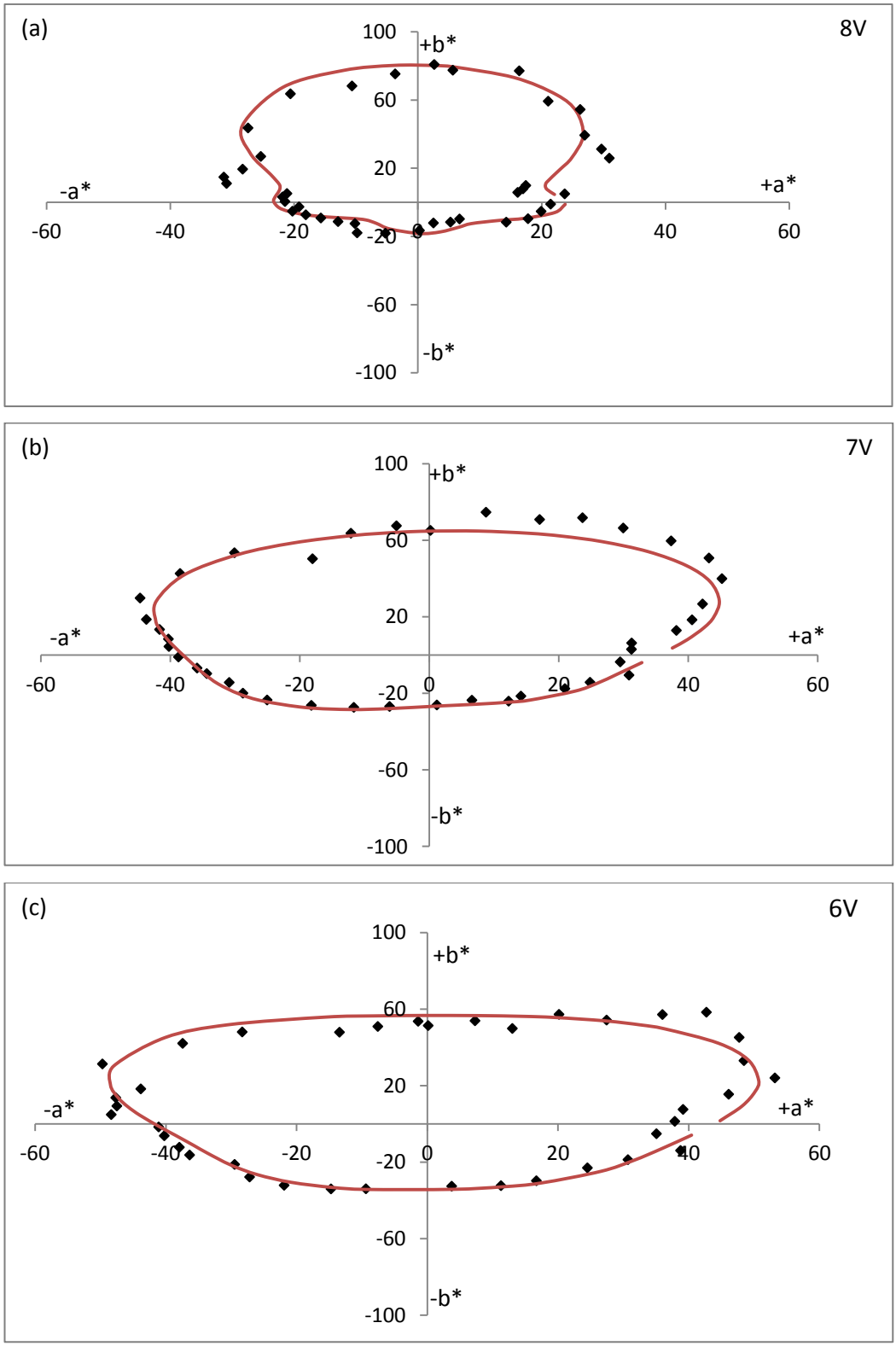

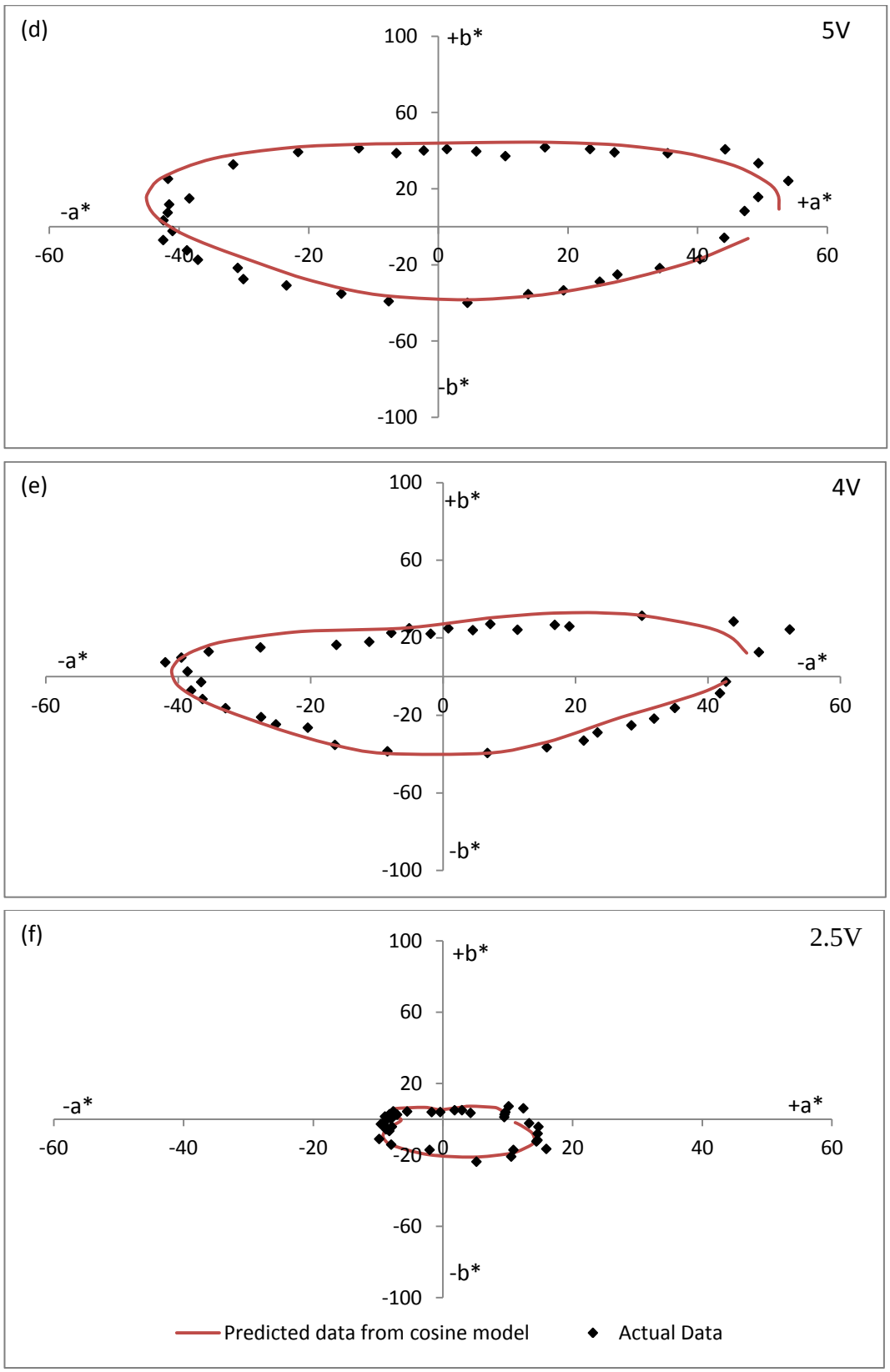


Figure 4.8 (a-f): Highest Munsell chroma values at different Munsell Value scales

Errors in fitting the cosine relation to the actual data were computed by using the Equation 4.12. The computed errors at different Munsell value scale are summerised in Table 4.3:

$$Error = \sqrt{\frac{\sum (C^*_{\max} - C^*_{\max(predicted)})^2}{n}}$$ Equation 4.12

Table 4.3: Calculated Error in term of $C^*_{max}$ to the Cosine Model

| Munsell Value scale | Error |
|---|---|
| 8V | 4.44 |
| 7V | 4.26 |
| 6V | 4.25 |
| 5V | 3.79 |
| 4V | 4.25 |
| 2.5 | 2.45 |

The cosine constants tabulated in Table 4.2 enabled to define the $C^*_{max}$ boundary around the hue circle for the six Munsell Value levels. In order to construct the $C^*_{max}$ boundary around the hue circle for any lightness lying in between these six levels, it was necessary to interpolate between these constants. However, it was observed that the lightness values of the Munsell highest chroma, computed from the reflectance values, for one Munsell value level, are not same round the hue circle. So, it was considered appropriate to use average lightness values for the optimisation of the cosine equation constants for every Munsell Value. The average lightness values for every Munsell hue is given in Table 4.4:

Table 4.4: Average lightness for Munsell Value scales

| Munsell Value scale | Average Lightness ($L^*_{av}$) |
|---|---|
| 8 | 82.70 |
| 7 | 72.85 |
| 6 | 63.04 |
| 5 | 53.20 |
| 4 | 42.86 |
| 2.5 | 27.40 |

The cosine constants are optimised by using the polynomial equations and are given in Table 4.5:

Table 4.5: Polynomial equations used to determine optimised cosine constants

$$m_1 = -0.03115(L^*)^2 + 3.7808(L^*) - 68.229$$
$$m_2 = 0.00211(L^*)^2 - 0.7612(L^*) + 25.599$$
$$m_3 = -0.00954(L^*)^2 + 0.7646(L^*) - 11.0251$$
$$m_4 = 0.0115(L^*)^2 - 1.1615(L^*) + 24.759$$
$$m_5 = 7.09E-06(L^*)^4 - 0.00114(L^*)^3 + 0.0586(L^*)^2 - 0.9747(L^*) + 1.0205$$
$$n_1 = 0.00304(L^*)^2 - 0.4415(L^*) + 23.642$$
$$n_2 = -0.00318(L^*)^2 + 0.4198(L^*) - 13.116$$
$$n_3 = -0.00242(L^*)^2 + 0.324(L^*) - 2.464$$

The optimised cosine costants ($m_1$tom$_5$ & $n_1$ton$_3$) are close to the cosine constant values as given in Table 4.2 and are represented graphically in Figure 4.9 (a-h):

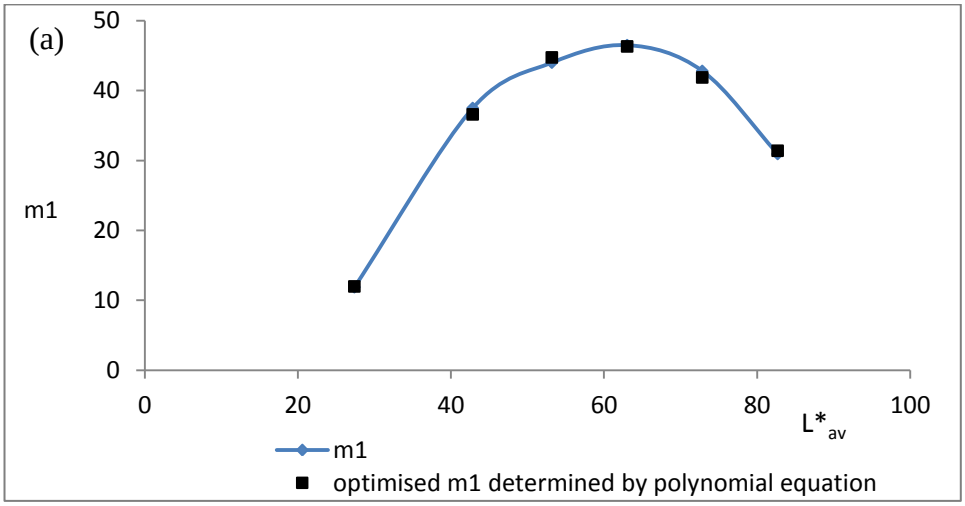


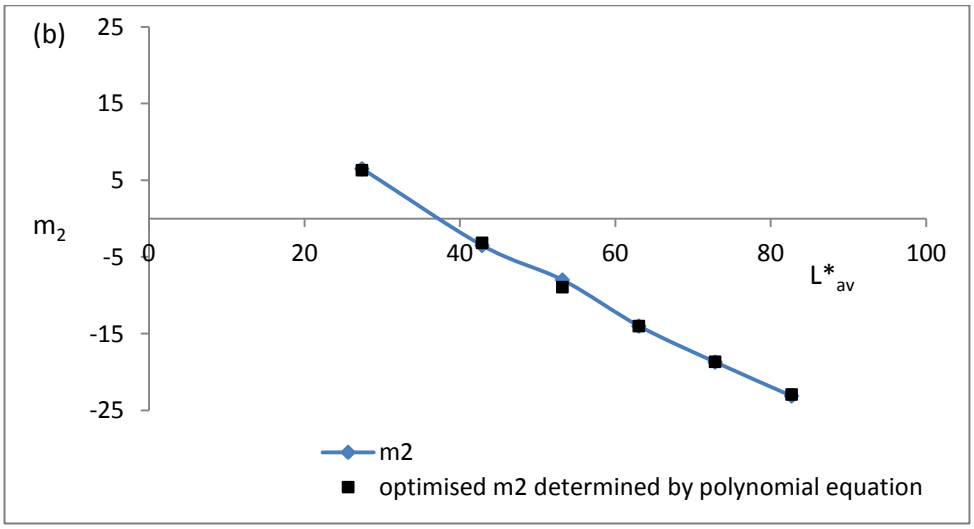

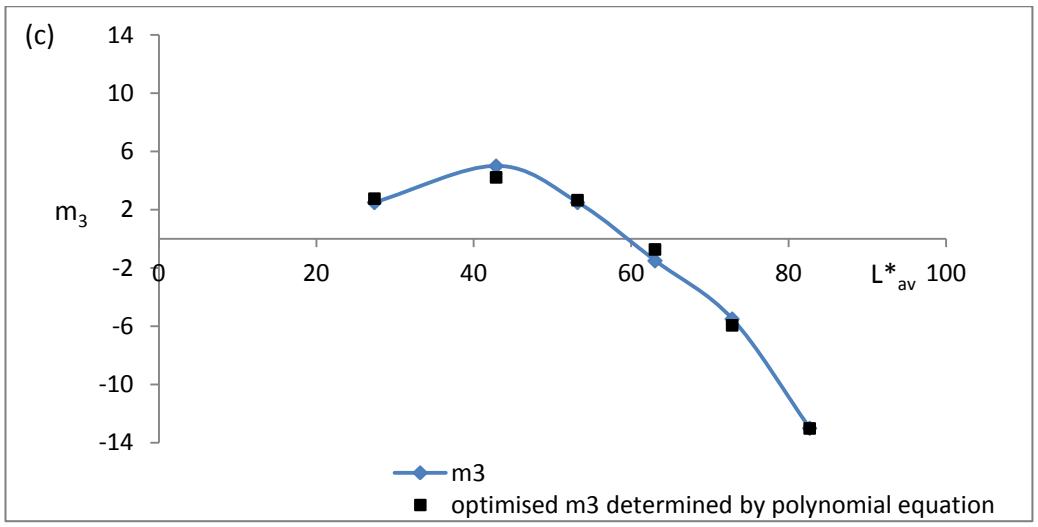
(c)
14
10
6
2
-2
-6
-10
-14
m3
0
20
40
60
80
100
L*av
m3
optimised m3 determined by polynomial equation

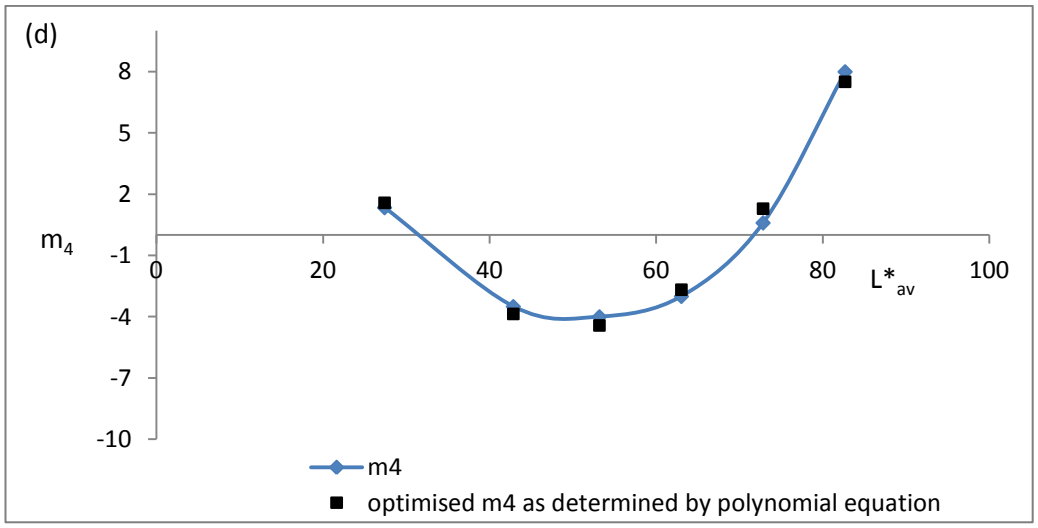
(d)
8
5
2
-1
-4
-7
-10
m4
0
20
40
60
80
100
L*av
m4
optimised m4 as determined by polynomial equation

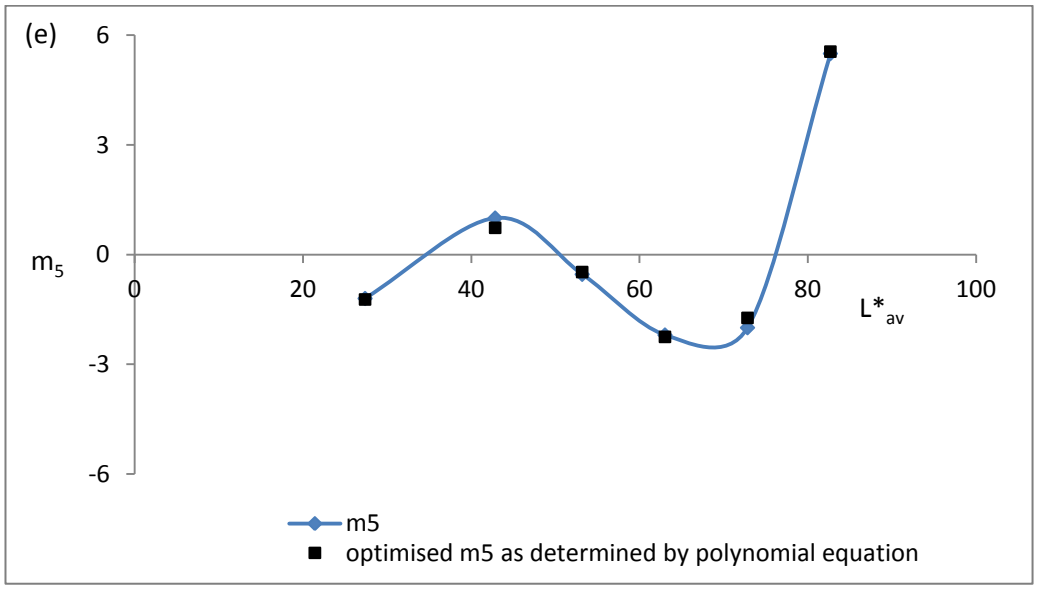
(e)
6
3
0
-3
-6
m5
0
20
40
60
80
100
L*av
m5
optimised m5 as determined by polynomial equation

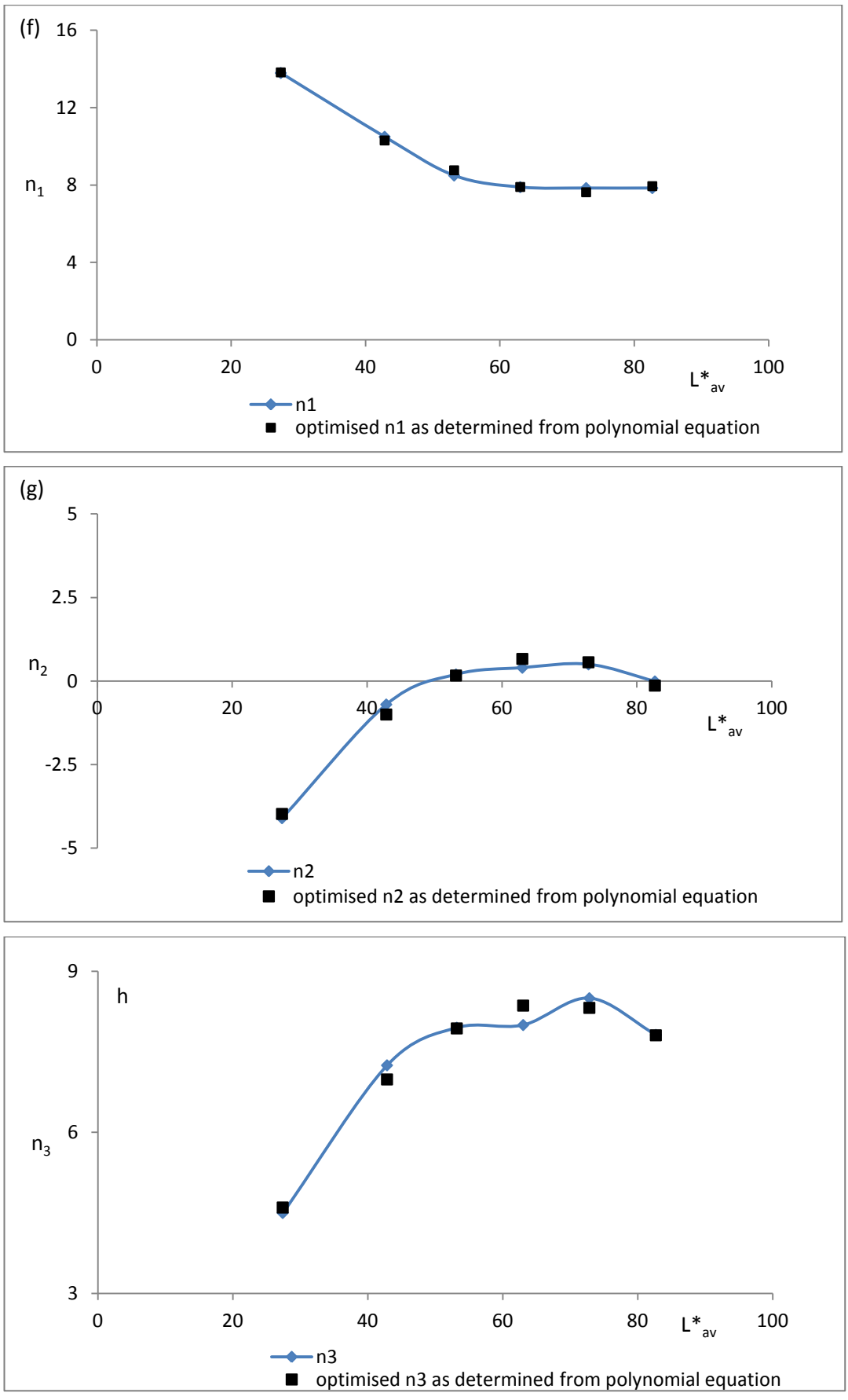


Figure 4.9 (a-h): Optimization of cosine formula constants ($m_1$ to $m_5$) and ($n_1$ to $n_3$)

The optimization was achieved by minimizing the errors computed from Equation 4.13 and the optimal constants are shown in Table 4.6 along with the minimised errors:

$$Error = \sqrt{\frac{\sum (const._{actual} - const._{predicted})^2}{n}} \qquad \text{Equation 4.13}$$

Table 4.6: Optimized cosine formula constants and calculated errors:

| Average Lightness | m1 | m2 | m3 | m4 | m5 | n1 | n2 | n3 |
|---|---|---|---|---|---|---|---|---|
| 82.70 | 31.39 | -22.92 | -13.01 | 7.51 | 5.55 | 7.95 | -0.13 | 7.81 |
| 72.85 | 41.88 | -18.65 | -5.93 | 1.30 | -1.73 | 7.63 | 0.56 | 8.32 |
| 63.04 | 46.32 | -14.00 | -0.72 | -2.67 | -2.25 | 7.91 | 0.66 | 8.36 |
| 53.20 | 44.75 | -8.92 | 2.66 | -4.42 | -0.48 | 8.77 | 0.17 | 7.94 |
| 42.86 | 36.59 | -3.15 | 4.23 | -3.86 | 0.73 | 10.31 | -1.00 | 6.99 |
| 27.40 | 11.98 | 6.33 | 2.77 | 1.58 | -1.23 | 13.83 | -3.97 | 4.60 |
| Error | 0.65 | 0.42 | 0.50 | 0.45 | 0.16 | 0.17 | 0.14 | 0.20 |

**4.5 Extension of the WSI algorithm to higher chroma colours**

The WSI algorithm when reported [15] was limited to the set chroma boundaries throughout the colour space as shown in Table 4.7:

Table 4.7: WSI set chroma boundaries throughout the colour space

| Standard depth | 0° | 45° | 90° | 135° | 180° | 225° | 270° | 315° |
|---|---|---|---|---|---|---|---|---|
| 2/1 | 25 | 15 | 15 | 15 | 20 | 20 | 20 | 20 |
| 1/1 | 45 | 40 | 45 | 40 | 40 | 35 | 35 | 35 |
| 1/3 | 45 | 45 | 45 | 40 | 35 | 40 | 35 | 35 |
| 1/6 | 40 | 45 | 45 | 35 | 35 | 40 | 30 | 30 |
| 1/12 | 35 | 35 | 30 | 30 | 30 | 30 | 25 | 25 |
| 1/25 | 25 | 20 | 25 | 25 | 25 | 25 | 20 | 20 |

Fabric dyeings of yellows, orange, reds and yellow-greens can have higher chroma values than reported in Table 4.7, especially at medium depth levels. It was therefore considered necessary to develop a procedure which could predict the lightness of highly saturated (non-fluorescent) equi-depth colours accurately. It was therefore considered that the more realistic behavior was to assume a linear extension, so a straight line equation was applied for higher chroma colours at the different depth levels. Figure 4.10 illustrates the situation clearly.

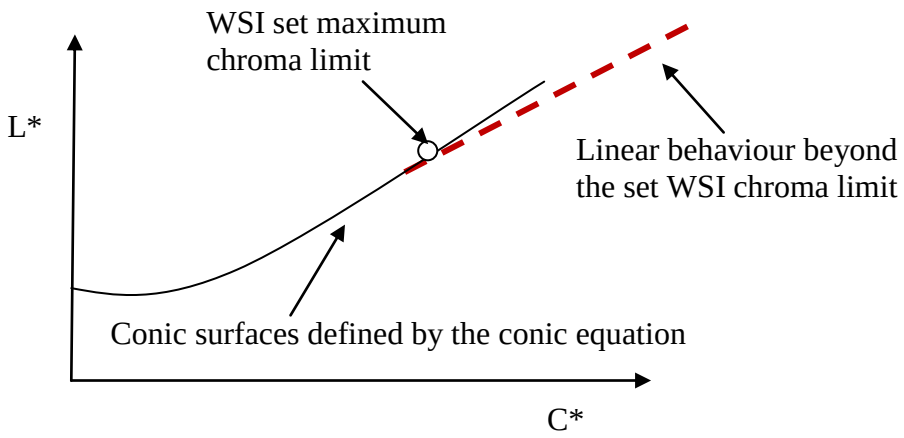


Figure 4.10: An illustration of the straight line fitting to the higher chroma dyeing beyond the set WSI maximum chroma limit

The procedure adopted to fit the straight line, beyond the set chroma boundaries, at each depth level around the hue circle was:

- The lightness of the standard at all the six established surfaces for a given hue and chroma of the standard was calculated. These lightness values were examined to find which two standard depth surfaces lay immediately above and below the standard. The conic constants of the line passing through the standard were then calculated using Equation 4.3:
- The chroma boundary limit for all the three surfaces: surface lying above, below and of the standard was determined from Table 4.7
- The slope (m) and intercept (c) for the straight line were calculated by using Equations 4.14 and 4.15 for all the three surfaces:

$$m = (L^*_{C^*(boundary-2)} - L^*_{C^* boundary}) / (C^*_{(boundary-2)} - C^*_{boundary}) \quad \text{Equation 4.14}$$

$$c = L^*_{C^* boundary} - m\, C^*_{boundary} \quad \text{Equation 4.15}$$

In Equations 4.14 and 4.15 $C^*_{boundary}$ is the chroma boundary limit as given in Table 4.7 and $L^*_{C\ boundary}$ is the lightness determined for the $C^*_{boundary}$ from the WSI algorithm. The $C^*_{(boundary-2)}$ is that chroma value which is two chroma less than the $C^*_{boundary}$ and $L^*_{C(boundary-2)}$ is the corresponding lightness determined from the WSI algorithm

- Finally the lightness of the sample was predicted by using the Equation 4.16

$L^*_{sample} = m\, C^*_{sample} + c$ Equation 4.16

Five different standards lying between different depth levels were investigated. The lightness of the standard was calculated by the WSI algorithm and also by the procedure given above to fit the straight line to the higher chroma lying beyond the set boundaries. The colorimetric data and the calculated lightness of the standards are given in Table 4.8. The calculated lightness from the WSI algorithm at higher chroma values was in satisfactory agreement with the lightness of the standard determined by straight line fitting.

Table 4.8: Calculated lightness of a standard from WSI algorithm and by fitting straight line to higher chroma colours

| S. No. | L* | C* | h | Lightness of the depth surface lying below and above the std. | | $L^*_{WSI}$ | $L^*$ st.line | $L^* - L^*_{st.\ line}$ | $L^* - L_{WSI}$ |
|---|---|---|---|---|---|---|---|---|---|
| 1 | 57.27 | 90.4 | 52.8 | 44.15 | 65.76 | 57.27 | 52.58 | 4.69 | 0 |
| 2 | 62.48 | 65.7 | 49.4 | 52.76 | 75.02 | 62.41 | 61.76 | 0.72 | 0.07 |
| 3 | 75.81 | 61.4 | 86.4 | 73.9 | 81.92 | 75.7 | 75.19 | 0.62 | 0.11 |
| 4 | 81 | 50 | 55 | 74.94 | 88,74 | 81.07 | 80.25 | 0.75 | -0.07 |
| 5 | 83.61 | 32.4 | 56.8 | 76.08 | 85.56 | 83.51 | 83.24 | 0.37 | 0.1 |

Though the straight line fitting for higher chroma colours was satisfactory for the standards lying between the 1/1 and the 1/12 depth levels, it fitted poorly for dark and pastel colours, as shown in Figure 4.11:

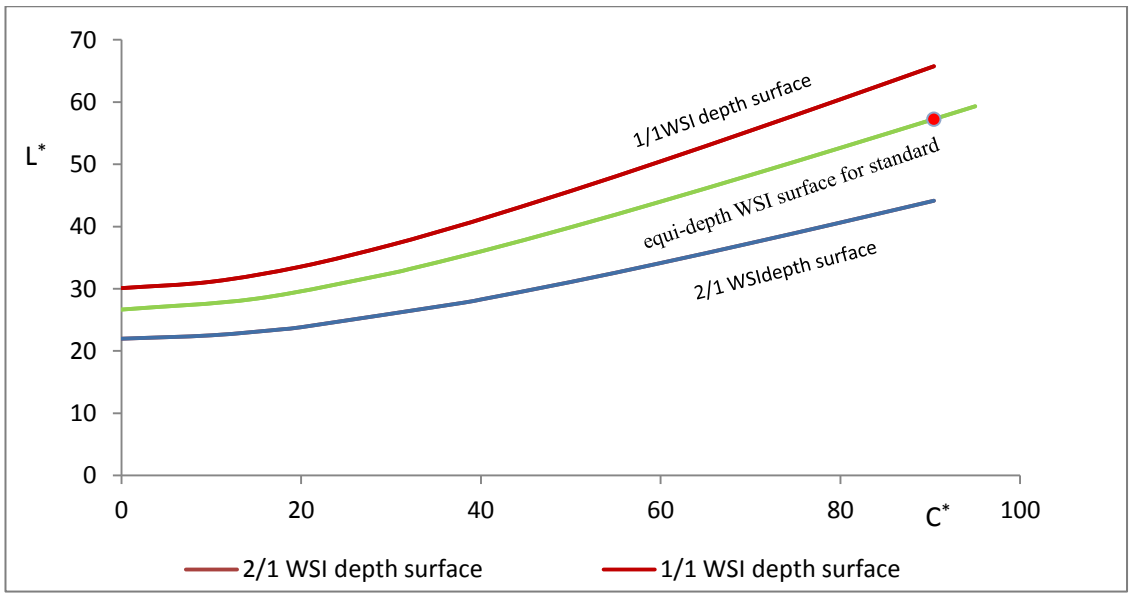
70
60
50
40
30
20
10
0
L*
0
20
40
60
80
C*
100
1/1WSI depth surface
equi-depth WSI surface for standard
2/1 WSIdepth surface
2/1 WSI depth surface
1/1 WSI depth surface

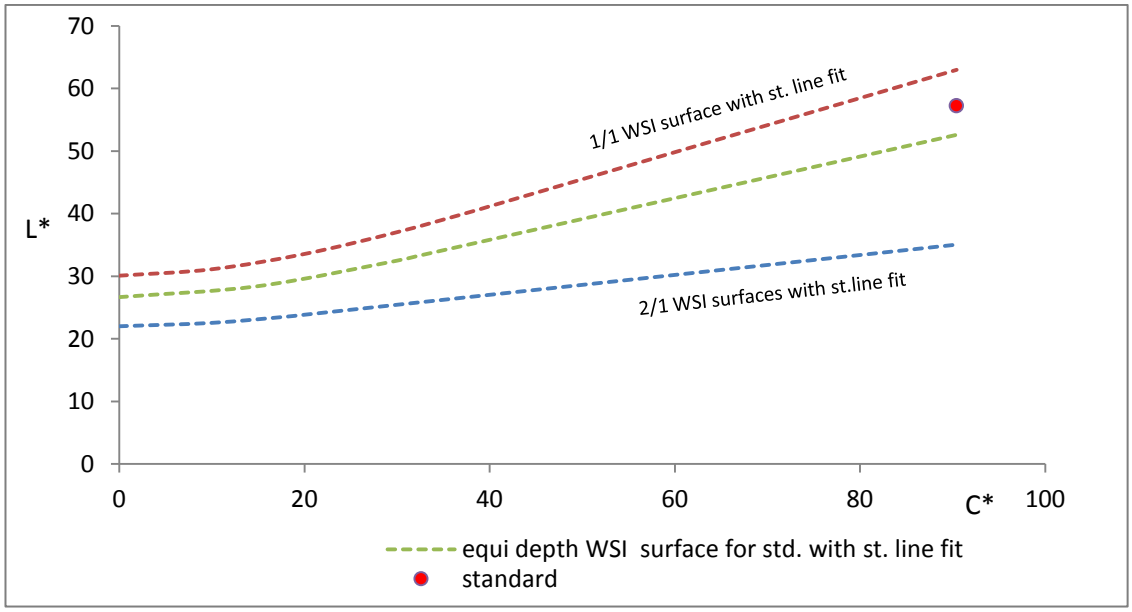
70
60
50
40
30
20
10
0
L*
0
20
40
60
80
C*
100
1/1 WSI surface with st. line fit
2/1 WSI surfaces with st.line fit
equi depth WSI surface for std. with st. line fit
standard

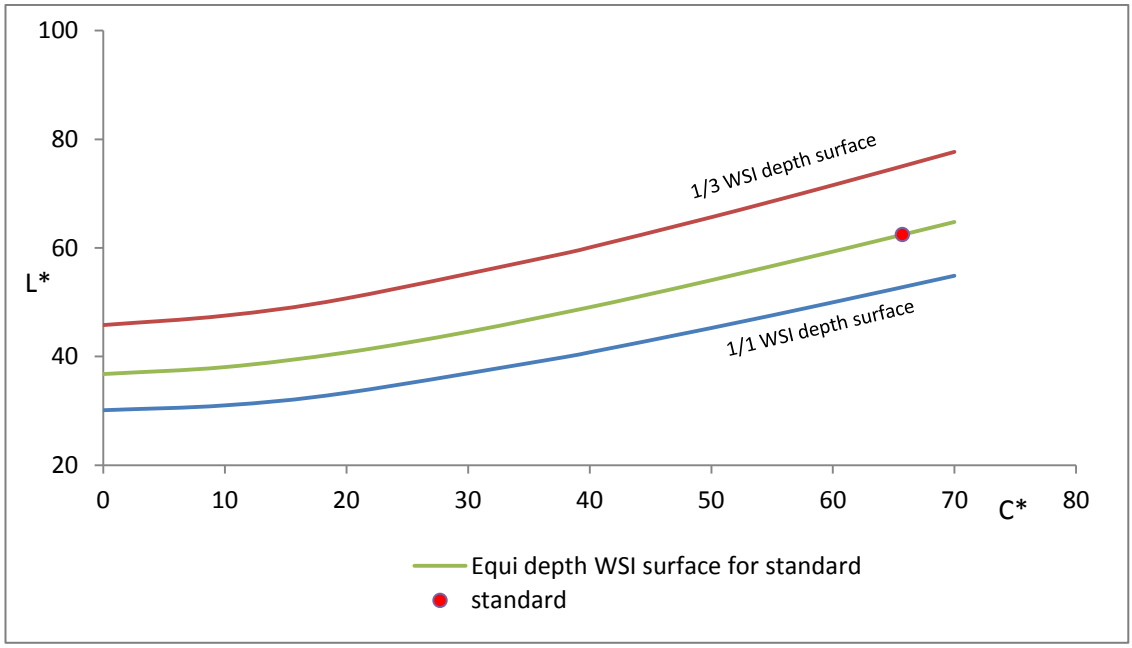
100
80
60
40
20
L*
0
10
20
30
40
50
60
70
80
C*
1/3 WSI depth surface
1/1 WSI depth surface
Equi depth WSI surface for standard
standard

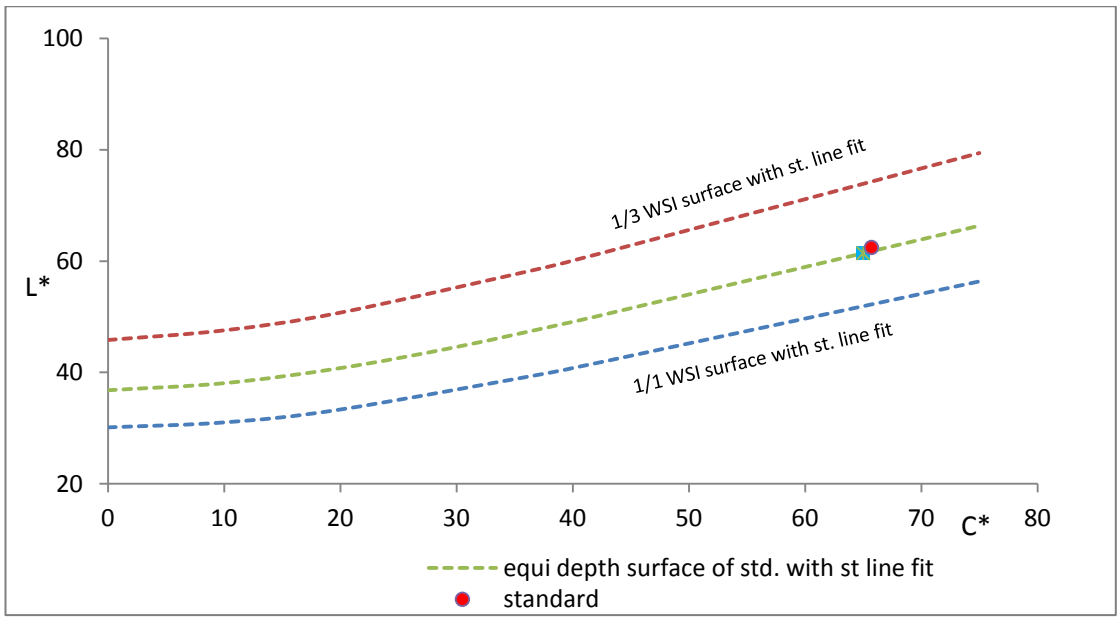
100
80
60
40
20
L*
0
10
20
30
40
50
60
70
80
C*
1/3 WSI surface with st. line fit
1/1 WSI surface with st. line fit
equi depth surface of std. with st line fit
standard

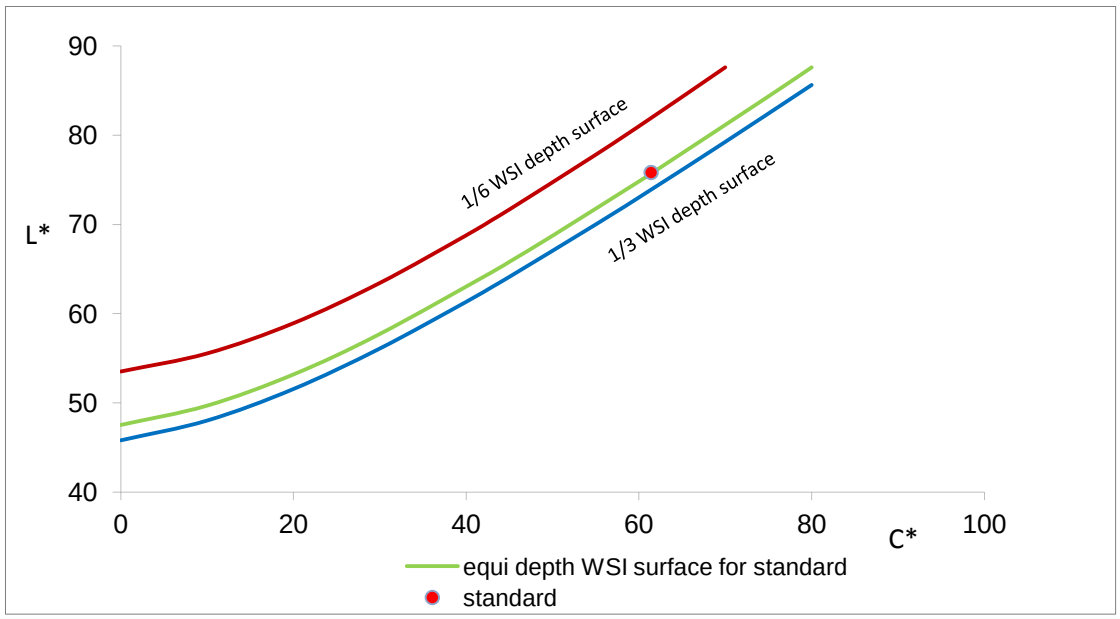
90
80
70
60
50
40
L*
0
20
40
60
80
100
C*
1/6 WSI depth surface
1/3 WSI depth surface
equi depth WSI surface for standard
standard

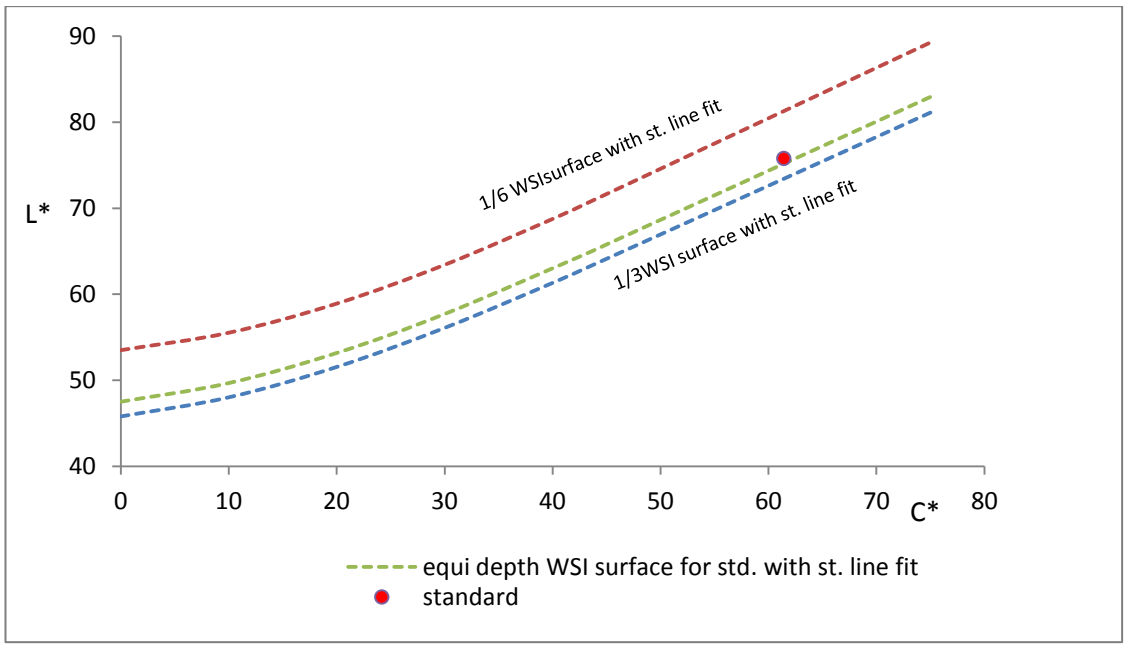
90
80
70
60
50
40
L*
0
10
20
30
40
50
60
70
80
C*
1/6 WSIsurface with st. line fit
1/3WSI surface with st. line fit
equi depth WSI surface for std. with st. line fit
standard

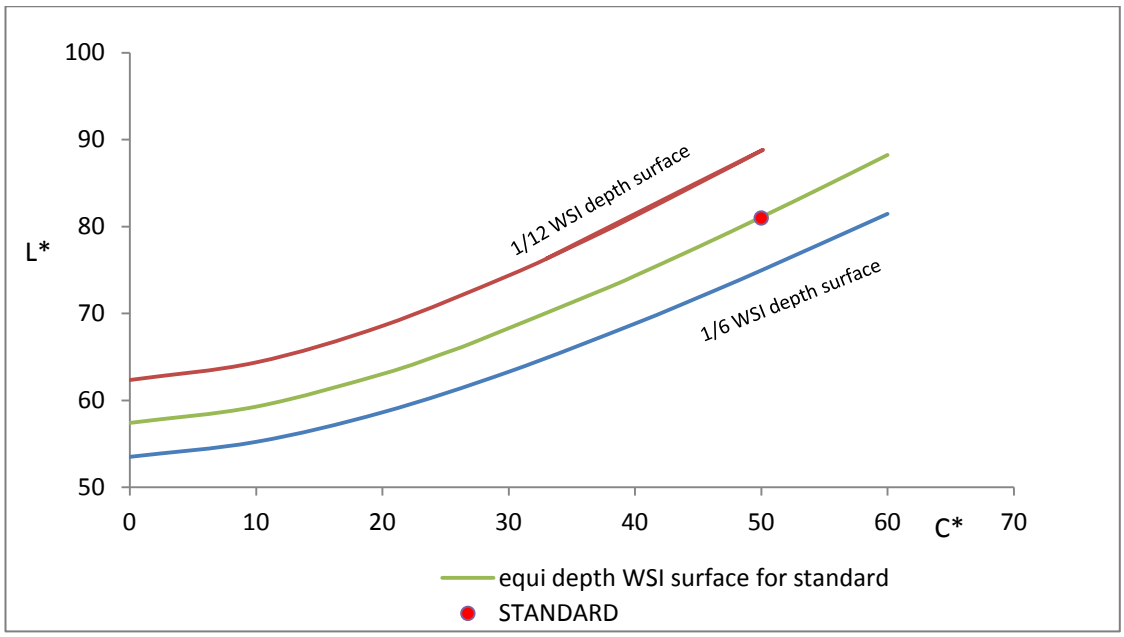
100
90
80
70
60
50
L*
0
10
20
30
40
50
60
70
C*
1/12 WSI depth surface
1/6 WSI depth surface
equi depth WSI surface for standard
STANDARD

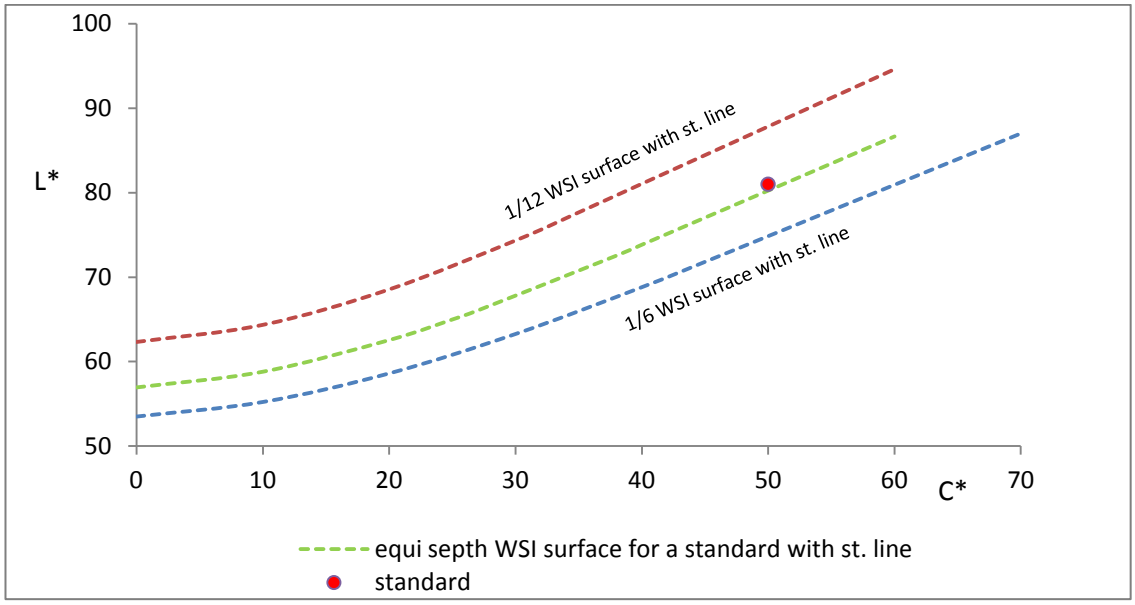
100
90
80
70
60
50
L*
0
10
20
30
40
50
60
70
C*
1/12 WSI surface with st. line
1/6 WSI surface with st. line
equi septh WSI surface for a standard with st. line
standard

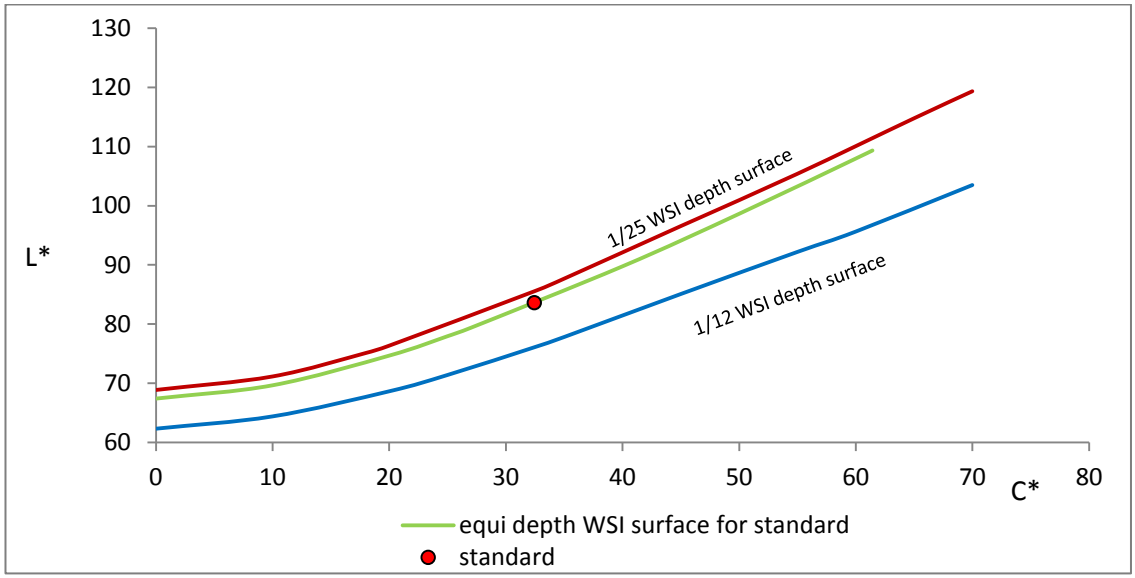
130
120
110
100
90
80
70
60
L*
0
10
20
30
40
50
60
70
80
C*
1/25 WSI depth surface
1/12 WSI depth surface
equi depth WSI surface for standard
standard

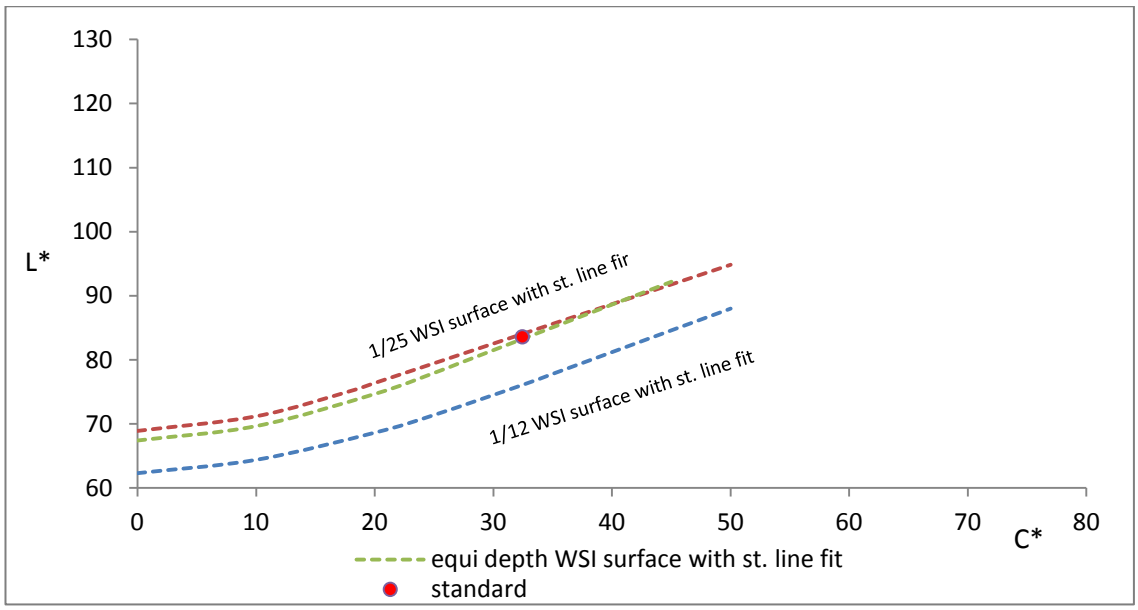


Figure 4.11: Extension of WSI algorithm and straight line fitting to higher chroma values.

In short an algorithm named WSF algorithm has been developed which can predict the differences in depth and brightness of a standard-batch pair by using the reflectance values of the batch on the depth plane. The Matlab *software for engineers* is used to iterate the K/S values of the batch. The WSF algorithm can be applied for the batch with similar or dissimilar hue angle from the standard and the respective Matlab iterative programs are given in Appendices A1 & A2.

### 4.6 Verification of the WSF Algorithm

The aim of the work was to develop an algorithm which could predict the dyers' variables of colour difference (ΔD, ΔB, ΔH) by using the reflectance values of a dyed pair. This work was grounded on extensive visual assessments to map various depth planes. In order to verify the WSF algorithm, it was decided to prepare dyed pairs (standard - batch) showing small to medium colour differences, ranging from 0.3 – 3.0 CIELAB units round the hue circle, at different chroma levels, as illustrated in Figure 4.12. It was decided to repeat that exercise at different lightness levels.

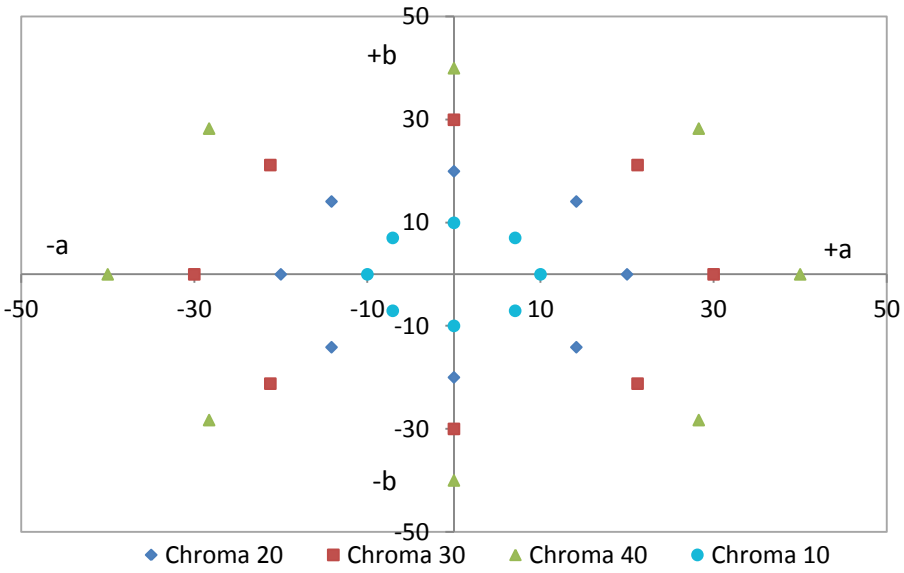


Figure 4.12: Plan for preparing the dyeing pairs round the hue circle

A total of 49 dyed pairs, with colour differences ranging from 0.3-3.00 CIELAB colour difference units, located round the hue circle were prepared by varying the concentration and sent for visual assessment to two professional colourists. Both of the colourists were male with more than twenty years of industrial experience. Colourists were asked to view the dyed pairs in D65 illuminant and gave their output in terms of differences in depth, brightness and hue to the overall colour difference perceived by them. Samples were assessed twice by each of the observer. The reproducibility of both of the observers was found satisfactory. These pairs were also run through the WSF algorithm and the output in terms of the difference in brightness and depth were computed. The CIELAB colour difference of these selected pairs is shown in Figure 4.13. The colorimetric data of these standard batch pairs are given in Appendix E1. The assessor's outputs in terms of percentage difference in depth, brightness and hue were noted and compared to the corresponding outputs from the WSF algorithm.

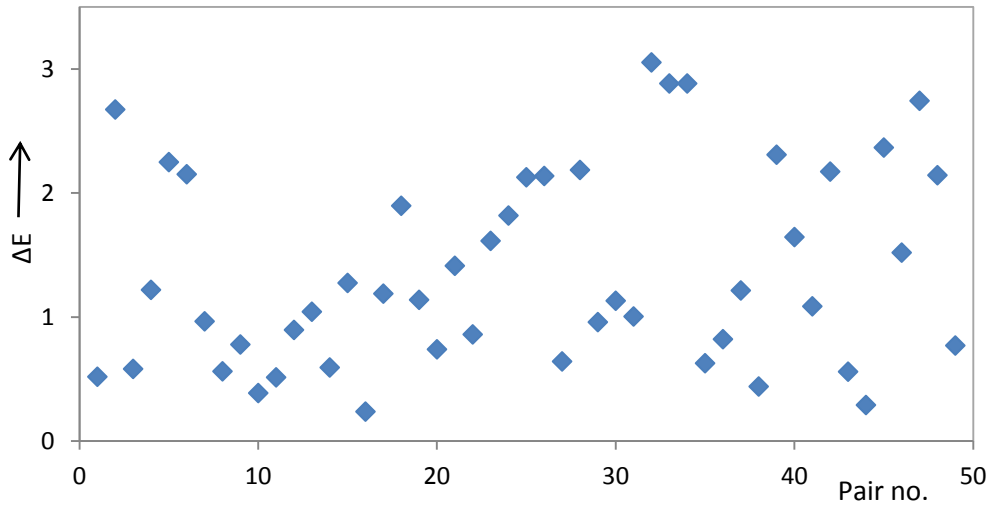


Figure 4.13: Colour difference of 49 dyeing pairs used for verifying the WSF algorithm

### *4.6.1 Preparation of dyeing pairs*:

The method adopted to produce dyeing pairs around the hue circle, at various lightness levels, is given in Figure 4.14:

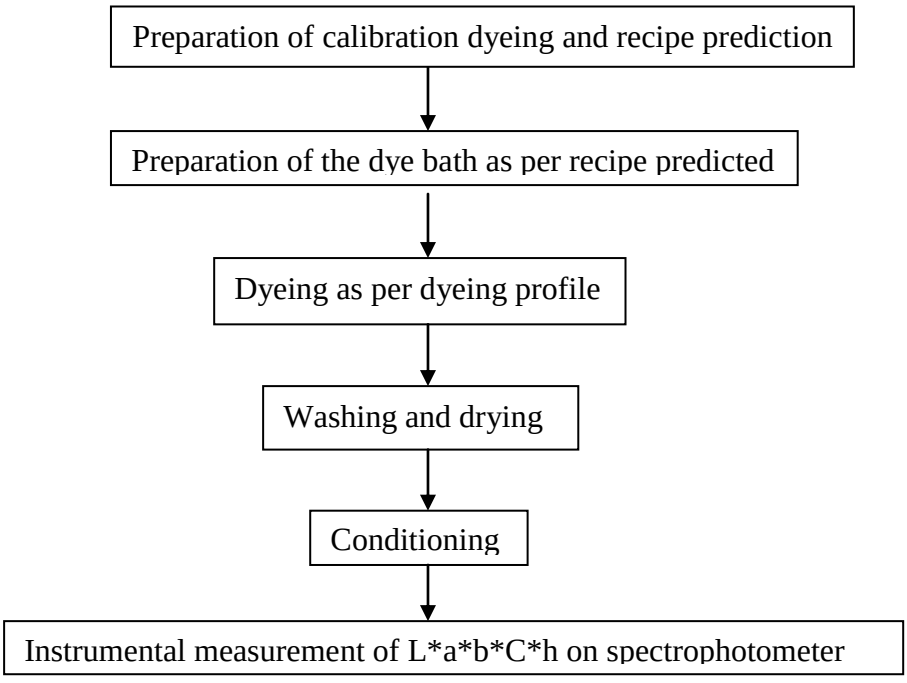


Figure 4.14: Method of dyeing to prepare dyeing pairs with small to medium colour difference round the hue circle

### *4.6.2 Recipe Prediction*

A Datacolour Match SF 600 colour measurement system, was used to predict the recipes for the L*, a*, b* values of the standard. Calibration dyeings were prepared at: 0.1%, 0.25%, 0.5%, 1.00%, 2.00%, 3.00% and 4.00% concentration levels, on the weight of fabric

### *4.6.3 Dyeing System Components*

**Dyeing material:** Pre-scoured wool satin was selected as a substrate. The wetability of the fabric was improved by first soaking for 25 -20 minutes in a solution containing 1-2g/l of a wetting agent, prior to dyeing and then fabric was introduced to the dyeing bath in the form of tube, after being squeezed.

**Dyes and Auxiliares**: The following acid dyes and auxilaries were used to prepare the required dyeings:

- Acid Red 57
- Acid Red 18
- Acid Blue 40
- Acid Blue 45
- Acid Yellow 17
- Acid Yellow 29
- Acid Red 52
- Duramine Violet V4B
- Sulphuric Acid
- Glauber Salt

**Dyeing machines**

- Pyrotec -S Laboratory Dyeing Machine
- Hot Box Oven with Fan

**Recipe**

Dyes = x% o.w.f

Sulphuric acid = 3%o.w.f

Glauber salt = 10% o.w.f

L:R = 40:1

### *4.6.4 Dye-Bath Preparation*

The amount of dyes and chemicals were calculated by using the Equation 4.17:

$$\frac{W \times P}{C}$$ Equation 4.17

Where

W =weight of the fabric

P = practical dyeing concentration of dyes or auxiliaries

C= concentration of the dye or auxiliary solution

The pre-calculated amount of the dye, acid and the salt was measured accurately from their stock solutions by means of a digital pipette to prepare the dye bath accurately. The fabric was introduced into the dye bath in the form of a tube. These dyeing bath tubes were then put into the Pyrotec-S machine and the dyeing was carried out as per dyeing profile given in Figure 4.16:

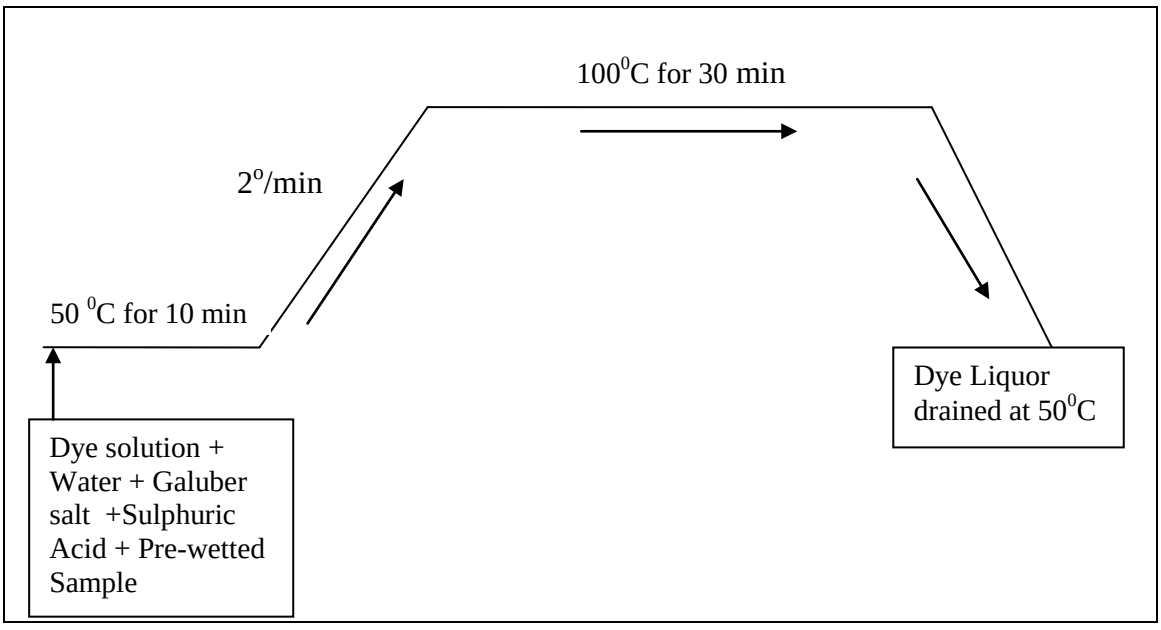


Figure 4.14: Dyeing profile of Acid levelling dyes on Wool

### *4.6.5 Washing and Drying*

After dyeing samples were rinsed at room temperature with water for 5 minutes, warm rinsed at 60°-70$^0$ for 5 min, and finally cold rinsed. The samples after washing were put

into the dryer at $80^0$- $90^0$C for 10-15minutes. The sample was conditioned at 65% RH and 21°C overnight after drying.

### *4.6.6 Instrumental Measurement*

The $L^*$, $a^*$, $b^*$, $C^*$ and $h°_{ab}$ values of the dyed samples were measured on a Datacolour SF600 spectrophotometer, using the large aperture, specular included, and UV filter off. The fabric sample was folded into four layers and measured twice, at 0° and 90°. The average values from these two readings for D65 illuminant were recorded.

The repeatability of the Spectroflash SF 600 was assessed by measuring the white, grey, black, red, blue and yellow BCRA tiles, each 20 times. Measurements were made firstly without removing the tile from the instrument between measurements, then secondly after removing then placing the tile between measurements. The mean and standard deviation of the resulting L*a*b* values are shown in Tables 4.9 and 4.10

Table 4.9: The repeatability of the Spectroflash SF 600 measured using standard BCRA tiles- tiles left to instrument between readings

| Std Tiles | Mean | | | Standard deviation | | |
|---|---|---|---|---|---|---|
| | L* | a* | b* | L* | a* | b* |
| White | 95.978 | -0.336 | 1.4255 | 0.004104 | 0.005026 | 0.00759 |
| Mid.grey | 60.2825 | -0.031 | 0.2955 | 0.004443 | 0.004472 | 0.00510 |
| Black | 25.387 | -0.1995 | -0.684 | 0.004702 | 0.007592 | 0.01391 |
| Red | 43.645 | 38.95 | 19.6005 | 0.024387 | 0.057947 | 0.05452 |
| Yellow | 83.436 | 2.328 | 77.338 | 0.022804 | 0.047639 | 0.01472 |
| Blue | 27.5555 | 8.441 | -18.7715 | 0.005104 | 0.006407 | 0.00933 |

Table 4.10: The repeatability of the Spectroflash SF 600 measured using standard BCRA tiles- tiles removed from instrument between readings

| Std Tiles | Mean | | | Standard deviation | | |
|---|---|---|---|---|---|---|
| | L* | a* | b* | L* | a* | b* |
| White | 95.973 | -0.329 | 1.428 | 0.009487 | 0.007379 | 0.00788 |
| Mid.grey | 60.284 | -0.031 | 0.296 | 0.005164 | 0.005676 | 0.00516 |
| Black | 25.385 | -0.203 | -0.686 | 0.007071 | 0.008233 | 0.01429 |
| Red | 43.659 | 38.981 | 19.635 | 0.013703 | 0.038427 | 0.04116 |
| Yellow | 83.449 | 2.298 | 77.348 | 0.016633 | 0.033928 | 0.02394 |
| Blue | 27.556 | 8.423 | -18.742 | 0.006992 | 0.020028 | 0.02898 |

The standard deviation for the tiles are all very low, even when the tiles are removed from the instrument between readings, showing that the spectroflash SF 600 has

excellent repeatability. Red and yellow gave higher standard deviation than rest of the colours which is due to the thermo-chromic nature of the red and yellow tiles.

# CHAPTER 5 RESULTS AND DISCUSSION

## 5.1 Comparison of ΔD, ΔB, and ΔH values calculated by the WSF, DBH and Sato algorithms

Two data sets (1 & 2) were used to compare the WSF, DBH and Sato algorithms. Data set 1 contained 49 pairs prepared in house with CIELAB colour differences ranging between from 0.3- 3 units. Data set 2 contained 117 pairs distributed round the hue circle at various lightness levels assessed by eleven observers, obtained from a private source [73]. After preparing the standard- batch pairs for data set 1, their reflectance values were measured on Datacolour SF600 spectrophotometer The reflectance values and colorimetric data for set 1 & 2 are given in Appendices E1 – E4. The computed values of ΔD and ΔB for all three algorithms are given in Tables 5.1 and 5.2 for both data sets. The same scaling factor calculation was used in all three models (WSF, DBH & Sato) to ensure that after scaling, the sum of the squares of the colorimetric variables were numerically equal to sum of squares of the dyers' variables. The three algorithms showed good agreement for both data sets in evaluating the difference in depth and brightness of a standard and batch pair as shown in Figure 5.1(a & b) and Figure 5.2 (a & b).

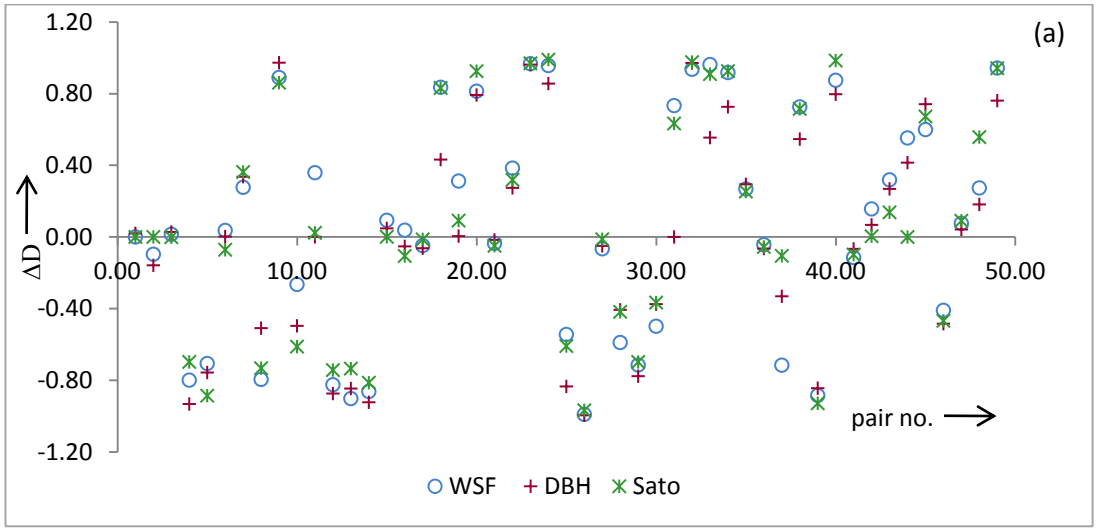

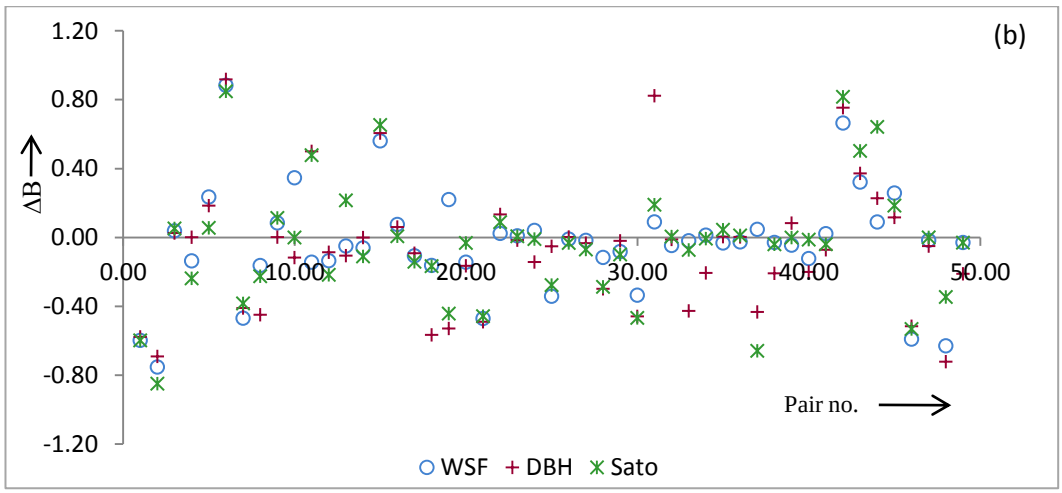


Figure 5.1 (a & b): Comparison of ΔD and ΔB values (a & b) computed by theWSF, DBH and Sato algorithms before performing any hue correction to the batch, for data set 1

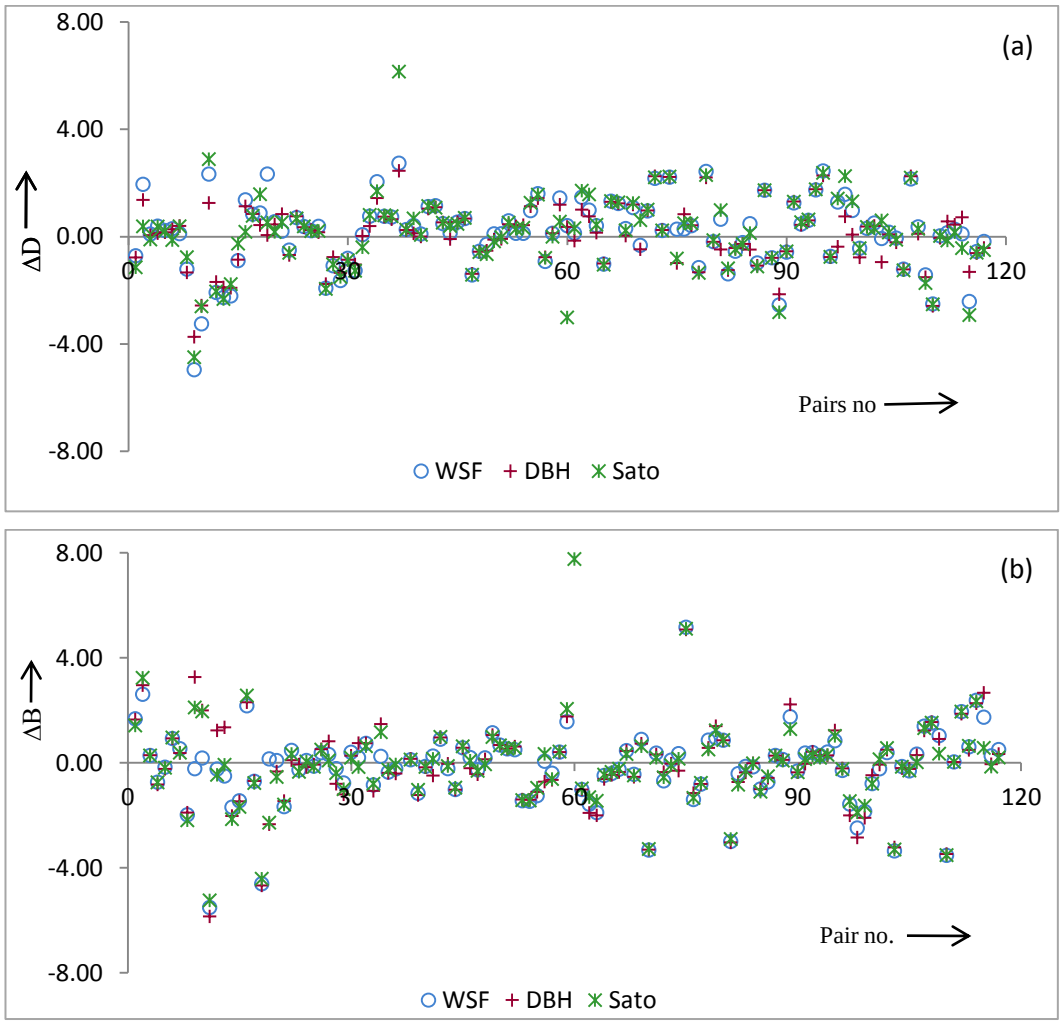


Figure 5.2 (a & b): Comparison of ΔD and ΔB values (a & b) computed by the WSF, DBH and Sato algorithms before performing any hue correction to the batch, for data set 2

Table 5.1: Comparison of the WSF algorithm with the DBH Model and the Sato formula, without any hue correction for data set 1

| Pair no. | WSF kΔD | DBH kΔD | Sato kΔD | WSF kΔB | DBH kΔB | Sato kΔB | ΔH |
|---|---|---|---|---|---|---|---|
| 1 | 0.00 | 0.02 | 0.00 | -0.60 | -0.58 | -0.60 | 0.40 |
| 2 | -0.10 | -0.16 | 0.00 | -0.75 | -0.69 | -0.85 | 0.15 |
| 3 | 0.02 | 0.03 | 0.00 | 0.04 | 0.03 | 0.05 | 0.95 |
| 4 | -0.80 | -0.93 | -0.70 | -0.14 | 0.00 | -0.24 | 0.07 |
| 5 | -0.71 | -0.76 | -0.89 | 0.24 | 0.19 | 0.06 | 0.06 |
| 6 | 0.04 | 0.00 | -0.07 | 0.88 | 0.92 | 0.85 | 0.08 |
| 7 | 0.28 | 0.34 | 0.36 | -0.47 | -0.41 | -0.38 | 0.25 |
| 8 | -0.79 | -0.51 | -0.73 | -0.16 | -0.45 | -0.22 | 0.04 |
| 9 | 0.89 | 0.97 | 0.86 | 0.09 | 0.00 | 0.11 | 0.02 |
| 10 | -0.26 | -0.50 | -0.61 | 0.35 | -0.12 | 0.00 | 0.39 |
| 11 | 0.36 | 0.00 | 0.02 | -0.14 | 0.50 | 0.48 | 0.50 |
| 12 | -0.82 | -0.87 | -0.74 | -0.13 | -0.09 | -0.22 | 0.04 |
| 13 | -0.90 | -0.85 | -0.73 | -0.05 | -0.10 | 0.22 | 0.05 |
| 14 | -0.86 | -0.92 | -0.81 | -0.06 | 0.00 | -0.11 | 0.08 |
| 15 | 0.09 | 0.05 | 0.00 | 0.56 | 0.61 | 0.65 | 0.35 |
| 16 | 0.04 | -0.05 | -0.11 | 0.08 | 0.06 | 0.01 | 0.89 |
| 17 | -0.05 | -0.06 | -0.01 | -0.11 | -0.09 | -0.14 | 0.85 |
| 18 | 0.84 | 0.43 | 0.83 | -0.16 | -0.57 | -0.17 | 0.00 |
| 19 | 0.31 | 0.00 | 0.09 | 0.22 | -0.53 | -0.44 | 0.47 |
| 20 | 0.81 | 0.79 | 0.93 | -0.14 | -0.16 | -0.03 | 0.04 |
| 21 | -0.04 | -0.02 | -0.05 | -0.47 | -0.49 | -0.46 | 0.49 |
| 22 | 0.38 | 0.27 | 0.32 | 0.02 | 0.13 | 0.09 | 0.59 |
| 23 | 0.97 | 0.96 | 0.97 | 0.01 | -0.01 | 0.01 | 0.02 |
| 24 | 0.96 | 0.86 | 0.99 | 0.04 | -0.14 | -0.01 | 0.00 |
| 25 | -0.54 | -0.83 | -0.61 | -0.34 | -0.05 | -0.28 | 0.12 |
| 26 | -0.99 | -1.00 | -0.97 | -0.01 | 0.00 | -0.03 | 0.00 |
| 27 | -0.07 | -0.05 | -0.01 | -0.02 | -0.03 | -0.07 | 0.92 |
| 28 | -0.59 | -0.41 | -0.42 | -0.12 | -0.30 | -0.29 | 0.30 |
| 29 | -0.71 | -0.78 | -0.70 | -0.08 | -0.02 | -0.10 | 0.20 |
| 30 | -0.50 | -0.37 | -0.37 | -0.33 | -0.46 | -0.47 | 0.17 |
| 31 | 0.73 | 0.00 | 0.63 | 0.09 | 0.82 | 0.19 | 0.18 |
| 32 | 0.94 | 0.97 | 0.98 | -0.05 | -0.01 | 0.01 | 0.02 |
| 33 | 0.96 | 0.55 | 0.91 | -0.02 | -0.43 | -0.07 | 0.02 |
| 34 | 0.92 | 0.73 | 0.93 | 0.01 | -0.21 | -0.01 | 0.07 |
| 35 | 0.27 | 0.29 | 0.25 | -0.03 | 0.01 | 0.05 | 0.70 |
| 36 | -0.04 | -0.06 | -0.06 | -0.03 | 0.00 | 0.01 | 0.93 |
| 37 | -0.72 | -0.33 | -0.11 | 0.05 | -0.43 | -0.66 | 0.24 |
| 38 | 0.73 | 0.55 | 0.71 | -0.03 | -0.21 | -0.04 | 0.25 |
| 39 | -0.88 | -0.84 | -0.93 | -0.04 | 0.08 | 0.00 | 0.07 |
| 40 | 0.87 | 0.80 | 0.98 | -0.12 | -0.20 | -0.01 | 0.00 |
| 41 | -0.11 | -0.07 | -0.10 | 0.02 | -0.07 | -0.04 | 0.86 |
| 42 | 0.16 | 0.07 | 0.00 | 0.67 | 0.75 | 0.82 | 0.18 |
| 43 | 0.32 | 0.27 | 0.14 | 0.32 | 0.37 | 0.50 | 0.36 |
| 44 | 0.55 | 0.41 | 0.00 | 0.09 | 0.23 | 0.64 | 0.36 |
| 45 | 0.60 | 0.74 | 0.67 | 0.26 | 0.12 | 0.19 | 0.14 |

| | | | | | | | |
|---|---|---|---|---|---|---|---|
| 46 | -0.41 | -0.48 | -0.47 | -0.59 | -0.52 | -0.53 | 0.00 |
| 47 | 0.08 | 0.04 | 0.09 | -0.02 | -0.05 | 0.00 | 0.91 |
| 48 | 0.27 | 0.18 | 0.56 | -0.63 | -0.72 | -0.35 | 0.10 |
| 49 | 0.94 | 0.76 | 0.94 | -0.03 | -0.21 | -0.03 | 0.03 |

Table 5.2: Comparison of the WSF algorithm with the DBH Model and the Sato formula, without any hue correction for data set 2

| Std. No | WSF KΔD | DBH KΔD | SATO KΔD | WSF KΔB | DBH KΔB | SATO KΔB | ΔH |
|---|---|---|---|---|---|---|---|
| 1 | -0.71 | -0.77 | -1.14 | 1.68 | 1.65 | 1.42 | 0.82 |
| 2 | 1.95 | 1.37 | 0.39 | 2.61 | 2.96 | 3.24 | 0.42 |
| 3 | 0.10 | 0.06 | -0.10 | 0.28 | 0.29 | 0.28 | 0.55 |
| 4 | 0.40 | 0.13 | 0.38 | -0.74 | -0.83 | -0.74 | 0.38 |
| 5 | 0.23 | 0.17 | 0.22 | -0.17 | -0.23 | -0.19 | 0.63 |
| 6 | 0.30 | 0.28 | -0.12 | 0.93 | 0.93 | 0.96 | 0.13 |
| 7 | 0.12 | 0.41 | 0.39 | 0.54 | 0.37 | 0.39 | 0.37 |
| 8 | -1.20 | -1.33 | -0.76 | -1.98 | -1.90 | -2.19 | 1.00 |
| 9 | -4.95 | -3.73 | -4.49 | -0.22 | 3.27 | 2.11 | 0.28 |
| 10 | -3.24 | -2.56 | -2.59 | 0.18 | 2.00 | 1.96 | 6.95 |
| 11 | 2.34 | 1.26 | 2.89 | -5.51 | -5.85 | -5.24 | 1.64 |
| 12 | -2.07 | -1.68 | -2.04 | -0.24 | 1.24 | -0.46 | 0.34 |
| 13 | -2.26 | -1.88 | -2.32 | -0.50 | 1.35 | -0.07 | 0.29 |
| 14 | -2.20 | -1.90 | -1.76 | -1.69 | -2.03 | -2.15 | 0.58 |
| 15 | -0.89 | -0.85 | -0.25 | -1.45 | -1.47 | -1.68 | 0.84 |
| 16 | 1.38 | 1.14 | 0.19 | 2.17 | 2.31 | 2.57 | 0.48 |
| 17 | 0.84 | 0.85 | 0.78 | -0.70 | -0.69 | -0.77 | 0.58 |
| 18 | 0.89 | 0.44 | 1.59 | -4.61 | -4.68 | -4.42 | 4.24 |
| 19 | 2.34 | 0.06 | 0.53 | 0.15 | -2.34 | -2.28 | 0.37 |
| 20 | 0.56 | 0.46 | 0.18 | 0.09 | -0.33 | -0.54 | 1.35 |
| 21 | 0.21 | 0.85 | 0.54 | -1.67 | -1.46 | -1.59 | 0.34 |
| 22 | -0.50 | -0.68 | -0.60 | 0.47 | 0.10 | 0.34 | 0.23 |
| 23 | 0.72 | 0.76 | 0.68 | -0.27 | -0.06 | -0.34 | 0.21 |
| 24 | 0.38 | 0.36 | 0.39 | 0.09 | -0.16 | 0.05 | 0.04 |
| 25 | 0.23 | 0.25 | 0.21 | -0.13 | -0.07 | -0.15 | 0.01 |
| 26 | 0.39 | 0.17 | 0.22 | 0.39 | 0.52 | 0.50 | 0.71 |
| 27 | -1.92 | -1.76 | -1.94 | 0.32 | 0.82 | 0.09 | 0.25 |
| 28 | -1.08 | -0.76 | -1.03 | -0.22 | -0.80 | -0.39 | 1.11 |
| 29 | -1.63 | -1.34 | -1.50 | -0.77 | -1.20 | -1.00 | 0.56 |
| 30 | -0.80 | -0.86 | -0.88 | 0.40 | 0.27 | 0.19 | 0.20 |
| 31 | -1.26 | -1.03 | -1.27 | 0.20 | 0.75 | -0.16 | 0.13 |
| 32 | 0.08 | 0.03 | -0.39 | 0.74 | 0.74 | 0.63 | 1.23 |
| 33 | 0.77 | 0.40 | 0.81 | -0.84 | -1.07 | -0.80 | 0.61 |
| 34 | 2.05 | 1.44 | 1.70 | 0.25 | 1.48 | 1.17 | 0.09 |
| 35 | 0.76 | 0.75 | 0.80 | -0.36 | -0.38 | -0.26 | 0.90 |
| 36 | 0.73 | 0.65 | 0.77 | -0.23 | -0.41 | -0.06 | 1.08 |
| 37 | 2.74 | 2.46 | 6.15 | -10.31 | -10.38 | -8.72 | 2.14 |
| 38 | 0.27 | 0.25 | 0.27 | 0.12 | 0.15 | 0.12 | 0.39 |
| 39 | 0.42 | 0.13 | 0.68 | -1.16 | -1.23 | -1.03 | 0.71 |
| 40 | 0.10 | 0.01 | 0.07 | -0.14 | -0.17 | -0.15 | 0.52 |
| 41 | 1.13 | 1.05 | 1.14 | 0.26 | -0.49 | 0.15 | 0.30 |
| 42 | 1.16 | 1.10 | 1.08 | 0.90 | 0.97 | 0.99 | 0.63 |
| 43 | 0.49 | 0.54 | 0.52 | -0.22 | -0.04 | -0.12 | 0.00 |
| 44 | 0.14 | -0.08 | 0.40 | -1.02 | -1.03 | -0.95 | 0.02 |
| 45 | 0.55 | 0.55 | 0.48 | 0.57 | 0.57 | 0.63 | 0.12 |

| | | | | | | | |
|---|---|---|---|---|---|---|---|
| 46 | 0.68 | 0.68 | 0.70 | 0.20 | -0.21 | 0.08 | 0.91 |
| 47 | -1.42 | -1.38 | -1.42 | -0.27 | -0.44 | -0.31 | 0.15 |
| 48 | -0.54 | -0.56 | -0.57 | 0.19 | 0.13 | -0.06 | 0.59 |
| 49 | -0.28 | -0.52 | -0.65 | 1.15 | 1.06 | 0.99 | 1.51 |
| 50 | 0.11 | -0.11 | -0.17 | 0.68 | 0.68 | 0.66 | 0.73 |
| 51 | 0.11 | -0.08 | -0.02 | 0.53 | 0.54 | 0.54 | 0.29 |
| 52 | 0.60 | 0.47 | 0.53 | 0.50 | 0.62 | 0.57 | 0.62 |
| 53 | 0.13 | 0.39 | 0.29 | -1.45 | -1.40 | -1.42 | 0.23 |
| 54 | 0.13 | 0.43 | 0.33 | -1.47 | -1.41 | -1.43 | 0.23 |
| 55 | 0.97 | 1.14 | 1.27 | -1.25 | -1.11 | -0.95 | 0.76 |
| 56 | 1.61 | 1.44 | 1.57 | 0.06 | -0.72 | 0.34 | 1.37 |
| 57 | -0.92 | -0.76 | -0.79 | -0.40 | -0.65 | -0.62 | 0.13 |
| 58 | 0.13 | 0.13 | 0.00 | 0.41 | 0.41 | 0.43 | 0.05 |
| 59 | 1.45 | 1.20 | 0.56 | 1.57 | 1.77 | 2.06 | 1.44 |
| 60 | 0.41 | 0.37 | -3.01 | 8.32 | 8.32 | 7.77 | 1.42 |
| 61 | 0.14 | -0.14 | 0.32 | -1.02 | -1.02 | -0.98 | 0.39 |
| 62 | 1.47 | 1.01 | 1.72 | -1.58 | -1.91 | -1.31 | 0.45 |
| 63 | 0.99 | 0.76 | 1.58 | -1.90 | -2.00 | -1.45 | 0.34 |
| 64 | 0.41 | 0.15 | 0.45 | -0.48 | -0.62 | -0.45 | 0.49 |
| 65 | -1.02 | -1.00 | -1.04 | -0.41 | -0.46 | -0.35 | 0.46 |
| 66 | 1.33 | 1.30 | 1.33 | -0.25 | -0.35 | -0.23 | 0.50 |
| 67 | 1.24 | 1.24 | 1.28 | 0.47 | 0.45 | 0.33 | 0.30 |
| 68 | 0.31 | 0.04 | 0.24 | -0.44 | -0.53 | -0.48 | 0.64 |
| 69 | 1.09 | 1.20 | 1.26 | 0.89 | 0.73 | 0.63 | 1.02 |
| 70 | -0.32 | -0.47 | 0.62 | -3.33 | -3.31 | -3.29 | 0.89 |
| 71 | 0.96 | 0.98 | 1.01 | 0.37 | 0.32 | 0.19 | 0.12 |
| 72 | 2.18 | 2.26 | 2.22 | -0.69 | -0.35 | -0.55 | 0.22 |
| 73 | 0.23 | 0.25 | 0.24 | 0.10 | -0.03 | -0.09 | 1.52 |
| 74 | 2.22 | 2.23 | 2.24 | 0.35 | -0.30 | 0.16 | 0.31 |
| 75 | 0.28 | -0.98 | -0.81 | 5.17 | 5.08 | 5.11 | 0.52 |
| 76 | 0.29 | 0.84 | 0.51 | -1.40 | -1.15 | -1.34 | 3.13 |
| 77 | 0.41 | 0.43 | 0.50 | -0.81 | -0.81 | -0.76 | 0.55 |
| 78 | -1.15 | -1.32 | -1.35 | 0.87 | 0.57 | 0.51 | 0.69 |
| 79 | 2.43 | 2.21 | 2.30 | 0.95 | 1.40 | 1.24 | 0.92 |
| 80 | -0.18 | -0.19 | -0.13 | 0.86 | 0.86 | 0.87 | 1.08 |
| 81 | 0.65 | -0.47 | 0.99 | -3.00 | -3.03 | -2.90 | 1.10 |
| 82 | -1.38 | -1.24 | -1.18 | -0.41 | -0.73 | -0.83 | 0.98 |
| 83 | -0.54 | -0.42 | -0.47 | -0.14 | -0.37 | -0.30 | 0.72 |
| 84 | -0.22 | -0.27 | -0.27 | -0.15 | -0.02 | -0.02 | 0.50 |
| 85 | 0.49 | -0.48 | 0.14 | -1.00 | -1.00 | -1.10 | 1.31 |
| 86 | -0.98 | -1.08 | -1.11 | -0.73 | -0.57 | -0.51 | 0.05 |
| 87 | 1.73 | 1.74 | 1.74 | 0.28 | 0.27 | 0.27 | 0.63 |
| 88 | -0.78 | -0.78 | -0.79 | 0.13 | 0.11 | 0.08 | 0.15 |
| 89 | -2.54 | -2.14 | -2.81 | 1.76 | 2.23 | 1.28 | 0.08 |
| 90 | -0.57 | -0.54 | -0.54 | -0.31 | -0.36 | -0.36 | 0.14 |
| 91 | 1.26 | 1.31 | 1.31 | 0.37 | -0.04 | 0.14 | 1.01 |
| 92 | 0.47 | 0.44 | 0.54 | 0.39 | 0.42 | 0.28 | 0.76 |
| 93 | 0.61 | 0.61 | 0.64 | 0.28 | 0.28 | 0.19 | 0.70 |
| 94 | 1.75 | 1.77 | 1.77 | 0.41 | 0.28 | 0.30 | 0.15 |
| 95 | 2.45 | 2.28 | 2.38 | 0.84 | 1.23 | 1.03 | 0.30 |
| 96 | -0.73 | -0.76 | -0.75 | -0.29 | -0.21 | -0.24 | 0.38 |

| | | | | | | | |
|---|---|---|---|---|---|---|---|
| 97 | 1.29 | -0.37 | 1.42 | -1.57 | -2.00 | -1.46 | 3.43 |
| 98 | 1.58 | 0.76 | 2.26 | -2.49 | -2.85 | -1.89 | 0.21 |
| 99 | 0.98 | 0.08 | 1.32 | -1.86 | -2.10 | -1.63 | 0.67 |
| 100 | -0.43 | -0.77 | -0.43 | -0.79 | -0.47 | -0.79 | 2.72 |
| 101 | 0.31 | 0.38 | 0.36 | -0.23 | -0.07 | 0.13 | 2.08 |
| 102 | 0.51 | 0.41 | 0.31 | 0.39 | 0.50 | 0.56 | 0.20 |
| 103 | -0.06 | -0.94 | 0.61 | -3.36 | -3.22 | -3.30 | 0.58 |
| 104 | 0.17 | 0.09 | 0.16 | -0.14 | -0.20 | -0.15 | 0.34 |
| 105 | -0.05 | -0.21 | -0.11 | -0.31 | -0.23 | -0.29 | 0.83 |
| 106 | -1.21 | -1.22 | -1.25 | 0.33 | 0.29 | 0.02 | 0.06 |
| 107 | 2.16 | 2.26 | 2.20 | 1.40 | 1.23 | 1.32 | 0.85 |
| 108 | 0.37 | 0.11 | 0.30 | 1.51 | 1.55 | 1.53 | 1.05 |
| 109 | -1.42 | -1.51 | -1.72 | 1.04 | 0.91 | 0.35 | 0.33 |
| 110 | -2.50 | -2.58 | -2.52 | -3.53 | -3.48 | -3.52 | 0.94 |
| 111 | 0.03 | -0.04 | 0.03 | 0.03 | 0.03 | 0.04 | 0.71 |
| 112 | 0.15 | 0.57 | -0.14 | 1.95 | 1.87 | 1.95 | 0.45 |
| 113 | 0.28 | 0.45 | 0.17 | 0.61 | 0.49 | 0.65 | 1.05 |
| 114 | 0.11 | 0.73 | -0.42 | 2.38 | 2.27 | 2.35 | 1.24 |
| 115 | -2.41 | -1.31 | -2.92 | 1.74 | 2.67 | 0.57 | 1.44 |
| 116 | -0.55 | -0.61 | -0.59 | 0.26 | -0.05 | -0.15 | 0.00 |
| 117 | -0.17 | -0.42 | -0.49 | 0.51 | 0.34 | 0.20 | 0.76 |

It has been explained earlier in the thesis that if the hue of the batch is different from the hue of the standard then hue correction of the batch is necessary. Here it is worth noting that the DBH and the Sato models include a hue correction procedure in any case. In the case of the DBH model, hue correction is achieved by defining a third parabola with the $L^*$ and $C^*$ coordinates of the standard, whose vertex is defined by the mixed coordinates of the standard and the batch. The $L^*$ coordinate is determined by the hue angle of the standard and $C^*$ coordinate is calculated from the batch parameters [69]. Sato's model predicts the depth and brightness of the batch and the standard by dividing the hue circle into three groups: samples with hue angle less than $110^\circ$ , samples with hue angle less than $290^\circ$ but greater than $110^\circ$, samples with hue angle greater than $290^\circ$ but less than $360^\circ$ [65, 66]. Figure 5.3 (a & b) and Figure 5.4 (a & b) shows the extent to which the hue correction to the WSF algorithm affects its correlation with DBH and Sato's output in terms of $\Delta D$ and $\Delta B$. The computed differences in depth and brightness by all three algorithms are given in Tables 5.3 and 5.4.

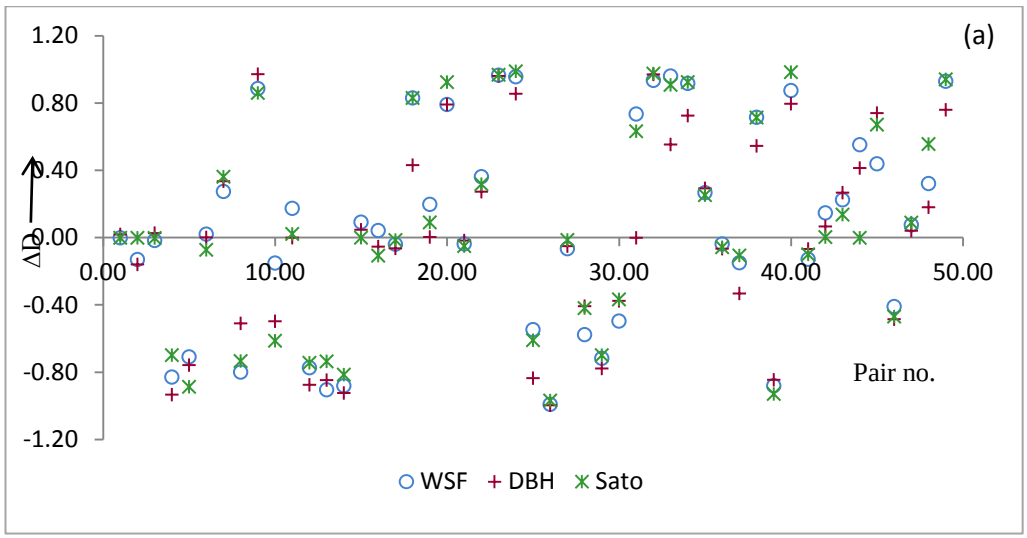


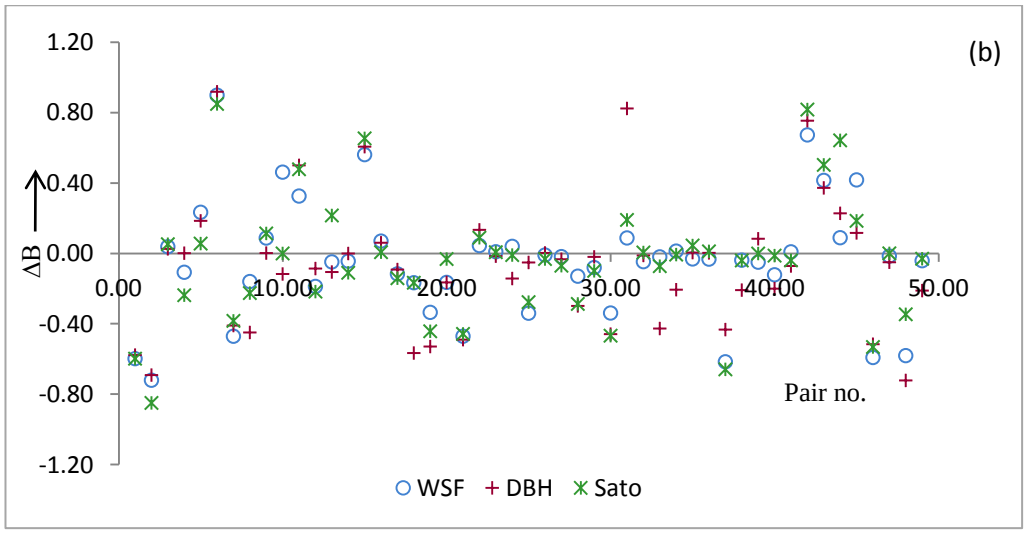


Figure 5.3 (a & b): Comparison of ΔD and ΔB values computed by the WSF, DBH and Sato algorithms after performing hue correction to the batch, for data set 1

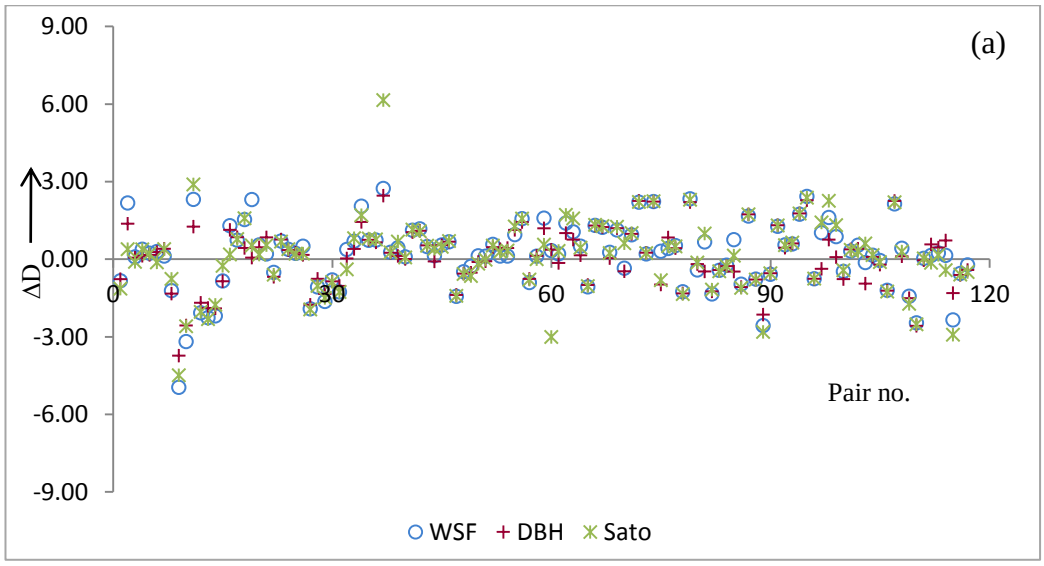

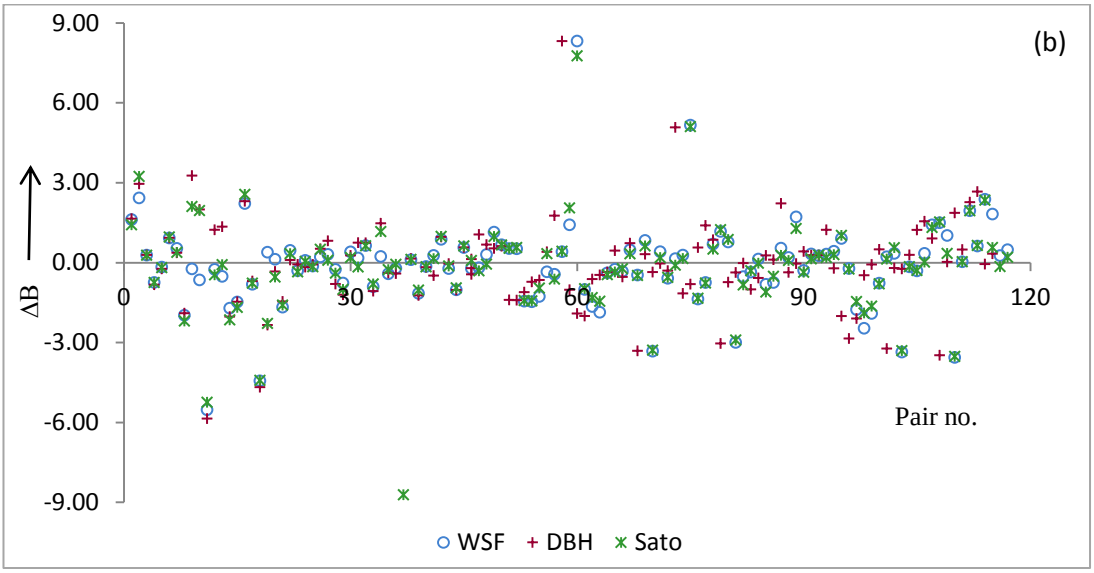


Figure 5.4(a & b): Comparison of ΔD and ΔB values computed by the WSF, DBH and Sato algorithms after performing hue correction to the batch, for data set 2

Table 5.3: Comparison of the WSF algorithm with the DBH Model and the Sato formula after hue correction, for data set 1

| Pair no. | WSF kΔD | DBH kΔD | Sato kΔD | WSF kΔB | DBH kΔB | Sato kΔB | ΔH |
|---|---|---|---|---|---|---|---|
| 1 | 0.00 | 0.02 | 0.00 | -0.60 | -0.58 | -0.60 | 0.40 |
| 2 | -0.13 | -0.16 | 0.00 | -0.72 | -0.69 | -0.85 | 0.15 |
| 3 | -0.02 | 0.03 | 0.00 | 0.04 | 0.03 | 0.05 | 0.95 |
| 4 | -0.83 | -0.93 | -0.70 | -0.11 | 0.00 | -0.24 | 0.07 |
| 5 | -0.71 | -0.76 | -0.89 | 0.23 | 0.19 | 0.06 | 0.06 |
| 6 | 0.02 | 0.00 | -0.07 | 0.90 | 0.92 | 0.85 | 0.08 |
| 7 | 0.28 | 0.34 | 0.36 | -0.47 | -0.41 | -0.38 | 0.25 |
| 8 | -0.80 | -0.51 | -0.73 | -0.16 | -0.45 | -0.22 | 0.04 |
| 9 | 0.89 | 0.97 | 0.86 | 0.09 | 0.00 | 0.11 | 0.02 |
| 10 | -0.15 | -0.50 | -0.61 | 0.46 | -0.12 | 0.00 | 0.39 |
| 11 | 0.18 | 0.00 | 0.02 | 0.33 | 0.50 | 0.48 | 0.50 |
| 12 | -0.77 | -0.87 | -0.74 | -0.19 | -0.09 | -0.22 | 0.04 |
| 13 | -0.90 | -0.85 | -0.73 | -0.05 | -0.10 | 0.22 | 0.05 |
| 14 | -0.88 | -0.92 | -0.81 | -0.04 | 0.00 | -0.11 | 0.08 |
| 15 | 0.09 | 0.05 | 0.00 | 0.56 | 0.61 | 0.65 | 0.35 |
| 16 | 0.04 | -0.05 | -0.11 | 0.07 | 0.06 | 0.01 | 0.89 |
| 17 | -0.04 | -0.06 | -0.01 | -0.12 | -0.09 | -0.14 | 0.85 |
| 18 | 0.83 | 0.43 | 0.83 | -0.17 | -0.57 | -0.17 | 0.00 |
| 19 | 0.20 | 0.00 | 0.09 | -0.33 | -0.53 | -0.44 | 0.47 |
| 20 | 0.79 | 0.79 | 0.93 | -0.16 | -0.16 | -0.03 | 0.04 |
| 21 | -0.04 | -0.02 | -0.05 | -0.47 | -0.49 | -0.46 | 0.49 |
| 22 | 0.36 | 0.27 | 0.32 | 0.05 | 0.13 | 0.09 | 0.59 |
| 23 | 0.97 | 0.96 | 0.97 | 0.01 | -0.01 | 0.01 | 0.02 |
| 24 | 0.96 | 0.86 | 0.99 | 0.04 | -0.14 | -0.01 | 0.00 |
| 25 | -0.55 | -0.83 | -0.61 | -0.34 | -0.05 | -0.28 | 0.12 |
| 26 | -0.99 | -1.00 | -0.97 | -0.01 | 0.00 | -0.03 | 0.00 |
| 27 | -0.06 | -0.05 | -0.01 | -0.02 | -0.03 | -0.07 | 0.92 |
| 28 | -0.58 | -0.41 | -0.42 | -0.13 | -0.30 | -0.29 | 0.30 |
| 29 | -0.72 | -0.78 | -0.70 | -0.08 | -0.02 | -0.10 | 0.20 |
| 30 | -0.49 | -0.37 | -0.37 | -0.34 | -0.46 | -0.47 | 0.17 |
| 31 | 0.74 | 0.00 | 0.63 | 0.09 | 0.82 | 0.19 | 0.18 |
| 32 | 0.94 | 0.97 | 0.98 | -0.05 | -0.01 | 0.01 | 0.02 |
| 33 | 0.96 | 0.55 | 0.91 | -0.02 | -0.43 | -0.07 | 0.02 |
| 34 | 0.92 | 0.73 | 0.93 | 0.01 | -0.21 | -0.01 | 0.07 |
| 35 | 0.27 | 0.29 | 0.25 | -0.03 | 0.01 | 0.05 | 0.70 |
| 36 | -0.04 | -0.06 | -0.06 | -0.03 | 0.00 | 0.01 | 0.93 |
| 37 | -0.15 | -0.33 | -0.11 | -0.62 | -0.43 | -0.66 | 0.24 |
| 38 | 0.72 | 0.55 | 0.71 | -0.04 | -0.21 | -0.04 | 0.25 |
| 39 | -0.88 | -0.84 | -0.93 | -0.05 | 0.08 | 0.00 | 0.07 |
| 40 | 0.88 | 0.80 | 0.98 | -0.12 | -0.20 | -0.01 | 0.00 |
| 41 | -0.13 | -0.07 | -0.10 | 0.01 | -0.07 | -0.04 | 0.86 |
| 42 | 0.15 | 0.07 | 0.00 | 0.67 | 0.75 | 0.82 | 0.18 |
| 43 | 0.23 | 0.27 | 0.14 | 0.42 | 0.37 | 0.50 | 0.36 |
| 44 | 0.55 | 0.41 | 0.00 | 0.09 | 0.23 | 0.64 | 0.36 |
| 45 | 0.44 | 0.74 | 0.67 | 0.42 | 0.12 | 0.19 | 0.14 |

| | | | | | | | |
|---|---|---|---|---|---|---|---|
| 46 | -0.41 | -0.48 | -0.47 | -0.59 | -0.52 | -0.53 | 0.00 |
| 47 | 0.08 | 0.04 | 0.09 | -0.01 | -0.05 | 0.00 | 0.91 |
| 48 | 0.32 | 0.18 | 0.56 | -0.58 | -0.72 | -0.35 | 0.10 |
| 49 | 0.93 | 0.76 | 0.94 | -0.04 | -0.21 | -0.03 | 0.03 |

Table 5.4: Comparison of the WSF algorithm with the DBH Model and the Sato formula after hue correction, for data set 2

| Pair no. | WSF kΔD | DBH kΔD | Sato kΔD | WSF kΔB | DBH kΔB | Sato kΔB | ΔH |
|---|---|---|---|---|---|---|---|
| 1 | -0.83 | -0.77 | -1.14 | 1.62 | 1.65 | 1.42 | 0.82 |
| 2 | 2.18 | 1.37 | 0.39 | 2.43 | 2.96 | 3.24 | 0.42 |
| 3 | 0.09 | 0.06 | -0.10 | 0.28 | 0.29 | 0.28 | 0.55 |
| 4 | 0.39 | 0.13 | 0.38 | -0.74 | -0.83 | -0.74 | 0.38 |
| 5 | 0.23 | 0.17 | 0.22 | -0.17 | -0.23 | -0.19 | 0.63 |
| 6 | 0.30 | 0.28 | -0.12 | 0.93 | 0.93 | 0.96 | 0.13 |
| 7 | 0.12 | 0.41 | 0.39 | 0.54 | 0.37 | 0.39 | 0.37 |
| 8 | -1.21 | -1.33 | -0.76 | -1.97 | -1.90 | -2.19 | 1.00 |
| 9 | -4.95 | -3.73 | -4.49 | -0.23 | 3.27 | 2.11 | 0.28 |
| 10 | -3.18 | -2.56 | -2.59 | -0.65 | 2.00 | 1.96 | 6.95 |
| 11 | 2.31 | 1.26 | 2.89 | -5.52 | -5.85 | -5.24 | 1.64 |
| 12 | -2.07 | -1.68 | -2.04 | -0.25 | 1.24 | -0.46 | 0.34 |
| 13 | -2.26 | -1.88 | -2.32 | -0.52 | 1.35 | -0.07 | 0.29 |
| 14 | -2.19 | -1.90 | -1.76 | -1.71 | -2.03 | -2.15 | 0.58 |
| 15 | -0.84 | -0.85 | -0.25 | -1.48 | -1.47 | -1.68 | 0.84 |
| 16 | 1.30 | 1.14 | 0.19 | 2.22 | 2.31 | 2.57 | 0.48 |
| 17 | 0.74 | 0.85 | 0.78 | -0.81 | -0.69 | -0.77 | 0.58 |
| 18 | 1.53 | 0.44 | 1.59 | -4.44 | -4.68 | -4.42 | 4.24 |
| 19 | 2.31 | 0.06 | 0.53 | 0.39 | -2.34 | -2.28 | 0.37 |
| 20 | 0.55 | 0.46 | 0.18 | 0.13 | -0.33 | -0.54 | 1.35 |
| 21 | 0.21 | 0.85 | 0.54 | -1.67 | -1.46 | -1.59 | 0.34 |
| 22 | -0.51 | -0.68 | -0.60 | 0.46 | 0.10 | 0.34 | 0.23 |
| 23 | 0.70 | 0.76 | 0.68 | -0.30 | -0.06 | -0.34 | 0.21 |
| 24 | 0.38 | 0.36 | 0.39 | 0.09 | -0.16 | 0.05 | 0.04 |
| 25 | 0.23 | 0.25 | 0.21 | -0.13 | -0.07 | -0.15 | 0.01 |
| 26 | 0.50 | 0.17 | 0.22 | 0.22 | 0.52 | 0.50 | 0.71 |
| 27 | -1.92 | -1.76 | -1.94 | 0.31 | 0.82 | 0.09 | 0.25 |
| 28 | -1.07 | -0.76 | -1.03 | -0.25 | -0.80 | -0.39 | 1.11 |
| 29 | -1.63 | -1.34 | -1.50 | -0.76 | -1.20 | -1.00 | 0.56 |
| 30 | -0.80 | -0.86 | -0.88 | 0.41 | 0.27 | 0.19 | 0.20 |
| 31 | -1.26 | -1.03 | -1.27 | 0.18 | 0.75 | -0.16 | 0.13 |
| 32 | 0.38 | 0.03 | -0.39 | 0.64 | 0.74 | 0.63 | 1.23 |
| 33 | 0.70 | 0.40 | 0.81 | -0.90 | -1.07 | -0.80 | 0.61 |
| 34 | 2.05 | 1.44 | 1.70 | 0.23 | 1.48 | 1.17 | 0.09 |
| 35 | 0.73 | 0.75 | 0.80 | -0.42 | -0.38 | -0.26 | 0.90 |
| 36 | 0.74 | 0.65 | 0.77 | -0.21 | -0.41 | -0.06 | 1.08 |
| 37 | 2.74 | 2.46 | 6.15 | -10.31 | -10.38 | -8.72 | 2.14 |
| 38 | 0.27 | 0.25 | 0.27 | 0.11 | 0.15 | 0.12 | 0.39 |
| 39 | 0.44 | 0.13 | 0.68 | -1.15 | -1.23 | -1.03 | 0.71 |
| 40 | 0.09 | 0.01 | 0.07 | -0.14 | -0.17 | -0.15 | 0.52 |
| 41 | 1.12 | 1.05 | 1.14 | 0.27 | -0.49 | 0.15 | 0.30 |
| 42 | 1.18 | 1.10 | 1.08 | 0.88 | 0.97 | 0.99 | 0.63 |
| 43 | 0.49 | 0.54 | 0.52 | -0.22 | -0.04 | -0.12 | 0.00 |
| 44 | 0.14 | -0.08 | 0.40 | -1.02 | -1.03 | -0.95 | 0.02 |
| 45 | 0.55 | 0.55 | 0.48 | 0.57 | 0.57 | 0.63 | 0.12 |

| | | | | | | | |
|---|---|---|---|---|---|---|---|
| 46 | 0.67 | 0.68 | 0.70 | -0.22 | -0.21 | 0.08 | 0.91 |
| 47 | -1.44 | -1.38 | -1.42 | -0.19 | -0.44 | -0.31 | 0.15 |
| 48 | -0.48 | -0.56 | -0.57 | 0.31 | 0.13 | -0.06 | 0.59 |
| 49 | -0.27 | -0.52 | -0.65 | 1.15 | 1.06 | 0.99 | 1.51 |
| 50 | 0.13 | -0.11 | -0.17 | 0.67 | 0.68 | 0.66 | 0.73 |
| 51 | 0.12 | -0.08 | -0.02 | 0.53 | 0.54 | 0.54 | 0.29 |
| 52 | 0.58 | 0.47 | 0.53 | 0.52 | 0.62 | 0.57 | 0.62 |
| 53 | 0.12 | 0.39 | 0.29 | -1.45 | -1.40 | -1.42 | 0.23 |
| 54 | 0.12 | 0.43 | 0.33 | -1.47 | -1.41 | -1.43 | 0.23 |
| 55 | 0.95 | 1.14 | 1.27 | -1.27 | -1.11 | -0.95 | 0.76 |
| 56 | 1.57 | 1.44 | 1.57 | -0.34 | -0.72 | 0.34 | 1.37 |
| 57 | -0.90 | -0.76 | -0.79 | -0.44 | -0.65 | -0.62 | 0.13 |
| 58 | 0.12 | 0.13 | 0.00 | 0.41 | 0.41 | 0.43 | 0.05 |
| 59 | 1.59 | 1.20 | 0.56 | 1.42 | 1.77 | 2.06 | 1.44 |
| 60 | 0.33 | 0.37 | -3.01 | 8.32 | 8.32 | 7.77 | 1.42 |
| 61 | 0.21 | -0.14 | 0.32 | -1.01 | -1.02 | -0.98 | 0.39 |
| 62 | 1.40 | 1.01 | 1.72 | -1.65 | -1.91 | -1.31 | 0.45 |
| 63 | 1.06 | 0.76 | 1.58 | -1.86 | -2.00 | -1.45 | 0.34 |
| 64 | 0.51 | 0.15 | 0.45 | -0.38 | -0.62 | -0.45 | 0.49 |
| 65 | -1.07 | -1.00 | -1.04 | -0.25 | -0.46 | -0.35 | 0.46 |
| 66 | 1.31 | 1.30 | 1.33 | -0.33 | -0.35 | -0.23 | 0.50 |
| 67 | 1.23 | 1.24 | 1.28 | 0.48 | 0.45 | 0.33 | 0.30 |
| 68 | 0.27 | 0.04 | 0.24 | -0.46 | -0.53 | -0.48 | 0.64 |
| 69 | 1.13 | 1.20 | 1.26 | 0.84 | 0.73 | 0.63 | 1.02 |
| 70 | -0.35 | -0.47 | 0.62 | -3.32 | -3.31 | -3.29 | 0.89 |
| 71 | 0.94 | 0.98 | 1.01 | 0.41 | 0.32 | 0.19 | 0.12 |
| 72 | 2.21 | 2.26 | 2.22 | -0.59 | -0.35 | -0.55 | 0.22 |
| 73 | 0.21 | 0.25 | 0.24 | 0.15 | -0.03 | -0.09 | 1.52 |
| 74 | 2.23 | 2.23 | 2.24 | 0.28 | -0.30 | 0.16 | 0.31 |
| 75 | 0.31 | -0.98 | -0.81 | 5.17 | 5.08 | 5.11 | 0.52 |
| 76 | 0.42 | 0.84 | 0.51 | -1.37 | -1.15 | -1.34 | 3.13 |
| 77 | 0.53 | 0.43 | 0.50 | -0.74 | -0.81 | -0.76 | 0.55 |
| 78 | -1.26 | -1.32 | -1.35 | 0.70 | 0.57 | 0.51 | 0.69 |
| 79 | 2.34 | 2.21 | 2.30 | 1.17 | 1.40 | 1.24 | 0.92 |
| 80 | -0.41 | -0.19 | -0.13 | 0.78 | 0.86 | 0.87 | 1.08 |
| 81 | 0.67 | -0.47 | 0.99 | -3.00 | -3.03 | -2.90 | 1.10 |
| 82 | -1.34 | -1.24 | -1.18 | -0.52 | -0.73 | -0.83 | 0.98 |
| 83 | -0.43 | -0.42 | -0.47 | -0.35 | -0.37 | -0.30 | 0.72 |
| 84 | -0.23 | -0.27 | -0.27 | 0.14 | -0.02 | -0.02 | 0.50 |
| 85 | 0.76 | -0.48 | 0.14 | -0.81 | -1.00 | -1.10 | 1.31 |
| 86 | -0.97 | -1.08 | -1.11 | -0.74 | -0.57 | -0.51 | 0.05 |
| 87 | 1.67 | 1.74 | 1.74 | 0.55 | 0.27 | 0.27 | 0.63 |
| 88 | -0.77 | -0.78 | -0.79 | 0.20 | 0.11 | 0.08 | 0.15 |
| 89 | -2.57 | -2.14 | -2.81 | 1.72 | 2.23 | 1.28 | 0.08 |
| 90 | -0.58 | -0.54 | -0.54 | -0.29 | -0.36 | -0.36 | 0.14 |
| 91 | 1.27 | 1.31 | 1.31 | 0.33 | -0.04 | 0.14 | 1.01 |
| 92 | 0.56 | 0.44 | 0.54 | 0.26 | 0.42 | 0.28 | 0.76 |
| 93 | 0.59 | 0.61 | 0.64 | 0.32 | 0.28 | 0.19 | 0.70 |
| 94 | 1.74 | 1.77 | 1.77 | 0.43 | 0.28 | 0.30 | 0.15 |
| 95 | 2.43 | 2.28 | 2.38 | 0.91 | 1.23 | 1.03 | 0.30 |
| 96 | -0.75 | -0.76 | -0.75 | -0.22 | -0.21 | -0.24 | 0.38 |

| | | | | | | | |
|---|---|---|---|---|---|---|---|
| 97 | 1.03 | -0.37 | 1.42 | -1.76 | -2.00 | -1.46 | 3.43 |
| 98 | 1.62 | 0.76 | 2.26 | -2.46 | -2.85 | -1.89 | 0.21 |
| 99 | 0.87 | 0.08 | 1.32 | -1.91 | -2.10 | -1.63 | 0.67 |
| 100 | -0.47 | -0.77 | -0.43 | -0.77 | -0.47 | -0.79 | 2.72 |
| 101 | 0.32 | 0.38 | 0.36 | 0.22 | -0.07 | 0.13 | 2.08 |
| 102 | 0.54 | 0.41 | 0.31 | 0.35 | 0.50 | 0.56 | 0.20 |
| 103 | -0.13 | -0.94 | 0.61 | -3.36 | -3.22 | -3.30 | 0.58 |
| 104 | 0.16 | 0.09 | 0.16 | -0.16 | -0.20 | -0.15 | 0.34 |
| 105 | -0.05 | -0.21 | -0.11 | -0.31 | -0.23 | -0.29 | 0.83 |
| 106 | -1.20 | -1.22 | -1.25 | 0.35 | 0.29 | 0.02 | 0.06 |
| 107 | 2.14 | 2.26 | 2.20 | 1.42 | 1.23 | 1.32 | 0.85 |
| 108 | 0.42 | 0.11 | 0.30 | 1.50 | 1.55 | 1.53 | 1.05 |
| 109 | -1.43 | -1.51 | -1.72 | 1.02 | 0.91 | 0.35 | 0.33 |
| 110 | -2.46 | -2.58 | -2.52 | -3.56 | -3.48 | -3.52 | 0.94 |
| 111 | 0.03 | -0.04 | 0.03 | 0.03 | 0.03 | 0.04 | 0.71 |
| 112 | 0.15 | 0.57 | -0.14 | 1.95 | 1.87 | 1.95 | 0.45 |
| 113 | 0.24 | 0.45 | 0.17 | 0.62 | 0.49 | 0.65 | 1.05 |
| 114 | 0.15 | 0.73 | -0.42 | 2.38 | 2.27 | 2.35 | 1.24 |
| 115 | -2.35 | -1.31 | -2.92 | 1.83 | 2.67 | 0.57 | 1.44 |
| 116 | -0.55 | -0.61 | -0.59 | 0.27 | -0.05 | -0.15 | 0.00 |
| 117 | -0.22 | -0.42 | -0.49 | 0.49 | 0.34 | 0.20 | 0.76 |

The correlation coefficients of WSF with DBH and with Sato's outputs are given in Table 5.5. They show very strong correlation between these three models in computing the difference in depth for both data sets. It is also clear that there is no noticeable effect for ΔD, both with and without any hue correction of the batch for the WSF algorithm. However, it was observed that correlation for brightness difference improves with the hue correction to the WSF algorithm of the batch for the data set 1. Strong relationships exist for all three models in evaluating the brightness differences as well.

Table 5.5: The correlation coefficient of the WSF algorithm with the DBH and the Sato models in evaluating ΔD and ΔB

| **Data set 1** | $(r)_{\Delta D}$ | $(r)_{\Delta B}$ |
|---|---|---|
| WSF with no hue correction and DBH | 0.96 | 0.76 |
| WSF with no hue correction and Sato | 0.96 | 0.80 |
| DBH and Sato | 0.96 | 0.87 |
| WSF with hue correction and DBH | 0.96 | 0.85 |
| WSF with hue correction and Sato | 0.97 | 0.91 |
| **Data set 2** | | |
| WSF with no hue correction and DBH | 0.94 | 0.96 |
| WSF with no hue correction and Sato | 0.90 | 0.97 |
| DBH and Sato | 0.87 | 0.97 |
| WSF with hue correction and DBH | 0.94 | 0.96 |
| WSF with hue correction and Sato | 0.90 | 0.97 |

### 5.2 Visual assessment results and their analysis

Two experienced colourists with an experience more than twenty years of making assessments of depth in colour manufacturing industries agreed to assess the 49 dyed pairs of data set 1. Both of the observers were male and over sixty years of age. They were asked to assess the samples with D65 illuminant and record the differences in terms of the percentage difference in depth, percentage difference in brightness and percentage difference in hue of the overall colour difference seen. The assessors returned the samples along with their assessment results to the university. Visual assessment data of two observers are given in Appendix F. The matt surface of the sample was taken for the assessment as well as for the instrumental measurement.

It is generally assumed that the difference in hue is simple to evaluate by the dyers [5, 6, 7]. A dyer usually uses a single term from redder, yellower, greener and bluer to express the difference in hue. In this work the assessors were asked to quantify the differences seen in hue along with its verbal description. It was found significant to compare the assessments of two colourists made for the differences in hue for the 49 pairs of data set 1. The quantified hue differences for data set 1 to the overall colour difference seen along with its verbal description made by both the assessors and as also from the CIELAB 1976 are summarized in Table 5.6:

Table 5.6: Qualitative and quantitative differences in hue made by two assessors and the CIELAB system

| | Assessor 1 | Assessor 2 | WSF |
|---|---|---|---|
| Pair no. | Hue difference | | Hue difference |
| 1.00 | 0.6Y | 0.5R | 0.40 R(Y) |
| 2.00 | 0.00 | 0.8Y | 0.15 Y(G) |
| 3.00 | 0.2Y | 1Y | -0.95 Y(R) |
| 4.00 | 0.00 | 0.4R | -0.07 Y(R) |
| 5.00 | 0.00 | 0.00 | -0.06 R(B) |
| 6.00 | 0.5Y | 0.4R | 0.08 Y(G) |
| 7.00 | 0.5B | 0.1R | 0.25 R(Y) |
| 8.00 | 0.6G | 1Y | -0.04G(Y) |
| 9.00 | 0.1Y | 0.1Y | -0.02G(Y) |
| 10.00 | 0.5R/B | 0.5B/R | -0.39 R(B) |
| 11.00 | 0.5R | 0.1R | -0.50 B(G) |
| 12.00 | 0.5B | 0.3B | -0.04 R(B) |
| 13.00 | 0.2B | 0.4R | 0.05 Y(G) |
| 14.00 | 0.2R | 0.5R/Y | 0.08 Y(G) |
| 15.00 | 0.5R | 0.5R | -0.35 R(B) |
| 16.00 | 1R | 0.5R | -0.89 R(B) |

| | | | |
|---|---|---|---|
| 17.00 | 1G | 0.6G | 0.85 Y(G) |
| 18.00 | 1B | 0.00 | 0.00 |
| 19.00 | 0.00 | 0.8Y | -0.47 Y(R) |
| 20.00 | 0.00 | 0.00 | -0.04 G(Y) |
| 21.00 | 0.00 | 0.1Y | -0.49 G(Y) |
| 22.00 | 0.8B | 0.8R | -0.59 B(G) |
| 23.00 | 1B | 0.00 | -0.02 Y(R) |
| 24.00 | 0.00 | 0.2G | 0.00 G(B) |
| 25.00 | 0.3G | 0.3Y/B | 0.12 G(B) |
| 26.00 | 0.00 | 0.3Y | 0.00 |
| 27.00 | 0.5R | 0.5R | -0.92 R(B) |
| 28.00 | 0.2Y | 0.00 | 0.30 R(Y) |
| 29.00 | 0.33G | 1Y | -0.20 G(Y) |
| 30.00 | 0.5B | 0.5B | -0.17B(G) |
| 31.00 | 0.5R | 1R | 0.18 B( R) |
| 32.00 | 0.5B | 0.00 | 0.02 Y(G) |
| 33.00 | 0.00 | 0.3B | -0.02 Y(R) |
| 34.00 | 0.00 | 0.8B | 0.07 G(B) |
| 35.00 | 0.5B | 0.00 | 0.70 G(B) |
| 36.00 | 0.5B | 0.3B | 0.93 G(B) |
| 37.00 | 0.5B | 0.8B | 0.24 G(B) |
| 38.00 | 0.00 | 1B | 0.25 Y(G) |
| 39.00 | 0.00 | 0.1B | 0.07 Y(G) |
| 40.00 | 0.4Y | 0.4Y | 0.00 |
| 41.00 | 1Y | 0.4Y | 0.86 Y(G) |
| 42.00 | 0.7Y | 0.6R | 0.18 R(Y) |
| 43.00 | 1Y | 0.00 | 0.36 R(Y) |
| 44.00 | 1R | 0.2B | -0.36 B(G) |
| 45.00 | 1B | 0.1B | -0.14 G(Y) |
| 46.00 | 0.33B | 0.00 | 0.00 B(R) |
| 47.00 | 1B | 0.9B | 0.91 B(R) |
| 48.00 | 0.5B | 0.3B | 0.10 G(B) |
| 49.00 | 0.00 | 0.00 | -0.03 Y(R) |

The CIELAB hue difference was calculated from Equation 2.32. The sign of the hue difference was taken as the same as the sign of the hue-angle difference, $\Delta h°_{ab}$ ($h_{batch}$-$h_{std}$) between the colour difference pair. The hue-angle difference, $\Delta h°_{ab}$ between the hue angles of batch and standard was calculated in the direction of lesser angular displacement and the verbal description of the hue difference component follow the same guideline given by Smith [69] which is in accordance with the guidelines given by Mclaren [53].

It was observed that both the assessors differ in their assessments for characterizing and quantifying the difference in hue component of standard-batch pair. Although the hue difference is the easiest of the colour attributes to evaluate, Table 5.6 shows that hue difference is not necessarily being perceived the same by the dyers. Further, the hue

difference component (ΔH*) calculated from the CIELAB 1976 system does not agree with the visual assessment results. It was realized that this lack of agreement between the two observers and to the CIELAB system was probably due to the assessment method used, rather than the competence of the observers concerned.

After comparing the assessments made by the two assessors for the hue difference component, next stage was to determine how well both of the assessors agreed in assessing the differences in depth and brightness of standard-batch pairs of data set 1. The visual assessment results of ΔD and ΔB by both the observers are given in Table 5.7.

Table 5.7: Visual assessment results of two assessors for the differences in depth and brightness

| Pair no. | Assessor1 ΔD | Assessor 1 qualitative output | Assessor 2 ΔD | Assessor 2 qualitative output | Assessor 1 ΔB | Assessor 1 qualitative output | Assessor 2 ΔB | Assessor 2 qualitative output |
|---|---|---|---|---|---|---|---|---|
| 1 | -0.40 | Thinner | -0.50 | Thinner | 0.00 | same | 0.00 | same |
| 2 | -0.80 | Thinner | -0.20 | Thinner | -0.20 | flatter | 0.00 | same |
| 3 | -0.80 | Thinner | 0.00 | same | 0.00 | same | 0.00 | same |
| 4 | -0.90 | Thinner | -0.40 | Thinner | -0.30 | flatter | -0.20 | flatter |
| 5 | -1.00 | Thinner | -0.50 | Thinner | 0.00 | same | 0.50 | brighter |
| 6 | 0.50 | Fuller | 0.10 | Fuller | 0.00 | same | 0.50 | brighter |
| 7 | 0.00 | same | 0.10 | Fuller | -0.50 | flatter | 0.80 | brighter |
| 8 | -0.40 | Thinner | 0.00 | same | 0.00 | same | 0.00 | same |
| 9 | 0.00 | same | 0.80 | Fuller | -0.90 | flatter | 0.10 | brighter |
| 10 | -0.50 | Thinner | 0.00 | same | 0.00 | same | 0.50 | brighter |
| 11 | 0.00 | same | 0.00 | same | 0.50 | brighter | 0.90 | brighter |
| 12 | -0.50 | Thinner | -0.20 | Thinner | 0.00 | same | -0.50 | flatter |
| 13 | -0.80 | Thinner | -0.20 | Thinner | 0.00 | same | 0.40 | brighter |
| 14 | -0.80 | Thinner | 0.00 | same | 0.00 | same | 0.50 | brighter |
| 15 | -0.50 | Thinner | 0.10 | Fuller | 0.00 | same | 0.40 | brighter |
| 16 | 0.00 | same | -0.50 | Thinner | 0.00 | same | 0.00 | same |
| 17 | 0.00 | same | -0.10 | Thinner | 0.00 | same | 0.30 | brighter |
| 18 | 0.00 | same | 0.60 | Fuller | 0.00 | same | -0.40 | flatter |
| 19 | -0.70 | Thinner | 0.00 | same | -0.30 | flatter | -0.20 | flatter |
| 20 | -1.00 | Thinner | 0.50 | Fuller | 0.00 | same | 0.50 | brighter |
| 21 | -1.00 | Thinner | -0.90 | Thinner | 0.00 | same | 0.00 | same |
| 22 | -0.20 | Thinner | 0.00 | same | 0.00 | same | 0.20 | brighter |
| 23 | 0.00 | same | 0.60 | Fuller | 0.00 | same | 0.40 | brighter |
| 24 | -1.00 | Thinner | 0.60 | Fuller | 0.00 | same | 0.20 | brighter |
| 25 | -0.70 | Thinner | -0.40 | Thinner | 0.00 | same | 0.30 | brighter |
| 26 | -1.00 | Thinner | -0.50 | Thinner | 0.00 | same | 0.20 | brighter |

| | | | | | | | | |
|---|---|---|---|---|---|---|---|---|
| 27 | -0.50 | Thinner | 0.00 | same | 0.00 | same | 0.50 | brighter |
| 28 | -0.80 | Thinner | -0.80 | Thinner | 0.00 | same | -0.20 | flatter |
| 29 | -0.33 | Thinner | 0.00 | same | 0.33 | brighter | 0.00 | same |
| 30 | -0.50 | Thinner | -0.50 | Thinner | 0.00 | same | 0.00 | same |
| 31 | 0.00 | same | 0.00 | same | 0.50 | brighter | 0.00 | same |
| 32 | 0.50 | Fuller | 0.80 | Fuller | 0.00 | same | 0.20 | brighter |
| 33 | 0.50 | Fuller | 0.20 | Fuller | -0.50 | flatter | -0.50 | flatter |
| 34 | 1.00 | Fuller | 0.00 | same | 0.00 | same | 0.20 | brighter |
| 35 | 0.00 | same | 0.00 | same | -0.50 | flatter | 1.00 | brighter |
| 36 | -0.50 | Thinner | 0.00 | same | 0.00 | same | 0.70 | brighter |
| 37 | 0.00 | same | 0.00 | same | -0.50 | flatter | -0.20 | flatter |
| 38 | 0.00 | same | 0.00 | same | -1.00 | flatter | 0.00 | same |
| 39 | -0.50 | Thinner | -0.80 | Thinner | -0.50 | flatter | -0.10 | flatter |
| 40 | 0.60 | Fuller | 0.20 | Fuller | 0.00 | same | -0.40 | flatter |
| 41 | 0.00 | same | -0.10 | Thinner | 0.00 | same | -0.50 | flatter |
| 42 | 0.00 | same | 0.00 | same | 0.30 | brighter | 0.40 | brighter |
| 43 | 0.00 | same | -1.00 | Thinner | 0.00 | same | 0.00 | same |
| 44 | 0.00 | same | 0.00 | same | 0.00 | same | 0.80 | brighter |
| 45 | -0.60 | Thinner | -0.80 | Thinner | 0.00 | same | -0.10 | flatter |
| 46 | -0.33 | Thinner | 0.00 | same | -0.33 | flatter | -1.00 | flatter |
| 47 | 0.00 | same | 0.00 | same | 0.00 | same | 0.10 | brighter |
| 48 | 0.00 | same | 0.00 | same | -0.50 | flatter | -0.70 | flatter |
| 49 | 0.00 | same | 0.00 | same | -1.00 | flatter | 0.00 | same |

Figure 5.5 (a & b) shows no relationship between the assessments made by observers 1 and 2 for both ΔD and ΔB. It was believed that the dyers found it very difficult to report these differences in terms of percentage difference of the overall colour difference seen. The agreement between the opinions of these two observers was found to be 0.57% and 0.35% in reporting the depth and the brightness differences on qualitative basis.

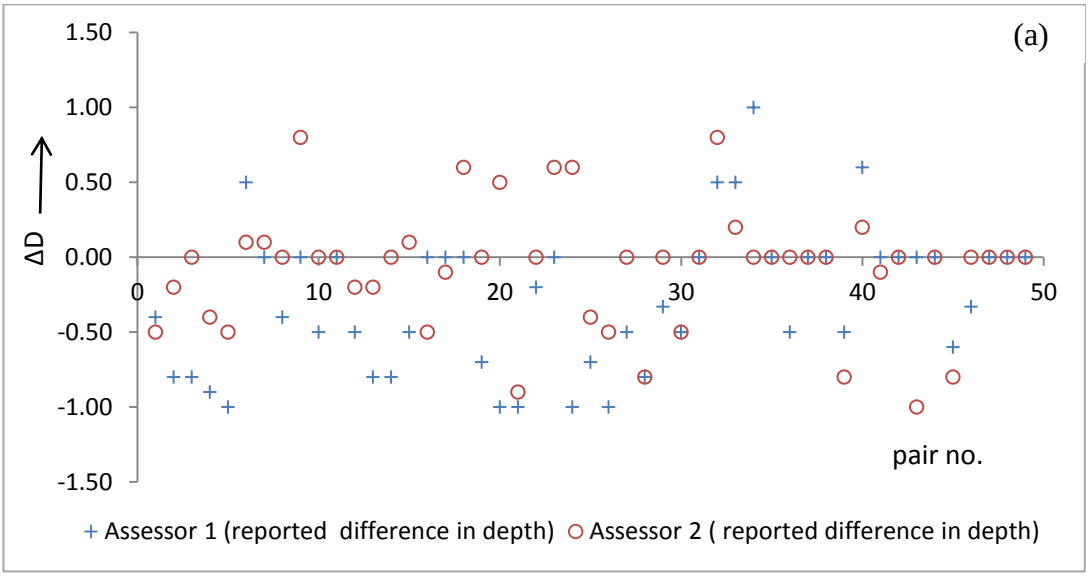

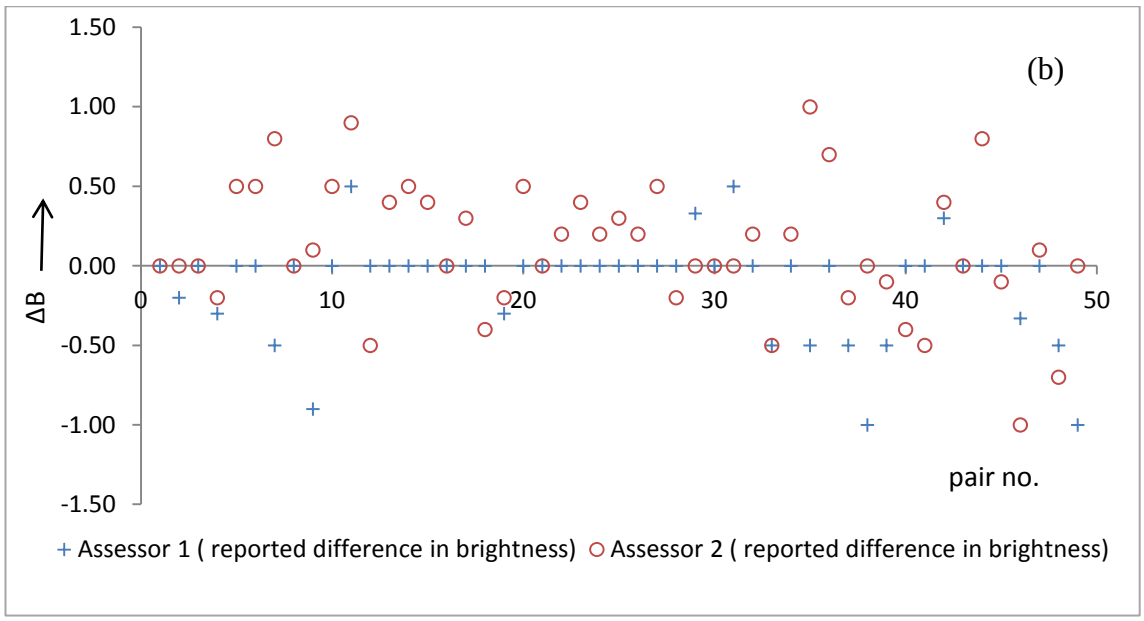


Figure 5.5: Inter-relationship between quantitative outputs of assessors 1 and 2 in terms of difference in depth (a) and difference in brightness (b)

### 5.3 Performance of WSF algorithm with visual assessments

In order to avoid the variation between the two assessors in assessing the difference in depth and brightness, the performance of the WSF algorithm is evaluated in relation to the average visual assessments of these two assessors and is given in Tables 5.8 and 5.9 The colorimetric data for each of the standard-batch pair of data set 1, given in Appendix E2, were entered to the WSF algorithm and its outputs in terms of ΔD and ΔB were computed. It was assumed that the difference in metric hue as computed from the colorimetric co-ordinates is equivalent to the ΔH computed from the WSF algorithm. The difference in depth, brightness and hue were computed twice from the WSF algorithm, one with no hue correction and other with the hue correction made to the batch chroma, using the procedure as stated earlier in section 4.4.

Table 5.8: Comparison of average visual assessments with the WSF algorithm for ΔD before and after the hue correction of the batch, for data set 1.

| Pair no. | Assessor (av) ΔD | Assessor (av) qualitative output | WSF $\Delta D_1$ | WSF qualitative output | WSF $\Delta D_2$ | WSF qualitative output |
|---|---|---|---|---|---|---|
| 1 | -0.45 | Thinner | 0.00 | same | 0.00 | same |
| 2 | -0.50 | Thinner | -0.10 | Thinner | -0.13 | Thinner |
| 3 | -0.40 | Thinner | 0.02 | Fuller | -0.02 | Thinner |
| 4 | -0.65 | Thinner | -0.80 | Thinner | -0.83 | Thinner |
| 5 | -0.75 | Thinner | -0.71 | Thinner | -0.71 | Thinner |
| 6 | 0.30 | Fuller | 0.04 | Fuller | 0.02 | Fuller |
| 7 | 0.05 | Fuller | 0.28 | Fuller | 0.28 | Fuller |
| 8 | -0.20 | Thinner | -0.79 | Thinner | -0.80 | Thinner |
| 9 | 0.40 | Fuller | 0.89 | Fuller | 0.89 | Fuller |
| 10 | -0.25 | Thinner | -0.26 | Thinner | -0.15 | Thinner |
| 11 | 0.00 | same | 0.36 | Fuller | 0.18 | Fuller |
| 12 | -0.35 | Thinner | -0.82 | Thinner | -0.77 | Thinner |
| 13 | -0.50 | Thinner | -0.90 | Thinner | -0.90 | Thinner |
| 14 | -0.40 | Thinner | -0.86 | Thinner | -0.88 | Thinner |
| 15 | -0.20 | Thinner | 0.09 | Fuller | 0.09 | Fuller |
| 16 | -0.25 | Thinner | 0.04 | Fuller | 0.04 | Fuller |
| 17 | -0.05 | Thinner | -0.05 | Thinner | -0.04 | Thinner |
| 18 | 0.30 | Fuller | 0.84 | Fuller | 0.83 | Fuller |
| 19 | -0.35 | Thinner | 0.31 | Fuller | 0.20 | Fuller |
| 20 | -0.25 | Thinner | 0.81 | Fuller | 0.79 | Fuller |
| 21 | -0.95 | Thinner | -0.04 | Thinner | -0.04 | Thinner |
| 22 | -0.10 | Thinner | 0.38 | Fuller | 0.36 | Fuller |
| 23 | 0.30 | Fuller | 0.97 | Fuller | 0.97 | Fuller |
| 24 | -0.20 | Thinner | 0.96 | Fuller | 0.96 | Fuller |
| 25 | -0.55 | Thinner | -0.54 | Thinner | -0.55 | Thinner |
| 26 | -0.75 | Thinner | -0.99 | Thinner | -0.99 | Thinner |
| 27 | -0.25 | Thinner | -0.07 | Thinner | -0.06 | Thinner |
| 28 | -0.80 | Thinner | -0.59 | Thinner | -0.58 | Thinner |
| 29 | -0.17 | Thinner | -0.71 | Thinner | -0.72 | Thinner |
| 30 | -0.50 | Thinner | -0.50 | Thinner | -0.49 | Thinner |
| 31 | 0.00 | same | 0.73 | Fuller | 0.74 | Fuller |
| 32 | 0.65 | Fuller | 0.94 | Fuller | 0.94 | Fuller |
| 33 | 0.35 | Fuller | 0.96 | Fuller | 0.96 | Fuller |
| 34 | 0.50 | Fuller | 0.92 | Fuller | 0.92 | Fuller |
| 35 | 0.00 | same | 0.27 | Fuller | 0.27 | Fuller |
| 36 | -0.25 | Thinner | -0.04 | Thinner | -0.04 | Thinner |
| 37 | 0.00 | same | -0.72 | Thinner | -0.15 | Thinner |
| 38 | 0.00 | same | 0.73 | Thinner | 0.72 | Fuller |
| 39 | -0.65 | Thinner | -0.88 | Thinner | -0.88 | Thinner |
| 40 | 0.40 | Fuller | 0.87 | Fuller | 0.88 | Fuller |
| 41 | -0.05 | Thinner | -0.11 | Thinner | -0.13 | Thinner |

| | | | | | | |
|---|---|---|---|---|---|---|
| 42 | 0.00 | same | 0.16 | Fuller | 0.15 | Fuller |
| 43 | -0.50 | Thinner | 0.32 | Fuller | 0.23 | Fuller |
| 44 | 0.00 | same | 0.55 | Fuller | 0.55 | Fuller |
| 45 | -0.70 | Thinner | 0.60 | Fuller | 0.44 | Fuller |
| 46 | -0.17 | Thinner | -0.41 | Thinner | -0.41 | Thinner |
| 47 | 0.00 | same | 0.08 | Fuller | 0.08 | Fuller |
| 48 | 0.00 | same | 0.27 | Fuller | 0.32 | Fuller |
| 49 | 0.00 | same | 0.94 | Fuller | 0.93 | Fuller |

$\Delta D_1$ & $\Delta D_2$ are the difference in depth before and after hue correction

Table 5.9 : Comparison of average visual assessments with the WSF algorithm for ΔB before and after the hue correction of the batch, for data set 1.

| Pair no. | Assessor (av) ΔB | Assessor (av) qualitative output | WSF $\Delta B_1$ | WSF qualitative output | WSF $\Delta B_2$ | WSF qualitative output |
|---|---|---|---|---|---|---|
| 1 | 0.00 | same | -0.60 | flatter | -0.60 | flatter |
| 2 | -0.10 | flatter | -0.75 | flatter | -0.72 | flatter |
| 3 | 0.00 | same | 0.04 | brighter | 0.04 | brighter |
| 4 | -0.25 | flatter | -0.14 | flatter | -0.11 | flatter |
| 5 | 0.25 | brighter | 0.24 | brighter | 0.23 | brighter |
| 6 | 0.25 | brighter | 0.88 | brighter | 0.90 | brighter |
| 7 | 0.15 | brighter | -0.47 | flatter | -0.47 | flatter |
| 8 | 0.00 | same | -0.16 | flatter | -0.16 | flatter |
| 9 | -0.40 | flatter | 0.09 | brighter | 0.09 | brighter |
| 10 | 0.25 | brighter | 0.35 | brighter | 0.46 | brighter |
| 11 | 0.70 | brighter | -0.14 | flatter | 0.33 | brighter |
| 12 | -0.25 | flatter | -0.13 | flatter | -0.19 | flatter |
| 13 | 0.20 | brighter | -0.05 | flatter | -0.05 | flatter |
| 14 | 0.25 | brighter | -0.06 | flatter | -0.04 | flatter |
| 15 | 0.20 | brighter | 0.56 | brighter | 0.56 | brighter |
| 16 | 0.00 | same | 0.08 | brighter | 0.07 | brighter |
| 17 | 0.15 | brighter | -0.11 | flatter | -0.12 | flatter |
| 18 | -0.20 | flatter | -0.16 | flatter | -0.17 | flatter |
| 19 | -0.25 | flatter | -0.22 | brighter | -0.33 | flatter |
| 20 | 0.25 | brighter | -0.14 | flatter | -0.16 | flatter |
| 21 | 0.00 | same | -0.47 | flatter | -0.47 | flatter |
| 22 | 0.10 | brighter | 0.02 | brighter | 0.05 | brighter |
| 23 | 0.20 | brighter | 0.01 | brighter | 0.01 | brighter |
| 24 | 0.10 | brighter | 0.04 | brighter | 0.04 | brighter |
| 25 | 0.15 | brighter | -0.34 | flatter | -0.34 | flatter |
| 26 | 0.10 | brighter | -0.01 | flatter | -0.01 | flatter |
| 27 | 0.25 | brighter | -0.02 | flatter | -0.02 | flatter |
| 28 | -0.10 | flatter | -0.12 | flatter | -0.13 | flatter |
| 29 | 0.17 | brighter | -0.08 | flatter | -0.08 | flatter |
| 30 | 0.00 | same | -0.33 | flatter | -0.34 | flatter |
| 31 | 0.25 | brighter | 0.09 | brighter | 0.09 | brighter |
| 32 | 0.10 | brighter | -0.05 | flatter | -0.05 | flatter |
| 33 | -0.50 | flatter | -0.02 | flatter | -0.02 | flatter |
| 34 | 0.10 | brighter | 0.01 | brighter | 0.01 | brighter |
| 35 | 0.25 | brighter | -0.03 | flatter | -0.03 | flatter |
| 36 | 0.35 | brighter | -0.03 | flatter | -0.03 | flatter |
| 37 | -0.35 | flatter | 0.05 | brighter | -0.62 | flatter |
| 38 | -0.50 | flatter | -0.03 | flatter | -0.04 | flatter |
| 39 | -0.30 | flatter | -0.04 | flatter | -0.05 | flatter |
| 40 | -0.20 | flatter | -0.12 | flatter | -0.12 | flatter |
| 41 | -0.25 | flatter | 0.02 | brighter | 0.01 | brighter |
| 42 | 0.35 | brighter | 0.67 | brighter | 0.67 | brighter |

| | | | | | | |
|---|---|---|---|---|---|---|
| 43 | 0.00 | same | 0.32 | brighter | 0.42 | brighter |
| 44 | 0.40 | brighter | 0.09 | brighter | 0.09 | brighter |
| 45 | -0.05 | flatter | 0.26 | brighter | 0.42 | brighter |
| 46 | -0.67 | flatter | -0.59 | flatter | -0.59 | flatter |
| 47 | 0.05 | brighter | -0.02 | flatter | -0.01 | flatter |
| 48 | -0.60 | flatter | -0.63 | flatter | -0.58 | flatter |
| 49 | -0.50 | flatter | -0.03 | flatter | -0.04 | flatter |

$\Delta B_1$ & $\Delta B_2$ are the difference in brightness before and after hue correction

Figure 5.6 shows that no strong relationship exists between the average visual assessments and the WSF algorithm both for ΔD and ΔB. It is clear from Figure 5.7 that the hue correction of the batch did not affect the performance of the WSF algorithm with the average visual assessments for ΔD but did make an improvement in its correlation for difference in brightness.

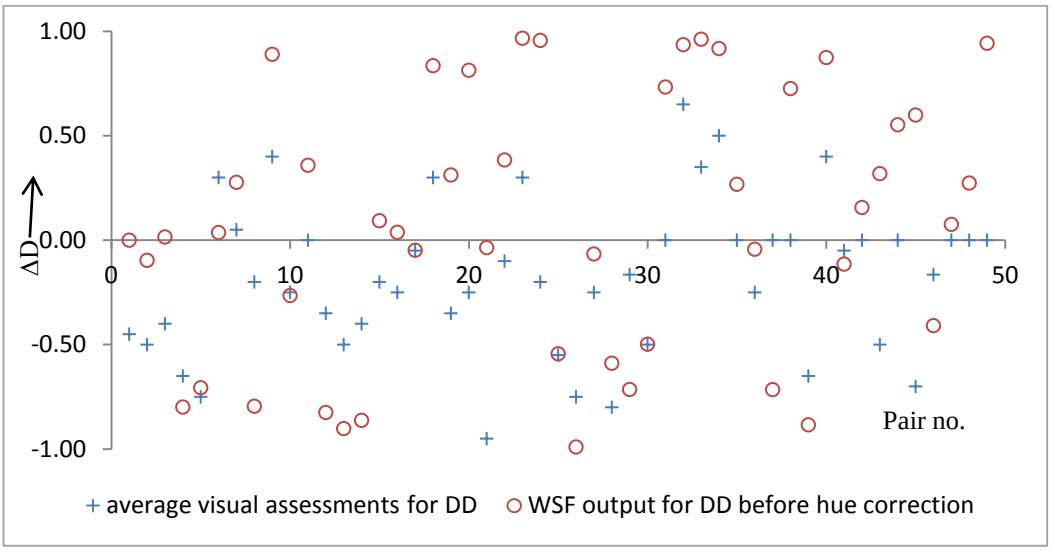


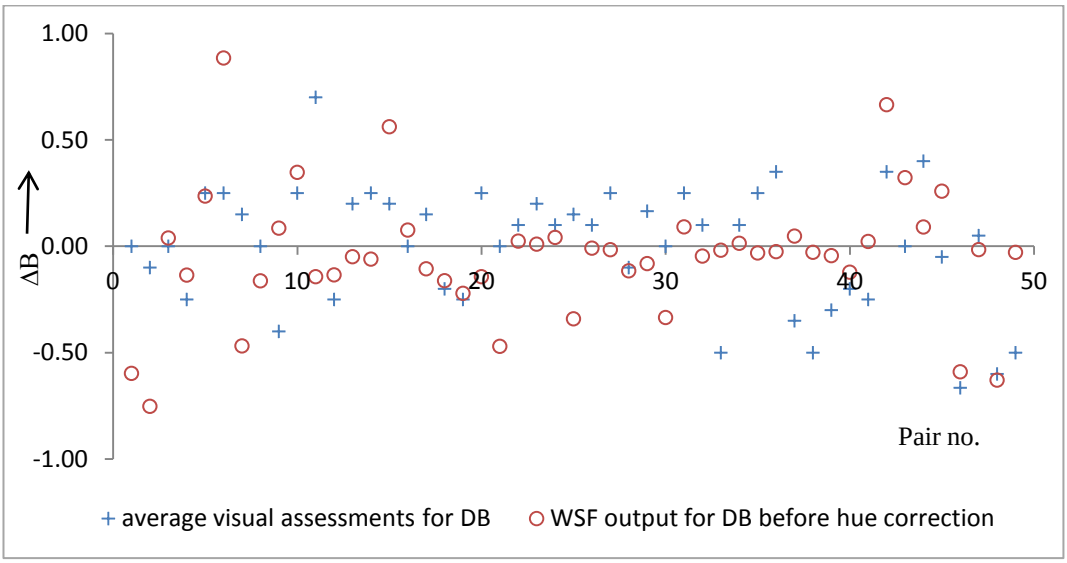


Figure 5.6: Performance of the WSF algorithm with visual assessments before any hue correction to the batch (ΔD & ΔB are the proportions of the overall visual difference)

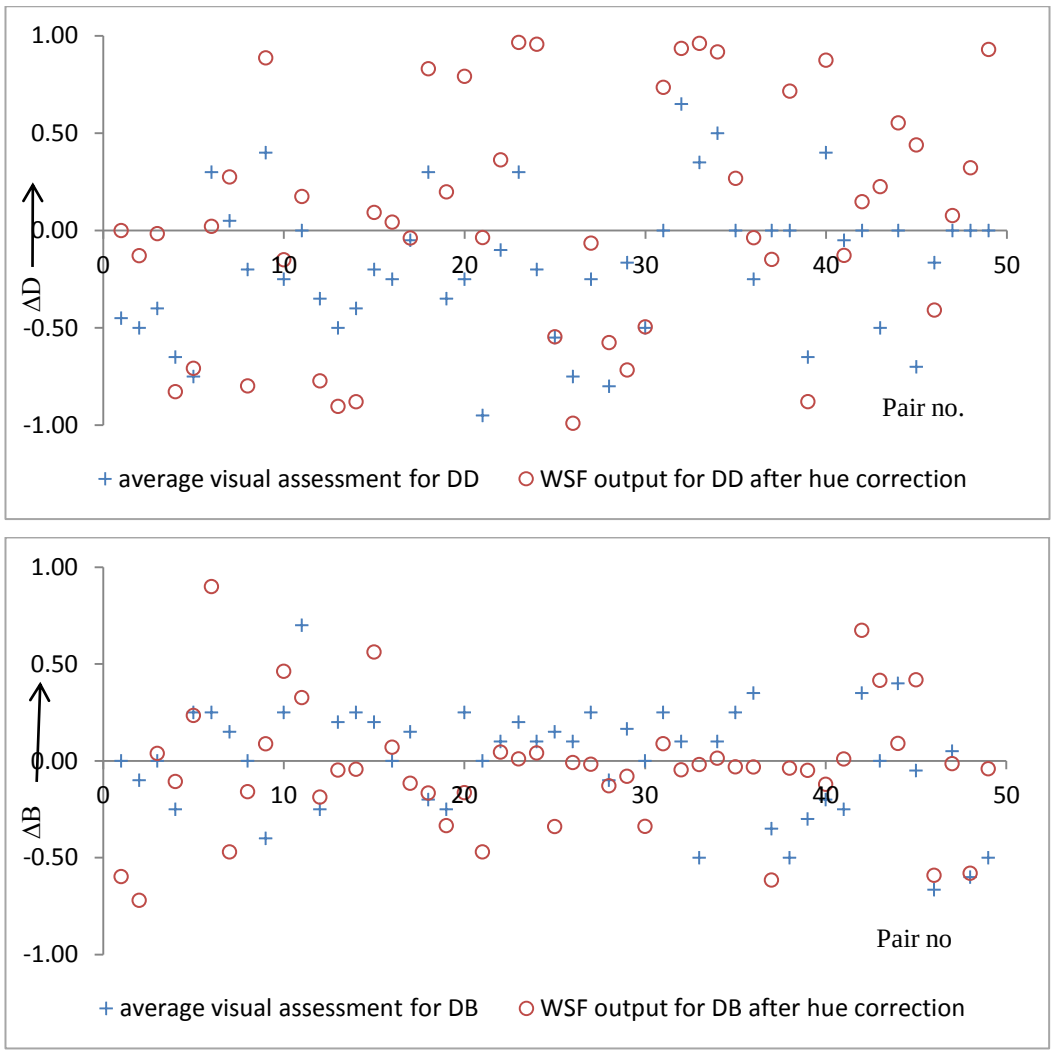


Figure 5.7: Performance of the WSF algorithm with visual assessments after hue correction to the batch (ΔD & ΔB are the proportions of the overall visual difference)

It was realized that more visual assessments were required to minimize the variation between the observers. Unfortunately it was not possible to find more assessors experienced in making assessments in terms of depth and brightness. Data set 2 which was used to compare the WSF algorithm with the DBH and the Sato models for ΔD and ΔB, reported these dyers' variables too. However only a qualitative assessment of the WSF algorithms with these visual results could be made, as the dyers' variables were reported purely on a descriptive basis, the assessors only stating which attribute (depth, brightness or hue) was the largest component in the difference seen. The extent of agreement of the WSF algorithm with the visual assessments both in terms of difference in depth and brightness is shown in Figure 5.8. Qualitative comparison of these visual assessments with the WSF algorithm with and without any hue correction to a batch is given in Table 5.10 and 5.11.

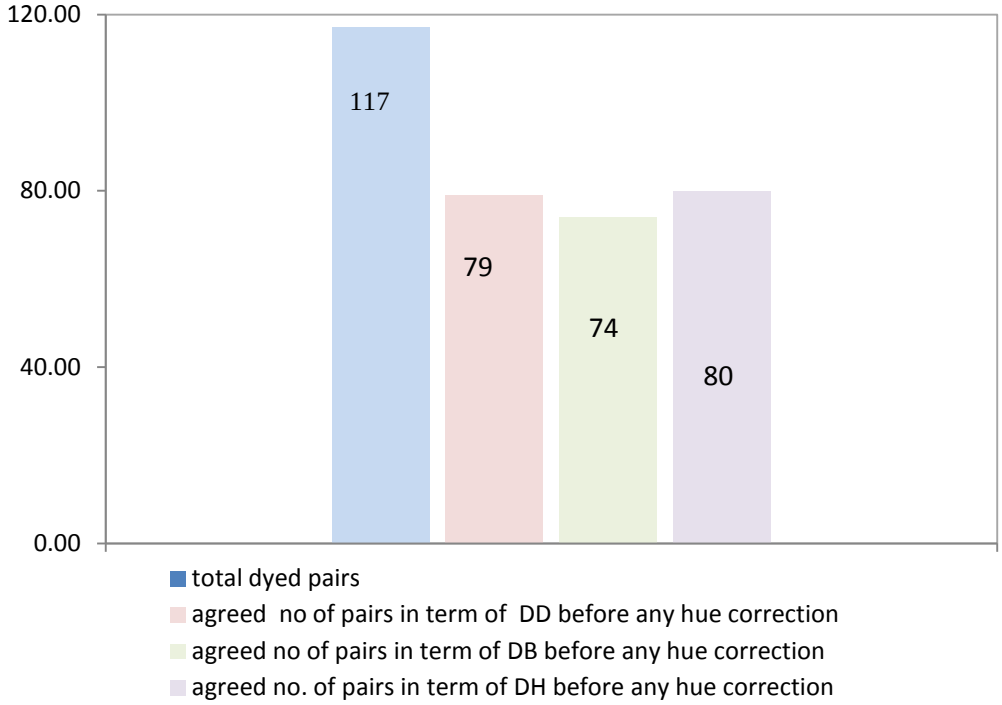


Figure 5.8: Qualitative comparison of the WSF algorithm with the visual assessments in term of ΔD, ΔB and ΔH*

The agreement of the qualitative visual results with the WSF algorithm was found to be 67.5%, 63.2% and 68% for ΔD, ΔB and ΔH* respectively. This agreement improves if very small differences computed from WSF (< 0.10) are round off to zero both for difference in depth, brightness and hue. Hence it was assumed that the WSF model performed well when compared qualitatively to the reported visual results of the given data. However no significant advantage of hue correction to the WSF model has been made in evaluating the difference in depth and brightness qualitatively and it remained the same for both the cases.

Table 5.10: Qualitative comparison of visual assessments with the WSF algorithm with and without any hue correction of the batch, for data set 2

| Std. No | Visual ΔD | WSF $\Delta D_1$ | WSF $\Delta D_2$ | Visual ΔB | WSF $\Delta B_1$ | WSF $\Delta B_2$ | VISUAL ΔH | WSF ΔH |
|---|---|---|---|---|---|---|---|---|
| 1 | thinner | thinner | thinner | brighter | brighter | brighter | Y(G) | Y(G |
| 2 | thinner | fuller | fuller | brighter | brighter | brighter | Y(G) | R(B) |
| 3 | thinner | fuller | fuller | brighter | brighter | brighter | Y(G) | Y(G |
| 4 | same | fuller | fuller | brighter | flatter | flatter | Y(G) | R(B) |
| 5 | thinner | fuller | fuller | flatter | flatter | flatter | Y(G) | R(B) |
| 6 | fuller | fuller | fuller | flatter | brighter | brighter | Y(G) | Y(G |
| 7 | fuller | fuller | fuller | brighter | brighter | brighter | R(B) | R(B) |
| 8 | thinner | thinner | thinner | flatter | flatter | flatter | R(B) | R(B) |
| 9 | thinner | thinner | thinner | brighter | flatter | flatter | Y(G) | Y(G |
| 10 | fuller | thinner | thinner | brighter | brighter | flatter | Y(R ) | G(B |
| 11 | fuller | fuller | fuller | flatter | flatter | flatter | Y(G) | G(B |
| 12 | thinner | thinner | thinner | flatter | flatter | flatter | Y(R ) | Y(G |
| 13 | thinner | thinner | thinner | flatter | flatter | flatter | Y(R ) | Y(G |
| 14 | fuller | thinner | thinner | flatter | flatter | flatter | R(B) | Y(G |
| 15 | thinner | thinner | thinner | brighter | flatter | flatter | Y(G) | G(B |
| 16 | fuller | fuller | fuller | brighter | brighter | brighter | Y(R ) | Y(R |
| 17 | fuller | fuller | fuller | flatter | flatter | flatter | G(B) | G(B |
| 18 | fuller | fuller | fuller | same | flatter | flatter | same | G(B |
| 19 | fuller | fuller | fuller | flatter | brighter | brighter | G(Y) | Y(R |
| 20 | fuller | fuller | fuller | flatter | brighter | brighter | R(B) | Y(R |
| 21 | fuller | fuller | fuller | flatter | flatter | flatter | B(R ) | G(Y |
| 22 | thinner | thinner | thinner | brighter | brighter | brighter | B(R ) | B(R |
| 23 | fuller | fuller | fuller | brighter | flatter | flatter | R(B) | B(R |
| 24 | fuller | fuller | fuller | flatter | brighter | brighter | R(B) | B(R |
| 25 | same | fuller | fuller | same | flatter | flatter | same | B(R |
| 26 | same | fuller | fuller | brighter | brighter | brighter | B(R ) | B(R |
| 27 | fuller | thinner | thinner | flatter | brighter | brighter | G(B) | R(Y |
| 28 | thinner | thinner | thinner | brighter | flatter | flatter | R(Y) | R(Y |
| 29 | thinner | thinner | thinner | flatter | flatter | flatter | B(G) | B(G |
| 30 | thinner | thinner | thinner | brighter | brighter | brighter | R(Y) | R(Y |
| 31 | thinner | thinner | thinner | brighter | brighter | brighter | B(G) | B(G |
| 32 | same | fuller | fuller | brighter | brighter | brighter | R(Y) | R(Y |
| 33 | same | fuller | fuller | flatter | flatter | flatter | Y(G) | R(B) |
| 34 | thinner | fuller | fuller | brighter | brighter | brighter | Y(G) | R(B) |
| 35 | fuller | fuller | fuller | flatter | flatter | flatter | R(B) | R(B) |
| 36 | fuller | fuller | fuller | same | flatter | flatter | R(B) | R(B) |
| 37 | fuller | fuller | fuller | flatter | flatter | flatter | R(B) | R(B) |
| 38 | fuller | fuller | fuller | same | brighter | brighter | Y(G) | Y(G |
| 39 | same | fuller | fuller | flatter | flatter | flatter | R(B) | R(B) |
| 40 | same | fuller | fuller | flatter | flatter | flatter | same | Y(G |
| 41 | fuller | fuller | fuller | same | brighter | brighter | R(B) | R(B) |
| 42 | thinner | fuller | fuller | flatter | brighter | brighter | R(Y) | Y(G |
| 43 | same | fuller | fuller | brighter | flatter | flatter | same | sam |
| 44 | same | fuller | fuller | flatter | flatter | flatter | R(B) | Y(G |
| 45 | fuller | fuller | fuller | brighter | brighter | brighter | R(B) | R(B) |

| | | | | | | | | |
|---|---|---|---|---|---|---|---|---|
| 46 | thinner | fuller | fuller | same | brighter | flatter | Y(R ) | G(B |
| 47 | thinner | thinner | thinner | flatter | flatter | flatter | R(B) | Y(R |
| 48 | thinner | thinner | thinner | flatter | brighter | brighter | Y(R ) | Y(R |
| 49 | same | thinner | thinner | brighter | brighter | brighter | G(Y) | G(Y |
| 50 | same | fuller | fuller | brighter | brighter | brighter | G(Y) | G(Y |
| 51 | same | fuller | fuller | brighter | brighter | brighter | B(R ) | B(R |
| 52 | fuller | fuller | fuller | brighter | brighter | brighter | R(Y) | R(Y |
| 53 | fuller | fuller | fuller | flatter | flatter | flatter | B(G) | B(G |
| 54 | fuller | fuller | fuller | flatter | flatter | flatter | B(G) | B(G |
| 55 | thinner | fuller | fuller | brighter | flatter | flatter | B(G) | R(B) |
| 56 | fuller | fuller | fuller | same | brighter | flatter | R(B) | R(B) |
| 57 | thinner | thinner | thinner | flatter | flatter | flatter | R(B) | R(B) |
| 58 | same | fuller | fuller | brighter | brighter | brighter | R(B) | Y(G |
| 59 | fuller | fuller | fuller | brighter | brighter | brighter | Y(G) | Y(G |
| 60 | thinner | fuller | fuller | brighter | brighter | brighter | R(B) | R(B) |
| 61 | fuller | fuller | fuller | brighter | flatter | flatter | B(G) | Y(G |
| 62 | fuller | fuller | fuller | flatter | flatter | flatter | Y(G) | Y(G |
| 63 | fuller | fuller | fuller | flatter | flatter | flatter | R(B) | R(B) |
| 64 | same | fuller | fuller | flatter | flatter | flatter | R(B) | R(B) |
| 65 | thinner | thinner | thinner | flatter | flatter | flatter | R(B) | R(B) |
| 66 | fuller | fuller | fuller | flatter | flatter | flatter | R(B) | G(B |
| 67 | same | fuller | fuller | flatter | brighter | brighter | R(B) | R(B) |
| 68 | same | fuller | fuller | flatter | flatter | flatter | Y(R ) | Y(R |
| 69 | fuller | fuller | fuller | brighter | brighter | brighter | Y(R ) | Y(R |
| 70 | fuller | thinner | thinner | flatter | flatter | flatter | G(Y) | Y(R |
| 71 | fuller | fuller | fuller | same | brighter | brighter | Y(R ) | Y(R |
| 72 | thinner | fuller | fuller | brighter | flatter | flatter | B(R ) | G(Y |
| 73 | fuller | fuller | fuller | same | brighter | brighter | G(Y) | G(Y |
| 74 | fuller | fuller | fuller | flatter | brighter | brighter | B(R ) | B(R |
| 75 | fuller | fuller | fuller | flatter | brighter | brighter | G(Y) | B(R |
| 76 | thinner | fuller | fuller | flatter | flatter | flatter | G(B) | G(Y |
| 77 | fuller | fuller | fuller | flatter | flatter | flatter | R(Y) | R(Y |
| 78 | thinner | thinner | thinner | brighter | brighter | brighter | B(G) | B(G |
| 79 | fuller | fuller | fuller | brighter | brighter | brighter | R(Y) | R(Y |
| 80 | thinner | thinner | thinner | brighter | brighter | brighter | R(B) | R(B) |
| 81 | same | fuller | fuller | flatter | flatter | flatter | R(B) | R(B) |
| 82 | fuller | thinner | thinner | brighter | flatter | flatter | Y(G) | R(B) |
| 83 | thinner | thinner | thinner | flatter | flatter | flatter | Y(G) | Y(G |
| 84 | thinner | thinner | thinner | same | flatter | brighter | R(B) | R(B) |
| 85 | thinner | fuller | fuller | flatter | flatter | flatter | R(B) | R(B) |
| 86 | thinner | thinner | thinner | flatter | flatter | flatter | same | Y(G |
| 87 | fuller | fuller | fuller | brighter | brighter | brighter | R(Y) | R(B) |
| 88 | thinner | thinner | thinner | same | brighter | brighter | R(B) | R(B) |
| 89 | thinner | thinner | thinner | brighter | brighter | brighter | Y(G) | Y(G |
| 90 | thinner | thinner | thinner | flatter | flatter | flatter | G(B) | G(B |
| 91 | fuller | fuller | fuller | same | brighter | brighter | Y(R ) | Y(R |
| 92 | fuller | fuller | fuller | brighter | brighter | brighter | B(R ) | B(R |
| 93 | fuller | fuller | fuller | same | brighter | brighter | B(R ) | B(R |
| 94 | fuller | fuller | fuller | brighter | brighter | brighter | B(R ) | B(R |
| 95 | fuller | fuller | fuller | same | brighter | brighter | B(R ) | B(R |
| 96 | thinner | thinner | thinner | flatter | flatter | flatter | B(G) | B(G |

| | | | | | | | | |
|---|---|---|---|---|---|---|---|---|
| 97 | fuller | fuller | fuller | brighter | flatter | flatter | Y(G) | R(B) |
| 98 | fuller | fuller | fuller | flatter | flatter | flatter | Y(G) | Y(G |
| 99 | thinner | fuller | fuller | flatter | flatter | flatter | R(B) | R(B) |
| 100 | fuller | thinner | thinner | brighter | flatter | flatter | R(B) | R(B) |
| 101 | fuller | fuller | fuller | same | flatter | brighter | Y(G) | Y(G |
| 102 | fuller | fuller | fuller | flatter | brighter | brighter | Y(G) | R(B) |
| 103 | thinner | thinner | thinner | flatter | flatter | flatter | R(B) | R(B) |
| 104 | same | fuller | fuller | flatter | flatter | flatter | Y(G) | Y(G |
| 105 | thinner | thinner | thinner | flatter | flatter | flatter | R(B) | R(B) |
| 106 | thinner | thinner | thinner | same | brighter | brighter | same | Y(R |
| 107 | fuller | fuller | fuller | brighter | brighter | brighter | B(R ) | B(R |
| 108 | same | fuller | fuller | brighter | brighter | brighter | B(R ) | B(R |
| 109 | thinner | thinner | thinner | brighter | brighter | brighter | G(Y) | G(Y |
| 110 | thinner | thinner | thinner | flatter | flatter | flatter | B(G) | B(G |
| 111 | same | fuller | fuller | same | brighter | brighter | B(G) | B(G |
| 112 | fuller | fuller | fuller | brighter | flatter | brighter | Y(G) | Y(G |
| 113 | fuller | fuller | fuller | same | brighter | brighter | Y(G) | Y(G |
| 114 | fuller | fuller | fuller | brighter | brighter | brighter | Y(G) | Y(G |
| 115 | thinner | thinner | thinner | brighter | brighter | brighter | Y(G) | Y(G |
| 116 | thinner | thinner | thinner | same | brighter | brighter | same | sam |
| 117 | thinner | thinner | thinner | brighter | brighter | brighter | B(G) | B(G |

$\Delta D_1$ & $\Delta B_1$ are the change in depth and brightness before any hue correction

$\Delta D_2$ & $\Delta B_2$ are the change in depth and brightness after hue correction

### 5.4 Effect of hue correction in the WSF algorithm to improve the qualitative & quantitative assessment of ΔD, ΔB and ΔH

Hue correction of the batch was considered mandatory for the WSF algorithm in all those situations where the hue angle of the batch differs from the standard. It is quite evident from Sections 5.1 and 5.3 that hue correction of the batch to the WSF algorithm improved the correlation with the DBH and the Sato models and its performance to the average visual assessments in evaluating the ΔB values. It was considered appropriate to analyze the significance of changes made by the hue correction through the colour space. This was achieved by comparing the output of the WSF algorithm with and without hue correction of the batch for data sets 1 and 2. The values of ΔD and ΔB computed by the WSF algorithm are given in Tables 5.1 to 5.4.

Figure 5.9 shows that no significant change was made in calculating the ΔD values before or after the hue correction round the hue circle with the exception of the batches with $350^{\circ}$-$5^{\circ}$, $40^{\circ}$-$50^{\circ}$, and $125^{\circ}$-$130^{\circ}$ hue angles.

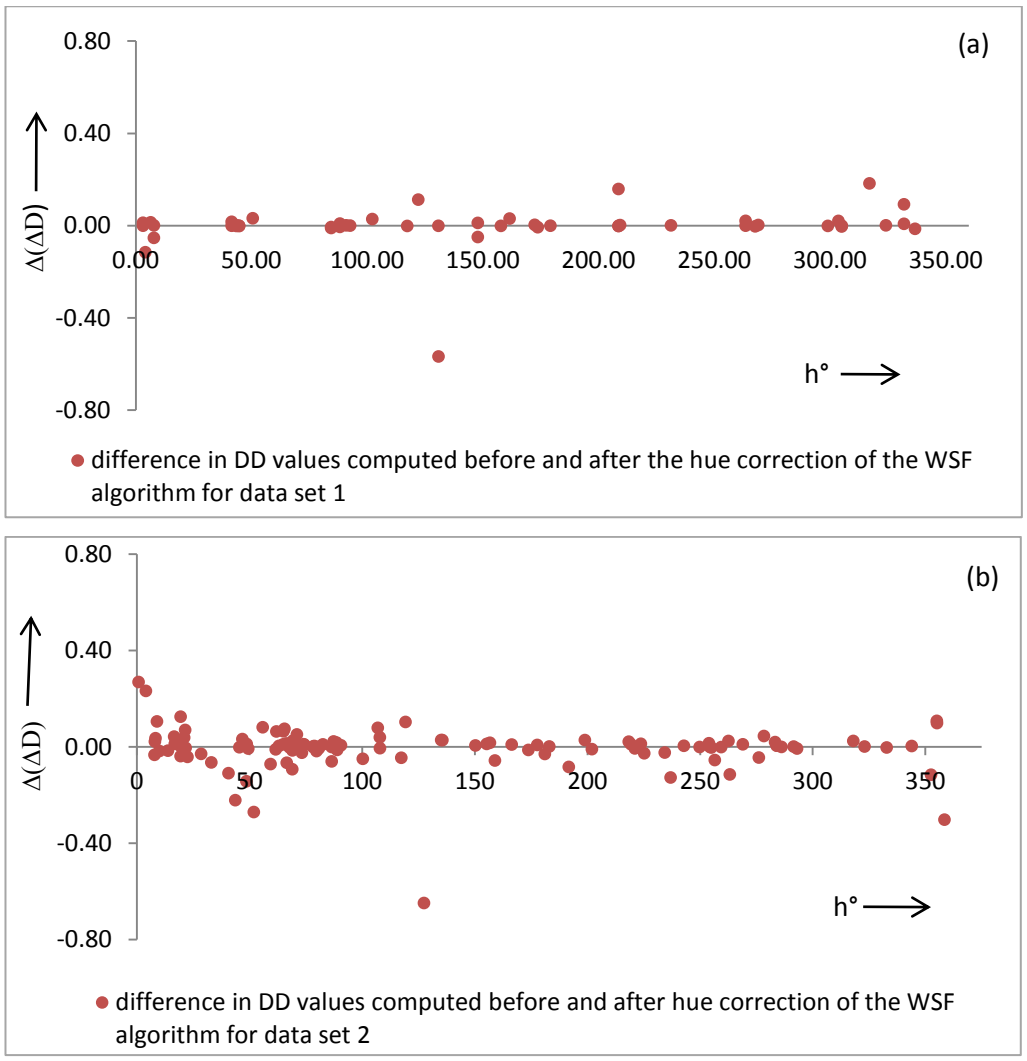


Figure 5.9 (a &b): Difference in ΔD values computed before and after the hue correction of the WSF algorithm for data set 2

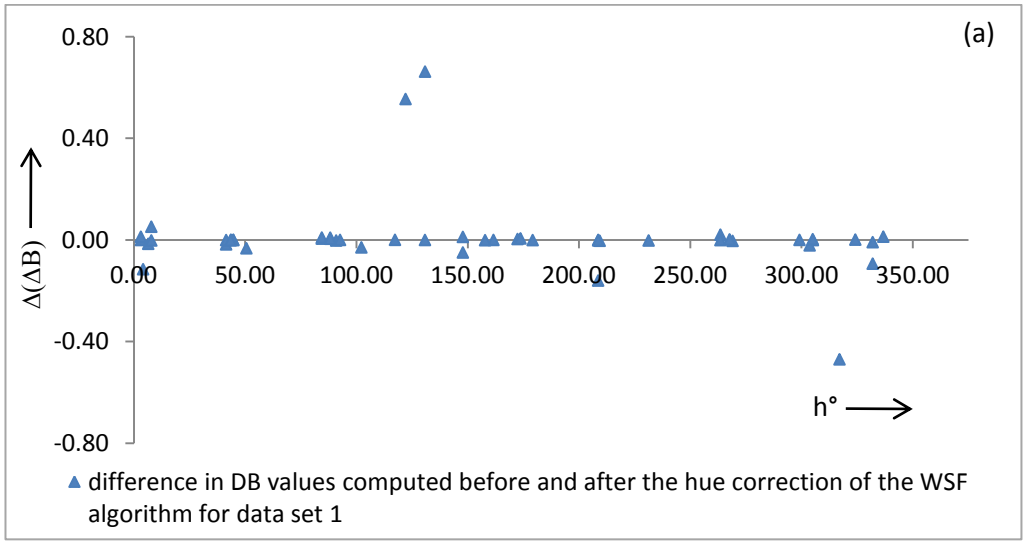

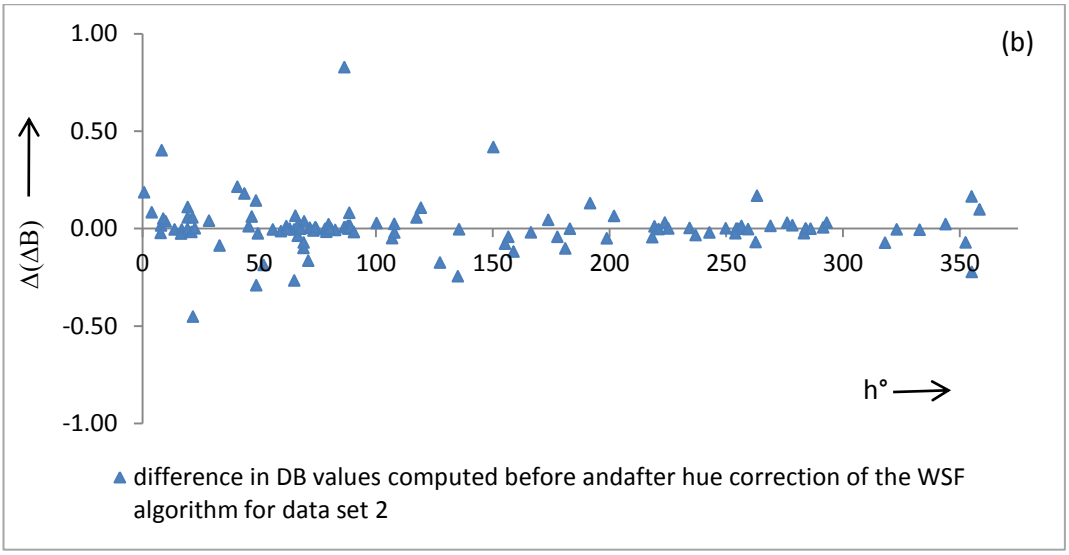


Figure 5.10 (a &b): Difference in ΔB values computed before and after the hue correction of the WSF algorithm through the colour space

It can be seen in Figures 5.10 that the ΔB values computed after the hue correction varied from the ΔB values computed before any hue correction, round the hue circle, from lower to higher extent. This disagreement is higher for the batches with hue angle 355°-5°, 30°-60°, 90°, and 130°-150°

# CHAPTER 6 DEVELOPMENT OF A LINEAR WSF ALGORITHM

The WSF algorithm, the development of which was explained in Chapter 4 of this thesis, is based upon the prediction of the intersection point of the batch on the equi depth line passing through the standard using an iterative procedure. MATLAB *software for engineers* was used to perform this task. Many software systems could easily utilize an iterative procedure but they are expensive and trained staffs are required to write and run the software. It was desired to develop a method which could eliminate the iterative step of the WSF algorithm and predict the same intersection point on the standard depth line as that given by the iterative method, so that the accurate difference in depth and brightness could be calculated in a simple and easy way.

It has already been pointed out that the WSI algorithm, which is used to define the equi-depth surfaces, is so structured that it determines the $L^*$ value that a colour of any given hue and chroma should possess for it to correspond to one of the levels of standard depth. Building on that principle, it is believed that the lightness of a batch, lying anywhere on the depth plane, should also vary round the hue circle, at each chroma value, for every WSI depth surface, if it is to lie on one of these equi-depth surfaces.

## 6.1 Description of linear WSF algorithm

The first stage of the linear WSF algorithm was to generate, using the WSI algorithm, the equi- depth line in the $L^* C^*$ plane that passes through the $L^* C^*$ coordinates of the standard. Secondly, the $L^*_{intersection}$ coordinate of the intersection point, as predicted by the iterative WSF algorithm, was determined from the $L^*C^*h$ coordinates of the standard and the batch, while the $C^*_{intersection}$ was determined from the $L^*C^*h$ values of the standard and the $L^*_{intersection}$ $C^*h$ values of the batch using the developed empirical models (see Equations 6.1 & 6.2). The hue correction of the batch was performed immediately after this step by the procedure detailed in Section 4.4. Finally the linear distances between the batch and the standard were calculated in a similar way as the iterative one, shown in Figure 4.1, to give the differences in depth and brightness between the standard and the batch.

It was found that the method for determining the intersection point of the batch on the equi-depth line depends upon the location of the standard in the depth plane. It was

therefore decided to develop separate strategies for predicting the intersection point of the batch if:

a. The standard is lying on one of the six WSI depth surfaces
b. The standard is lying either between any two of these six WSI depth surfaces or above the 1/25 standard depth surface or below the 2/1 standard depth surface

## 6.2 Methodology and calculation for the determination of difference in depth and brightness between the standard and the batch by the linear WSF algorithm

### *6.2.1 When the standard is lying on one of the six WSI depth surfaces*

If the standard lies on one of the six defined WSI depth surfaces; the equation for that surface will serve as equi-depth line of the standard. It was decided to compute the lightness of the standard for given chroma values ($C^*_1$, $C^*_2$, $C^*_3$, $C^*_4$ and $C^*_5$) as shown in Table 6.1 for the eight hue directions of the WSI algorithm, for every depth level. The eight hue directions are shown in Figure 6.1.

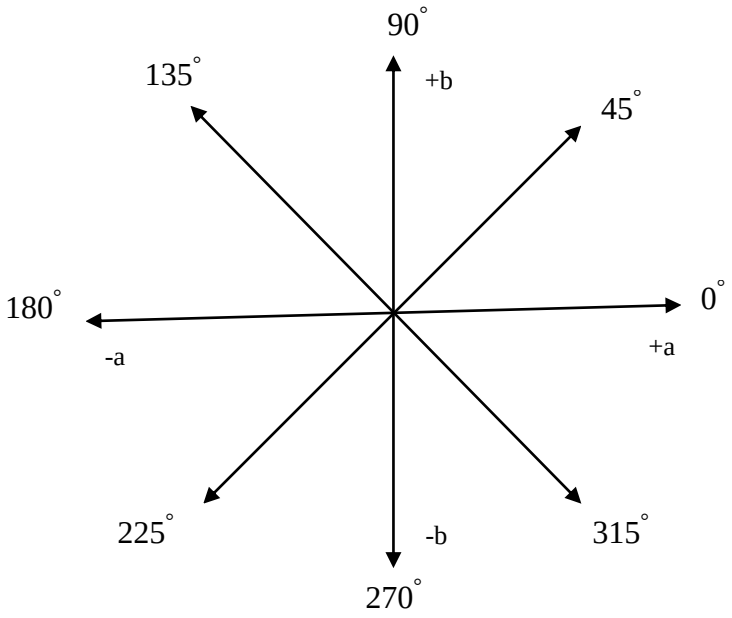


Figure 6.1: Eight hue directions used to develop the linear WSF model

Table 6.1: The chroma levels at which the linear WSF algorithm developed

| | 0° | 45° | 90° | 135° | 180° | 225° | 270° | 315° |
|---|---|---|---|---|---|---|---|---|
| 2/1 | | | | | | | | |
| $C^*_1$ | 5 | 5 | 5 | 5 | 5 | 5 | 5 | 5 |
| $C^*_2$ | 10 | 10 | 10 | 10 | 10 | 10 | 10 | 10 |
| $C^*_3$ | 15 | 15 | 15 | 15 | 15 | 15 | 15 | 15 |
| $C^*_4$ | 20 | 20 | 20 | 20 | 20 | 20 | 20 | 20 |
| $C^*_5$ | 30 | 30 | 30 | 30 | 30 | 30 | 30 | 30 |
| 1/1 | | | | | | | | |
| $C^*_1$ | 5 | 5 | 5 | 5 | 5 | 5 | 5 | 5 |
| $C^*_2$ | 10 | 10 | 10 | 10 | 10 | 10 | 10 | 10 |
| $C^*_3$ | 20 | 20 | 20 | 20 | 20 | 20 | 20 | 20 |
| $C^*_4$ | 30 | 30 | 30 | 30 | 30 | 30 | 30 | 30 |
| $C^*_5$ | 40 | 40 | 40 | 40 | 40 | 40 | 40 | 40 |
| 1/3 | | | | | | | | |
| $C^*_1$ | 5 | 5 | 5 | 5 | 5 | 5 | 5 | 5 |
| $C^*_2$ | 10 | 10 | 10 | 10 | 10 | 10 | 10 | 10 |
| $C^*_3$ | 20 | 20 | 20 | 20 | 20 | 20 | 20 | 20 |
| $C^*_4$ | 30 | 30 | 30 | 30 | 30 | 30 | 30 | 30 |
| $C^*_5$ | 40 | 40 | 40 | 40 | 40 | 40 | 40 | 40 |
| 1/6 | | | | | | | | |
| $C^*_1$ | 5 | 5 | 5 | 5 | 5 | 5 | 5 | 5 |
| $C^*_2$ | 10 | 10 | 10 | 10 | 10 | 10 | 10 | 10 |
| $C^*_3$ | 20 | 20 | 20 | 20 | 20 | 20 | 20 | 20 |
| $C^*_4$ | 30 | 30 | 30 | 30 | 30 | 30 | 30 | 30 |
| $C^*_5$ | 35 | 35 | 35 | 35 | 35 | 35 | 35 | 35 |
| 1/12 | | | | | | | | |
| $C^*_1$ | 5 | 5 | 5 | 5 | 5 | 5 | 5 | 5 |
| $C^*_2$ | 10 | 10 | 10 | 10 | 10 | 10 | 10 | 10 |
| $C^*_3$ | 20 | 20 | 20 | 20 | 20 | 20 | 20 | 20 |
| $C^*_4$ | 30 | 30 | 30 | 30 | 30 | 30 | 30 | 30 |
| 1/25 | | | | | | | | |
| $C^*_1$ | 5 | 5 | 5 | 5 | 5 | 5 | 5 | 5 |
| $C^*_2$ | 10 | 10 | 10 | 10 | 10 | 10 | 10 | 10 |
| $C^*_3$ | 15 | 15 | 15 | 15 | 15 | 15 | 15 | 15 |
| $C^*_4$ | 20 | 20 | 20 | 20 | 20 | 20 | 20 | 20 |

The $L^*_{SD}$, $a^*$ and $b^*$ of the standard were entered to the recipe prediction software to predict the recipe of the batch. Acid dyes on wool were used to prepare these standard-batch pairs. The %R values of the batches were measured on a Datacolour SF600 spectrophotometer and converted to the corresponding K/S values using Equation 3.11. These K/S values of the batch were then either increased or decreased, until its depth became equal to that of standard (see Section 4.3.2). This iterative procedure was performed with the condition that the difference between the lightness of the batch and the lightness predicted by the equation of the standard depth line was less than 0.1 ($\Delta L^* \leq 0.1$). The coordinates of the intersection point ($L^*_{intersection}$, $C^*_{intersection}$) of the batch on

the standard depth surface were recorded. This practice was repeated for all the eight hue directions of the given chroma levels at each WSI depth surface. It was kept in mind that the colour industry deals with small to medium colour differences (0.3-3.5) in normal routine, so pairs with a colour difference higher than the given range were not considered for this work.

The $L^*_{intersection}$ and $C^*_{intersection}$ of the batch as predicted by the iteration were re-predicted by the mathematical models which are given in Equations 6.1 and 6.2:

$$(L^*_{intersection})_2 = L^*_{batch} + \{m\,(C^*_{batch} - C^*_{std})/(C_{batch})\ (\cos(360 - r_1 h_{std})) + (n\,(L^*_{batch} - L^*_{stdWSI})/(L^*_{batch})\}$$

Equation 6.1

$$(C^*_{intersection})_2 = C^*_{batch} + \{(p\,(L^*_{batch} - (L^*_{intersection})_2) / (L^*_{intersection})_2\,(\sin(360 - r_2 h_{std})) + (q\,(C^*_{batch} - C^*_{std}) / (C^*_{batch})\}$$

Equation 6.2

In Equations 6.1 and 6.2 m, n, $r_1$, p, q & $r_2$ are constants. The values of these constants calculated for given chroma values at each depth level are given in Table 6.2. $L^*_{std\ WSI}$, $C^*_{std}$ , and $h_{std}$ stand for the lightness, chroma and hue angle of the standard respectively. $L^*_{batch}$ and $C^*_{batch}$ are the lightness and chroma of the batch respectively.

Table 6.2: The optimal constants of the linear WSF algorithm for six WSI depth surfaces

| | m | n | $r_1$ | p | q | $r_2$ |
|---|---|---|---|---|---|---|
| 2/1 | | | | | | |
| $C^*_1$ | 2 | -22 | -0.06 | -91 | 0.2 | -0.006 |
| $C^*_2$ | -2 | -25 | -0.0061 | -227 | -0.35 | 0.005 |
| $C^*_3$ | -2.23 | -26 | -0.042 | -313 | -0.24 | .006 |
| $C^*_4$ | -4.20 | -27 | 0.026 | -411 | 0.1 | 0.002 |
| $C^*_5$ | -18.63 | -28 | 0.0256 | -522 | 0.71 | -0.006 |
| 1/1 | | | | | | |
| $C^*_1$ | -2 | -34 | 0 | -293 | -0.9 | -0.0003 |
| $C^*_2$ | -8 | -31 | 0.0559 | -256 | -0.6 | 0.002 |
| $C^*_3$ | -29 | -33 | 0.0498 | -257 | -0.4 | 0.003 |
| $C^*_4$ | -52 | -38 | 0.03 | -397 | -0.2 | -0.0016 |
| $C^*_5$ | -63 | -44 | 0.03 | -828 | 0.1 | -0.02 |
| 1/3 | | | | | | |
| $C^*_1$ | -5 | -50.42 | 0.04 | 344 | 0.23 | -0.10 |
| $C^*_2$ | 2.99 | -46.79 | 0.04 | 215 | 0.74 | -0.08 |
| $C^*_3$ | -14 | -46 | 0.05 | 96 | 1 | -0.06 |
| $C^*_4$ | -51 | -46.92 | 0.03 | -315 | 1.5 | -0.02 |

| | | | | | | |
|---|---|---|---|---|---|---|
| $C^*_5$ | -69 | -56.41 | 0.02 | -1045 | 2.7 | 0.01 |
| 1/6 | | | | | | |
| $C^*_1$ | -2.87 | -57 | 0 | 149 | -0.1 | 0.16 |
| $C^*_2$ | -9 | -54 | 0.05 | 181 | -0.2 | 0.14 |
| $C^*_3$ | -20 | -46 | 0.043 | 251 | -0.3 | 0.12 |
| $C^*_4$ | -28 | -46 | 0.05 | 457 | -0.5 | 0.07 |
| $C^*_5$ | -40 | -53 | 0.06 | 633 | -0.8 | -0.05 |
| 1/12 | | | | | | |
| $C^*_1$ | -5 | -69 | 0.06 | 54 | -0.333 | 0 |
| $C^*_2$ | -15 | -61 | 0.04 | 747 | -0.028 | 0 |
| $C^*_3$ | -18 | -57 | -0.08 | 1099 | -1 | 0 |
| $C^*_4$ | -48 | -67 | -0.004 | 471 | -5 | 0.044 |
| 1/25 | | | | | | |
| $C^*_1$ | -10 | -75 | 0.02428 | 1110 | -1.4 | 0 |
| $C^*_2$ | -14.5 | -66 | 0.0328 | 981 | -1 | 0 |
| $C^*_3$ | -22 | -61 | 0.0327 | 806 | -3 | 0 |
| $C^*_4$ | -32 | -59 | 0.0224 | 501 | -5 | 0 |

The constant values were calculated so that the errors in predicting the $L^*_{(intersection)\,2}$ and $C^*_{(intersection)\,2}$ for the given chroma and the hue at each depth level was minimum. These errors were computed from Equations 6.3 and 6.4 respectively.

$$Error_{lightness} = \sqrt{(L^*_{intersection} - L^*_{(intersection)_2})^2} \qquad \text{Equation 6.3}$$

$$Error_{chroma} = \sqrt{(C^*_{intersection} - C^*_{(intersection)_2})^2} \qquad \text{Equation 6.4}$$

The values of the constants tabulated in Table 6.2 enabled the determination of the coordinates of the intersection point of the batch, around the hue circle, only for the given chroma values at each of the six depth levels. In order to determine the $L^*_{(intersection)2}$ for any chroma value lying in between these given chroma values, and the $C^*_{(intersection)2}$ corresponding to $L^*_{(intersection)2}$ value, it was necessary to interpolate between these constants. This was achieved by optimising these constants at each of the six depth levels. Polynomial equations were used to optimise these constants and are given in Table 6.3

Table 6.3: Polynomial equations used to determine optimised constants

| 2/1 |
| --- |
| $m = 11.02 - 2.55\ C^* + 0.167\ (C^*)^2 - 0.004\ (C^*)^3$ |
| $n = -19.55 - 0.597\ C^* + 0.011\ (C^*)^2$ |
| $r_1 = -0.084 + 0.006\ C^* - 8.9E^{-05}\ (C^*)^2$ |
| $p = -1618.82 + 200.99\ L^* - 6.11\ (L^*)^2$ |
| $q = 67.07 - 5.84\ L^* + 0.126\ (L^*)^2$ |
| $r_2 = -1.03 + 0.088\ L^* - 0.0019\ (L^*)^2$ |
| 1/1 |
| $m = 0.030 + 0.382C^* - 0.147(C^*)^2 + 0.0029\ (C^*)^3 - 0.00001\ (C^*)^4$ |
| $n = -38.89 + 1.326C^* - 0.065\ (C^*)^2 + 0.001\ (C^*)^3$ |
| $r_1 = 0.019 + 0.003\ C^* - 6.4E^{-05}\ (C^*)^2 - 1.30E^{-08}\ (C^*)^3$ |
| $p = -12.46 - 143.22\ L^* + 7.826\ (L^*)^2 - 0.112\ (L^*)^3$ |
| $q = -65.05 + 4.96\ L^* - 0.126\ (L^*)^2 + 0.001\ (L^*)^3$ |
| $r_2 = -0.214 + 0.013\ L^* - 0.00018\ (L^*)^2$ |
| 1/3 |
| $m = -31.78 + 7.39\ C^* - 0.45\ (C^*)^2 + 0.01\ (C^*)^3$ |
| $n = -54.77 + 1.01\ C^* - 0.03\ (C^*)^2$ |
| $r_1 = -0.04 + 6.3E^{-04}\ C^* - 3.04E^{-05}\ (C^*)^2$ |
| $p = 1.59 + 34.82\ L^* - 0.41\ (L^*)^2 - 0.004\ (L^*)^3$ |
| $q = -2.07 + 0.03\ L^* + 0.00058\ (L^*)^2$ |
| $r_2 = -0.67 + 0.02\ L^* - 0.0001\ (L^*)^2$ |
| 1/6 |
| $m = 0.013 + 0.099\ C^* - 0.175\ (C^*)^2 + 0.009\ (C^*)^3 - 0.00014\ (C^*)^4$ |
| $n = =57.14 - 0.356\ C^* + 0.088\ (C^*)^2 - 0.002\ (C^*)^3$ |
| $r_1 = -0.008 + 0.005\ C^* + 7.8E^{-05}\ (C^*)^2$ |
| $p = 6109.57 - 228.8\ L^* + 2.195\ (L^*)^2$ |
| $q = -0.206 + 0.043\ L^* - 0.001\ (L^*)^2$ |
| $r_2 = -0.137 + 0.022\ L^* - 0.0003\ (L^*)^2$ |
| 1/12 |
| $m = 20.6 - 7.18\ C^* + 0.461\ (C^*)^2 - 0.01\ (C^*)^3$ |
| $n = -80.18 + 2.62\ C^* - 0.073\ (C^*)^2$ |
| $r_1 = 0.200 - 0.023\ C^* + 0.001\ (C^*)^2$ |
| $p = -57504.36 + 1637.71\ L^* - 11.44\ (L^*)^2$ |
| $q = -108.25 + 3.32\ L^* - 0.026\ (L^*)^2$ |
| $r_2 = -0.168 + 0.003\ L^*$ |

| 1/25 |
|---|
| $m = -8.13 - 0.095\ C^* - 0.055\ (C^*)^2$ |
| $n = -87.25 + 2.81\ C^* - 0.07\ (C^*)^2$ |
| $r1 = 0.007 + 0.004\ C^* + 1.8\ E^{-04}\ (C^*)^2$ |
| $p = -8591.4 + 316\ L^* - 2.55\ (L^*)^2$ |
| $q = -1.398 + 0.188\ L^* - 0.003\ (L^*)^2$ |
| $r2 = 0$ |

The constants in Equations 6.1 and 6.2 were optimized at every depth level by minimizing the errors in determining their values by the Equations given in Table 6.3. Equation 6.5 was used to determine the errors and the calculated errors in optimizing these constants are given in Table 6.4:

$$Error = \sqrt{\frac{(S - S_1)^2}{N}} \qquad \text{Equation 6.5}$$

Where

N = number of chroma levels at each WSI depth surface

S = the value of the constants tabulated in Table 6.2. Constants are m, n, $r_1$, p, q or $r_2$

$S_1$ = the value of the constants (m, n, $r_1$, p, q or $r_2$) computed from the equations given in Table 6.3.

Table 6.4: Calculated errors in optimizing the constants for the chroma values lying between $C^*_1$ to $C^*_5$ at every depth level

| | 2/1 | 1/1 | 1/3 | 1/6 | 1/12 | 1/25 |
|---|---|---|---|---|---|---|
| m | 0.30 | 0.47 | 0.37 | 0.41 | 0.01 | 0.06 |
| n | 0.33 | 0.32 | 0.63 | 0.011 | 0.17 | 0.13 |
| $r_1$ | 0.02 | 0.018 | 0.01 | 0.012 | 0.03 | 0.0003 |
| p | 0.50 | 0.73 | 0.73 | 0.38 | 0.59 | 0.60 |
| q | 0.007 | 0.12 | 0.1 | 0.05 | 0.04 | 0.25 |
| $r_2$ | 0.0005 | 0.002 | 0 | 0.02 | 0.01 | 0 |

Because the errors in optimizing these constants are small, it was assumed that the values of the constants calculated from these polynomial equations (given in Table 6.3) were reliable.

Later on the hue correction of the batch was achieved by following the procedure mentioned in Section 4.4 and using Equation 6.6:

Hue corrected $(C^*_{intersection})_2$ = (g/h) $(C^*_{intersection})_2$ Equation 6.6

g = $C^*_{max}$ of the batch for batch's hue angle

h = $C^*_{max}$ of the standard for standard's hue angle

A batch is said to be equal in depth to the standard if the difference in $L_{(intersection)2}$, determined from WSF non-iterative model, and $L_{bxWSI}$ computed from the WSI algorithm for the hue corrected $C_{(intersection)2}$ of the batch, is less than 0.5. The difference in depth and brightness were calculated from Equations 6.7 and 6.8 respectively:

$$\Delta D = \sqrt{(C^*_{batch,final} - C^*_{batch,initial})^2 + (L^*_{batch,final} - L^*_{batch,initial})^2} \quad \text{Equation 6.7}$$

$$\Delta B = \sqrt{(C^*_{batch,final} - C^*_{std})^2 + (L^*_{batch,final} - L^*_{std})^2} \quad \text{Equation 6.8}$$

where

- $C^*_{batch\ final}$ is the hue corrected $(C^*_{intersection})_2$ and $L^*_{batch\ final}$ is the $L^*_{(intersection)2}$ values determined from WSF non iterative model
- $C^*_{batch}$ initial and $L^*_{batch\ initial}$ are the chroma and lightness values of the batch measured on spectrophotometer
- $C^*_{std}$ and $L^*_{std}$ are the chroma and lightness values of the standard

ΔD and ΔB are scaled with scaling factor k. It was calculated by the equation 6.9

$$k = \sqrt{\frac{(L^*_{batch,initial} - L^*_{std})^2 + (C^*_{batch,initial} - C^*_{std})^2}{((\Delta D)^2 + (\Delta B)^2)}} \quad \text{Equation 6.9}$$

$\Delta D_1 = k \times \Delta D$ Equation 6.10

$\Delta B_1 = k \times \Delta B$ Equation 6.11

A positive sign is assigned to $\Delta D_1$ if the lightness of the batch is lower than the lightness of the batch at the intersection point and vice versa. Similarly a positive sign is assigned to $\Delta B_1$ if the chroma of the standard is lower than the adjusted chroma of the batch at the intersection point and vice versa.

### *6.2.2 When the standard is lying between any two of the six WSI depth surfaces*

It has been mentioned earlier that the standard does not necessarily lie on one of the defined WSI depth surfaces. In those situations the equi-depth line for the standard was generated by following the procedure described in Section 4.3.1, for which the conic equation constants ($k_1$ to $k_6$) were calculated by the Equation 4.3. The method for these situations, to determine the intersection point of the batch ($L^*_{(intersection)2}$, $C^*_{(intersection2)}$), by the non-iterative WSF algorithm is illustrated in Figure 6.2:

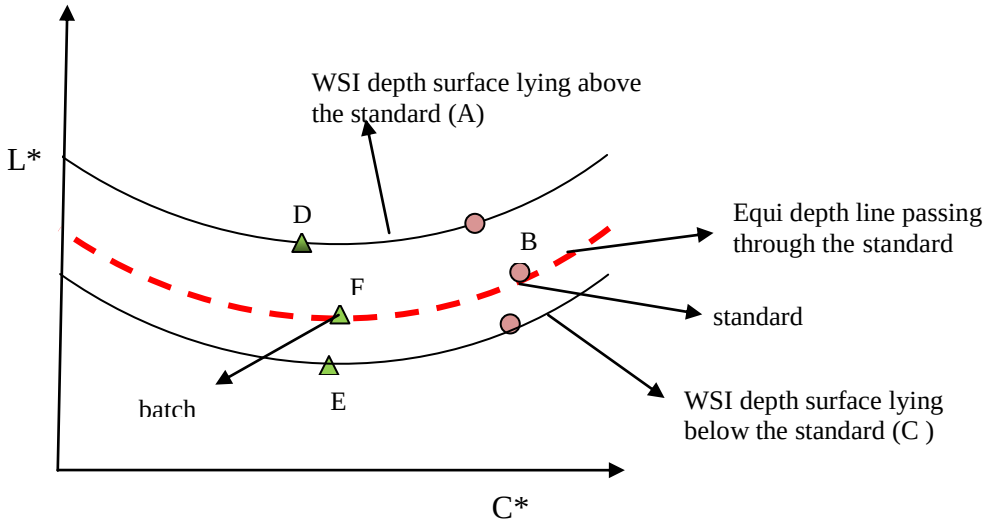


Figure 6.2: An illustration to describe the methodology to calculate the ΔD and ΔB by the non- iterative WSF algorithm for the standard lying between the WSI depth surfaces

The surfaces lying immediately above and below the standard were found. D and E are the intersection points of the batch on the WSI surfaces lying above and below the equi-depth surface passing through the standard. The $L_{(intersection)2}$ coordinate of these intersection points was calculated by the Equations 6.1. For the small to medium colour difference a linear relationship may be assumed for the change in lightness of a standard and a batch from one depth surface to another. If $L^*_{C\ std}$ and $L^*_{A\ std}$ are the corresponding lightness values of a standard at the depth surfaces C and A, the lightness of the batch at F, the intersection point of the batch at the equi-depth line of a standard, was calculated from Equation 6.12:

$$L^*_{F\ bx\ intersection} = L^*_{D\ bx} - \{(L^*_{std} - L^*_{C\ std})(L^*_{D\ bx} - L^*_{E\ bx}) / (L^*_{A\ std} - L^*_{C\ std})\}$$

Equation 6.12

The corresponding chroma values for $L^*_{D\,bx}$ & $L^*_{E\,bx}$ of the batch at the surfaces lying above and below the equi-depth line for the standard were computed from Equation 6.2. Since change in lightness is always accompanied with a change in chroma the chroma of the batch at F was computed using the relation given in Equation 6.13

$$C^*_{F\,bx\,intersection} = C^*_{D\,bx} + (C^*_{E\,bx} - C^*_{D\,bx}) \{(L^*_{D\,bx} - L^*_{F\,bx\,intersection})/(L^*_{D\,bx} - L^*_{E\,bx})\}$$

Equation 6.13

Following on determination of the intersection point of the batch on the equi-depth line of the standard, the hue correction of the batch was achieved using the Equation 6.6. The differences in depth, brightness and the scaling factor were determined using the Equations 6.7, 6.8 and 6.9 respectively.

### 6.3 Verification of the linear WSF algorithm

The non-iterative WSF algorithm was developed to predict the same differences in depth and brightness as those determined from the iterative model. Verification of the non-iterative WSF algorithm was achieved by comparing its output in terms of ΔD & ΔB with the output from the iterative WSF algorithm for both the data sets (data set 1 and data set 2). Differences in depth and brightness computed from both the models for data set 1 and 2 are shown in Figures 6.3 and 6.4

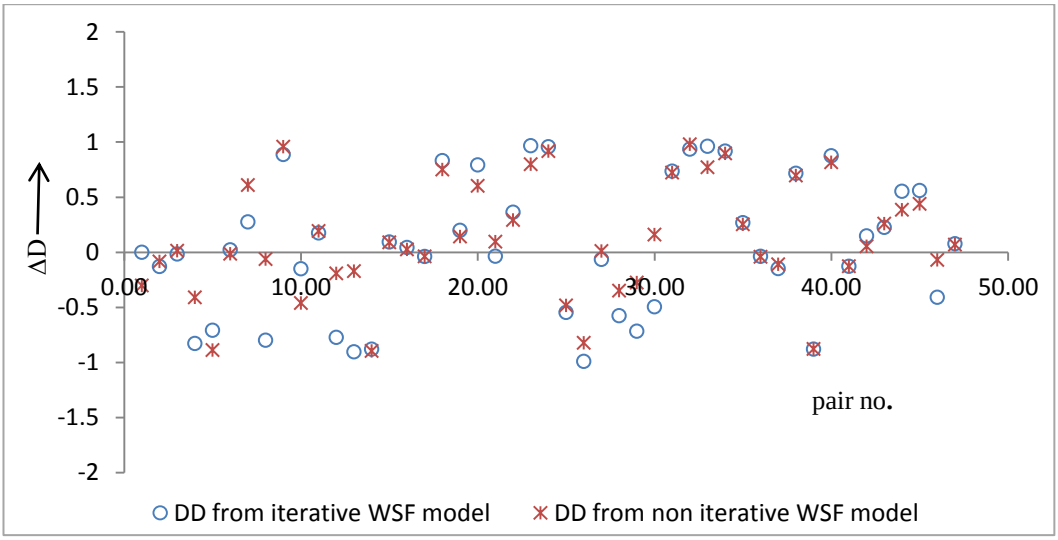

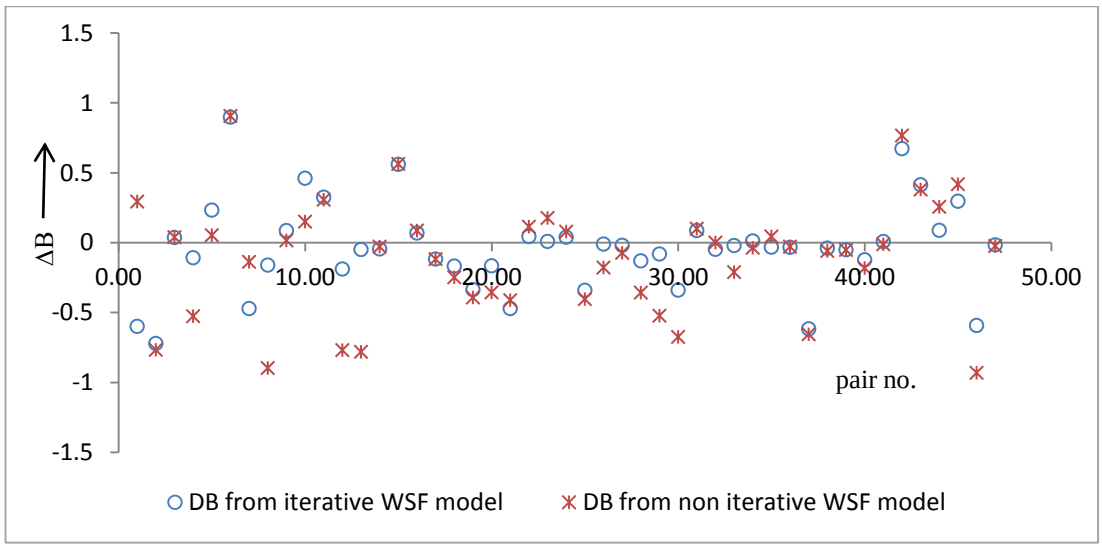


Figure 6.3: Comparison in computing the differences in depth and brightness of the dyed pairs for data set 1

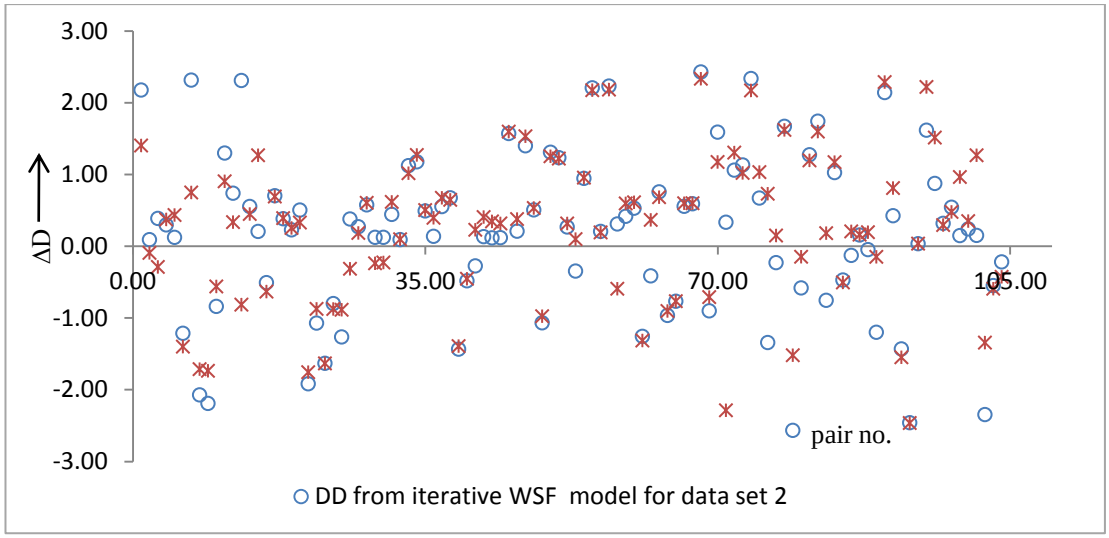


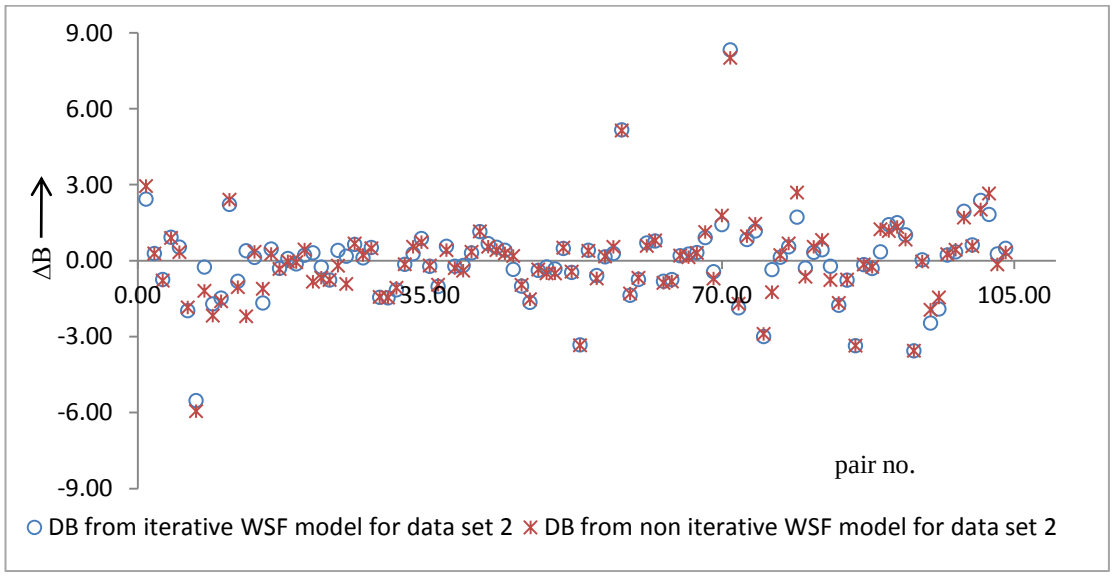


Figure 6.4: Comparison in computing the differences in depth and brightness of the dyed pairs for data set 2

It is evident from the Figures 6.3 and 6.4 that both approaches (iterative and non-iterative) to determine the ΔD and ΔB strongly relate to each other. It was observed that the interpolation between the six WSI depth surfaces was very encouraging but extrapolation of the samples with higher chroma values or samples lying above the 1/25 depth surface did not come up to expectations. It was decided to explore the WSF algorithm further for higher chroma colours and for very pale colours.

Performance of the non-iterative WSF algorithm was also evaluated in terms of its correlation to DBH and Sato algorithms. The calculated correlation coefficients of the WSF non-iterative algorithm with the DBH and Sato algorithms for combined data sets (data 1 and 2) are given in Table 6.5:

Table 6.5: Correlation co-efficients of the WSF algorithm with DBH and Sato algorithms

| | r (ΔD) | r (ΔB) |
|---|---|---|
| Non-iterative WSF with iterative WSF algorithm | 0.85 | 0.96 |
| Non-iterative WSF with Sato's algorithm | 0.90 | 0.97 |
| Non-iterative WSF with DBH algorithm | 0.86 | 0.95 |

It is apparent from Table 6.5 that all four algorithms agree with each other well, both in determining the difference in depth and difference in brightness of a coloured pair. Whilst the methodologies of each of the four algorithms (WSF (iterative and non-iterative, DBH, Sato) are different, the outcomes are strongly related.

For all dyed pairs lying below the 2/1 standard depth surface and with chroma less than 5 units, the method to determine the intersection point of a batch on the standard depth line needed to be different than for the rest of the colour space. It was observed from the WSI algorithm that there is no noticeable change in lightness with change in chroma for the samples lying on the 2/1WSI standard depth surface from C* = 0 to C* = 5.

Table 6.6 shows the marginal differences calculated from the lightness values for the 2/1 standard depth surface round the hue circle at C*= 0 and C*= 5. It is important to point out that if the standard-batch pair is lying close to achromatic axis, a dyer usually considers only the difference in depth as tangible to the overall difference seen between the standard-batch pair, while the difference in brightness is insignificant. It was therefore decided that the chroma of the batch at the intersection point on the equi-depth line for the standard be taken as the same as the chroma of the batch at its initial point, while the lightness of the batch at this intersection point for that chroma was calculated

from the conic equation of the standard. The co-ordinates of this intersection point were then used to calculate the differences in depth and brightness by using Equation 6.7 and 6.8.

Table 6.6: Marginal differences in lightness for 2/1 standard depth surface at C*= 0 and C*= 5 around the hue circle calculated using the WSI algorithm.

| C* | $h°_{ab}$ | L* at 2/1 std. depth level | difference in L* |
|---|---|---|---|
| 0 | 0 | 21.99 | -0.09 |
| 5 | 0 | 21.90 | |
| 0 | 30 | 21.99 | 0.06 |
| 5 | 30 | 22.04 | |
| 0 | 60 | 21.99 | 0.21 |
| 5 | 60 | 22.20 | |
| 0 | 90 | 21.99 | 0.30 |
| 5 | 90 | 22.29 | |
| 0 | 120 | 21.99 | 0.30 |
| 5 | 120 | 22.29 | |
| 0 | 150 | 21.99 | 0.21 |
| 5 | 150 | 22.20 | |
| 0 | 180 | 21.99 | 0.10 |
| 5 | 180 | 22.09 | |
| 0 | 210 | 21.99 | 0.04 |
| 5 | 210 | 22.03 | |
| 0 | 240 | 21.99 | -0.02 |
| 5 | 240 | 21.97 | |
| 0 | 270 | 21.99 | -0.10 |
| 5 | 270 | 21.89 | |
| 0 | 300 | 21.99 | -0.15 |
| 5 | 300 | 21.83 | |
| 0 | 330 | 21.99 | -0.16 |
| 5 | 330 | 21.83 | |
| 0 | 350 | 21.99 | -0.12 |
| 5 | 350 | 21.87 | |

### 6.4 Behaviour of the WSF algorithm for batches possessing identical L* C* $h°_{ab}$ values but different %R values

Broadly speaking the following four stages were involved to determine the differences in depth and brightness between a standard and a batch by both the WSF iterative and non-iterative methods:

1) Generation of an equi-depth line for the standard
2) Determination of the strength of the batch to intersect the equi-depth line of the standard
3) Hue correction of the batch
4) Determination of differences in depth, brightness and hue between the standard and the batch

The methods followed to achieve each of these stages were same for both of the models with the exception of stage 2. The intersection point of the batch on the equi-depth line for the standard was determined through iteration of the %R values of the batch with the WSF iterative model and from L*C* $h°_{ab}$ values of the batch and the standard with the WSF non-iterative algorithm. It was found that both of the algorithms correlated well to each other at different depth levels round the hue circle as shown in Table 6.5.

While working with the WSF iterative algorithm it was found that two batches with identical L*C* $h°_{ab}$ values but different %R values when compared against the same standard, gave different intersection points. Figures 6.5 and 6.6 illustrate this phenomenon.

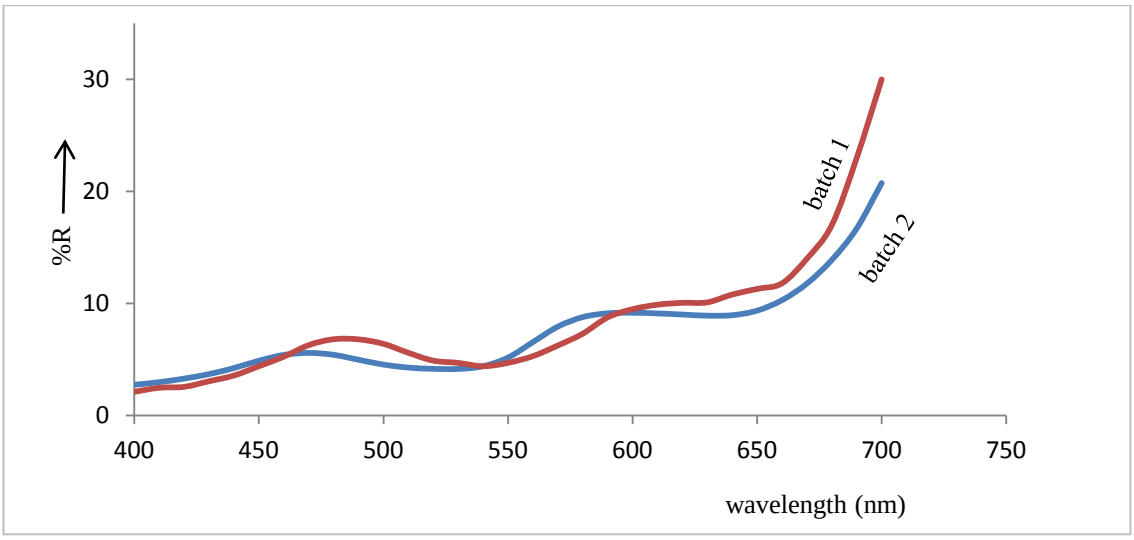


Figure 6.5: Two batches with same L*a* b* C* $h°_{ab}$ values but with different %R values

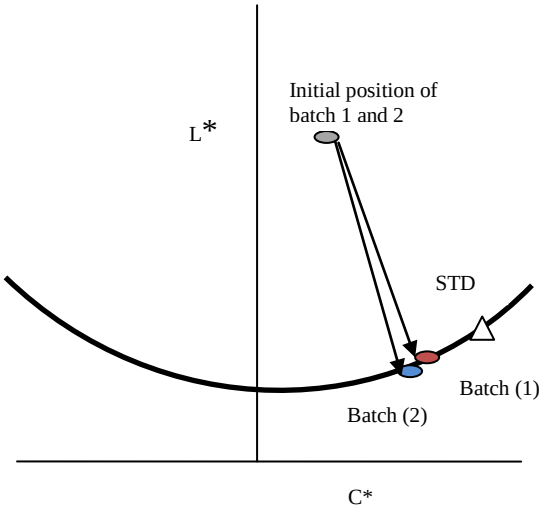


Figure 6.6: An illustration of different intersection points on equi depth line of the standard for two batches with same L*a* b* C* $h°_{ab}$ values but different reflectance values

Figure 6.5 shows the reflectance curves of two batches with identical L* a* b* C* $h°_{ab}$ values. It had been believed that the intersection point of these batches would be the same and there would be no difference in change in depth and brightness between the standard and these batches. However it was found that iteration in concentration of these batches to determine the ΔD & ΔB values of the batches for the same standard, as illustrated in Figure 6.6, gave two different intersection points, hence different depth and brightness differences were obtained for batch 1 and batch 2. This behaviour was also investigated for the linear WSF algorithm and the DBH model along with non-iterative WSF algorithm. The same data were used to analyse the outcome of these three algorithms. The data used to investigate these three algorithms and their outcomes are summarised in Table 6.7

Table 6.7: ΔD and ΔB values of standard – batch pairs calculated from the iterative WSF, DBH, and the WSF non iterative algorithm

| | | DARK BLUE | | DARK KHAKI | | YELLOW-GREEN | | GREEN | | PURPLE | | YELLOW | | BLUE-RED | |
|---|---|---|---|---|---|---|---|---|---|---|---|---|---|---|---|
| | | pair 1 | | pair 2 | | pair 3 | | pair 4 | | pair 5 | | pair 6 | | pair 7 | |
| | | batch 1 | batch 2 | batch 1 | batch 2 | batch 1 | batch 2 | batch 1 | batch 2 | batch 1 | batch 2 | batch 1 | batch 2 | batch 1 | batch 2 |
| | $L^*_{std}$ | 31 | 31 | 31.26 | 31.26 | 58 | 58 | 57 | 57 | 28 | 28 | 36 | 36 | 21 | 21 |
| | $C^*_{std}$ | 8.22 | 8.22 | 12.50 | 12.50 | 16 | 16 | 26.50 | 26.50 | 13 | 13 | 18 | 18 | 24 | 24 |
| | $h_{std}$ | 256 | 256 | 43.69 | 43.69 | 110 | 110 | 165 | 165 | 307 | 307 | 87 | 87 | 280 | 280 |
| | $L^*_{batch}$ | 29.3 | 29.3 | 30.7 | 30.7 | 56.0 | 56.0 | 61.7 | 61.7 | 25.1 | 25.1 | 34.3 | 34.3 | 19.3 | 19.3 |
| | $C^*_{batch}$ | 7.0 | 7.0 | 13.5 | 13.5 | 13.8 | 13.9 | 29.9 | 29.9 | 15.1 | 15.1 | 20.3 | 20.3 | 26.5 | 26.5 |
| | $h_{batch}$ | 268.8 | 268.8 | 36.5 | 36.5 | 106.1 | 106.2 | 162.7 | 162.7 | 304.8 | 304.8 | 85.7 | 85.4 | 282.3 | 282.5 |
| ΔD | WSF (iterative) | 1.91 | 1.76 | 1.05 | 1.01 | 1.42 | 1.34 | -4.05 | -3.63 | 2.94 | 2.96 | 2.25 | 2.24 | 3.01 | 3.05 |
| ΔD | WSF (noniterative) | 2.03 | 2.03 | 1.12 | 1.12 | 1.41 | 1.41 | -3.13 | -3.12 | 3.37 | 3.36 | 2.62 | 2.61 | 1.45 | 1.45 |
| ΔD | DBH | 1.65 | 1.67 | 0.64 | 0.64 | 0.97 | 0.98 | -2.90 | -2.89 | 2.50 | 2.49 | 2.47 | 2.47 | 1.29 | 1.30 |
| ΔB | WSF (iterative) | -0.79 | -1.10 | -0.47 | -0.58 | -2.60 | -2.61 | 4.14 | 4.56 | -2.01 | -1.98 | 2.03 | 2.00 | 0.15 | 0.18 |
| ΔB | WSF (noniterative) | -0.39 | -0.39 | -0.29 | -0.30 | -2.61 | -2.58 | 4.88 | 4.92 | -1.18 | -1.17 | 1.51 | 1.49 | 2.64 | 2.68 |
| ΔB | DBH | -1.24 | -1.23 | 0.96 | 0.97 | -2.80 | -2.77 | 5.01 | 5.06 | 2.55 | 2.54 | 1.74 | 1.71 | 2.72 | 2.76 |

Table 6.7 shows the different values of ΔD & ΔB for the batch 1and 2 (having very similar L*, C*, $h°_{ab}$ values) when determined by WSF iterative model. This behaviour is due to the different reflectance curves of the batches. There is no change in ΔD & ΔB when computed by WSF linear and DBH algorithms which use just L*C* $h°_{ab}$ of the standard and the batch as input values. The response of the WSF iterative model in these circumstances is disappointing though and requires to be explored further. The non-iterative WSF algorithm worked sensibly well for these pairs. Figure 6.7 (a-g) shows the intersection points of the two batches on the equi-depth line of the same standard when determined by the WSF (iterative) algorithm.

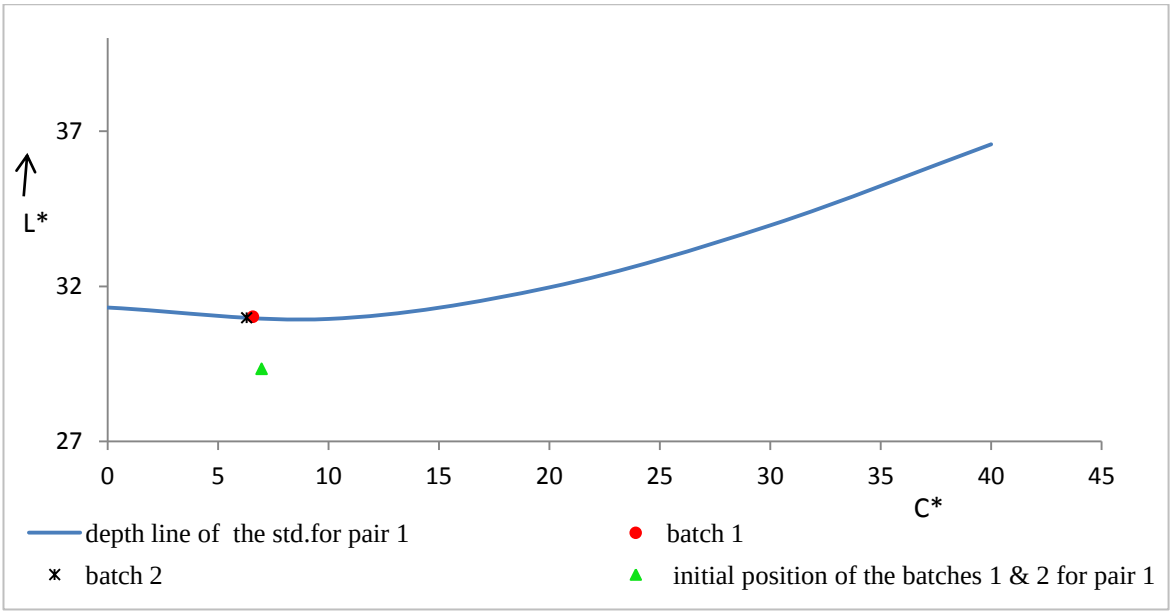
37
32
27
L*
0
5
10
15
20
25
30
35
40
45
C*
depth line of the std.for pair 1
batch 1
batch 2
initial position of the batches 1 & 2 for pair 1

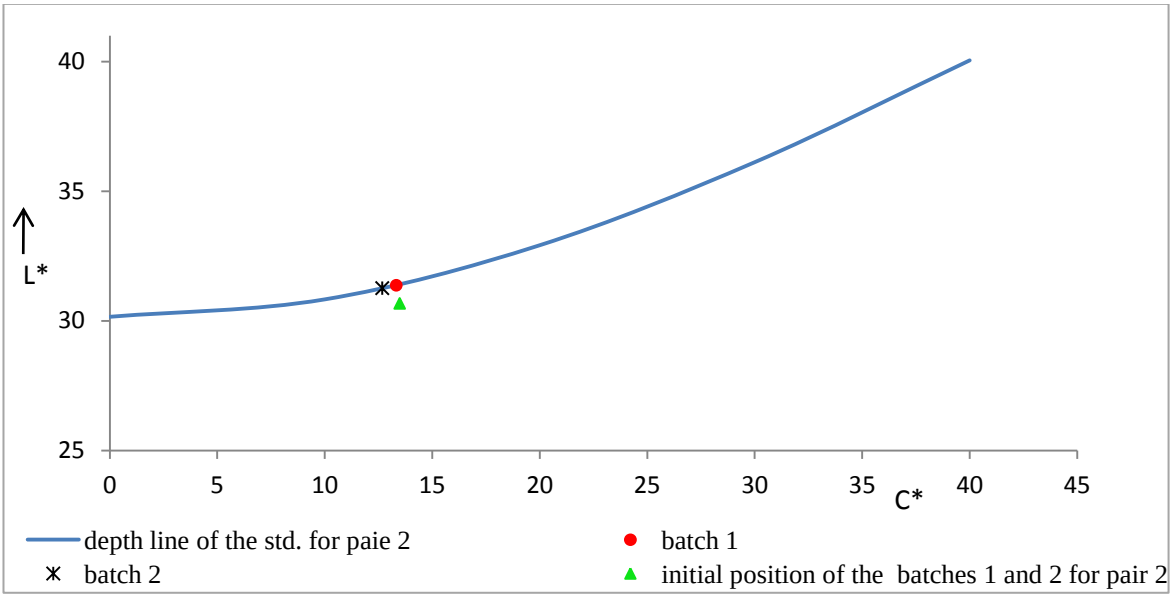
40
35
30
25
L*
0
5
10
15
20
25
30
35
40
45
C*
depth line of the std. for paie 2
batch 1
batch 2
initial position of the batches 1 and 2 for pair 2

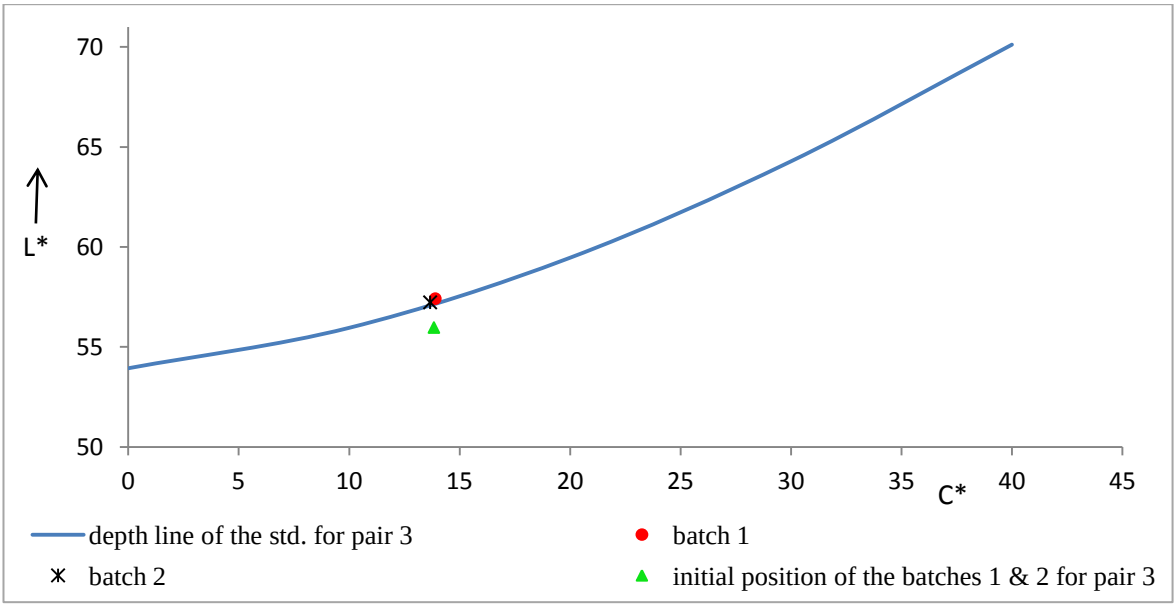
70
65
60
55
50
L*
0
5
10
15
20
25
30
35
40
45
C*
depth line of the std. for pair 3
batch 1
batch 2
initial position of the batches 1 & 2 for pair 3

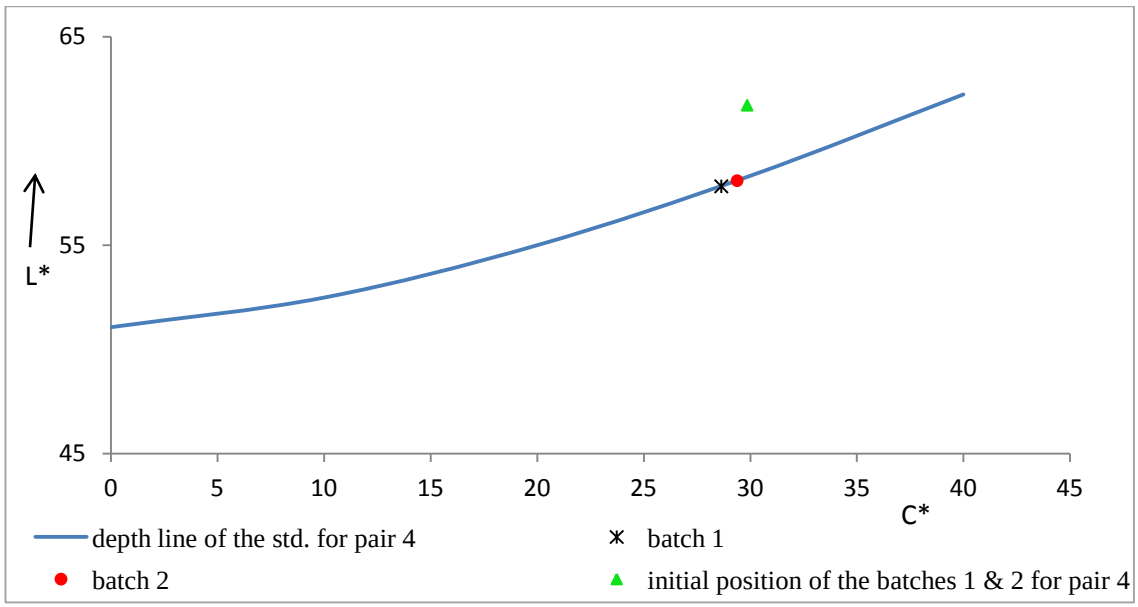
65
55
45
L*
0
5
10
15
20
25
30
35
40
45
C*
depth line of the std. for pair 4
batch 1
batch 2
initial position of the batches 1 & 2 for pair 4

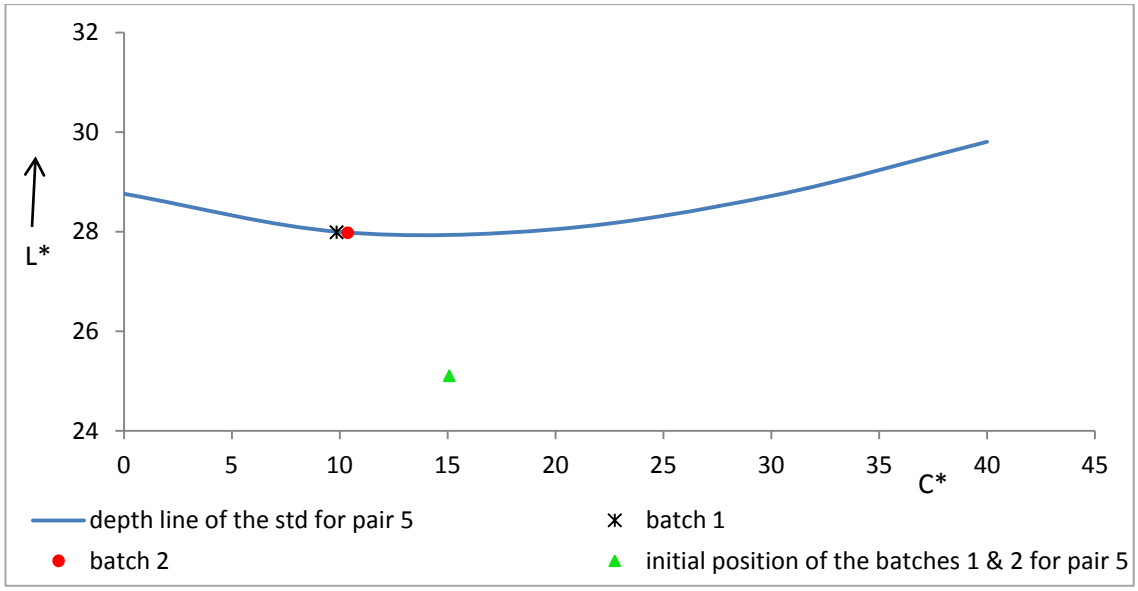
32
30
28
26
24
L*
0
5
10
15
20
25
30
35
40
45
C*
depth line of the std for pair 5
batch 1
batch 2
initial position of the batches 1 & 2 for pair 5

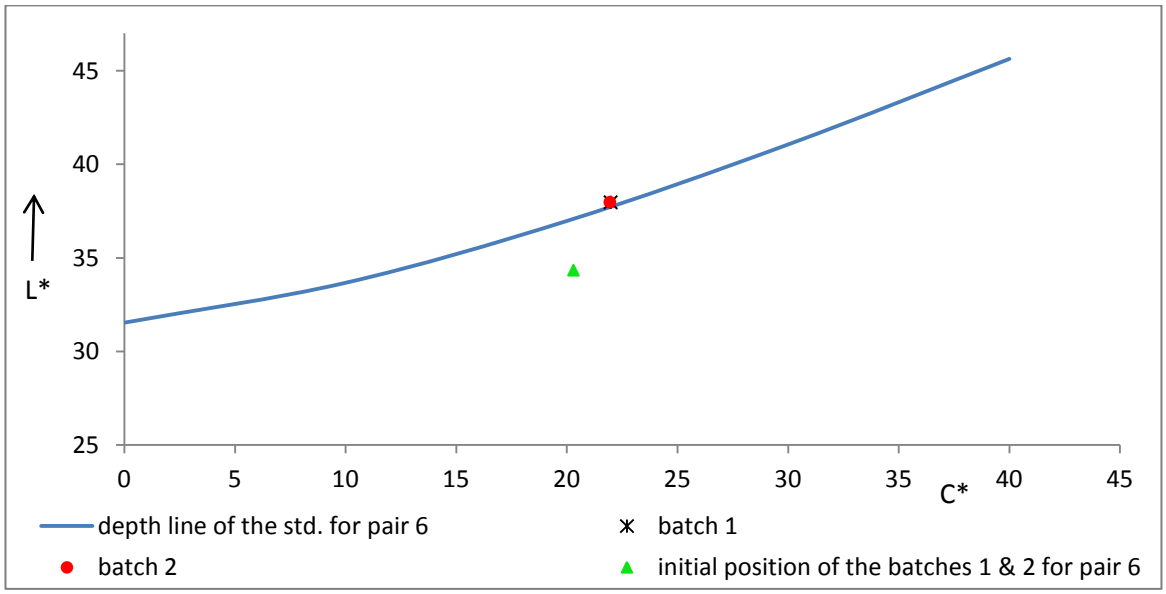
45
40
35
30
25
L*
0
5
10
15
20
25
30
35
40
45
C*
depth line of the std. for pair 6
batch 1
batch 2
initial position of the batches 1 & 2 for pair 6

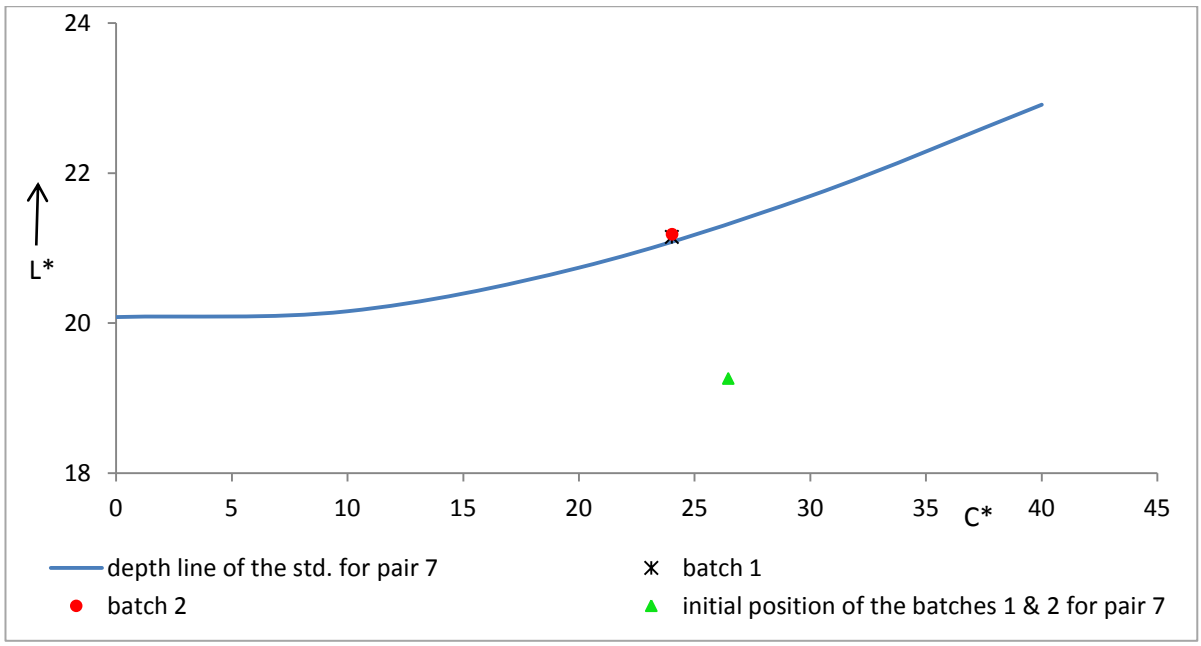


Figure 6.7: Determination of the intersection points of the batches on the equi-depth line of the same standard

It is clear from Figure 6.7 that the intersection points did not necessarily be different for all the dyed pairs studied but it differ in few of them.

# CHAPTER 7 CONCLUSIONS

This research has achieved its aim to develop an algorithm which computes the dyers' variables of ΔD, ΔB and ΔH from the spectral reflectance values of a standard and a batch. The developed algorithm is named the WSF algorithm and it was achieved by iterating the K/S values of the batch. It is believed that this algorithm will help the dyer in minimizing the errors to reconcile the output of colour physics software. The algorithm also intends to reduce the percentage disagreement in reporting the colour errors between an experienced and an inexperienced dyer.

## 7.1 Outcome of the thesis

The principle outcomes of the thesis are:

### *i. Development of the WSF algorithm*

It has been mentioned earlier in this thesis that a dyer is normally trained since the beginning of his career to assess the effect of changing the concentration of a dye on depth and brightness of a dyed pair. This fundamental principle is applied to develop this WSF algorithm. It involved the following stages (given in Section 4.3) to determine the differences in depth, brightness and hue of the batch from the standard:

- Generation of the equi-depth line for the standard
- Determination of how the strength of a batch can be altered to intersect the equi-depth line of a standard
- Hue correction of the batch
- Determination of difference in depth, brightness and hue of standard and batch & its description

### *ii. Extension of the WSI algorithm to calculate the standard depth of the samples lying above, below or in between these six WSI depth surfaces*

Although the six WSI depth surfaces were used in all those situations where the standard was lying on any one of these surfaces, but it was most unlikely for the standard to always lie on one of these six depth surfaces. Therefore, a new methodology was devised as given in Section 4.3.1, which enabled to generate an equi-depth line passing through the standard for any L* C* $h°_{ab}$ values of the standard. It is important to note that the WSI algorithm is currently the subject of a round- robin trial as a pre-curser to being adopted as an ISO standard.

***iii. Extension of the WSI algorithm for high chroma colours***

The WSI algorithm when reported [15] was limited to the set chroma boundaries throughout the colour space. These limitations are given in Table 4.7 of Section 4.5. An investigation for all the colours with high chroma values than the set chroma boundaries revealed that their behaviour was not linear and an extrapolation of the conic equation to determine the L* of the sample for any C* $h°_{ab}$ value was more reliable instead.

***iv. Hue correction of the batch in all those situations where it is different from standard***

It was considered necessary to perform a hue correction for all those situations where the hue angle of the batch is different from the standard. A new methodology was devised and implemented by using the $C^*$values of the Munsell coloured chips of highest chroma. Details of this methodology are given in Section 4.4. One of the limitations of this hue correction strategy is the extent of lightness levels covered. The extrapolation of this strategy for very pale and dark colours needs to be explored further. Here it is worth reminding that the DBH and the Sato models include a hue correction procedure as well but those procedures are principally different than one used in WSF algorithm, as highlighted in Section 5.1.

***v. Development of the WSF algorithm from the colorimetric variables of the standard and the batch (the linear model)***

One of the important outcomes of this thesis is the determination of ΔD, ΔB & ΔH values from the ΔL*, ΔC* & ΔH* values of a dyed pair. A new method was developed which can predict the L* and C* coordinate of the batch at the intersection point on the equi-depth line for the standard without involving any iteration. This new WSF algorithm is named the linear WSF algorithm. This linear WSF algorithm was found superior in computing the ΔD, ΔB & ΔH values for all those batches which have same L* a* b* C* $h°_{ab}$ values but different reflectance curves.

## 7.2 Performance of the WSF algorithm in comparison to the visual assessments

The WSF model performed well when compared qualitatively to the reported visual results of data set 2. No significant difference of hue correction to the WSF model was made in evaluating the difference in depth and brightness of the batch from the standard

but the extent of agreement remains same when the hue correction was made. The quantitative comparison of the WSF algorithm with the visual assessments was disappointing however. It is known that observers vary in their opinions; the assessments of only two observers were available to estimate the accuracy of the WSF algorithm, which does not truly reflect the average assessments of the experienced observers in terms of evaluating the differences in depth, brightness and hue. It is recommended that more reliable quantitative visual assessments are required to make a good comparison with the outcome of the WSF algorithm. The decisions of the two observers were not in good agreement, though this was probably due to the assessment method used, rather than the competence of the observers concerned. The method used in this work required the observers to apportion the overall colour difference into its components of depth, brightness and hue which in reality is very difficult to do. It is therefore suggested that an alternative assessment strategy (ranking method, grey scale method or ratio method etc) might affect the dyers' output in term of assessing the difference in depth and brightness between the standard and the batch.

### 7.3 Comparison of the WSF algorithm with the DBH, Sato and WSF linear algorithms

The correlation coefficients of the WSF algorithm with the DBH, Sato and the linear WSF algorithms were calculated for cumulative data sets (data set 1and 2) and are given in Table 7.1. Comparison with the DBH, Sato and WSF linear models shows good agreement in predicting the change in depth and brightness.

Table 7.1: Correlation coefficients of the WSF algorithm with the DBH, Sato and the linear WSF algorithms

| | $(r)_{\Delta D}$ | $(r)_{\Delta B}$ |
|---|---|---|
| WSF and DBH | 0.94 | 0.95 |
| WSF and Sato | 0.90 | 0.96 |
| WSF and linear WSF | 0.85 | 0.96 |
| Linear WSF and Sato | 0.90 | 0.97 |
| linear WSF and DBH | 0.86 | 0.95 |
| DBH and Sato | 0.88 | 0.97 |

This level of agreement with the DBH and Sato models between the three algorithms is significant because they are based on fundamentally different principles.

### 7.4 Future direction

The following work is recommended to validate the outcome of the WSF algorithm and to widen the scope of the thesis:

- More quantitative visual data are required to compare the performance of the WSF algorithm with the visual assessments.
- Hue correction strategy for very pale and very dark shades needs to be investigated further.
- More data are required to investigate the behaviour of the WSF algorithm (iterative) for all those batches with same L* a* b* C* $h°_{ab}$ values but different %R values.
- A general guide line how to develop the linear WSF algorithm is proposed. It is required that this linear model be explored further for very pale colours and for very rich chroma colours. Its quantitative comparison to reliable visual assessments needs also to be established.
- The WSF algorithm applies only to non-fluorescent coloured pairs. It is possible that its application for fluorescent coloured pairs be explored.
- It is recommended to develop the WSI depth surfaces and the WSF algorithm to predict the difference in depth, brightness and hue of dyed pairs for other illuminants as well.

# REFERENCES


1. "Colour Terms and Definitions", S.D.C., (1988) second edition
2. M. R. Luo, "Development of Colour Difference Formulae", Rev. Prog. Col., **32,** 28−39 (2002)
3. EN ISO 105: Textiles –Tests for colour fastness, Part J03: "Calculation of colour differences", (1995)
4. K. McLaren, "Lab Space: The key to successful instrumental shade passing", J.S.D.C., **97,** 498−502 (1981)
5. K. McLaren, "Adams-Nickerson Colour Space and the Dyer's Variables of Perceived Colour", J. Col. App., **11,** 12−18 (1972)
6. E.Waters, "Colour Matching – What the Dyer Sees ", S.D.C., **59**, 261−269 (1943)
7. A.C. Cooper and K. Mclaren, "The ANLAB Colour System and the Dyers Variables of Shade and Strength", J.S.D.C., **89**, 41−45 (1973)
8. T.H. Morton, "Dyers Terms for Colour Differences", J.S.D.C., **92**, 342 (1976)
9. E. I. Stearns, "Measurement of Dye Strengths", Amer. Dyestuff Rep., **39,** 358−366 (1950)
10. H. R. Davidson, "Accuracy of Visual Judgements of Colour Differences on Wool Flannel", Amer. Dyestuff Rep., **40**, 247−254 (1951)
11. R.G. Kuehni, "Standard Depth and its Determination", Text. Chem. Col., **4,** 22−25 (1978)
12. EN ISO 105: Textiles- Tests For Colour Fastness, Part AO1: "General Principles of Fastness Testing", (1995)
13. EN ISO 105: Textiles- Tests For Colour Fastness, Part AO6: "Instrumental Determination of 1/1 Standard Depth", (1997)
14. R.H. Wardman, Chao-Chi Chen and K. J. Smith, "The Mapping of a Surface of Constant Visual Depth in CIELAB Colour Space", Col. Tech., **118**, 281−294 (2002)
15. R.H. Wardman, S.Islam and K. J. Smith, "Proposal for the Numerical Definition of Standard Depths", Col. Tech., **122**, 350−355 (2006)
16. R.W.G. Hunt, "Measuring Colour", John Wiley and Sons, 74−103 (1987)
17. M. D. Fairchild, "Colour Appearance Models", Addison–Wesley, 97−107 (1998)

18. Billmeyer and Saltzman , “Principles of Colour Technology”, John Wiley and Sons, 25−66 (1981)
19. F. W. Billmeyer Jr., “Survey of Colour Order Systems”, Col. Res. Appln., **12**, 173−185 (1987)
20. G. Tonnquist, “Philosophy of Perceptive Colour Order Systems”, Col. Res. Appln., **11,** 51−55 (1988)
21. W.D Wright, “The Basic Concepts and Attributes of Colour Order Systems”, Col. Res. Appln., **9,** 229−233 (1984)
22. S. M. Newhall, D. Nickerson, and D. B. Judd, “Final Report of the O.S.A. Subcommittee on the Spacing of the Munsell Colours”, J. Opt. Soc., **33,** 385−418 (1943)
23. M. R. Witt, “The Story of the DIN Colour System”, Col. Res. Appln., **11,** 138−145 (1986)
24. A. Hard and L. Sivik, “NCS-Natural Colour System: A Swedish Standard for Colour Notation”, Col. Res. Appln., **6,** 129−138 (1981)
25. D. Nickerson, “OSA Uniform Colour Scale Samples: A Unique Set”, Col. Res. Appln., **6,** 7−28 (1981)
26. F. W. Billmeyer Jr., “Notes on the Geometry of the OSA Uniform Colour Scales Committee Space”, Col. Res. Appln., **6,** 34−36 (1981)
27. A. Nemcsics, “The Coloriod Colour System”, Col. Res. Appln., **5,** 113−120 (1980)
28. R. McDonald, “Colour Physics For Industry ”, Society Of Dyers and Colourists, 162−184 (1997)
29. R.W.Hunt, “Colour Measurement”, Review of Progress in Coloration, **2,** 11−19 (1971)
30. ASTM E 308-06, “Standard Practice for Computing the Colous of Objects by using the CIE System”, (1994)
31. Chamberlin, “The C.I.E. International Colour System Explained”, Salisbury, U.K., Tintometer, (1951)
32. Y. Ohuo, “ CIE Fundamentals For Colour Measurements”, Paper for IS&T NIP 16 Conference, Canada, (Oct 2000)
33. E. Coates and B. Rigg, “The Measurement of Colour (1) – An Introduction to Tristimulus Colorimerty”, J.S.D.C., **81,** 469−475 (1965)
34. E.Coates And B. Rigg, “The Measurement of Colour (2) – The CIE System”, J.S.D.C., **83,** 328−339 (1967)

35. E. I. Stearns, “A New Look at the Calculation of Tristimulus Values”, Col.Res. Appln., **6,** 203−206 (1981)
36. E. I. Stearns, “ Calculation of Tristimulus Weights by Integration”, Col. Res. Appln., **6,** 207−209 (1981)
37. E. I. Stearns, “Calculation of Tristimulus Values and Weights with the revised CIE recommendations”, Text. Chem. Col., **17,** 162−168 (1985)
38. “Colorimerty,” CIE., **15** (1986) Second Edition
39. R. G. Kuehni, “Colour Difference Formulas: an unsatisfactory state of affairs”, Col. Res. Appln., **33,** 324−326 ( 2008)
40. K. McLaren, “The Adams-Nickerson Colour Difference Formula”, J.S.D.C., **86,** 354−366 (1970)
41. K. McLaren, “The development of the CIE1976(LAB) uniform colour space and colour difference formula”, J.S.D.C., **92,** 338−341 (1976)
42. K. McLaren and B.Rigg, “The SDC recommended colour difference formula: change to CIELAB”, J.S.D.C., **92,** 337−338 (1976)
43. R. McDonald, “Industrial Pass/Fail Colour Matching. Part I –Preparation of visual colour matching data”, J.S.D.C., **96,** 372−376 (1980)
44. R. McDonald, “Industrial Pass/Fail Colour Matching. Part II –Methods of fitting tolerance ellipsoids”, J.S.D.C., **96,** 418−422 (1980)
45. R. McDonald, “Industrial Pass/Fail Colour Matching. Part III–Development of a Pass/Fail formula for use with Instrumental Measurement of Colour Difference”, J.S.D.C., **96,** 486−496 (1980)
46. R. McDonald, “The development of Pass/Fail Colour Matching Formulae for Single Number Shade Passing”, J.S.D.C., **97,** 517−521 (1981)
47. F.J. Clarke, R. McDonald and B. Rigg, “Modification to the JPC79 Colour Difference Formula”, J.S.D.C., **100,** 128−132 (1984)
48. M.R. Luo and B. Rigg, “BFD (*l:c*) Colour-Difference Formula Part 1 – Development of the Formula”, J.S.D.C., **103,** 87−93 (1987)
49. M.R. Luo and B. Rigg, “BFD (*l:c*) Colour-Difference Formula Part 2 – Development of the Formula”, J.S.D.C., **103,** 126−132 (1987)
50. R. McDonald and K. J. Smith, “CIE94-A new Colour Difference Formula”, J.S.D.C., **111,** 376−379 (1995)
51. M.R. Luo, G.Cui, and B. Rigg, “The Development of the CIE 2000 Colour Difference Formula: CIEDE 2000”, Col. Res. Appln., **5,** 340−350 (2001)

52. J. H. Xin, “Total Colour Management Of Textiles”, Wood Head Publishing Limited, 62−65, (2006)
53. K. McLaren and P. F. Taylor, “The Derivation of Hue Difference terms from CIELAB Coordinates”, Col. Res. Appln., **6**, 75−79 (1981)
54. K. J. Smith , “ Instrumental Evaluation of Dyers Depth of Shade”, Proceeding of the International Conference and Exhibition, University of Leeds, 77−87 (1998)
55. M. E. Taylor, “An Instrumental Method for determining Equal Depth of Shade”, Text. Chem. Col., **2,** 149−158 (1970)
56. R. Commerford, “Difficulties in Preparing Dye Solutions for Accurate Strength Measurements”, Text. Chem. Col., **6,** 39−48 (1974)
57. R. G. Kuehni, “Determination of Relative Strength and Shade of Textile Dyes”, Text. Chem. Col., **16,** 27−28 (1984)
58. C. E. Garland, “Shade and Strength Predictions and Tolerances from Spectral Analysis of Solutions”, Text. Chem. Col., **5,** 227−231 (1973)
59. A. N. Derbyshire and W. J. Marshall , “Value Analysis of Dyes-A new method based on Colour Measurement”, J.S.D.C., **96,** 166−175 (1980)
60. W. Baumann, R. Brossman, and A. T. Leaver, “Determination of Relative Colour Strength and Residual Colour Difference by means of Reflectance Measurements”, J.S.D.C., **103,** 100−105 (1987)
61. H. Godlove , “Tinctorial Strength, Depth (Apparent Strength ) of Dyeings and Money Value of Dyes”, Amer. Dyestuff Rep., **43,** 685−690 (1954)
62. P. Rabe, “The Standard Depth of Shade in Relation to the Assessment of Colorfastness of Dyes on Textiles”, Amer. Dyestuff Rep., **15,** 504−508 (1957)
63. L. Gall and G. Riedel, “Farbe−Frankfurtthen Gottingen”, Die Farbe, **14,** 342−353 (1965)
64. H. A. Christ., Textilveredlung , **20,** 241−243 (1985)
65. T. Sato, M. Ueda, and S.M. Burkinshaw, “Numerical Expression of Colour Depth and Brightness for Dyeing”, Proceeding of the International Conference U.M.I,S.T., 205−206 (1995)
66. T. Sato, “Dyers Scales for Assessing the Colour of Dyed Fabrics”, Proceeding of the International Conference and Exhibition, University of Leeds, 259−262 (1998)
67. C. J. Hawkyard and A. Haque, “Depth Assessment for Mixture Shades”, Col. Tech., **121,** 86−89 (2005)

68. C. J. Hawkyard and M. Kelly , “A New Approach to the Assessment of Standard Depth”, J.S.D.C., **116,** 339−344 (2000)
69. K. J. Smith, “Partitioning Colour Differences into Dyers Components; The DBH Model”, Col. Tech., **123,** 170-177 (2007)
70. C.C. Chin, “The Inter-conversion of Colorimetric Components of Colour Difference and Dyer’s Perceived Variables”, PhD Thesis, School of Textiles, Heriot-Watt University, (October 2001)
71. S. Islam., “Development of an Algorithm for the Numerical Specification of Standard Depths of Colour”, PhD Thesis, School of Textiles and Design, Heriot -Watt University, (July 2006)
72. Munsell Book of Colour
73. S. Williams, Private Communication.
74. http:www.colorsystem.com
75. http://en.wikipedia.org/wiki/CIE_1931_colour_space
76. http://hyperphysics.phy-astr.gsu.edu/hbase/vision/cie.html

# APPENDICES

**Appendix A1 Flow chart for the WSF algorithm for the determination of the batch strength by iterating the K/S values of the batch until its depth becomes equal to the standard**

**When standard is lying on one of the six WSI equi-depth surfaces**

```
ref=[26.16 28.15 30.66 33.65 37.33 41.52 45.37 47.87 48.78 48.13 46.24 43.56 40.54
37.37 34.23 31.43 29.04 26.89 24.92 23.36 22.4 21.91 21.65 21.47 21.6 22.4 24.16
26.93 30.88 35.74 41.79];

KS=(100^2-2*ref.*100+ref.^2)./(ref.*200);

EX=[0.097020374 0.616129387 1.650346573 2.377499275 3.512737675 3.789795857 3.103651767
1.937406855 0.747156903 0.110023105 0.00700147 0.314065954 1.027215715 2.174456636
3.380709949 4.735994559 6.082277278 7.311535422 8.3947629 8.604807009 8.772842297
7.997679513 6.477360246 4.635973554 3.074645676 1.81438102 1.031216555 0.557116995
0.261054822 0.114023945 0.057011973];

EY=[0.0100021 0.064013443 0.171035918 0.283059442 0.549115314 0.888186519 1.277268226
1.81738165 2.545534562 3.16466458 4.30990508 5.632182758 6.897448464 8.137708919 8.685824023
8.904870023 8.61580932 7.951669851 7.165504756 5.946248712 5.111073325 4.067854249
2.990628032 2.020424289 1.275267806 0.724152072 0.407085488 0.21804579 0.102021424
0.044009242 0.022004621];

EZ=[0.436091579 2.808589804 7.859650527 11.70545815 17.96177197 20.36227608 17.8647516
13.08774843 7.511577431 3.743786195 2.003420718 1.004210884 0.529111113 0.271056922
0.116024365 0.030006301 -0.00300063 0.00100021 0 0 0 0 0 0 0 0 0 0 0 0];

Xn=sum(EX);
Yn=sum(EY);
Zn=sum(EZ);

c=1;
%c is the orignal concentration at which reflectance is measured

k=KS;
g=k.*c;

R=(200+g.*200-sqrt(200^2+g.*200*2*200+200^2*g.^2-40000))/2;

X=(sum(R.*EX.*1))/100;
Y=(sum(R.*EY.*1))/100;
Z=(sum(R.*EZ.*1))/100;

power=1/3;
Ll=(116*(Y/Yn)^power)-16;
a1=((500*(X/Xn)^power-(500*(Y/Yn)^power)));
b1=((200*(Y/Yn)^power-(200*(Z/Zn)^power)));
C1=(a1^2+b1^2)^0.5 ;
%chroma of the dyed fabric

STDL=65.75;
STDC=20;
STDh=225;

BXL=67
BXC=22
BXh=228
```

```
k1=0.0142;
k2=-0.00944;
k3=-1;
k4=0.00301;
k5=-0.1492;
k6=7.166;

aa=k1
bb=k3+k4*STDC
cc=k2*(STDC)^2+k5*STDC+k6
Lwsisample =(-bb+sqrt((bb^2)-4*aa*cc))/2/aa

diffinL=STDL-Lwsisample

C=[1.0];
L=[1.0];
Co=0;
i=1;
while Co<70

aa=k1;
bb=k3+k4*Co;
cc=k2*(Co)^2+k5*Co+k6;
Lwsisample =(-bb+sqrt((bb^2)-4*aa*cc))/2/aa;

C(i)=Co;
L(i)=Lwsisample;
Co=Co+5;
i=i+1;
end

Coo = C1;
%Co is the input chroma to the algorithm.
%C1 is the chroma of the dyed fabric

aaa=k1; %constant for quadratic equation to solve conic equation
bbb=k3+k4*Coo; %constant for quadratic equation to solve conic equation
ccc=k2*Coo^2+k5*Coo+k6; %constant for quadratic equation to solve conic equation

dyedlightness=Ll;
Lwsi=(-bbb+sqrt((bbb^2)-4*aaa*ccc))/2/aaa;
 %lightness calculated by the WSI Algorithm

formulalightness=Lwsi;
difference=dyedlightness-formulalightness;%lightness difference to predicted lightness and dyed fabric
lightness

DL=[1.0 ];%lightness of the dyed fabric will appear in a vector form
DC=[1.0 ];%chroma of the dyed fabric will appear in vector form
DIFF=[1.0];%DIFFERENCE IN LIGHTNESSFROM PREDICTED TO ORIGNAL IN VECTOR FORM

conc=1;
inc=0.01;
concc=conc*inc;
i=1;
while ((abs(difference)>=0.1))

k=KS;
g=k.*concc;
R=(200+g.*200-sqrt(200^2+g.*200*2*200+200^2*g.^2-40000))/2;
```

```
X=(sum(R.*EX.*1))/100;
Y=(sum(R.*EY.*1))/100;
Z=(sum(R.*EZ.*1))/100;
power=1/3;
Ll=(116*(Y/Yn)^power)-16;
a1=((500*(X/Xn)^power-(500*(Y/Yn)^power)));
b1=((200*(Y/Yn)^power-(200*(Z/Zn)^power)));
C1=(a1^2+b1^2)^0.5;

dyedlightness=Ll;
Coo=C1;
aaa=k1;%constant for quadratic equation to solve conic equation
bbb=k3+k4*Coo;
ccc=k2*Coo^2+k5*Coo+k6;
Lwsi=(-bbb+sqrt((bbb^2)-4*aaa*ccc))/2/aaa;

formulalightness=Lwsi;
difference=dyedlightness-formulalightness;

DL(i)=dyedlightness;
DC(i)=C1;
DIFF(i)=difference;

concc=conc*inc;

inc=(inc+0.01);
i=i+1;
end

hue=BXh-STDh;
concc=concc-0.01

FINALL= DL(i-1)
FINALC =DC(i-1)

brightness=sqrt((STDL-FINALL)^2+((STDC-FINALC)^2));
depth=sqrt(((BXL-FINALL))^2+((BXC-FINALC)^2));

weaker=-1*depth;
stronger=1*depth;
flatter=-1*brightness ;
brighter=1*brightness ;

if concc>=1
       weaker
else
      stronger
end

if STDC>=DC(i-1)
     flatter
else
       brighter
end


dyedfabriclightness=DL;
dyedfabricchroma=DC;
differenceinlightness=DIFF;
```

```
graph1=plot(BXC,BXL,'+r',DC,DL,'-+g',C,L,'y',STDC,STDL,'p')
```

**Appendix A 2 When standard is lying between the six wsi equi-depth surfaces**

```
Ref= [15.2   22.13   30.96   36.8    38.59   36.95   33.17   29.19   25.68   22.54   20.1    18.19   16.69
15.77   15.58   15.99   16.61   17.6    19.9    24.77   32.9    43.27   52.96   59.86   63.83   66.19   68.32
70.91   74.26   77.61   80.61];

KS= (100^2-2*ref.*100+ref.^2)./(ref.*200);

EX= [0.097 0.616 1.650 2.377 3.512 3.789795857 3.103651767 1.937406855 0.747156903 0.110023105
0.00700147 0.314065954 1.027215715 2.174456636 3.380709949 4.735994559 6.082277278
7.311535422 8.3947629 8.604807009 8.772842297 7.997679513 6.477360246 4.635973554
3.074645676 1.81438102 1.031216555 0.557116995 0.261054822 0.114023945 0.057011973];

EY= [0.0100021 0.064013443 0.171035918 0.283059442 0.549115314 0.888186519 1.277268226
1.81738165 2.545534562 3.16466458 4.30990508 5.632182758 6.897448464 8.137708919 8.685824023
8.904870023 8.61580932 7.951669851 7.165504756 5.946248712 5.111073325 4.067854249
2.990628032 2.020424289 1.275267806 0.724152072 0.407085488 0.21804579 0.102021424
0.044009242 0.022004621];

EZ= [0.436091579 2.808589804 7.859650527 11.70545815 17.96177197 20.36227608 17.8647516
13.08774843 7.511577431 3.743786195 2.003420718 1.004210884 0.529111113 0.271056922
0.116024365 0.030006301 -0.00300063 0.00100021 0 0 0 0 0 0 0 0 0 0 0 0];

Xn=sum(EX);
Yn=sum(EY);
Zn=sum(EZ);

c=1;
%c is the optimal concentration at which reflectance is measured

k=KS./c;
conc=0.1;
g=k.*conc;
%conc is the new concentration and g is the k/s of the new
%concentration

R=(200+g.*200-sqrt(200^2+g.*200*2*200+200^2*g.^2-40000))/2;

X=(sum(R.*EX.*1))/100;
Y=(sum(R.*EY.*1))/100;
Z=(sum(R.*EZ.*1))/100;

Ll=(116*(Y/Yn)^0.33)-16;
%lightness of the dyed fabric

a1=((500*(X/Xn)^0.33-(500*(Y/Yn)^0.33)));
b1=((200*(Y/Yn)^0.33-(200*(Z/Zn)^0.33)));
C1=(a1^2+b1^2)^0.5 ;
%chroma of the dyed fabric
STDL=54.95;
STDC=38.83;
STDh=336.81;

BXL=56.05;
BXC=37.36;
BXh=338.6;
```

```
k1below=0.0195;
k2below=-0.0038;
k3below=-1;
k4below=0.0029;
k5below=-0.057;
k6below=4.892;

k1above=0.0167;
k2above=-0.0056;
k3above=-1;
k4above=0.00158;
k5above=-0.0209;
k6above=5.691;

deltakt1= k1above-k1below;
deltakt2= k2above-k2below;
deltakt3= k3above-k3below;
deltakt4= k4above-k4below;
deltakt5= k5above-k5below;
deltakt6= k6above-k6below;

Lsample=54.95;
Lbelow =48.84;
Labove =59.78;

deltaL1= Lsample-Lbelow;
deltaLt= Labove-Lbelow;

deltakt1= k1above-k1below;
deltak1=(deltaL1/deltaLt)*deltakt1;
deltak2=(deltaL1/deltaLt)*deltakt2;
deltak3=(deltaL1/deltaLt)*deltakt3;
deltak4=(deltaL1/deltaLt)*deltakt4;
deltak5=(deltaL1/deltaLt)*deltakt5;
deltak6=(deltaL1/deltaLt)*deltakt6;

k1sample=k1below+deltak1;
k2sample=k2below+deltak2;
k3sample=k3below+deltak3;
k4sample=k4below+deltak4;
k5sample=k5below+deltak5;
k6sample=k6below+deltak6;


aa=k1sample;
bb=k3sample+k4sample*STDC;
cc=k2sample*(STDC)^2+k5sample*STDC+k6sample;
Lwsisample =(-bb+sqrt((bb^2)-4*aa*cc))/2/aa;

diffinL=Lsample-Lwsisample;
k1s=[1.0];
deltak1new=(-1);
i=1;

while(abs(diffinL)>=0.1)&&(deltak1new <(1))
deltaL1= Lsample-Lbelow;
deltaLt= Labove-Lbelow;
deltakt1= k1above-k1below;
```

```
k1sample=k1below+deltak1new;

aa=k1sample;
bb=k3sample+k4sample*STDC;
cc=k2sample*(STDC)^2+k5sample*STDC+k6sample;
Lwsisample =(-bb+sqrt((bb^2)-4*aa*cc))/2/aa;

diffinL=Lsample-Lwsisample;
deltak1new=deltak1new+0.0001;
i=i+1;
end

diffinL=Lsample-Lwsisample
k1s=k1sample
C=[1.0];
L=[1.0];
Co=0;
i=1;

while Co<50

a=k1s;
b=k3sample+k4sample*Co;
c=k2sample*(Co)^2+k5sample*Co+k6sample;
LLwsisample =(-b+sqrt((b^2)-4*a*c))/2/a;
C(i)=Co;
L(i)=LLwsisample;
Co=Co+5;
i=i+1;
end

Coo=C1;
%Co is the input chroma to the algorithm.
%C1 is the chroma of the dyed fabric

aaa=k1s; %constant for quadratic equation to solve conic equation
bbb=k3sample+k4sample*Coo; %constant for quadratic equation to solve conic equation
ccc=k2sample*Coo^2+k5sample*Coo+k6sample; %constant for quadratic equation to solve conic
equation

dyedlightness=Ll;
Lwsi=(-bbb+sqrt((bbb^2)-4*aaa*ccc))/2/aaa;
%lightness calculated by the WSI Algorithm

formulalightness=Lwsi;
difference=dyedlightness-formulalightness;%lightness difference to predicted lightness and dyed fabric
lightness
DL=[1.0 ];%lightness of the dyed fabric will appear in a vector form
DC=[1.0 ];%chroma of the dyed fabric will appear in vector form
DIFF=[1.0];%DIFFERENCE IN LIGHTNESSFROM PREDICTED TO ORIGNAL IN VECTOR FORM

conc=0.1;
i=1;
while ((abs(difference)>=0.1))&&(conc<2)
c=1;
k=KS./c;
g=k.*conc;
R=(200+g.*200-sqrt(200^2+g.*200*2*200+200^2*g.^2-40000))/2;
X=(sum(R.*EX.*1))/100;
Y=(sum(R.*EY.*1))/100;
Z=(sum(R.*EZ.*1))/100;
```

```
Ll=(116*(Y/Yn)^0.33)-16;
a1=((500*(X/Xn)^0.33-(500*(Y/Yn)^0.33)));
b1=((200*(Y/Yn)^0.33-(200*(Z/Zn)^0.33)));
C1=(a1^2+b1^2)^0.5;

dyedlightness=Ll;
Coo=C1;
aaa=k1s;%constant for quadratic equation to solve conic equation
bbb=k3sample+k4sample*Coo;
ccc=k2sample*Coo^2+k5sample*Coo+k6sample;
Lwsi=(-bbb+sqrt((bbb^2)-4*aaa*ccc))/2/aaa;

formulalightness=Lwsi;
difference=dyedlightness(1)-formulalightness(1);

DL(i)=dyedlightness;
DC(i)=C1;
DIFF(i)=difference;

hue=BXh-STDh;
conc=conc+0.01;
i=i+1;
end

hue=BXh-STDh
conc=conc-0.01
FINALL= DL(i-1)
FINALC =DC(i-1)

brightness=sqrt((STDL-DL(i-1))^2+((STDC-DC(i-1))^2))
depth=sqrt((BXL-DL(i-1))^2+((BXC-DC(i-1))^2))

weaker=(-1*depth);
stronger=1*depth;
flatter=-1*brightness ;
brighter=1*brightness ;

if STDC>=DC(i-1)
     flatter
else
       brighter
end

if (conc>=1.03)
   weaker
else
        stronger
end

  dyedfabriclightness=DL;
  dyedfabricchroma=DC;
  differenceinlightness=DIFF;

  graph1=plot(DC,DL,'-+g',C,L,'y',STDC,STDL,'p')
```

**Appendix B The ICI (x,y) equivalents of the Theoretical Pigment Maxima for 40 Hues on nine Value levels viewed in illuminant C at $2^0$ observer and the calculated X, Y, Z values.**

**R**

| HUE | value | x | y | X | Y | Z |
|---|---|---|---|---|---|---|
| 2.5R | 9 | 0.372 | 0.318 | 92.017 | 78.66 | 76.681 |
| 5.0R | | 0.378 | 0.326 | 91.207 | 78.66 | 71.421 |
| 7.5R | | 0.384 | 0.335 | 90.165 | 78.66 | 65.980 |
| 10.0R | | 0.39 | 0.344 | 89.178 | 78.66 | 60.824 |
| 2.5R | 8 | 0.432 | 0.315 | 81.051 | 59.1 | 47.468 |
| 5.0R | | 0.442 | 0.327 | 79.884 | 59.1 | 41.750 |
| 7.5R | | 0.458 | 0.344 | 78.685 | 59.1 | 34.017 |
| 10.0R | | 0.476 | 0.364 | 77.285 | 59.1 | 25.978 |
| 2.5R | 7 | 0.49 | 0.304 | 69.406 | 43.06 | 29.179 |
| 5.0R | | 0.51 | 0.322 | 68.201 | 43.06 | 22.466 |
| 7.5R | | 0.535 | 0.345 | 66.774 | 43.06 | 14.977 |
| 10.0R | | 0.567 | 0.374 | 65.281 | 43.06 | 6.793 |
| 2.5R | 6 | 0.54 | 0.289 | 56.149 | 30.05 | 17.780 |
| 5.0R | | 0.57 | 0.311 | 55.076 | 30.05 | 11.498 |
| 7.5R | | 0.604 | 0.336 | 54.018 | 30.05 | 5.366 |
| 10.0R | | 0.627 | 0.372 | 50.649 | 30.05 | 0.081 |
| 2.5R | 5 | 0.585 | 0.269 | 42.994 | 19.77 | 10.730 |
| 5.0R | | 0.624 | 0.294 | 41.961 | 19.77 | 5.514 |
| 7.5R | | 0.658 | 0.315 | 41.297 | 19.77 | 1.695 |
| 10.0R | | 0.635 | 0.364 | 34.489 | 19.77 | 0.054 |
| 2.5R | 4 | 0.613 | 0.253 | 29.075 | 12 | 6.356 |
| 5.0R | | 0.659 | 0.278 | 28.446 | 12 | 2.719 |
| 7.5R | | 0.69 | 0.294 | 28.163 | 12 | 0.653 |
| 10.0R | | 0.647 | 0.353 | 21.994 | 12 | 0.000 |
| 2.5R | 3 | 0.627 | 0.238 | 17.269 | 6.555 | 3.718 |
| 5.0R | | 0.668 | 0.259 | 16.906 | 6.555 | 1.848 |
| 7.5R | | 0.703 | 0.277 | 16.636 | 6.555 | 0.473 |
| 10.0R | | 0.677 | 0.322 | 13.782 | 6.555 | 0.020 |
| 2.5R | 2 | 0.58 | 0.204 | 8.888 | 3.126 | 3.310 |
| 5.0R | | 0.632 | 0.228 | 8.665 | 3.126 | 1.919 |
| 7.5R | | 0.68 | 0.251 | 8.469 | 3.126 | 0.859 |
| 10.0R | | 0.721 | 0.271 | 8.317 | 3.126 | 0.092 |
| 2.5R | 1 | 0.526 | 0.172 | 3.700 | 1.21 | 2.125 |
| 5.0R | | 0.581 | 0.198 | 3.551 | 1.21 | 1.351 |
| 7.5R | | 0.628 | 0.22 | 3.454 | 1.21 | 0.836 |
| 10.0R | | 0.679 | 0.244 | 3.367 | 1.21 | 0.382 |

**YR**

| HUE | value | x | y | X | Y | Z |
|---|---|---|---|---|---|---|
| 2.5YR | 9 | 0.399 | 0.358 | 87.669 | 78.66 | 53.392 |
| 5.0YR | | 0.409 | 0.373 | 86.252 | 78.66 | 45.973 |
| 7.5YR | | 0.423 | 0.393 | 84.665 | 78.66 | 36.828 |
| 10.0YR | | 0.442 | 0.422 | 82.388 | 78.66 | 25.350 |
| 2.5YR | 8 | 0.497 | 0.388 | 75.703 | 59.1 | 17.517 |
| 5.0YR | | 0.527 | 0.422 | 73.805 | 59.1 | 7.142 |
| 7.5YR | | 0.545 | 0.455 | 70.790 | 59.1 | 0.000 |
| 10.0YR | | 0.527 | 0.472 | 65.987 | 59.1 | 0.125 |
| 2.5YR | 7 | 0.593 | 0.407 | 62.739 | 43.06 | 0.000 |
| 5.0YR | | 0.569 | 0.431 | 56.847 | 43.06 | 0.000 |
| 7.5YR | | 0.547 | 0.452 | 52.110 | 43.06 | 0.095 |
| 10.0YR | | 0.529 | 0.471 | 48.363 | 43.06 | 0.000 |
| 2.5YR | 6 | 0.596 | 0.403 | 44.441 | 30.05 | 0.075 |
| 5.0YR | | 0.572 | 0.427 | 40.254 | 30.05 | 0.070 |
| 7.5YR | | 0.55 | 0.449 | 36.810 | 30.05 | 0.067 |

| | | | | | | |
|---|---|---|---|---|---|---|
| 10.0YR | | 0.53 | 0.468 | 34.031 | 30.05 | 0.128 |
| 2.5YR | 5 | 0.6 | 0.4 | 29.655 | 19.77 | 0.000 |
| 5.0YR | | 0.576 | 0.423 | 26.921 | 19.77 | 0.047 |
| 7.5YR | | 0.553 | 0.446 | 24.513 | 19.77 | 0.044 |
| 10.0YR | | 0.533 | 0.466 | 22.612 | 19.77 | 0.042 |
| 2.5YR | 4 | 0.605 | 0.394 | 18.426 | 12 | 0.030 |
| 5.0YR | | 0.581 | 0.419 | 16.640 | 12 | 0.000 |
| 7.5YR | | 0.556 | 0.443 | 15.061 | 12 | 0.027 |
| 10.0YR | | 0.536 | 0.463 | 13.892 | 12 | 0.026 |
| 2.5YR | 3 | 0.617 | 0.382 | 10.588 | 6.555 | 0.017 |
| 5.0YR | | 0.586 | 0.413 | 9.301 | 6.555 | 0.016 |
| 7.5YR | | 0.56 | 0.439 | 8.362 | 6.555 | 0.015 |
| 10.0YR | | 0.539 | 0.46 | 7.681 | 6.555 | 0.014 |
| 2.5YR | 2 | 0.646 | 0.353 | 5.721 | 3.126 | 0.009 |
| 5.0YR | | 0.598 | 0.402 | 4.650 | 3.126 | 0.000 |
| 7.5YR | | 0.566 | 0.434 | 4.077 | 3.126 | 0.000 |
| 10.0YR | | 0.543 | 0.456 | 3.722 | 3.126 | 0.007 |
| 2.5YR | 1 | 0.713 | 0.287 | 3.006 | 1.21 | 0.000 |
| 5.0YR | | 0.616 | 0.384 | 1.941 | 1.21 | 0.000 |
| 7.5YR | | 0.581 | 0.418 | 1.682 | 1.21 | 0.003 |
| 10.0YR | | 0.55 | 0.449 | 1.482 | 1.21 | 0.003 |

**Y**

| HUE | value | x | y | X | Y | Z |
|---|---|---|---|---|---|---|
| 2.5Y | 9 | 0.468 | 0.461 | 79.854 | 78.66 | 12.115 |
| 5.0Y | | 0.484 | 0.51 | 74.650 | 78.66 | 0.925 |
| 7.5Y | | 0.47 | 0.523 | 70.689 | 78.66 | 1.053 |
| 10.0Y | | 0.457 | 0.537 | 66.942 | 78.66 | 0.879 |
| 2.5Y | 8 | 0.509 | 0.49 | 61.392 | 59.1 | 0.121 |
| 5.0Y | | 0.488 | 0.51 | 56.551 | 59.1 | 0.232 |
| 7.5Y | | 0.474 | 0.526 | 53.257 | 59.1 | 0.000 |
| 10.0Y | | 0.46 | 0.54 | 50.344 | 59.1 | 0.000 |
| 2.5Y | 7 | 0.511 | 0.489 | 44.997 | 43.06 | 0.000 |
| 5.0Y | | 0.491 | 0.508 | 41.619 | 43.06 | 0.085 |
| 7.5Y | | 0.475 | 0.524 | 39.033 | 43.06 | 0.082 |
| 10.0Y | | 0.459 | 0.539 | 36.669 | 43.06 | 0.160 |
| 2.5Y | 6 | 0.512 | 0.487 | 31.593 | 30.05 | 0.062 |
| 5.0Y | | 0.493 | 0.506 | 29.278 | 30.05 | 0.059 |
| 7.5Y | | 0.476 | 0.523 | 27.350 | 30.05 | 0.057 |
| 10.0Y | | 0.46 | 0.54 | 25.598 | 30.05 | 0.000 |
| 2.5Y | 5 | 0.514 | 0.485 | 20.952 | 19.77 | 0.041 |
| 5.0Y | | 0.495 | 0.504 | 19.417 | 19.77 | 0.039 |
| 7.5Y | | 0.478 | 0.522 | 18.104 | 19.77 | 0.000 |
| 10.0Y | | 0.459 | 0.54 | 16.805 | 19.77 | 0.037 |
| 2.5Y | 4 | 0.516 | 0.483 | 12.820 | 12 | 0.025 |
| 5.0Y | | 0.498 | 0.502 | 11.904 | 12 | 0.000 |
| 7.5Y | | 0.479 | 0.52 | 11.054 | 12 | 0.023 |
| 10.0Y | | 0.459 | 0.54 | 10.200 | 12 | 0.022 |
| 2.5Y | 3 | 0.519 | 0.48 | 7.088 | 6.555 | 0.014 |
| 5.0Y | | 0.5 | 0.5 | 6.555 | 6.555 | 0.000 |
| 7.5Y | | 0.48 | 0.519 | 6.062 | 6.555 | 0.013 |
| 10.0Y | | 0.459 | 0.54 | 5.572 | 6.555 | 0.012 |
| 2.5Y | 2 | 0.522 | 0.477 | 3.421 | 3.126 | 0.007 |
| 5.0Y | | 0.502 | 0.497 | 3.157 | 3.126 | 0.006 |
| 7.5Y | | 0.482 | 0.517 | 2.914 | 3.126 | 0.006 |
| 10.0Y | | 0.459 | 0.54 | 2.657 | 3.126 | 0.006 |
| 2.5Y | 1 | 0.526 | 0.473 | 1.346 | 1.21 | 0.003 |
| 5.0Y | | 0.504 | 0.495 | 1.232 | 1.21 | 0.002 |
| 7.5Y | | 0.484 | 0.515 | 1.137 | 1.21 | 0.002 |
| 10.0Y | | 0.459 | 0.54 | 1.029 | 1.21 | 0.002 |

**GY**

| HUE | value | x | y | X | Y | Z |
|---|---|---|---|---|---|---|
| 2.5GY | 9 | 0.438 | 0.555 | 62.078 | 78.66 | 0.992 |
| 5.0GY | | 0.413 | 0.576 | 56.400 | 78.66 | 1.502 |
| 7.5GY | | 0.361 | 0.603 | 47.092 | 78.66 | 4.696 |
| 10.0GY | | 0.303 | 0.579 | 41.164 | 78.66 | 16.031 |
| 2.5GY | 8 | 0.439 | 0.56 | 46.330 | 59.1 | 0.106 |
| 5.0GY | | 0.413 | 0.586 | 41.652 | 59.1 | 0.101 |
| 7.5GY | | 0.36 | 0.632 | 33.665 | 59.1 | 0.748 |
| 10.0GY | | 0.278 | 0.686 | 23.950 | 59.1 | 3.101 |
| 2.5GY | 7 | 0.438 | 0.561 | 33.619 | 43.06 | 0.077 |
| 5.0GY | | 0.41 | 0.588 | 30.025 | 43.06 | 0.146 |
| 7.5GY | | 0.356 | 0.64 | 23.952 | 43.06 | 0.269 |
| 10.0GY | | 0.267 | 0.711 | 16.170 | 43.06 | 1.332 |
| 2.5GY | 6 | 0.437 | 0.562 | 23.366 | 30.05 | 0.053 |
| 5.0GY | | 0.407 | 0.591 | 20.694 | 30.05 | 0.102 |
| 7.5GY | | 0.349 | 0.648 | 16.184 | 30.05 | 0.139 |
| 10.0GY | | 0.257 | 0.726 | 10.638 | 30.05 | 0.704 |
| 2.5GY | 5 | 0.435 | 0.563 | 15.275 | 19.77 | 0.070 |
| 5.0GY | | 0.404 | 0.594 | 13.446 | 19.77 | 0.067 |
| 7.5GY | | 0.342 | 0.655 | 10.323 | 19.77 | 0.091 |
| 10.0GY | | 0.247 | 0.74 | 6.599 | 19.77 | 0.347 |
| 2.5GY | 4 | 0.434 | 0.565 | 9.218 | 12 | 0.021 |
| 5.0GY | | 0.401 | 0.597 | 8.060 | 12 | 0.040 |
| 7.5GY | | 0.333 | 0.663 | 6.027 | 12 | 0.072 |
| 10.0GY | | 0.238 | 0.747 | 3.823 | 12 | 0.241 |
| 2.5GY | 3 | 0.432 | 0.567 | 4.994 | 6.555 | 0.012 |
| 5.0GY | | 0.396 | 0.602 | 4.312 | 6.555 | 0.022 |
| 7.5GY | | 0.322 | 0.673 | 3.136 | 6.555 | 0.049 |
| 10.0GY | | 0.222 | 0.76 | 1.915 | 6.555 | 0.155 |
| 2.5GY | 2 | 0.43 | 0.57 | 2.358 | 3.126 | 0.000 |
| 5.0GY | | 0.39 | 0.607 | 2.008 | 3.126 | 0.015 |
| 7.5GY | | 0.311 | 0.683 | 1.423 | 3.126 | 0.027 |
| 10.0GY | | 0.188 | 0.785 | 0.749 | 3.126 | 0.108 |
| 2.5GY | 1 | 0.424 | 0.575 | 0.892 | 1.21 | 0.002 |
| 5.0GY | | 0.38 | 0.618 | 0.744 | 1.21 | 0.004 |
| 7.5GY | | 0.292 | 0.701 | 0.504 | 1.21 | 0.012 |
| 10.0GY | | 0.147 | 0.81 | 0.220 | 1.21 | 0.064 |

**G**

| HUE | value | x | y | X | Y | Z |
|---|---|---|---|---|---|---|
| 2.5G | 9 | 0.263 | 0.497 | 41.625 | 78.66 | 37.985 |
| 5.0G | | 0.244 | 0.428 | 44.844 | 78.66 | 60.281 |
| 7.5G | | 0.238 | 0.403 | 46.454 | 78.66 | 70.072 |
| 10.0G | | 0.232 | 0.38 | 48.024 | 78.66 | 80.316 |
| 2.5G | 8 | 0.202 | 0.615 | 19.412 | 59.1 | 17.586 |
| 5.0G | | 0.18 | 0.496 | 21.448 | 59.1 | 38.606 |
| 7.5G | | 0.175 | 0.456 | 22.681 | 59.1 | 47.824 |
| 10.0G | | 0.172 | 0.417 | 24.377 | 59.1 | 58.250 |
| 2.5G | 7 | 0.149 | 0.682 | 9.408 | 43.06 | 10.670 |
| 5.0G | | 0.129 | 0.541 | 10.268 | 43.06 | 26.266 |
| 7.5G | | 0.128 | 0.488 | 11.294 | 43.06 | 33.883 |
| 10.0G | | 0.129 | 0.439 | 12.653 | 43.06 | 42.373 |
| 2.5G | 6 | 0.105 | 0.724 | 4.358 | 30.05 | 7.097 |
| 5.0G | | 0.085 | 0.574 | 4.450 | 30.05 | 17.852 |
| 7.5G | | 0.086 | 0.513 | 5.038 | 30.05 | 23.489 |
| 10.0G | | 0.091 | 0.454 | 6.023 | 30.05 | 30.116 |
| 2.5G | 5 | 0.066 | 0.753 | 1.733 | 19.77 | 4.752 |
| 5.0G | | 0.047 | 0.6 | 1.549 | 19.77 | 11.631 |
| 7.5G | | 0.049 | 0.528 | 1.835 | 19.77 | 15.838 |
| 10.0G | | 0.057 | 0.459 | 2.455 | 19.77 | 20.847 |
| 2.5G | 4 | 0.042 | 0.762 | 0.661 | 12 | 3.087 |

| | | | | | | |
|---|---|---|---|---|---|---|
| 5.0G | | 0.023 | 0.614 | 0.450 | 12 | 7.094 |
| 7.5G | | 0.027 | 0.532 | 0.609 | 12 | 9.947 |
| 10.0G | | 0.036 | 0.456 | 0.947 | 12 | 13.368 |
| 2.5G | 3 | 0.027 | 0.759 | 0.233 | 6.555 | 1.848 |
| 5.0G | | 0.012 | 0.617 | 0.127 | 6.555 | 3.941 |
| 7.5G | | 0.017 | 0.529 | 0.211 | 6.555 | 5.626 |
| 10.0G | | 0.028 | 0.446 | 0.412 | 6.555 | 7.731 |
| 2.5G | 2 | 0.019 | 0.75 | 0.079 | 3.126 | 0.963 |
| 5.0G | | 0.008 | 0.612 | 0.041 | 3.126 | 1.941 |
| 7.5G | | 0.014 | 0.522 | 0.084 | 3.126 | 2.779 |
| 10.0G | | 0.025 | 0.433 | 0.180 | 3.126 | 3.913 |
| 2.5G | 1 | 0.013 | 0.737 | 0.021 | 1.21 | 0.410 |
| 5.0G | | 0.006 | 0.605 | 0.012 | 1.21 | 0.778 |
| 7.5G | | 0.012 | 0.513 | 0.028 | 1.21 | 1.120 |
| 10.0G | | 0.024 | 0.417 | 0.070 | 1.21 | 1.622 |

BG

| HUE | value | x | y | X | Y | Z |
|---|---|---|---|---|---|---|
| 2.5BG | 9 | 0.229 | 0.361 | 49.898 | 78.6 | 89.337 |
| 5.0BG | | 0.225 | 0.342 | 51.750 | 78.66 | 99.590 |
| 7.5BG | | 0.221 | 0.323 | 53.820 | 78.66 | 111.049 |
| 10.0BG | | 0.232 | 0.309 | 59.059 | 78.66 | 116.844 |
| 2.5BG | 8 | 0.17 | 0.38 | 26.439 | 59.1 | 69.987 |
| 5.0BG | | 0.168 | 0.346 | 28.696 | 59.1 | 83.013 |
| 7.5BG | | 0.168 | 0.316 | 31.420 | 59.1 | 96.505 |
| 10.0BG | | 0.168 | 0.29 | 34.237 | 59.1 | 110.456 |
| 2.5BG | 7 | 0.13 | 0.388 | 14.427 | 43.06 | 53.492 |
| 5.0BG | | 0.133 | 0.342 | 16.746 | 43.06 | 66.101 |
| 7.5BG | | 0.136 | 0.306 | 19.138 | 43.06 | 78.521 |
| 10.0BG | | 0.138 | 0.273 | 21.767 | 43.06 | 92.902 |
| 2.5BG | 6 | 0.097 | 0.389 | 7.493 | 30.05 | 39.706 |
| 5.0BG | | 0.104 | 0.334 | 9.357 | 30.05 | 50.563 |
| 7.5BG | | 0.11 | 0.295 | 11.205 | 30.05 | 60.609 |
| 10.0BG | | 0.116 | 0.257 | 13.563 | 30.05 | 73.313 |
| 2.5BG | 5 | 0.068 | 0.386 | 3.483 | 19.77 | 27.965 |
| 5.0BG | | 0.078 | 0.321 | 4.804 | 19.77 | 37.015 |
| 7.5BG | | 0.086 | 0.28 | 6.072 | 19.77 | 44.765 |
| 10.0BG | | 0.095 | 0.241 | 7.793 | 19.77 | 54.470 |
| 2.5BG | 4 | 0.048 | 0.38 | 1.516 | 12 | 18.063 |
| 5.0BG | | 0.062 | 0.306 | 2.431 | 12 | 24.784 |
| 7.5BG | | 0.072 | 0.265 | 3.260 | 12 | 30.023 |
| 10.0BG | | 0.082 | 0.226 | 4.354 | 12 | 36.743 |
| 2.5BG | 3 | 0.04 | 0.37 | 0.709 | 6.555 | 10.453 |
| 5.0BG | | 0.056 | 0.294 | 1.249 | 6.555 | 14.492 |
| 7.5BG | | 0.065 | 0.254 | 1.677 | 6.555 | 17.575 |
| 10.0BG | | 0.076 | 0.213 | 2.339 | 6.555 | 21.881 |
| 2.5BG | 2 | 0.037 | 0.359 | 0.322 | 3.126 | 5.259 |
| 5.0BG | | 0.053 | 0.28 | 0.592 | 3.126 | 7.447 |
| 7.5BG | | 0.062 | 0.244 | 0.794 | 3.126 | 8.891 |
| 10.0BG | | 0.073 | 0.2 | 1.141 | 3.126 | 11.363 |
| 2.5BG | 1 | 0.037 | 0.345 | 0.130 | 1.21 | 2.167 |
| 5.0BG | | 0.053 | 0.267 | 0.240 | 1.21 | 3.082 |
| 7.5BG | | 0.063 | 0.227 | 0.336 | 1.21 | 3.785 |
| 10.0BG | | 0.074 | 0.19 | 0.471 | 1.21 | 4.687 |

**B**

| HUE | value | x | y | X | Y | Z |
|---|---|---|---|---|---|---|
| 2.5B | 9 | 0.248 | 0.302 | 64.595 | 78.66 | 117.209 |
| 5.0B | | 0.259 | 0.297 | 68.596 | 78.66 | 117.593 |
| 7.5B | | 0.265 | 0.295 | 70.661 | 78.66 | 117.323 |

| | | | | | | |
|---|---|---|---|---|---|---|
| 10.0B | | 0.271 | 0.292 | 73.003 | 78.66 | 117.721 |
| 2.5B | 8 | 0.181 | 0.272 | 39.328 | 59.1 | 118.852 |
| 5.0B | | 0.205 | 0.264 | 45.892 | 59.1 | 118.872 |
| 7.5B | | 0.217 | 0.26 | 49.326 | 59.1 | 118.882 |
| 10.0B | | 0.227 | 0.257 | 52.201 | 59.1 | 118.660 |
| 2.5B | 7 | 0.141 | 0.246 | 24.681 | 43.06 | 107.300 |
| 5.0B | | 0.156 | 0.226 | 29.723 | 43.06 | 117.748 |
| 7.5B | | 0.172 | 0.222 | 33.362 | 43.06 | 117.542 |
| 10.0B | | 0.186 | 0.219 | 36.572 | 43.06 | 116.989 |
| 2.5B | 6 | 0.121 | 0.23 | 15.809 | 30.05 | 84.793 |
| 5.0B | | 0.127 | 0.202 | 18.893 | 30.05 | 99.820 |
| 7.5B | | 0.132 | 0.183 | 21.675 | 30.05 | 112.482 |
| 10.0B | | 0.144 | 0.177 | 24.447 | 30.05 | 115.277 |
| 2.5B | 5 | 0.102 | 0.212 | 9.512 | 19.77 | 63.973 |
| 5.0B | | 0.11 | 0.183 | 11.884 | 19.77 | 76.379 |
| 7.5B | | 0.115 | 0.164 | 13.863 | 19.77 | 86.916 |
| 10.0B | | 0.12 | 0.15 | 15.816 | 19.77 | 96.214 |
| 2.5B | 4 | 0.09 | 0.197 | 5.482 | 12 | 43.431 |
| 5.0B | | 0.1 | 0.17 | 7.059 | 12 | 51.529 |
| 7.5B | | 0.106 | 0.151 | 8.424 | 12 | 59.046 |
| 10.0B | | 0.111 | 0.137 | 9.723 | 12 | 65.869 |
| 2.5B | 3 | 0.084 | 0.185 | 2.976 | 6.555 | 25.901 |
| 5.0B | | 0.094 | 0.158 | 3.900 | 6.555 | 31.033 |
| 7.5B | | 0.1 | 0.141 | 4.649 | 6.555 | 35.285 |
| 10.0B | | 0.105 | 0.127 | 5.419 | 6.555 | 39.640 |
| 2.5B | 2 | 0.082 | 0.175 | 1.465 | 3.126 | 13.272 |
| 5.0B | | 0.09 | 0.149 | 1.888 | 3.126 | 15.966 |
| 7.5B | | 0.096 | 0.133 | 2.256 | 3.126 | 18.121 |
| 10.0B | | 0.102 | 0.119 | 2.679 | 3.126 | 20.463 |
| 2.5B | 1 | 0.082 | 0.166 | 0.598 | 1.21 | 5.481 |
| 5.0B | | 0.09 | 0.143 | 0.762 | 1.21 | 6.490 |
| 7.5B | | 0.096 | 0.127 | 0.915 | 1.21 | 7.403 |
| 10.0B | | 0.101 | 0.114 | 1.072 | 1.21 | 8.332 |

**PB**

| HUE | value | x | y | X | Y | Z |
|---|---|---|---|---|---|---|
| 2.5PB | 9 | 0.277 | 0.29 | 75.134 | 78.66 | 117.448 |
| 5.0PB | | 0.281 | 0.288 | 76.748 | 78.66 | 117.717 |
| 7.5PB | | 0.286 | 0.286 | 78.660 | 78.66 | 117.715 |
| 10.0PB | | 0.29 | 0.281 | 81.179 | 78.66 | 120.089 |
| 2.5PB | 8 | 0.238 | 0.254 | 55.377 | 59.1 | 118.200 |
| 5.0PB | | 0.246 | 0.251 | 57.923 | 59.1 | 118.435 |
| 7.5PB | | 0.258 | 0.247 | 61.732 | 59.1 | 118.439 |
| 10.0PB | | 0.268 | 0.244 | 64.913 | 59.1 | 118.200 |
| 2.5PB | 7 | 0.201 | 0.215 | 40.256 | 43.06 | 116.963 |
| 5.0PB | | 0.213 | 0.212 | 43.263 | 43.06 | 116.790 |
| 7.5PB | | 0.23 | 0.207 | 47.844 | 43.06 | 117.115 |
| 10.0PB | | 0.245 | 0.204 | 51.714 | 43.06 | 116.304 |
| 2.5PB | 6 | 0.163 | 0.173 | 28.313 | 30.05 | 115.336 |
| 5.0PB | | 0.177 | 0.17 | 31.287 | 30.05 | 115.427 |
| 7.5PB | | 0.202 | 0.166 | 36.567 | 30.05 | 114.407 |
| 10.0PB | | 0.224 | 0.161 | 41.809 | 30.05 | 114.787 |
| 2.5PB | 5 | 0.127 | 0.13 | 19.314 | 19.77 | 112.993 |
| 5.0PB | | 0.14 | 0.122 | 22.687 | 19.77 | 119.592 |
| 7.5PB | | 0.177 | 0.118 | 29.655 | 19.77 | 118.117 |
| 10.0PB | | 0.205 | 0.115 | 35.242 | 19.77 | 116.901 |
| 2.5PB | 4 | 0.119 | 0.117 | 12.205 | 12 | 78.359 |
| 5.0PB | | 0.127 | 0.1 | 15.240 | 12 | 92.760 |
| 7.5PB | | 0.164 | 0.078 | 25.231 | 12 | 116.615 |
| 10.0PB | | 0.195 | 0.076 | 30.789 | 12 | 115.105 |
| 2.5PB | 3 | 0.113 | 0.107 | 6.923 | 6.555 | 47.784 |

| | | | | | | |
|---|---|---|---|---|---|---|
| 5.0PB | | 0.121 | 0.087 | 9.117 | 6.555 | 59.673 |
| 7.5PB | | 0.16 | 0.046 | 22.800 | 6.555 | 113.145 |
| 10.0PB | | 0.191 | 0.048 | 26.083 | 6.555 | 103.924 |
| 2.5PB | 2 | 0.11 | 0.099 | 3.473 | 3.126 | 24.976 |
| 5.0PB | | 0.119 | 0.078 | 4.769 | 3.126 | 32.182 |
| 7.5PB | | 0.162 | 0.026 | 19.477 | 3.126 | 97.627 |
| 10.0PB | | 0.191 | 0.032 | 18.658 | 3.126 | 75.903 |
| 2.5PB | 1 | 0.109 | 0.093 | 1.418 | 1.21 | 10.383 |
| 5.0PB | | 0.119 | 0.071 | 2.028 | 1.21 | 13.804 |
| 7.5PB | | 0.168 | 0.013 | 15.637 | 1.21 | 76.230 |
| 10.0PB | | 0.192 | 0.022 | 10.560 | 1.21 | 43.230 |

**P**

| HUE | value | x | y | X | Y | Z |
|---|---|---|---|---|---|---|
| 2.5P | 9 | 0.295 | 0.283 | 81.995 | 78.66 | 117.295 |
| 5.0P | | 0.298 | 0.281 | 83.419 | 78.66 | 117.850 |
| 7.5P | | 0.312 | 0.275 | 89.243 | 78.66 | 118.133 |
| 10.0P | | 0.325 | 0.273 | 93.643 | 78.66 | 115.829 |
| 2.5P | 8 | 0.277 | 0.241 | 67.928 | 59.1 | 118.200 |
| 5.0P | | 0.287 | 0.238 | 71.268 | 59.1 | 117.952 |
| 7.5P | | 0.312 | 0.23 | 80.170 | 59.1 | 117.686 |
| 10.0P | | 0.336 | 0.226 | 87.865 | 59.1 | 114.539 |
| 2.5P | 7 | 0.261 | 0.2 | 56.193 | 43.06 | 116.047 |
| 5.0P | | 0.277 | 0.196 | 60.855 | 43.06 | 115.779 |
| 7.5P | | 0.309 | 0.187 | 71.153 | 43.06 | 116.055 |
| 10.0P | | 0.343 | 0.186 | 79.406 | 43.06 | 109.039 |
| 2.5P | 6 | 0.247 | 0.157 | 47.276 | 30.05 | 114.075 |
| 5.0P | | 0.268 | 0.152 | 52.983 | 30.05 | 114.664 |
| 7.5P | | 0.305 | 0.146 | 62.776 | 30.05 | 112.996 |
| 10.0P | | 0.347 | 0.154 | 67.710 | 30.05 | 97.370 |
| 2.5P | 5 | 0.234 | 0.112 | 41.305 | 19.77 | 115.443 |
| 5.0P | | 0.261 | 0.109 | 47.339 | 19.77 | 114.267 |
| 7.5P | | 0.301 | 0.108 | 55.100 | 19.77 | 108.186 |
| 10.0P | | 0.25 | 0.126 | 39.226 | 19.77 | 97.909 |
| 2.5P | 4 | 0.226 | 0.075 | 36.160 | 12 | 111.840 |
| 5.0P | | 0.257 | 0.079 | 39.038 | 12 | 100.861 |
| 7.5P | | 0.296 | 0.088 | 40.364 | 12 | 84.000 |
| 10.0P | | 0.344 | 0.108 | 38.222 | 12 | 60.889 |
| 2.5P | 3 | 0.223 | 0.053 | 27.580 | 6.555 | 89.544 |
| 5.0P | | 0.255 | 0.062 | 26.960 | 6.555 | 72.211 |
| 7.5P | | 0.292 | 0.075 | 25.521 | 6.555 | 55.324 |
| 10.0P | | 0.335 | 0.092 | 23.869 | 6.555 | 40.826 |
| 2.5P | 2 | 0.222 | 0.04 | 17.349 | 3.126 | 57.675 |
| 5.0P | | 0.256 | 0.052 | 15.390 | 3.126 | 41.600 |
| 7.5P | | 0.288 | 0.065 | 13.851 | 3.126 | 31.116 |
| 10.0P | | 0.323 | 0.081 | 12.465 | 3.126 | 23.001 |
| 2.5P | 1 | 0.225 | 0.035 | 7.779 | 1.21 | 25.583 |
| 5.0P | | 0.259 | 0.048 | 6.529 | 1.21 | 17.469 |
| 7.5P | | 0.283 | 0.059 | 5.804 | 1.21 | 13.495 |
| 10.0P | | 0.306 | 0.07 | 5.289 | 1.21 | 10.786 |

**RP**

| HUE | value | x | y | X | Y | Z |
|---|---|---|---|---|---|---|
| 2.5RP | 9 | 0.34 | 0.282 | 94.838 | 78.66 | 105.438 |
| 5.0RP | | 0.352 | 0.294 | 94.178 | 78.66 | 94.713 |
| 7.5RP | | 0.36 | 0.302 | 93.767 | 78.66 | 88.037 |
| 10.0RP | | 0.367 | 0.311 | 92.824 | 78.66 | 81.442 |
| 2.5RP | 8 | 0.366 | 0.243 | 89.015 | 59.1 | 95.095 |
| 5.0RP | | 0.39 | 0.268 | 86.004 | 59.1 | 75.419 |

| | | | | | | |
|---|---|---|---|---|---|---|
| 7.5RP | | 0.404 | 0.284 | 84.072 | 59.1 | 64.927 |
| 10.0RP | | 0.419 | 0.301 | 82.269 | 59.1 | 54.977 |
| 2.5RP | 7 | 0.383 | 0.211 | 78.161 | 43.06 | 82.855 |
| 5.0RP | | 0.423 | 0.242 | 75.266 | 43.06 | 59.608 |
| 7.5RP | | 0.446 | 0.263 | 73.022 | 43.06 | 47.644 |
| 10.0RP | | 0.471 | 0.286 | 70.913 | 43.06 | 36.586 |
| 2.5RP | 6 | 0.396 | 0.183 | 65.026 | 30.05 | 69.131 |
| 5.0RP | | 0.447 | 0.22 | 61.056 | 30.05 | 45.485 |
| 7.5RP | | 0.479 | 0.243 | 59.234 | 30.05 | 34.378 |
| 10.0RP | | 0.514 | 0.269 | 57.419 | 30.05 | 24.241 |
| 2.5RP | 5 | 0.405 | 0.158 | 50.676 | 19.77 | 54.680 |
| 5.0RP | | 0.469 | 0.197 | 47.067 | 19.77 | 33.519 |
| 7.5RP | | 0.509 | 0.222 | 45.329 | 19.77 | 23.956 |
| 10.0RP | | 0.551 | 0.248 | 43.924 | 19.77 | 16.023 |
| 2.5RP | 4 | 0.406 | 0.141 | 34.553 | 12 | 38.553 |
| 5.0RP | | 0.472 | 0.176 | 32.182 | 12 | 24.000 |
| 7.5RP | | 0.522 | 0.203 | 30.857 | 12 | 16.256 |
| 10.0RP | | 0.571 | 0.23 | 29.791 | 12 | 10.383 |
| 2.5RP | 3 | 0.403 | 0.126 | 20.966 | 6.555 | 24.503 |
| 5.0RP | | 0.461 | 0.155 | 19.496 | 6.555 | 16.239 |
| 7.5RP | | 0.519 | 0.185 | 18.389 | 6.555 | 10.488 |
| 10.0RP | | 0.579 | 0.215 | 17.653 | 6.555 | 6.281 |
| 2.5RP | 2 | 0.38 | 0.108 | 10.999 | 3.126 | 14.820 |
| 5.0RP | | 0.434 | 0.133 | 10.201 | 3.126 | 10.177 |
| 7.5RP | | 0.478 | 0.154 | 9.703 | 3.126 | 7.470 |
| 10.0RP | | 0.526 | 0.178 | 9.238 | 3.126 | 5.198 |
| 2.5RP | 1 | 0.337 | 0.083 | 4.913 | 1.21 | 8.455 |
| 5.0RP | | 0.383 | 0.105 | 4.414 | 1.21 | 5.900 |
| 7.5RP | | 0.431 | 0.128 | 4.074 | 1.21 | 4.169 |
| 10.0RP | | 0.47 | 0.146 | 3.895 | 1.21 | 3.182 |

**Appendix C1 Colour co-ordinates of the theoretical Pigment Maxima for 40 Hues at 9V determined from Appendix B**

| L* | a* | b* | C* | h |
|---|---|---|---|---|
| 91.08 | 27.94 | 11.50 | 30.21 | 22.38 |
| 91.08 | 26.49 | 15.55 | 30.72 | 30.41 |
| 91.08 | 24.63 | 19.96 | 31.70 | 39.02 |
| 91.08 | 22.85 | 24.37 | 33.40 | 46.84 |
| 91.08 | 20.10 | 31.18 | 37.10 | 57.19 |
| 91.08 | 17.49 | 38.64 | 42.42 | 65.65 |
| 91.08 | 14.53 | 49.05 | 51.15 | 73.49 |
| 91.08 | 10.23 | 64.92 | 65.72 | 81.05 |
| 91.08 | 5.34 | 91.03 | 91.19 | 86.64 |
| 91.08 | -5.03 | 144.91 | 145.00 | 91.99 |
| 91.08 | -21.32 | 145.59 | 147.14 | 98.33 |
| 91.08 | -32.25 | 143.98 | 147.55 | 102.63 |
| 91.08 | -45.76 | 137.95 | 145.34 | 108.35 |
| 91.08 | -70.02 | 116.38 | 135.82 | 121.03 |
| 91.08 | -87.19 | 81.87 | 119.61 | 136.80 |
| 91.08 | -85.80 | 47.64 | 98.14 | 150.96 |
| 91.08 | -76.35 | 24.84 | 80.29 | 161.98 |
| 91.08 | -71.80 | 16.62 | 73.70 | 166.96 |
| 91.08 | -67.45 | 8.81 | 68.03 | 172.56 |
| 91.08 | -62.39 | 2.46 | 62.44 | 177.74 |
| 91.08 | -57.51 | -4.26 | 57.67 | 184.24 |
| 91.08 | -52.20 | -11.24 | 53.40 | 192.16 |
| 91.08 | -39.33 | -14.59 | 41.95 | 200.36 |
| 91.08 | -26.52 | -14.80 | 30.37 | 209.16 |
| 91.08 | -17.72 | -15.02 | 23.23 | 220.28 |
| 91.08 | -13.31 | -14.87 | 19.95 | 228.16 |
| 91.08 | -8.41 | -15.09 | 17.28 | 240.86 |
| 91.08 | -4.05 | -14.94 | 15.47 | 254.84 |
| 91.08 | -0.79 | -15.09 | 15.11 | 266.99 |
| 91.08 | 3.00 | -15.09 | 15.38 | 281.25 |
| 91.08 | 7.91 | -16.42 | 18.23 | 295.72 |
| 91.08 | 9.48 | -14.85 | 17.62 | 302.55 |
| 91.08 | 12.19 | -15.16 | 19.45 | 308.79 |
| 91.08 | 22.97 | -15.32 | 27.61 | 326.29 |
| 91.08 | 30.80 | -14.01 | 33.84 | 335.53 |
| 91.08 | 32.89 | -7.89 | 33.82 | 346.51 |
| 91.08 | 31.74 | -1.13 | 31.76 | 357.97 |
| 91.08 | 31.02 | 3.35 | 31.20 | 366.16 |
| 91.08 | 29.36 | 7.99 | 30.43 | 375.22 |

**Appendix C2 Colour co-ordinates of the theoretical Pigment Maxima for 40 Hues at 8V determined from Appendix B**

| L* | a* | b* | C* | HUE |
|---|---|---|---|---|
| 81.35 | 49.62 | 20.30 | 53.61 | 22.25 |
| 81.35 | 47.36 | 26.48 | 54.25 | 29.21 |
| 81.35 | 45.01 | 35.81 | 57.51 | 38.50 |
| 81.35 | 42.23 | 47.15 | 63.30 | 48.15 |
| 81.35 | 39.06 | 62.01 | 73.29 | 57.79 |
| 81.35 | 35.20 | 89.36 | 96.04 | 68.50 |
| 81.35 | 18.53 | 147.45 | 148.61 | 82.84 |
| 81.35 | 8.12 | 147.71 | 147.93 | 86.85 |
| 81.35 | -3.43 | 142.81 | 142.85 | 91.38 |
| 81.35 | -30.19 | 148.58 | 151.62 | 101.48 |

| | | | | |
|---|---|---|---|---|
| 81.35 | -43.76 | 148.87 | 155.17 | 106.38 |
| 81.35 | -69.51 | 130.85 | 148.16 | 117.98 |
| 81.35 | -107.07 | 108.41 | 152.37 | 134.64 |
| 81.35 | -128.21 | 61.87 | 142.36 | 154.24 |
| 81.35 | -118.36 | 30.12 | 122.13 | 165.72 |
| 81.35 | -112.69 | 19.93 | 114.44 | 169.97 |
| 81.35 | -105.22 | 9.88 | 105.69 | 174.64 |
| 81.35 | -96.60 | -0.09 | 96.60 | 180.05 |
| 81.35 | -87.66 | -9.92 | 88.22 | 186.46 |
| 81.35 | -77.47 | -19.07 | 79.78 | 193.83 |
| 81.35 | -67.54 | -27.68 | 72.99 | 202.28 |
| 81.35 | -50.89 | -32.51 | 60.39 | 212.57 |
| 81.35 | -31.42 | -32.52 | 45.22 | 225.99 |
| 81.35 | -21.97 | -32.53 | 39.25 | 235.96 |
| 81.35 | -14.39 | -32.40 | 35.45 | 246.06 |
| 81.35 | -6.33 | -32.14 | 32.76 | 258.86 |
| 81.35 | -0.09 | -32.28 | 32.28 | 269.83 |
| 81.35 | 8.91 | -32.28 | 33.48 | 285.43 |
| 81.35 | 16.14 | -32.14 | 35.97 | 296.67 |
| 81.35 | 22.79 | -32.14 | 39.40 | 305.34 |
| 81.35 | 29.92 | -32.00 | 43.81 | 313.08 |
| 81.35 | 47.91 | -31.85 | 57.53 | 326.38 |
| 81.35 | 62.42 | -30.06 | 69.28 | 334.29 |
| 81.35 | 64.51 | -18.16 | 67.01 | 344.28 |
| 81.35 | 58.99 | -4.33 | 59.14 | 355.81 |
| 81.35 | 55.38 | 4.06 | 55.52 | 364.19 |
| 81.35 | 51.96 | 12.89 | 53.53 | 373.94 |

**Appendix C3 Colour co-ordinates of the theoretical Pigment Maxima for 40 Hues at 7V determined from Appendix B**

| L* | a* | b* | C* | HUE |
|---|---|---|---|---|
| 71.60 | 68.00 | 25.58 | 72.65 | 20.61 |
| 71.60 | 65.41 | 36.05 | 74.68 | 28.86 |
| 71.60 | 62.30 | 50.58 | 80.25 | 39.07 |
| 71.60 | 59.00 | 73.85 | 94.52 | 51.38 |
| 71.60 | 53.25 | 151.03 | 160.14 | 70.58 |
| 71.60 | 39.32 | 151.03 | 156.06 | 75.41 |
| 71.60 | 17.45 | 151.03 | 152.03 | 83.41 |
| 71.60 | 8.07 | 151.03 | 151.24 | 86.94 |
| 71.60 | -27.64 | 133.71 | 136.54 | 101.68 |
| 71.60 | -40.58 | 129.55 | 135.75 | 107.39 |
| 71.60 | -65.03 | 124.72 | 140.65 | 117.54 |
| 71.60 | -103.40 | 106.19 | 148.21 | 134.24 |
| 71.60 | -148.69 | 61.32 | 160.83 | 157.59 |
| 71.60 | -141.91 | 29.90 | 145.03 | 168.10 |
| 71.60 | -134.31 | 19.17 | 135.67 | 171.88 |
| 71.60 | -124.92 | 8.96 | 125.24 | 175.90 |
| 71.60 | -113.62 | -2.51 | 113.65 | 181.27 |
| 71.60 | -100.18 | -13.73 | 101.12 | 187.81 |
| 71.60 | -87.56 | -23.47 | 90.65 | 195.00 |
| 71.60 | -74.84 | -33.53 | 82.01 | 204.13 |
| 71.60 | -61.89 | -42.61 | 75.14 | 214.54 |
| 71.60 | -41.71 | -48.70 | 64.12 | 229.42 |
| 71.60 | -28.53 | -48.58 | 56.34 | 239.57 |
| 71.60 | -17.68 | -48.27 | 51.41 | 249.88 |
| 71.60 | -5.98 | -48.25 | 48.62 | 262.94 |
| 71.60 | 3.05 | -48.16 | 48.25 | 273.63 |
| 71.60 | 16.04 | -48.34 | 50.93 | 288.36 |
| 71.60 | 26.38 | -47.88 | 54.66 | 298.85 |
| 71.60 | 37.72 | -47.73 | 60.84 | 308.32 |

| | | | | |
|---|---|---|---|---|
| 71.60 | 48.90 | -47.58 | 68.23 | 315.78 |
| 71.60 | 71.71 | -47.74 | 86.15 | 326.35 |
| 71.60 | 88.45 | -43.65 | 98.64 | 333.73 |
| 71.60 | 86.00 | -26.62 | 90.03 | 342.80 |
| 71.60 | 80.21 | -8.15 | 80.62 | 354.20 |
| 71.60 | 75.61 | 3.30 | 75.68 | 362.50 |
| 71.60 | 71.21 | 15.75 | 72.93 | 372.47 |

**Appendix C4 Colour co-ordinates of the theoretical Pigment Maxima for 40 Hues at 6V determined from Appendix B**

| L* | a* | b* | C* | HUE |
|---|---|---|---|---|
| 61.70 | 80.27 | 27.60 | 84.89 | 18.98 |
| 61.70 | 77.61 | 41.99 | 88.24 | 28.41 |
| 61.70 | 74.96 | 62.62 | 97.67 | 39.88 |
| 61.70 | 66.25 | 116.35 | 133.89 | 60.34 |
| 61.70 | 49.14 | 116.81 | 126.73 | 67.18 |
| 61.70 | 36.68 | 117.14 | 122.75 | 72.61 |
| 61.70 | 25.76 | 117.42 | 120.21 | 77.62 |
| 61.70 | 7.85 | 117.86 | 118.12 | 86.19 |
| 61.70 | -0.73 | 118.06 | 118.06 | 90.36 |
| 61.70 | -8.24 | 118.24 | 118.52 | 93.99 |
| 61.70 | -24.94 | 118.61 | 121.20 | 101.87 |
| 61.70 | -37.23 | 114.94 | 120.82 | 107.95 |
| 61.70 | -60.65 | 112.85 | 128.11 | 118.26 |
| 61.70 | -96.45 | 97.72 | 137.30 | 134.63 |
| 61.70 | -157.80 | 55.65 | 167.33 | 160.57 |
| 61.70 | -156.57 | 27.46 | 158.96 | 170.05 |
| 61.70 | -149.04 | 17.26 | 150.03 | 173.39 |
| 61.70 | -137.63 | 7.18 | 137.82 | 177.01 |
| 61.70 | -122.74 | -5.06 | 122.84 | 182.36 |
| 61.70 | -106.43 | -16.72 | 107.74 | 188.93 |
| 61.70 | -92.28 | -26.10 | 95.91 | 195.79 |
| 61.70 | -76.33 | -36.59 | 84.65 | 205.61 |
| 61.70 | -62.79 | -45.06 | 77.28 | 215.67 |
| 61.70 | -46.13 | -55.07 | 71.84 | 230.04 |
| 61.70 | -32.60 | -62.74 | 70.71 | 242.54 |
| 61.70 | -20.23 | -64.36 | 67.46 | 252.55 |
| 61.70 | -4.45 | -64.39 | 64.55 | 266.05 |
| 61.70 | 6.74 | -64.44 | 64.80 | 275.97 |
| 61.70 | 24.97 | -63.86 | 68.57 | 291.36 |
| 61.70 | 41.40 | -64.08 | 76.29 | 302.87 |
| 61.70 | 57.14 | -63.67 | 85.55 | 311.91 |
| 61.70 | 72.32 | -64.01 | 96.58 | 318.49 |
| 61.70 | 96.00 | -63.04 | 114.85 | 326.71 |
| 61.70 | 107.01 | -53.51 | 119.64 | 333.43 |
| 61.70 | 101.09 | -33.28 | 106.43 | 341.78 |
| 61.70 | 92.03 | -11.50 | 92.75 | 352.88 |
| 61.70 | 87.74 | 1.46 | 87.76 | 360.95 |
| 61.70 | 83.38 | 16.03 | 84.91 | 370.88 |

**Appendix C5 Colour co-ordinates of the theoretical Pigment Maxima for 40 Hues at 5V determined from Appendix B**

| L* | a* | b* | C* | HUE |
|---|---|---|---|---|
| 51.58 | 88.55 | 26.63 | 92.47 | 16.74 |
| 51.58 | 85.49 | 44.52 | 96.38 | 27.51 |

| | | | | |
|---|---|---|---|---|
| 51.58 | 83.49 | 67.93 | 107.63 | 39.13 |
| 51.58 | 61.65 | 101.08 | 118.39 | 58.62 |
| 51.58 | 33.67 | 101.83 | 107.26 | 71.70 |
| 51.58 | 23.68 | 102.09 | 104.80 | 76.94 |
| 51.58 | 15.32 | 102.30 | 103.44 | 81.48 |
| 51.58 | 7.62 | 102.49 | 102.77 | 85.75 |
| 51.58 | 0.14 | 102.67 | 102.67 | 89.92 |
| 51.58 | -13.57 | 102.98 | 103.87 | 97.50 |
| 51.58 | -22.26 | 99.70 | 102.15 | 102.59 |
| 51.58 | -33.46 | 100.00 | 105.44 | 108.50 |
| 51.58 | -55.20 | 98.21 | 112.66 | 119.34 |
| 51.58 | -87.91 | 87.87 | 124.29 | 135.01 |
| 51.58 | -161.05 | 48.00 | 168.05 | 163.40 |
| 51.58 | -165.84 | 24.18 | 167.59 | 171.70 |
| 51.58 | -158.54 | 14.18 | 159.18 | 174.89 |
| 51.58 | -145.01 | 4.36 | 145.08 | 178.28 |
| 51.58 | -126.93 | -7.18 | 127.13 | 183.24 |
| 51.58 | -108.33 | -19.29 | 110.04 | 190.10 |
| 51.58 | -93.47 | -28.18 | 97.63 | 196.78 |
| 51.58 | -76.32 | -37.96 | 85.24 | 206.44 |
| 51.58 | -61.55 | -46.46 | 77.12 | 217.05 |
| 51.58 | -43.86 | -56.38 | 71.43 | 232.12 |
| 51.58 | -30.82 | -63.99 | 71.03 | 244.29 |
| 51.58 | -19.12 | -70.21 | 72.77 | 254.77 |
| 51.58 | -0.38 | -80.49 | 80.49 | 269.73 |
| 51.58 | 15.66 | -84.25 | 85.70 | 280.53 |
| 51.58 | 44.32 | -83.42 | 94.47 | 297.98 |
| 51.58 | 64.20 | -82.74 | 104.72 | 307.81 |
| 51.58 | 83.51 | -81.90 | 116.97 | 315.56 |
| 51.58 | 100.94 | -81.23 | 129.56 | 321.18 |
| 51.58 | 121.30 | -77.66 | 144.03 | 327.37 |
| 51.58 | 109.95 | -38.16 | 116.38 | 340.86 |
| 51.58 | 100.19 | -14.87 | 101.28 | 351.55 |
| 51.58 | 95.31 | -0.96 | 95.31 | 359.42 |
| 51.58 | 91.27 | 13.78 | 92.31 | 368.59 |

**Appendix C6 Colour co-ordinates of the theoretical Pigment Maxima for 40 Hues at 4V determined from Appendix B**

| L* | a* | b* | C* | HUE |
|---|---|---|---|---|
| 41.22 | 86.77 | 23.17 | 89.81 | 14.95 |
| 41.22 | 84.35 | 41.77 | 94.13 | 26.34 |
| 41.22 | 83.25 | 63.29 | 104.58 | 37.25 |
| 41.22 | 57.16 | 98.65 | 114.01 | 59.91 |
| 41.22 | 21.13 | 86.41 | 88.96 | 76.26 |
| 41.22 | 14.02 | 86.59 | 87.72 | 80.80 |
| 41.22 | 7.13 | 86.76 | 87.05 | 85.30 |
| 41.22 | -5.10 | 87.05 | 87.20 | 93.35 |
| 41.22 | -11.49 | 87.19 | 87.95 | 97.50 |
| 41.22 | -19.29 | 87.36 | 89.47 | 102.45 |
| 41.22 | -29.23 | 84.69 | 89.59 | 109.04 |
| 41.22 | -49.31 | 81.66 | 95.40 | 121.12 |
| 41.22 | -77.08 | 73.29 | 106.37 | 136.44 |
| 41.22 | -152.15 | 39.32 | 157.15 | 165.51 |
| 41.22 | -163.57 | 20.35 | 164.83 | 172.91 |
| 41.22 | -154.72 | 11.01 | 155.11 | 175.93 |
| 41.22 | -140.14 | 1.94 | 140.15 | 179.21 |
| 41.22 | -122.07 | -8.27 | 122.35 | 183.88 |
| 41.22 | -100.83 | -20.16 | 102.82 | 191.31 |
| 41.22 | -85.85 | -28.00 | 90.30 | 198.06 |

| | | | | |
|---|---|---|---|---|
| 41.22 | -69.58 | -36.82 | 78.72 | 207.89 |
| 41.22 | -55.44 | -44.59 | 71.15 | 218.81 |
| 41.22 | -38.64 | -52.99 | 65.58 | 233.90 |
| 41.22 | -26.01 | -60.03 | 65.42 | 246.57 |
| 41.22 | -15.21 | -65.92 | 67.65 | 257.01 |
| 41.22 | 3.01 | -75.73 | 75.79 | 272.28 |
| 41.22 | 22.19 | -85.81 | 88.64 | 284.50 |
| 41.22 | 71.38 | -100.44 | 123.22 | 305.40 |
| 41.22 | 93.20 | -99.57 | 136.39 | 313.11 |
| 41.22 | 111.91 | -97.68 | 148.54 | 318.88 |
| 41.22 | 121.18 | -91.03 | 151.56 | 323.09 |
| 41.22 | 125.30 | -79.81 | 148.56 | 327.50 |
| 41.22 | 118.60 | -61.66 | 133.67 | 332.53 |
| 41.22 | 106.52 | -39.01 | 113.44 | 339.89 |
| 41.22 | 98.25 | -18.89 | 100.05 | 349.12 |
| 41.22 | 93.45 | -4.58 | 93.56 | 357.20 |
| 41.22 | 89.49 | 9.75 | 90.02 | 366.22 |
| 41.22 | 89.49 | 9.75 | 90.02 | 366.22 |

**Appendix C7 Colour co-ordinates of the theoretical Pigment Maxima for 40 Hues at 3V determined from Appendix B**

| L* | a* | b* | C* | HUE |
|---|---|---|---|---|
| 30.77 | 78.64 | 17.51 | 80.57 | 12.55 |
| 30.77 | 76.67 | 30.64 | 82.57 | 21.78 |
| 30.77 | 75.18 | 48.88 | 89.67 | 33.03 |
| 30.77 | 58.35 | 69.51 | 90.76 | 49.99 |
| 30.77 | 36.47 | 70.13 | 79.05 | 62.52 |
| 30.77 | 26.41 | 70.40 | 75.19 | 69.44 |
| 30.77 | 18.46 | 70.61 | 72.98 | 75.35 |
| 30.77 | 12.32 | 70.76 | 71.83 | 80.12 |
| 30.77 | 6.66 | 70.90 | 71.21 | 84.63 |
| 30.77 | -3.90 | 71.15 | 71.26 | 93.14 |
| 30.77 | -9.39 | 71.28 | 71.89 | 97.50 |
| 30.77 | -16.27 | 71.43 | 73.26 | 102.83 |
| 30.77 | -25.13 | 69.26 | 73.68 | 109.94 |
| 30.77 | -42.90 | 65.76 | 78.51 | 123.12 |
| 30.77 | -66.97 | 58.74 | 89.08 | 138.74 |
| 30.77 | -134.87 | 30.63 | 138.30 | 167.20 |
| 30.77 | -137.09 | 8.17 | 137.33 | 176.59 |
| 30.77 | -120.96 | 0.07 | 120.96 | 179.97 |
| 30.77 | -104.94 | -8.46 | 105.28 | 184.61 |
| 30.77 | -84.85 | -18.71 | 86.89 | 192.43 |
| 30.77 | -72.78 | -25.30 | 77.05 | 199.17 |
| 30.77 | -57.68 | -33.33 | 66.62 | 210.02 |
| 30.77 | -45.64 | -39.93 | 60.64 | 221.18 |
| 30.77 | -30.94 | -47.41 | 56.62 | 236.87 |
| 30.77 | -20.65 | -53.01 | 56.89 | 248.72 |
| 30.77 | -11.16 | -58.30 | 59.36 | 259.17 |
| 30.77 | 5.04 | -67.23 | 67.42 | 274.28 |
| 30.77 | 24.90 | -78.60 | 82.45 | 287.58 |
| 30.77 | 105.84 | -116.45 | 157.36 | 312.27 |
| 30.77 | 119.94 | -110.94 | 163.38 | 317.23 |
| 30.77 | 125.98 | -101.66 | 161.88 | 321.10 |
| 30.77 | 123.50 | -89.05 | 152.26 | 324.21 |
| 30.77 | 117.61 | -74.63 | 139.29 | 327.60 |
| 30.77 | 110.57 | -59.67 | 125.65 | 331.65 |
| 30.77 | 97.36 | -37.72 | 104.41 | 338.83 |
| 30.77 | 90.21 | -22.55 | 92.98 | 345.96 |
| 30.77 | 84.58 | -8.56 | 85.01 | 354.22 |
| 30.77 | 80.71 | 5.46 | 80.89 | 363.87 |

| | | | | |
|---|---|---|---|---|
| 30.77 | 84.58 | -8.56 | 85.01 | 354.22 |
| 30.77 | 80.71 | 5.46 | 80.89 | 363.87 |

**Appendix C8 Colour co-ordinates of the theoretical Pigment Maxima for 40 Hues at 2V determined from Appendix B**

| L* | a* | b* | C* | HUE |
|---|---|---|---|---|
| 20.54 | 67.08 | 2.27 | 67.12 | 1.94 |
| 20.54 | 65.19 | 12.36 | 66.35 | 10.74 |
| 20.54 | 63.49 | 24.26 | 67.97 | 20.91 |
| 20.54 | 62.16 | 44.59 | 76.50 | 35.65 |
| 20.54 | 36.40 | 54.57 | 65.60 | 56.29 |
| 20.54 | 10.53 | 55.26 | 56.26 | 79.22 |
| 20.54 | 5.86 | 55.38 | 55.69 | 83.96 |
| 20.54 | 1.55 | 55.48 | 55.50 | 88.40 |
| 20.54 | -2.64 | 55.58 | 55.64 | 92.72 |
| 20.54 | -7.34 | 55.69 | 56.17 | 97.50 |
| 20.54 | -20.71 | 52.85 | 56.77 | 111.40 |
| 20.54 | -35.54 | 50.71 | 61.93 | 125.03 |
| 20.54 | -59.06 | 43.63 | 73.42 | 143.55 |
| 20.54 | -110.95 | 22.77 | 113.26 | 168.40 |
| 20.54 | -120.16 | 12.17 | 120.78 | 174.22 |
| 20.54 | -110.05 | 5.71 | 110.20 | 177.03 |
| 20.54 | -96.23 | -1.21 | 96.24 | 180.72 |
| 20.54 | -83.18 | -7.86 | 83.55 | 185.40 |
| 20.54 | -66.48 | -16.57 | 68.52 | 194.00 |
| 20.54 | -57.10 | -21.42 | 60.98 | 200.56 |
| 20.54 | -44.21 | -28.61 | 52.66 | 212.91 |
| 20.54 | -34.37 | -33.48 | 47.98 | 224.24 |
| 20.54 | -23.50 | -39.61 | 46.05 | 239.32 |
| 20.54 | -15.30 | -44.03 | 46.61 | 250.84 |
| 20.54 | -6.92 | -48.46 | 48.95 | 261.88 |
| 20.54 | 6.69 | -56.11 | 56.51 | 276.80 |
| 20.54 | 24.99 | -66.61 | 71.15 | 290.57 |
| 20.54 | 134.21 | -124.63 | 183.15 | 317.12 |
| 20.54 | 130.06 | -109.53 | 170.04 | 319.90 |
| 20.54 | 123.17 | -94.44 | 155.21 | 322.52 |
| 20.54 | 112.18 | -78.19 | 136.74 | 325.12 |
| 20.54 | 102.87 | -65.16 | 121.78 | 327.65 |
| 20.54 | 93.89 | -52.88 | 107.76 | 330.61 |
| 20.54 | 83.61 | -37.09 | 91.47 | 336.08 |
| 20.54 | 77.63 | -25.30 | 81.65 | 341.95 |
| 20.54 | 73.74 | -16.65 | 75.60 | 347.27 |
| 20.54 | 69.99 | -7.59 | 70.40 | 353.81 |

**Appendix D1 Real Munsell highest chroma values at 8V measured from actual Munsell Atlas**

| | L* | a* | b* | C* | h |
|---|---|---|---|---|---|
| MUNSELL 10 RP V 8 | 80.72 | 23.74 | 4.96 | 24.25 | 11.8 |
| MUNSELL 2.5 R V 8 | 81.07 | 16.14 | 5.8 | 17.15 | 19.77 |
| MUNSELL 5 R V 8 | 80.62 | 17 | 7.91 | 18.75 | 24.95 |
| MUNSELL 7.5 R V 8 | 80.23 | 17.45 | 9.89 | 20.06 | 29.54 |
| MUNSELL 10 R V 8 | 79.08 | 30.95 | 25.91 | 40.36 | 39.93 |
| MUNSELL 2.5 YR V 8 | 79.16 | 29.68 | 31.24 | 43.09 | 46.46 |
| MUNSELL 5 YR V 8 | 78.85 | 26.98 | 39.35 | 47.71 | 55.57 |
| MUNSELL 7.5 YR V 8 | 78.71 | 26.24 | 54.45 | 60.44 | 64.27 |
| MUNSELL 10 YR V 8 | 78.76 | 21.07 | 59.3 | 62.93 | 70.44 |
| MUNSELL 2.5 Y V 8 | 78.43 | 16.38 | 77.11 | 78.83 | 78 |
| MUNSELL 5 Y V 8 | 78.42 | 5.67 | 77.48 | 77.69 | 85.82 |
| MUNSELL 7.5 Y V 8 | 78.56 | 2.66 | 80.81 | 80.86 | 88.12 |
| MUNSELL 10 Y V 8 | 78.64 | -3.66 | 75.3 | 75.39 | 92.78 |
| MUNSELL 2.5 GY V 8 | 79.29 | -10.64 | 68.25 | 69.07 | 98.86 |
| MUNSELL 5 GY V 8 | 79.46 | -20.59 | 63.63 | 66.88 | 107.93 |
| MUNSELL 7.5 GY V 8 | 80.61 | -27.44 | 43.61 | 51.52 | 122.18 |
| MUNSELL 10 GY V 8 | 81.07 | -25.37 | 26.9 | 36.98 | 133.33 |
| MUNSELL 2.5 G V 8 | 81.06 | -28.31 | 19.45 | 34.35 | 145.5 |
| MUNSELL 5 G V 8 | 81.15 | -31.35 | 14.8 | 34.67 | 154.73 |
| MUNSELL 7.5 G V 8 | 80.74 | -30.91 | 11.06 | 32.83 | 160.31 |
| MUNSELL 10 G V 8 | 81.33 | -21.15 | 5.16 | 21.77 | 166.29 |
| MUNSELL 2.5 BG V 8 | 81.34 | -21.87 | 3.15 | 22.09 | 171.8 |
| MUNSELL 5 BG V 8 | 81.3 | -21.47 | 0.46 | 21.47 | 178.78 |
| MUNSELL 7.5 BG V 8 | 81.9 | -19.19 | -2.65 | 19.38 | 187.87 |
| MUNSELL 10 BG V 8 | 81.93 | -20.27 | -5.21 | 20.92 | 194.42 |
| MUNSELL 2.5 B V 8 | 81.91 | -18.1 | -7.3 | 19.52 | 201.98 |
| MUNSELL 5 B V 8 | 81.47 | -15.67 | -9.2 | 18.17 | 210.42 |
| MUNSELL 7.5 B V 8 | 82.14 | -12.89 | -11.3 | 17.14 | 221.25 |
| MUNSELL 10 B V 8 | 81.64 | -10.16 | -12.45 | 16.07 | 230.77 |
| MUNSELL 2.5 PB V 8 | 81.59 | -9.81 | -17.9 | 20.41 | 241.27 |
| MUNSELL 5 PB V 8 | 81.13 | -5.23 | -18.14 | 18.88 | 253.9 |
| MUNSELL 7.5 PB V 8 | 82.02 | 0.27 | -16.52 | 16.52 | 270.93 |
| MUNSELL 10 PB V 8 | 81.31 | 2.53 | -12.12 | 12.38 | 281.78 |
| MUNSELL 2.5 P V 8 | 81.7 | 5.28 | -11.59 | 12.74 | 294.47 |
| MUNSELL 5 P V 8 | 81.65 | 6.74 | -9.77 | 11.87 | 304.6 |
| MUNSELL 7.5 P V 8 | 81.31 | 14.3 | -11.64 | 18.43 | 320.86 |
| MUNSELL 10 P V 8 | 80.95 | 17.81 | -9.61 | 20.24 | 331.65 |
| MUNSELL 2.5 RP V 8 | 80.58 | 19.93 | -5.3 | 20.62 | 345.12 |
| MUNSELL 5 RP V 8 | 80.77 | 21.47 | -1.07 | 21.49 | 357.16 |

**Appendix D2 Real Munsell highest chroma values at 7V measured from actual Munsell Atlas**

| | L* | a* | b* | C* | h |
|---|---|---|---|---|---|
| MUNSELL 7.5 RP V 7 | 71.59 | 31.24 | 3.07 | 31.4 | 5.61 |
| MUNSELL 10 RP V 7 | 70.98 | 31.28 | 6.35 | 31.92 | 11.48 |
| MUNSELL 2.5 R V 7 | 69.98 | 38.19 | 12.93 | 40.32 | 18.7 |
| MUNSELL 5 R V 7 | 69.39 | 40.61 | 18.46 | 44.61 | 24.45 |
| MUNSELL 7.5 R V 7 | 70.09 | 42.24 | 26.76 | 50 | 32.36 |
| MUNSELL 10 R V 7 | 69.32 | 45.23 | 40 | 60.38 | 41.49 |
| MUNSELL 2.5 YR V 7 | 68.98 | 43.22 | 50.79 | 66.69 | 49.6 |
| MUNSELL 5 YR V 7 | 68.48 | 37.38 | 59.73 | 70.46 | 57.96 |
| MUNSELL 7.5 YR V 7 | 68.85 | 29.98 | 66.46 | 72.91 | 65.72 |
| MUNSELL 10 YR V 7 | 69.24 | 23.69 | 71.83 | 75.64 | 71.75 |
| MUNSELL 2.5 Y V 7 | 68.95 | 17.06 | 70.9 | 72.92 | 76.47 |
| MUNSELL 5 Y V 7 | 69.44 | 8.77 | 74.7 | 75.22 | 83.3 |
| MUNSELL 7.5 Y V 7 | 69.55 | 0.19 | 65.2 | 65.2 | 89.83 |
| MUNSELL 10 Y V 7 | 70.25 | -5.06 | 67.6 | 67.79 | 94.28 |
| MUNSELL 2.5 GY V 7 | 70.6 | -12.1 | 63.73 | 64.87 | 100.75 |
| MUNSELL 5 GY V 7 | 70.07 | -18.03 | 50.38 | 53.51 | 109.69 |

| | | | | | |
|---|---|---|---|---|---|
| MUNSELL 7.5 GY V 7 | 70.22 | -30.09 | 53.54 | 61.41 | 119.34 |
| MUNSELL 10 GY V 7 | 71.51 | -38.49 | 42.69 | 57.48 | 132.04 |
| MUNSELL 2.5 G V 7 | 71 | -44.67 | 29.85 | 53.73 | 146.24 |
| MUNSELL 5 G V 7 | 70.81 | -43.7 | 18.68 | 47.53 | 156.85 |
| MUNSELL 7.5 G V 7 | 71.57 | -41.66 | 13.43 | 43.77 | 162.14 |
| MUNSELL 10 G V 7 | 71.81 | -40.3 | 8.46 | 41.17 | 168.15 |
| MUNSELL 2.5 BG V 7 | 72.12 | -40.21 | 4.54 | 40.47 | 173.56 |
| MUNSELL 5 BG V 7 | 72.05 | -38.74 | -0.95 | 38.75 | 181.41 |
| MUNSELL 7.5 BG V 7 | 71.74 | -35.87 | -6.72 | 36.49 | 190.61 |
| MUNSELL 10 BG V 7 | 72.98 | -34.36 | -9.63 | 35.69 | 195.65 |
| MUNSELL 2.5 B V 7 | 72.93 | -30.9 | -14.25 | 34.03 | 204.77 |
| MUNSELL 5 B V 7 | 72.48 | -28.78 | -19.87 | 34.97 | 214.61 |
| MUNSELL 7.5 B V 7 | 73.14 | -25.05 | -23.44 | 34.3 | 223.1 |
| MUNSELL 10 B V 7 | 73.36 | -18.21 | -26.24 | 31.94 | 235.24 |
| MUNSELL 2.5 PB V 7 | 73.13 | -11.65 | -27.27 | 29.66 | 246.88 |
| MUNSELL 5 PB V 7 | 71.93 | -6.12 | -26.81 | 27.5 | 257.14 |
| MUNSELL 7.5 PB V 7 | 72.1 | 1.18 | -26.03 | 26.05 | 272.6 |
| MUNSELL 10 PB V 7 | 71.91 | 6.6 | -23.54 | 24.45 | 285.66 |
| MUNSELL 2.5 P V 7 | 72.52 | 12.27 | -24.04 | 26.99 | 297.04 |
| MUNSELL 5 P V 7 | 71.34 | 14.17 | -21.39 | 25.66 | 303.52 |
| MUNSELL 7.5 P V 7 | 71.55 | 20.97 | -17.5 | 27.31 | 320.15 |
| MUNSELL 10 P V 7 | 71.65 | 24.85 | -14.18 | 28.61 | 330.29 |
| MUNSELL 2.5 RP V 7 | 70.94 | 30.87 | -10.44 | 32.59 | 341.32 |
| MUNSELL 5 RP V 7 | 70.93 | 29.51 | -3.53 | 29.72 | 353.19 |

**Appendix D3 Real Munsell highest chroma values at 6V measured from actual Munsell Atlas**

| | L* | a* | b* | C* | h |
|---|---|---|---|---|---|
| MUNSELL 7.5 RP V 6 | 61.11 | 37.88 | 1.54 | 37.91 | 2 |
| MUNSELL 10 RP V 6 | 60.75 | 39.15 | 7.54 | 39.87 | 10.9 |
| MUNSELL 2.5 R V 6 | 60.18 | 46.13 | 15.48 | 48.66 | 18.55 |
| MUNSELL 5 R V 6 | 59.62 | 53.2 | 24.01 | 58.37 | 24.29 |
| MUNSELL 7.5 R V 6 | 59.31 | 48.46 | 33.06 | 58.67 | 34.3 |
| MUNSELL 10 R V 6 | 58.9 | 47.75 | 45.19 | 65.74 | 43.43 |
| MUNSELL 2.5 YR V 6 | 59.16 | 42.72 | 58.38 | 72.34 | 53.8 |
| MUNSELL 5 YR V 6 | 59.32 | 36 | 57.16 | 67.55 | 57.8 |
| MUNSELL 7.5 YR V 6 | 59.46 | 27.46 | 54.27 | 60.82 | 63.17 |
| MUNSELL 10 YR V 6 | 59.41 | 20.16 | 57.24 | 60.69 | 70.59 |
| MUNSELL 2.5 Y V 6 | 59.67 | 13.03 | 49.87 | 51.55 | 75.36 |
| MUNSELL 5 Y V 6 | 59.75 | 7.32 | 53.89 | 54.39 | 82.27 |
| MUNSELL 7.5 Y V 6 | 59.89 | 0.15 | 51.39 | 51.39 | 89.83 |
| MUNSELL 10 Y V 6 | 60.02 | -1.38 | 53.62 | 53.64 | 91.48 |
| MUNSELL 2.5 GY V 6 | 60.02 | -7.55 | 50.92 | 51.48 | 98.44 |
| MUNSELL 5 GY V 6 | 59.91 | -13.43 | 47.91 | 49.76 | 105.65 |
| MUNSELL 7.5 GY V 6 | 61.22 | -28.3 | 48.05 | 55.77 | 120.5 |
| MUNSELL 10 GY V 6 | 60.81 | -37.43 | 42.09 | 56.32 | 131.64 |
| MUNSELL 2.5 G V 6 | 61.35 | -49.7 | 31.32 | 58.74 | 147.78 |
| MUNSELL 5 G V 6 | 61.84 | -43.82 | 18.27 | 47.48 | 157.37 |
| MUNSELL 7.5 G V 6 | 62.09 | -47.66 | 13.68 | 49.58 | 163.98 |
| MUNSELL 10 G V 6 | 62.27 | -47.49 | 9.34 | 48.4 | 168.88 |
| MUNSELL 2.5 BG V 6 | 62.49 | -48.35 | 4.85 | 48.59 | 174.28 |
| MUNSELL 5 BG V 6 | 63.6 | -41.08 | -1.63 | 41.12 | 182.27 |
| MUNSELL 7.5 BG V 6 | 63.56 | -40.23 | -6.23 | 40.71 | 188.81 |
| MUNSELL 10 BG V 6 | 63.4 | -37.92 | -12.25 | 39.85 | 197.9 |
| MUNSELL 2.5 B V 6 | 63.08 | -36.36 | -16.3 | 39.84 | 204.14 |
| MUNSELL 5 B V 6 | 63.25 | -29.47 | -21.21 | 36.31 | 215.75 |
| MUNSELL 7.5 B V 6 | 64.3 | -27.17 | -27.79 | 38.87 | 225.64 |
| MUNSELL 10 B V 6 | 64.05 | -21.9 | -32.13 | 38.88 | 235.73 |
| MUNSELL 2.5 PB V 6 | 63.9 | -14.72 | -34.02 | 37.07 | 246.6 |
| MUNSELL 5 PB V 6 | 63.32 | -9.38 | -33.96 | 35.23 | 254.56 |
| MUNSELL 7.5 PB V 6 | 63.23 | 3.75 | -32.6 | 32.82 | 276.56 |
| MUNSELL 10 PB V 6 | 62.42 | 11.29 | -32.33 | 34.24 | 289.25 |

| | | | | | |
|---|---|---|---|---|---|
| MUNSELL 2.5 P V 6 | 62.12 | 16.71 | -29.76 | 34.13 | 299.31 |
| MUNSELL 7.5 P V 6 | 61.7 | 24.52 | -23.01 | 33.62 | 316.82 |
| MUNSELL 10 P V 6 | 62 | 30.72 | -18.73 | 35.98 | 328.63 |
| MUNSELL 2.5 RP V 6 | 61.38 | 38.77 | -13.94 | 41.2 | 340.22 |
| MUNSELL 5 RP V 6 | 61.7 | 35.08 | -5.17 | 35.46 | 351.61 |

**Appendix D4 Real Munsell highest chroma values at 5V measured from actual Munsell Atlas**

| | L* | a* | b* | C* | h |
|---|---|---|---|---|---|
| MUNSELL 10 RP V 5 | 51.68 | 47.23 | 8.46 | 47.98 | 10 |
| MUNSELL 2.5 R V 5 | 50.94 | 49.35 | 15.67 | 51.78 | 17.62 |
| MUNSELL 5 R V 5 | 49.35 | 54 | 24.12 | 59.14 | 24.07 |
| MUNSELL 7.5 R V 5 | 49.91 | 49.38 | 33.4 | 59.62 | 34.07 |
| MUNSELL 10 R V 5 | 49.78 | 44.26 | 40.72 | 60.14 | 42.61 |
| MUNSELL 2.5 YR V 5 | 49.72 | 35.38 | 38.67 | 52.42 | 47.54 |
| MUNSELL 5 YR V 5 | 49.54 | 27.18 | 39.12 | 47.64 | 55.21 |
| MUNSELL 7.5 YR V 5 | 50.16 | 23.42 | 40.87 | 47.1 | 60.19 |
| MUNSELL 10 YR V 5 | 50.42 | 16.47 | 41.77 | 44.9 | 68.49 |
| MUNSELL 2.5 Y V 5 | 50.67 | 10.35 | 37.15 | 38.56 | 74.43 |
| MUNSELL 5 Y V 5 | 50.46 | 5.86 | 39.63 | 40.06 | 81.58 |
| MUNSELL 7.5 Y V 5 | 50.15 | 1.33 | 40.87 | 40.89 | 88.14 |
| MUNSELL 10 Y V 5 | 50.03 | -2.23 | 40.09 | 40.15 | 93.19 |
| MUNSELL 2.5 GY V 5 | 50.46 | -6.45 | 38.71 | 39.25 | 99.46 |
| MUNSELL 5 GY V 5 | 49.73 | -12.25 | 41.28 | 43.06 | 106.52 |
| MUNSELL 7.5 GY V 5 | 50.53 | -21.62 | 39.31 | 44.86 | 118.81 |
| MUNSELL 10 GY V 5 | 51.31 | -31.62 | 32.74 | 45.52 | 134.01 |
| MUNSELL 2.5 G V 5 | 52.19 | -41.69 | 25.22 | 48.72 | 148.83 |
| MUNSELL 5 G V 5 | 52.79 | -38.4 | 14.94 | 41.2 | 158.74 |
| MUNSELL 7.5 G V 5 | 52.22 | -41.51 | 11.79 | 43.15 | 164.15 |
| MUNSELL 10 G V 5 | 52.21 | -41.73 | 7.47 | 42.4 | 169.85 |
| MUNSELL 2.5 BG V 5 | 53.25 | -42.39 | 3.45 | 42.53 | 175.35 |
| MUNSELL 5 BG V 5 | 53.92 | -40.99 | -2.16 | 41.05 | 183.02 |
| MUNSELL 7.5 BG V 5 | 53.86 | -42.43 | -6.92 | 42.99 | 189.26 |
| MUNSELL 10 BG V 5 | 53.96 | -38.77 | -12.3 | 40.67 | 197.6 |
| MUNSELL 2.5 B V 5 | 54.07 | -37.07 | -17.27 | 40.9 | 204.98 |
| MUNSELL 5 B V 5 | 54.55 | -30.93 | -21.54 | 37.69 | 214.85 |
| MUNSELL 7.5 B V 5 | 54.32 | -30.06 | -27.41 | 40.68 | 222.36 |
| MUNSELL 10 B V 5 | 55.29 | -23.41 | -30.73 | 38.63 | 232.7 |
| MUNSELL 2.5 PB V 5 | 54.77 | -14.94 | -35.03 | 38.09 | 246.9 |
| MUNSELL 5 PB V 5 | 54.52 | -7.65 | -39.03 | 39.77 | 258.92 |
| MUNSELL 7.5 PB V 5 | 53.8 | 4.5 | -39.84 | 40.09 | 276.45 |
| MUNSELL 10 PB V 5 | 53.17 | 13.87 | -35.3 | 37.93 | 291.45 |
| MUNSELL 2.5 P V 5 | 52.59 | 19.32 | -33.31 | 38.51 | 300.12 |
| MUNSELL 5 P V 5 | 52.44 | 24.91 | -28.75 | 38.04 | 310.91 |
| MUNSELL 7.5 P V 5 | 52.09 | 27.64 | -25.04 | 37.29 | 317.83 |
| MUNSELL 10 P V 5 | 51.03 | 34.17 | -21.63 | 40.44 | 327.67 |
| MUNSELL 2.5 RP V 5 | 51.28 | 40.35 | -16.9 | 43.75 | 337.28 |
| MUNSELL 5 RP V 5 | 51.63 | 44.13 | -5.71 | 44.49 | 352.62 |
| MUNSELL 7.5 RP V 5 | 50.14 | 44.91 | -0.09 | 44.91 | 359.88 |

**Appendix D5 Real Munsell highest chroma values at 4V measured from actual Munsell Atlas**

| | L* | a* | b* | C* | h |
|---|---|---|---|---|---|
| MUNSELL 2.5 R V 4 | 39.8 | 47.72 | 12.55 | 49.34 | 14.74 |
| MUNSELL 5 R V 4 | 39.13 | 52.37 | 24.28 | 57.73 | 24.87 |
| MUNSELL 7.5 R V 4 | 40.33 | 43.9 | 28.37 | 52.27 | 32.87 |
| MUNSELL 10 R V 4 | 40.79 | 30.23 | 25.12 | 39.3 | 39.72 |
| MUNSELL 2.5 YR V 4 | 41.05 | 30.04 | 31.35 | 43.42 | 46.21 |
| MUNSELL 5 YR V 4 | 40.58 | 19.09 | 25.86 | 32.14 | 53.56 |
| MUNSELL 7.5 YR V 4 | 41.04 | 16.89 | 26.64 | 31.54 | 57.63 |
| MUNSELL 10 YR V 4 | 40.9 | 11.25 | 24.12 | 26.62 | 64.99 |
| MUNSELL 2.5 Y V 4 | 40.15 | 7.15 | 27.08 | 28 | 75.21 |

| | | | | | |
|---|---|---|---|---|---|
| MUNSELL 5 Y V 4 | 41.04 | 4.51 | 23.92 | 24.34 | 79.33 |
| MUNSELL 7.5 Y V 4 | 40.96 | 0.81 | 24.84 | 24.86 | 88.14 |
| MUNSELL 10 Y V 4 | 41.18 | -1.86 | 22.06 | 22.14 | 94.82 |
| MUNSELL 2.5 GY V 4 | 41.42 | -5.1 | 24.89 | 25.41 | 101.59 |
| MUNSELL 5 GY V 4 | 41.31 | -7.8 | 22.52 | 23.83 | 109.11 |
| MUNSELL 7.5 GY V 4 | 41.11 | -11.14 | 17.91 | 21.09 | 121.88 |
| MUNSELL 10 GY V 4 | 41.78 | -16.1 | 16.31 | 22.92 | 134.61 |
| MUNSELL 2.5 G V 4 | 41.04 | -27.58 | 15.01 | 31.4 | 151.43 |
| MUNSELL 5 G V 4 | 42.11 | -35.39 | 12.87 | 37.66 | 160.02 |
| MUNSELL 7.5 G V 4 | 41.77 | -39.52 | 9.77 | 40.71 | 166.12 |
| MUNSELL 10 G V 4 | 42.77 | -41.94 | 7.34 | 42.58 | 170.08 |
| MUNSELL 2.5 BG V 4 | 42.42 | -38.6 | 2.59 | 38.68 | 176.17 |
| MUNSELL 5 BG V 4 | 42.27 | -36.53 | -2.86 | 36.64 | 184.47 |
| MUNSELL 7.5 BG V 4 | 43.34 | -38.05 | -7.18 | 38.72 | 190.69 |
| MUNSELL 10 BG V 4 | 42.88 | -36.32 | -11.61 | 38.13 | 197.72 |
| MUNSELL 2.5 B V 4 | 44.15 | -32.85 | -16.31 | 36.68 | 206.41 |
| MUNSELL 5 B V 4 | 43.49 | -27.47 | -20.94 | 34.55 | 217.32 |
| MUNSELL 7.5 B V 4 | 43.85 | -25.23 | -24.68 | 35.3 | 224.37 |
| MUNSELL 10 B V 4 | 43.62 | -20.42 | -26.38 | 33.36 | 232.26 |
| MUNSELL 2.5 PB V 4 | 45.8 | -16.33 | -35.27 | 38.86 | 245.16 |
| MUNSELL 5 PB V 4 | 43.42 | -8.39 | -38.58 | 39.48 | 257.73 |
| MUNSELL 7.5 PB V 4 | 43.01 | 6.71 | -39.44 | 40.01 | 279.66 |
| MUNSELL 10 PB V 4 | 42.6 | 15.68 | -36.5 | 39.72 | 293.25 |
| MUNSELL 2.5 P V 4 | 42.47 | 21.26 | -33.06 | 39.3 | 302.75 |
| MUNSELL 5 P V 4 | 41.64 | 23.34 | -28.87 | 37.13 | 308.95 |
| MUNSELL 7.5 P V 4 | 42.01 | 28.46 | -25.18 | 38 | 318.5 |
| MUNSELL 10 P V 4 | 41.71 | 31.89 | -21.71 | 38.58 | 325.75 |
| MUNSELL 2.5 RP V 4 | 41.43 | 35.03 | -16.21 | 38.59 | 335.17 |
| MUNSELL 5 RP V 4 | 41.02 | 41.84 | -8.63 | 42.72 | 348.34 |
| MUNSELL 7.5 RP V 4 | 40.09 | 42.75 | -2.66 | 42.83 | 356.45 |
| MUNSELL 10 RP V 4 | 40.13 | 44.64 | 4.36 | 44.85 | 5.58 |

**Appendix D6 Real Munsell highest chroma values at 2.5V measured from actual Munsell Atlas**

| | L* | a* | b* | C* | h |
|---|---|---|---|---|---|
| MUNSELL 2.5R V 2.5 | 25.87 | 9.47 | 1.21 | 9.55 | 7.25 |
| MUNSELL 5R V 2.5 | 25.67 | 9.52 | 2.69 | 9.89 | 15.78 |
| MUNSELL 7.5R V 2.5 | 26.1 | 9.65 | 3.96 | 10.43 | 22.31 |
| MUNSELL 10.0R V 2.5 | 26.75 | 12.42 | 6.13 | 13.85 | 26.29 |
| MUNSELL 2.5YR V 2.5 | 24.84 | 10.15 | 7.25 | 12.47 | 35.55 |
| MUNSELL 5 YR V 2.5 | 26.29 | 4.27 | 3.54 | 5.55 | 39.66 |
| MUNSELL10.0YRV 2.5 | 25.84 | 2.95 | 5.09 | 5.88 | 59.94 |
| MUNSELL 5.0 Y V 2.5 | 26.78 | 1.82 | 5.04 | 5.36 | 70.16 |
| MUNSELL 10.0 Y V 2.5 | 25.81 | -0.4 | 4.02 | 4.04 | 95.69 |
| MUNSELL 5.0 GYV 2.5 | 25.54 | -1.72 | 4.01 | 4.36 | 113.26 |
| MUNSELL 0.0 GY V2.5 | 26.85 | -5.51 | 4.35 | 7.01 | 141.72 |
| MUNSELL 2.5 G V2.5 | 27.66 | -7.65 | 4.44 | 8.84 | 149.87 |
| MUNSELL 5.0 G V2.5 | 26.9 | -7.05 | 2.58 | 7.51 | 159.88 |
| MUNSELL 7.5 G V2.5 | 27.14 | -8.22 | 2.84 | 8.69 | 160.93 |
| MUNSELL 10.0 GV 2.5 | 27.18 | -8.93 | 1.53 | 9.06 | 170.27 |
| MUNSELL 2.5 BG V2.5 | 26.14 | -7.98 | 0.23 | 7.98 | 178.35 |
| MUNSELL 5.0 BG V2.5 | 26.61 | -8.83 | -0.98 | 8.89 | 186.35 |
| MUNSELL 7.5 BG V2.5 | 26.67 | -9.55 | -2.71 | 9.93 | 195.87 |
| MUNSELL 10 BG V2.5 | 26.37 | -9 | -3.55 | 9.67 | 201.52 |
| MUNSELL 2.5 B V2.5 | 27.64 | -7.86 | -4.17 | 8.89 | 207.93 |
| MUNSELL 5 B V2.5 | 27.17 | -8.76 | -5.63 | 10.41 | 212.76 |
| MUNSELL 7.5 B V2.5 | 26.83 | -8.26 | -6.58 | 10.56 | 218.56 |
| MUNSELL 10.0 B V2.5 | 27.63 | -9.82 | -11.07 | 14.8 | 228.44 |
| MUNSELL 2.5 PB V2.5 | 27.84 | -7.96 | -14.23 | 16.31 | 240.77 |
| MUNSELL 5.0 PB V2.5 | 26.75 | -2.04 | -17.19 | 17.31 | 263.23 |
| MUNSELL 7.5 PB V2.5 | 27.3 | 5.18 | -23.83 | 24.38 | 282.27 |
| MUNSELL 10 PB V2.5 | 26.58 | 10.55 | -20.95 | 23.45 | 296.72 |
| MUNSELL 2.5 P V2.5 | 26.05 | 10.89 | -17.21 | 20.36 | 302.32 |

| | | | | | |
|---|---|---|---|---|---|
| MUNSELL 5.0 P V2.5 | 25.84 | 15.96 | -16.64 | 23.06 | 313.79 |
| MUNSELL 7.5 P V2.5 | 26.69 | 14.43 | -12.44 | 19.05 | 319.24 |
| MUNSELL 10 P V2.5 | 26.88 | 14.6 | -11.75 | 18.74 | 321.17 |
| MUNSELL 2.5 RP V2.5 | 26.62 | 14.63 | -8.04 | 16.69 | 331.19 |
| MUNSELL 5 RP V2.5 | 27.14 | 14.74 | -4.23 | 15.34 | 344.01 |
| MUNSELL 7.5 RP V2.5 | 25.89 | 13.31 | -2.25 | 13.5 | 350.42 |
| MUNSELL 10 RP V2.5 | 27.98 | 18.51 | -1.57 | 18.58 | 355.16 |

**Appendix E1 Reflectance values of data set 1**

| REF. | PAIR NUMBERS | | | | | | | | | | | | |
|---|---|---|---|---|---|---|---|---|---|---|---|---|---|
| nm | 1 | 2 | 3 | 4 | 5 | 6 | 7 | 8 | 9 | 10 | 11 | 12 | 13 |
| 400 | 20.8 | 11.17 | 15.36 | 10.54 | 8.58 | 15.25 | 16.84 | 16.65 | 4.87 | 2.97 | 5.31 | 4.62 | 4.63 |
| 410 | 30.6 | 14.6 | 22.46 | 13.43 | 10.69 | 21.69 | 27.79 | 28.11 | 5.68 | 3.2 | 6.38 | 5.31 | 5.35 |
| 420 | 45.39 | 18.68 | 31.37 | 16.53 | 13.19 | 29.71 | 42.75 | 44.13 | 6.78 | 3.46 | 7.54 | 6.24 | 6.26 |
| 430 | 57.56 | 21.47 | 36.98 | 18.67 | 15.31 | 35.15 | 53.4 | 54.82 | 7.89 | 3.65 | 8.28 | 7.35 | 7.33 |
| 440 | 62.62 | 23.37 | 39.99 | 20.56 | 17.32 | 38.13 | 56.39 | 56.73 | 9.16 | 3.77 | 8.77 | 8.71 | 8.68 |
| 450 | 63.7 | 25.5 | 42.7 | 23.1 | 19.61 | 40.25 | 53.99 | 54.25 | 10.77 | 3.72 | 8.93 | 10.17 | 10.11 |
| 460 | 63.15 | 28.06 | 45.96 | 26.63 | 22.04 | 41.89 | 48.84 | 50.08 | 12.63 | 3.41 | 8.52 | 11.32 | 11.23 |
| 470 | 62.22 | 30.82 | 49.97 | 31.36 | 24.07 | 43.03 | 43.68 | 46.18 | 14.33 | 2.99 | 7.69 | 11.73 | 11.63 |
| 480 | 61.56 | 33.39 | 54.7 | 37.5 | 25.24 | 43.4 | 39.41 | 43.3 | 15.45 | 2.63 | 6.71 | 11.21 | 11.11 |
| 490 | 59.99 | 34.57 | 58.21 | 43.42 | 25.1 | 42.21 | 35.34 | 40.4 | 15.56 | 2.35 | 5.69 | 9.98 | 9.91 |
| 500 | 58.14 | 34.52 | 60 | 48.06 | 24.23 | 40.2 | 32.13 | 37.97 | 14.68 | 2.17 | 4.79 | 8.66 | 8.63 |
| 510 | 55.88 | 33.74 | 59.87 | 50.74 | 23.12 | 37.83 | 29.53 | 35.96 | 13.04 | 2.07 | 4.06 | 7.44 | 7.45 |
| 520 | 53.38 | 32.97 | 58.33 | 51.77 | 22.29 | 35.5 | 27.42 | 34.29 | 11.18 | 2.05 | 3.47 | 6.43 | 6.49 |
| 530 | 51.04 | 32.76 | 56.06 | 52.07 | 22.03 | 33.83 | 26.06 | 32.86 | 9.38 | 2.06 | 2.98 | 5.81 | 5.89 |
| 540 | 49.16 | 33.16 | 53.36 | 52.47 | 22.31 | 33.19 | 25.71 | 31.75 | 7.73 | 2.14 | 2.63 | 5.61 | 5.69 |
| 550 | 47.82 | 34.34 | 50.62 | 53.66 | 23.29 | 33.2 | 26.11 | 31.17 | 6.37 | 2.44 | 2.48 | 5.65 | 5.72 |
| 560 | 46.94 | 36.73 | 48.17 | 55.26 | 25.3 | 33.37 | 26.76 | 30.85 | 5.36 | 3.1 | 2.45 | 5.71 | 5.82 |
| 570 | 46.66 | 40.83 | 45.93 | 56.3 | 28.84 | 34.14 | 27.8 | 30.09 | 4.6 | 4 | 2.47 | 5.97 | 6.16 |
| 580 | 47.15 | 46.7 | 43.59 | 56.34 | 34.05 | 36.79 | 30.3 | 28.6 | 3.94 | 4.84 | 2.5 | 7.05 | 7.29 |
| 590 | 48.33 | 53.33 | 41.35 | 55.73 | 40.14 | 42.53 | 35.32 | 26.81 | 3.41 | 5.42 | 2.49 | 9.87 | 10.11 |
| 600 | 50.24 | 59.25 | 39.8 | 55.11 | 45.74 | 51.35 | 42.65 | 25.44 | 3.08 | 5.72 | 2.56 | 15.53 | 15.67 |
| 610 | 53.84 | 63.56 | 39.13 | 54.88 | 49.9 | 61.03 | 50.1 | 24.81 | 2.95 | 5.83 | 2.97 | 24.19 | 24.21 |
| 620 | 59.76 | 66.15 | 39.01 | 54.91 | 52.44 | 68.67 | 55.3 | 24.66 | 2.94 | 5.83 | 4.18 | 34.18 | 34.15 |
| 630 | 67.27 | 67.37 | 38.63 | 54.64 | 53.55 | 73.33 | 57.7 | 24.28 | 2.91 | 5.81 | 7.11 | 43.32 | 43.3 |
| 640 | 74.13 | 67.84 | 37.96 | 54.05 | 53.81 | 75.74 | 58.25 | 23.6 | 2.83 | 5.88 | 12.59 | 50.02 | 50.04 |
| 650 | 78.74 | 68.34 | 37.87 | 53.99 | 54.23 | 77.09 | 58.52 | 23.37 | 2.8 | 6.2 | 20.38 | 54.38 | 54.47 |
| 660 | 81.84 | 69.35 | 39.3 | 55.31 | 55.61 | 78.24 | 59.81 | 24.4 | 3 | 6.94 | 30.05 | 57.79 | 57.97 |
| 670 | 83.21 | 71.02 | 42.87 | 58.4 | 58.42 | 79.48 | 62.71 | 27.36 | 3.61 | 8.17 | 39.87 | 61.43 | 61.69 |
| 680 | 83.76 | 73.31 | 48.95 | 63.27 | 62.74 | 81.05 | 67.31 | 32.76 | 4.95 | 10.07 | 49.17 | 66.04 | 66.3 |
| 690 | 84.05 | 75.55 | 56.15 | 68.51 | 67.42 | 82.58 | 72.21 | 39.68 | 7.15 | 12.64 | 57.35 | 70.91 | 71.02 |
| 700 | 84.81 | 77.48 | 63.64 | 73.41 | 71.87 | 83.92 | 76.75 | 47.75 | 10.51 | 16.28 | 65.94 | 75.6 | 75.5 |

| Ref. | Pair numbers | | | | | | | | | | | | |
|---|---|---|---|---|---|---|---|---|---|---|---|---|---|
| nm | 14 | 15 | 16 | 17 | 18 | 19 | 20 | 21 | 22 | 23 | 24 | 25 | 26 |
| 400 | 2.45 | 2.42 | 2.09 | 2.25 | 1.99 | 2.38 | 12.95 | 12.97 | 15.76 | 11.98 | 3.82 | 6.51 | 5.84 |
| 410 | 2.5 | 2.52 | 2.06 | 2.23 | 1.98 | 2.43 | 19.03 | 18.63 | 22.66 | 17.12 | 4.32 | 7.56 | 6.98 |
| 420 | 2.64 | 2.64 | 2.07 | 2.17 | 2.02 | 2.5 | 26.63 | 26.41 | 31.72 | 22.45 | 4.98 | 8.78 | 8.37 |
| 430 | 2.87 | 2.82 | 2.12 | 2.2 | 2.1 | 2.63 | 31.63 | 31.77 | 38.18 | 25.92 | 5.81 | 9.89 | 9.76 |
| 440 | 3.26 | 3.2 | 2.24 | 2.31 | 2.25 | 2.84 | 33.48 | 33.85 | 40.47 | 28.3 | 7.02 | 11.18 | 11.31 |
| 450 | 3.94 | 3.82 | 2.57 | 2.6 | 2.65 | 3.33 | 33.31 | 33.83 | 39.01 | 30.89 | 8.97 | 13.12 | 13.32 |
| 460 | 4.88 | 4.7 | 3.24 | 3.27 | 3.48 | 4.26 | 31.7 | 32.32 | 35.15 | 34.3 | 11.92 | 15.96 | 15.62 |
| 470 | 5.84 | 5.57 | 4.48 | 4.54 | 4.92 | 5.77 | 29.35 | 30.04 | 30.89 | 38.64 | 15.88 | 19.81 | 17.69 |
| 480 | 6.49 | 6.11 | 6.53 | 6.62 | 7 | 7.98 | 26.8 | 27.5 | 26.88 | 43.68 | 20.77 | 24.74 | 18.96 |
| 490 | 6.57 | 6.14 | 8.88 | 9.01 | 8.76 | 10.17 | 24.04 | 24.74 | 23.06 | 47.11 | 25.39 | 29.28 | 19.01 |
| 500 | 6.26 | 5.82 | 10.58 | 10.76 | 9.04 | 11.49 | 21.24 | 21.96 | 19.8 | 47.99 | 28.84 | 32.17 | 18.29 |
| 510 | 5.81 | 5.4 | 10.99 | 11.19 | 7.75 | 11.64 | 18.42 | 19.15 | 16.92 | 46.32 | 30.57 | 32.79 | 17.32 |

| | | | | | | | | | | | | | |
|---|---|---|---|---|---|---|---|---|---|---|---|---|---|
| 520 | 5.47 | 5.09 | 10.39 | 10.6 | 5.85 | 11.09 | 15.83 | 16.52 | 14.38 | 43.1 | 30.81 | 31.78 | 16.58 |
| 530 | 5.37 | 5.01 | 9.62 | 9.81 | 4.23 | 10.41 | 13.54 | 14.19 | 12.3 | 39.44 | 30.25 | 30.48 | 16.34 |
| 540 | 5.48 | 5.14 | 9.17 | 9.34 | 3.17 | 9.81 | 11.54 | 12.15 | 10.8 | 35.77 | 29.55 | 29.73 | 16.57 |
| 550 | 5.88 | 5.54 | 8.98 | 9.11 | 2.6 | 9.37 | 9.88 | 10.44 | 9.8 | 32.49 | 29.22 | 29.42 | 17.41 |
| 560 | 6.79 | 6.44 | 8.82 | 8.95 | 2.32 | 9.15 | 8.59 | 9.11 | 9.19 | 29.78 | 29.07 | 29.2 | 19.21 |
| 570 | 8.56 | 8.19 | 8.85 | 8.99 | 2.18 | 9.06 | 7.55 | 8.02 | 8.95 | 27.43 | 28.45 | 29.36 | 22.48 |
| 580 | 11.49 | 11.11 | 9.5 | 9.59 | 2.09 | 8.93 | 6.63 | 7.06 | 9.1 | 25.22 | 27.11 | 30.63 | 27.36 |
| 590 | 15.35 | 15.01 | 11.05 | 10.99 | 2.02 | 8.72 | 5.88 | 6.28 | 9.56 | 23.34 | 25.45 | 33.33 | 33.12 |
| 600 | 19.28 | 19.11 | 13.26 | 12.94 | 2 | 8.53 | 5.43 | 5.78 | 10.46 | 22.09 | 24.17 | 36.77 | 38.42 |
| 610 | 22.49 | 22.57 | 15.37 | 14.82 | 2.11 | 8.41 | 5.25 | 5.59 | 12.6 | 21.49 | 23.59 | 39.75 | 42.43 |
| 620 | 24.62 | 24.89 | 16.77 | 16.06 | 2.51 | 8.3 | 5.22 | 5.55 | 17.06 | 21.26 | 23.46 | 41.62 | 44.94 |
| 630 | 25.54 | 25.92 | 17.24 | 16.43 | 3.45 | 8.24 | 5.13 | 5.45 | 24.74 | 20.97 | 23.13 | 42.21 | 45.9 |
| 640 | 25.59 | 26.04 | 17.09 | 16.21 | 5 | 8.33 | 4.98 | 5.29 | 34.97 | 20.71 | 22.52 | 42.02 | 45.81 |
| 650 | 25.68 | 26.21 | 17.02 | 16.17 | 6.92 | 8.81 | 5 | 5.32 | 45.61 | 20.98 | 22.33 | 42.08 | 45.83 |
| 660 | 26.74 | 27.42 | 17.87 | 17.09 | 9.11 | 9.84 | 5.51 | 5.82 | 55.89 | 22.3 | 23.37 | 43.43 | 47.11 |
| 670 | 29.47 | 30.35 | 20.25 | 19.56 | 11.54 | 11.51 | 6.84 | 7.08 | 63.88 | 25.06 | 26.24 | 46.71 | 50.38 |
| 680 | 34.37 | 35.44 | 24.68 | 24.07 | 14.5 | 13.99 | 9.45 | 9.48 | 69.79 | 29.63 | 31.48 | 52.25 | 55.89 |
| 690 | 40.64 | 41.85 | 30.62 | 30.1 | 18.05 | 17.21 | 13.29 | 12.96 | 74.07 | 35.41 | 38.3 | 58.7 | 62.24 |
| 700 | 47.95 | 49.23 | 38.01 | 37.6 | 22.83 | 21.57 | 18.55 | 17.79 | 78.96 | 42.41 | 46.38 | 65.35 | 68.54 |

| Ref. | Pair numbers | | | | | | | | | | | | |
|---|---|---|---|---|---|---|---|---|---|---|---|---|---|
| nm | 27 | 28 | 29 | 30 | 31 | 32 | 33 | 34 | 35 | 36 | 37 | 38 | 39 |
| 400 | 5.58 | 15.2 | 6.43 | 14.27 | 10.51 | 6.9 | 2.96 | 3.01 | 7.54 | 9.71 | 2.45 | 4.17 | 4.73 |
| 410 | 6.53 | 22.13 | 8.25 | 20.27 | 14.72 | 8.55 | 3.04 | 3.22 | 9.14 | 12.25 | 2.47 | 4.5 | 5.23 |
| 420 | 7.73 | 30.96 | 10.64 | 28.25 | 19.63 | 10.49 | 3.17 | 3.55 | 10.86 | 15.25 | 2.53 | 4.91 | 5.87 |
| 430 | 8.88 | 36.8 | 13.03 | 33.9 | 22.86 | 12.32 | 3.37 | 4.04 | 12.27 | 17.48 | 2.67 | 5.43 | 6.52 |
| 440 | 10.3 | 38.59 | 15.96 | 35.9 | 24.21 | 14.27 | 3.76 | 4.83 | 13.89 | 19.49 | 3 | 6.21 | 7.5 |
| 450 | 12.1 | 36.95 | 19.76 | 34.14 | 24.11 | 16.23 | 4.54 | 6.21 | 16.25 | 22.09 | 3.71 | 7.56 | 9.05 |
| 460 | 14.18 | 33.17 | 23.55 | 30.02 | 22.81 | 17.74 | 5.92 | 8.39 | 19.62 | 25.53 | 4.98 | 9.72 | 11.44 |
| 470 | 16.02 | 29.19 | 25.72 | 25.69 | 20.85 | 18.33 | 8.13 | 11.38 | 24.08 | 29.75 | 6.87 | 12.86 | 14.87 |
| 480 | 17.07 | 25.68 | 25.58 | 21.72 | 18.63 | 17.75 | 11.37 | 15.01 | 29.65 | 34.53 | 9.28 | 17.13 | 19.39 |
| 490 | 17.05 | 22.54 | 23.36 | 18.14 | 16.34 | 16.18 | 14.82 | 18.25 | 34.55 | 37.95 | 11.41 | 21.35 | 23.78 |
| 500 | 16.38 | 20.1 | 20.2 | 15.18 | 14.07 | 14.41 | 17.27 | 20.33 | 37.02 | 38.88 | 12.71 | 24.18 | 26.71 |
| 510 | 15.51 | 18.19 | 16.94 | 12.65 | 11.85 | 12.71 | 17.9 | 20.97 | 36.51 | 37.35 | 13.06 | 24.83 | 27.41 |
| 520 | 14.86 | 16.69 | 14.03 | 10.49 | 9.88 | 11.24 | 17.14 | 20.56 | 33.94 | 34.38 | 12.74 | 23.86 | 26.47 |
| 530 | 14.67 | 15.77 | 11.51 | 8.78 | 8.19 | 10.27 | 16.09 | 19.58 | 30.64 | 31.01 | 12.08 | 22.62 | 25.25 |
| 540 | 14.93 | 15.58 | 9.39 | 7.57 | 6.78 | 9.91 | 15.44 | 18.48 | 27.35 | 27.66 | 11.4 | 21.92 | 24.55 |
| 550 | 15.76 | 15.99 | 7.78 | 6.79 | 5.66 | 9.93 | 15.12 | 17.61 | 24.51 | 24.7 | 10.96 | 21.65 | 24.26 |
| 560 | 17.48 | 16.61 | 6.56 | 6.34 | 4.84 | 10 | 14.85 | 16.9 | 22.17 | 22.28 | 10.64 | 21.4 | 24.04 |
| 570 | 20.58 | 17.6 | 5.6 | 6.17 | 4.2 | 10.4 | 14.85 | 15.99 | 20.13 | 20.22 | 10.11 | 21.5 | 24.23 |
| 580 | 25.2 | 19.9 | 4.82 | 6.31 | 3.67 | 11.95 | 15.63 | 14.73 | 18.3 | 18.31 | 9.26 | 22.71 | 25.53 |
| 590 | 30.72 | 24.77 | 4.27 | 6.7 | 3.25 | 15.73 | 17.45 | 13.38 | 16.84 | 16.67 | 8.31 | 25.46 | 28.32 |
| 600 | 35.94 | 32.9 | 3.95 | 7.43 | 3.02 | 22.61 | 19.89 | 12.39 | 15.93 | 15.59 | 7.61 | 29.17 | 32.03 |
| 610 | 39.98 | 43.27 | 3.79 | 9.15 | 2.94 | 32.04 | 22.07 | 11.96 | 15.48 | 15.06 | 7.3 | 32.49 | 35.36 |
| 620 | 42.53 | 52.96 | 3.7 | 12.84 | 2.92 | 41.51 | 23.42 | 11.86 | 15.26 | 14.86 | 7.24 | 34.58 | 37.47 |
| 630 | 43.54 | 59.86 | 3.66 | 19.53 | 2.88 | 48.68 | 23.75 | 11.65 | 15.07 | 14.63 | 7.12 | 35.2 | 38.08 |
| 640 | 43.52 | 63.83 | 3.7 | 29.05 | 2.81 | 52.91 | 23.41 | 11.24 | 15.07 | 14.4 | 6.86 | 34.91 | 37.77 |
| 650 | 43.64 | 66.19 | 3.92 | 39.74 | 2.83 | 55.18 | 23.28 | 11.11 | 15.56 | 14.57 | 6.77 | 34.8 | 37.7 |
| 660 | 44.99 | 68.32 | 4.44 | 50.91 | 3.1 | 56.89 | 24.24 | 11.79 | 16.9 | 15.59 | 7.24 | 36.05 | 39.07 |
| 670 | 48.26 | 70.91 | 5.34 | 60.35 | 3.82 | 58.78 | 26.88 | 13.77 | 19.28 | 17.82 | 8.65 | 39.4 | 42.61 |
| 680 | 53.66 | 74.26 | 6.81 | 67.72 | 5.39 | 61.21 | 31.58 | 17.48 | 22.97 | 21.61 | 11.45 | 45.39 | 48.73 |

| | | | | | | | | | | | | | |
|---|---|---|---|---|---|---|---|---|---|---|---|---|---|
| 690 | 59.92 | 77.61 | 8.89 | 73.13 | 7.94 | 63.85 | 37.5 | 22.47 | 27.61 | 26.56 | 15.45 | 52.74 | 56.1 |
| 700 | 66.27 | 80.61 | 12.02 | 78.78 | 11.79 | 66.9 | 44.34 | 28.68 | 33.5 | 32.85 | 20.82 | 60.64 | 63.78 |

| Ref. | Pair numbers | | | | | | | | | |
|---|---|---|---|---|---|---|---|---|---|---|
| nm | 40 | 41 | 42 | 43 | 44 | 45 | 46 | 47 | 48 | 49 |
| 400 | 3.76 | 9.23 | 15.35 | 15.53 | 15.7 | 9.27 | 8.74 | 8.39 | 4.84 | 4.94 |
| 410 | 4.15 | 11.97 | 22.75 | 23.11 | 23.32 | 11.85 | 10.77 | 10.92 | 5.63 | 5.74 |
| 420 | 4.69 | 15.26 | 33.15 | 33.74 | 33.21 | 15.01 | 13.49 | 13.81 | 6.73 | 6.8 |
| 430 | 5.35 | 18.14 | 40.72 | 41.51 | 38.77 | 17.6 | 15.85 | 16.12 | 7.97 | 7.94 |
| 440 | 6.27 | 20.69 | 43.13 | 43.9 | 39.53 | 19.83 | 17.96 | 18.13 | 9.59 | 9.55 |
| 450 | 7.59 | 23.04 | 41.59 | 42.16 | 37.82 | 22.29 | 20.27 | 20.28 | 11.98 | 11.93 |
| 460 | 9.2 | 24.81 | 37.7 | 38.02 | 34.76 | 24.94 | 22.74 | 22.56 | 15.41 | 15.41 |
| 470 | 10.67 | 25.54 | 33.56 | 33.67 | 31.68 | 27.37 | 24.94 | 24.54 | 19.87 | 19.99 |
| 480 | 11.57 | 25 | 29.93 | 29.9 | 29.16 | 29.15 | 26.45 | 25.77 | 25.2 | 25.51 |
| 490 | 11.59 | 23.18 | 26.57 | 26.44 | 26.86 | 29.52 | 26.62 | 25.68 | 30.04 | 30.68 |
| 500 | 11.06 | 21.05 | 23.92 | 23.74 | 25.1 | 28.51 | 25.53 | 24.36 | 33.19 | 34.17 |
| 510 | 10.36 | 18.95 | 21.81 | 21.62 | 23.93 | 26.28 | 23.39 | 22.05 | 33.74 | 34.94 |
| 520 | 9.84 | 17.06 | 20.15 | 19.94 | 23.24 | 23.57 | 20.82 | 19.42 | 32.13 | 33.44 |
| 530 | 9.69 | 15.78 | 19.09 | 18.87 | 22.87 | 20.79 | 18.23 | 16.81 | 29.53 | 30.81 |
| 540 | 9.87 | 15.32 | 18.87 | 18.66 | 23.07 | 18.04 | 15.73 | 14.32 | 26.64 | 27.79 |
| 550 | 10.5 | 15.34 | 19.27 | 19.15 | 24.25 | 15.62 | 13.56 | 12.17 | 23.92 | 24.95 |
| 560 | 11.87 | 15.41 | 19.94 | 19.86 | 26 | 13.72 | 11.85 | 10.51 | 21.65 | 22.6 |
| 570 | 14.39 | 15.89 | 20.99 | 20.86 | 27.09 | 12.15 | 10.45 | 9.18 | 19.71 | 20.6 |
| 580 | 18.26 | 17.89 | 23.34 | 23.26 | 26.98 | 10.68 | 9.15 | 7.95 | 17.87 | 18.65 |
| 590 | 22.91 | 22.76 | 28.05 | 28.3 | 26.12 | 9.36 | 8.03 | 6.88 | 16.2 | 16.87 |
| 600 | 27.3 | 31.44 | 35.31 | 36.24 | 25.29 | 8.49 | 7.3 | 6.2 | 15.06 | 15.64 |
| 610 | 30.64 | 43.13 | 43.52 | 45.26 | 24.93 | 8.14 | 7.03 | 5.93 | 14.55 | 15.1 |
| 620 | 32.7 | 54.86 | 50.1 | 52.43 | 24.87 | 8.07 | 6.98 | 5.88 | 14.41 | 14.95 |
| 630 | 33.42 | 64.09 | 53.95 | 56.51 | 24.59 | 7.9 | 6.84 | 5.76 | 14.15 | 14.67 |
| 640 | 33.25 | 70.1 | 55.64 | 58.12 | 24.04 | 7.57 | 6.58 | 5.53 | 13.74 | 14.2 |
| 650 | 33.22 | 73.68 | 56.69 | 58.94 | 23.97 | 7.47 | 6.53 | 5.48 | 13.66 | 14.08 |
| 660 | 34.3 | 76.05 | 58.44 | 60.46 | 25.16 | 8.05 | 7.11 | 5.96 | 14.51 | 14.9 |
| 670 | 37.07 | 77.99 | 61.51 | 63.42 | 28.23 | 9.75 | 8.72 | 7.28 | 16.77 | 17.18 |
| 680 | 41.77 | 80.07 | 66.03 | 68.05 | 33.69 | 13.1 | 11.86 | 9.87 | 20.86 | 21.36 |
| 690 | 47.31 | 82.08 | 70.77 | 73.01 | 40.69 | 17.89 | 16.39 | 13.67 | 26.28 | 26.93 |
| 700 | 53.26 | 83.82 | 75.27 | 77.53 | 48.81 | 24.18 | 22.38 | 18.88 | 33.05 | 33.88 |

**Appendix E2 Colorimetric co-ordinates of data set 1**

| Pair no. | $L_s$ | $C_s$ | $a_s$ | $b_s$ | $h_s$ | $L_{bx}$ | $C_{bx}$ | $a_{bx}$ | $b_{bx}$ | $h_{bx}$ |
|---|---|---|---|---|---|---|---|---|---|---|
| 1 | 77.72 | 8.96 | 5.16 | -7.32 | 305.17 | 77.68 | 8.56 | 5.19 | -6.81 | 307.33 |
| 2 | 70.72 | 29.12 | 18.49 | 22.50 | 50.59 | 70.45 | 26.67 | 16.15 | 21.22 | 52.73 |
| 3 | 75.56 | 18.20 | -17.27 | 5.74 | 161.60 | 75.60 | 18.33 | -17.20 | 6.32 | 159.82 |
| 4 | 76.46 | 35.04 | -7.44 | 34.24 | 102.26 | 77.07 | 34.03 | -6.92 | 33.32 | 101.74 |
| 5 | 59.52 | 25.98 | 18.81 | 17.92 | 43.62 | 61.70 | 26.13 | 19.29 | 17.63 | 42.43 |
| 6 | 69.35 | 15.95 | 15.85 | 1.80 | 6.47 | 70.14 | 17.86 | 17.66 | 2.65 | 8.52 |
| 7 | 65.40 | 30.97 | 25.13 | -18.10 | 324.23 | 64.71 | 30.50 | 25.03 | -17.43 | 325.14 |
| 8 | 62.99 | 21.77 | -0.35 | -21.77 | 269.08 | 63.39 | 21.39 | -0.46 | -21.39 | 268.77 |
| 9 | 33.59 | 24.32 | -21.20 | -11.92 | 209.36 | 32.82 | 24.35 | -21.28 | -11.83 | 209.07 |
| 10 | 21.66 | 15.00 | 14.96 | 1.09 | 4.17 | 21.93 | 15.14 | 15.12 | 0.86 | 3.25 |
| 11 | 23.76 | 25.24 | 18.50 | -17.17 | 317.12 | 23.70 | 25.60 | 18.51 | -17.69 | 316.30 |
| 12 | 38.91 | 36.03 | 35.69 | 4.93 | 7.87 | 39.74 | 35.74 | 35.43 | 4.71 | 7.58 |
| 13 | 38.91 | 36.03 | 35.69 | 4.93 | 7.87 | 39.87 | 35.69 | 35.32 | 5.12 | 8.24 |
| 14 | 37.14 | 33.87 | 25.37 | 22.43 | 41.48 | 37.71 | 33.83 | 25.24 | 22.53 | 41.76 |
| 15 | 37.14 | 33.87 | 25.37 | 22.43 | 41.48 | 37.22 | 34.90 | 26.64 | 22.54 | 40.23 |
| 16 | 38.22 | 27.99 | 2.69 | 27.86 | 84.48 | 38.29 | 28.03 | 2.92 | 27.88 | 84.02 |
| 17 | 38.22 | 27.99 | 2.69 | 27.86 | 84.48 | 38.30 | 27.53 | 1.57 | 27.49 | 86.74 |
| 18 | 24.80 | 16.60 | -16.46 | 2.18 | 172.44 | 23.34 | 15.39 | -15.27 | 1.93 | 172.81 |
| 19 | 36.92 | 24.01 | -12.77 | 20.33 | 122.12 | 36.58 | 23.25 | -11.71 | 20.09 | 120.23 |
| 20 | 42.05 | 35.68 | -3.98 | -35.46 | 263.60 | 41.39 | 35.38 | -4.10 | -35.14 | 263.35 |
| 21 | 42.05 | 35.68 | -3.98 | -35.46 | 263.60 | 42.23 | 34.69 | -4.84 | -34.35 | 261.98 |
| 22 | 45.89 | 40.26 | 22.34 | -33.49 | 303.71 | 45.41 | 40.53 | 21.94 | -34.08 | 302.77 |
| 23 | 65.46 | 22.88 | -22.88 | 0.30 | 179.24 | 63.98 | 23.48 | -23.47 | 0.56 | 178.63 |
| 24 | 60.66 | 36.02 | -16.55 | 31.99 | 117.36 | 58.87 | 36.34 | -16.77 | 32.24 | 117.49 |
| 25 | 61.47 | 30.35 | -0.49 | 30.35 | 90.93 | 62.75 | 28.81 | -1.17 | 28.79 | 92.33 |
| 26 | 53.78 | 30.03 | 21.35 | 21.12 | 44.70 | 55.80 | 29.33 | 20.79 | 20.69 | 44.86 |
| 27 | 53.78 | 30.03 | 21.35 | 21.12 | 44.70 | 53.82 | 29.85 | 21.65 | 20.55 | 43.52 |
| 28 | 54.95 | 38.83 | 35.69 | -15.29 | 336.81 | 56.05 | 37.36 | 34.78 | -13.63 | 338.60 |
| 29 | 36.97 | 29.31 | -18.31 | -22.89 | 231.34 | 37.82 | 29.20 | -18.58 | -22.53 | 230.49 |
| 30 | 39.31 | 45.38 | 26.09 | -37.13 | 305.09 | 40.00 | 44.61 | 25.27 | -36.76 | 304.50 |
| 31 | 33.93 | 35.51 | -1.41 | -35.48 | 267.73 | 33.02 | 35.59 | -0.99 | -35.58 | 268.41 |
| 32 | 50.27 | 29.48 | 29.43 | 1.63 | 3.17 | 47.25 | 29.69 | 29.62 | 2.06 | 3.97 |
| 33 | 50.16 | 31.70 | -1.48 | 31.67 | 92.68 | 47.48 | 30.71 | -1.04 | 30.69 | 91.94 |
| 34 | 50.05 | 31.32 | -20.48 | 23.70 | 130.83 | 47.29 | 30.95 | -20.80 | 22.92 | 132.22 |
| 35 | 56.72 | 29.49 | -27.31 | 11.12 | 157.85 | 56.44 | 29.69 | -27.69 | 10.70 | 158.87 |
| 36 | 56.90 | 26.12 | -25.97 | 2.84 | 173.76 | 57.10 | 26.20 | -26.12 | 2.06 | 175.50 |
| 37 | 37.75 | 27.64 | -18.09 | 20.90 | 130.87 | 38.01 | 26.61 | -17.85 | 19.74 | 132.12 |
| 38 | 56.09 | 32.20 | 0.98 | 32.19 | 88.26 | 55.71 | 32.15 | 0.76 | 32.14 | 88.65 |
| 39 | 56.09 | 32.20 | 0.98 | 32.19 | 88.26 | 58.28 | 31.80 | 0.35 | 31.80 | 89.37 |
| 40 | 47.95 | 31.26 | 22.67 | 21.53 | 43.52 | 46.34 | 30.93 | 22.36 | 21.37 | 43.71 |
| 41 | 55.05 | 29.99 | 29.94 | 1.65 | 3.15 | 55.34 | 29.71 | 29.59 | 2.64 | 5.09 |
| 42 | 58.69 | 31.88 | 28.16 | -14.95 | 332.04 | 58.77 | 33.85 | 30.33 | -15.03 | 333.64 |
| 43 | 58.69 | 31.88 | 28.16 | -14.95 | 332.04 | 58.56 | 32.31 | 28.70 | -14.85 | 332.64 |
| 44 | 57.78 | 15.31 | 7.46 | -13.37 | 299.14 | 57.60 | 15.46 | 7.37 | -13.59 | 298.49 |
| 45 | 49.74 | 24.08 | -21.13 | -11.55 | 208.65 | 47.93 | 25.32 | -22.64 | -11.33 | 206.58 |
| 46 | 44.37 | 26.13 | -22.92 | -12.54 | 208.67 | 45.25 | 24.89 | -21.78 | -12.05 | 208.96 |
| 47 | 44.37 | 26.13 | -22.92 | -12.54 | 208.67 | 43.54 | 26.13 | -21.55 | -14.77 | 214.42 |
| 48 | 56.62 | 35.21 | -29.81 | 18.73 | 147.86 | 54.98 | 34 | -29.14 | 17.52 | 148.98 |

| | | | | | | | | | | |
|---|---|---|---|---|---|---|---|---|---|---|
| 49 | 56.62 | 35.21 | -29.81 | 18.73 | 147.86 | 55.86 | 35.18 | -29.72 | 18.83 | 147.65 |

**Appendix F1 Colorimetric co-ordinates of data set 2**

| Pair . No | L*std | astd* | b*std | C*std | h°std | L*bx | a*bx | b*bx | C*bx | h°bx |
|---|---|---|---|---|---|---|---|---|---|---|
| 1.00 | 73.00 | 8.14 | 2.87 | 8.63 | 19.42 | 74.36 | 8.95 | 4.08 | 9.83 | 24.49 |
| 2.00 | 74.11 | 15.23 | 14.55 | 21.07 | 43.69 | 74.05 | 17.90 | 16.48 | 24.33 | 42.63 |
| 3.00 | 70.27 | 8.18 | 17.54 | 19.36 | 64.99 | 70.41 | 7.79 | 18.00 | 19.62 | 66.59 |
| 4.00 | 76.97 | 2.72 | 9.73 | 10.10 | 74.36 | 76.44 | 2.90 | 9.00 | 9.45 | 72.12 |
| 5.00 | 71.70 | 1.81 | 8.69 | 8.88 | 78.23 | 71.46 | 2.39 | 8.39 | 8.72 | 74.10 |
| 6.00 | 75.34 | 2.71 | 13.23 | 13.50 | 78.43 | 75.58 | 2.76 | 14.18 | 14.44 | 78.96 |
| 7.00 | 71.73 | 2.28 | 14.04 | 14.23 | 80.76 | 71.42 | 2.73 | 14.42 | 14.68 | 79.28 |
| 8.00 | 71.30 | 1.71 | 13.13 | 13.24 | 82.59 | 71.78 | 2.32 | 10.72 | 10.97 | 77.81 |
| 9.00 | 75.81 | 3.80 | 61.32 | 61.44 | 86.45 | 78.73 | 3.28 | 57.34 | 57.43 | 86.73 |
| 10.00 | 78.13 | 3.51 | 57.39 | 57.50 | 86.50 | 80.14 | -3.44 | 54.84 | 54.95 | 93.59 |
| 11.00 | 78.31 | 0.55 | 11.86 | 11.87 | 87.33 | 74.40 | -0.95 | 7.28 | 7.34 | 97.43 |
| 12.00 | 77.38 | 0.87 | 25.20 | 25.22 | 88.03 | 78.84 | 0.49 | 23.72 | 23.73 | 88.82 |
| 13.00 | 69.43 | 1.52 | 49.45 | 49.47 | 88.24 | 71.09 | 1.18 | 47.84 | 47.85 | 88.58 |
| 14.00 | 71.06 | 0.51 | 26.45 | 26.45 | 88.90 | 72.27 | -0.09 | 23.95 | 23.95 | 90.21 |
| 15.00 | 71.97 | -4.35 | 23.95 | 24.34 | 100.30 | 72.04 | -4.84 | 22.12 | 22.64 | 102.35 |
| 16.00 | 74.62 | -6.47 | 21.23 | 22.20 | 106.95 | 74.70 | -6.73 | 23.84 | 24.77 | 105.77 |
| 17.00 | 78.79 | -5.13 | 9.15 | 10.49 | 119.27 | 77.79 | -5.39 | 8.46 | 10.03 | 122.53 |
| 18.00 | 74.04 | -36.05 | 47.06 | 59.28 | 127.46 | 70.96 | -37.07 | 41.63 | 55.74 | 131.69 |
| 19.00 | 78.57 | -16.71 | 16.64 | 23.58 | 135.12 | 77.57 | -14.96 | 15.39 | 21.46 | 134.18 |
| 20.00 | 81.29 | -19.50 | 0.77 | 19.51 | 177.75 | 80.93 | -18.96 | 2.08 | 19.07 | 173.74 |
| 21.00 | 79.88 | -22.38 | -1.21 | 22.41 | 183.10 | 78.85 | -21.06 | -0.81 | 21.08 | 182.20 |
| 22.00 | 75.20 | -10.07 | -8.25 | 13.02 | 219.32 | 75.88 | -10.01 | -8.49 | 13.13 | 220.32 |
| 23.00 | 73.29 | -18.11 | -17.35 | 25.08 | 223.76 | 72.52 | -18.01 | -17.54 | 25.14 | 224.25 |
| 24.00 | 70.83 | -5.57 | -15.19 | 16.18 | 249.85 | 70.47 | -5.59 | -15.36 | 16.34 | 250.01 |
| 25.00 | 73.14 | -4.80 | -17.14 | 17.80 | 254.36 | 72.89 | -4.77 | -17.08 | 17.73 | 254.40 |
| 26.00 | 74.43 | -1.78 | -15.07 | 15.18 | 263.25 | 74.27 | -1.13 | -15.66 | 15.70 | 265.87 |
| 27.00 | 77.54 | 5.72 | -14.45 | 15.54 | 291.59 | 79.30 | 5.64 | -13.60 | 14.72 | 292.52 |
| 28.00 | 76.98 | 6.33 | -14.85 | 16.14 | 293.10 | 77.82 | 7.03 | -13.72 | 15.42 | 297.14 |
| 29.00 | 74.50 | 12.47 | -9.37 | 15.60 | 323.07 | 75.68 | 11.05 | -8.98 | 14.24 | 320.92 |
| 30.00 | 71.83 | 22.14 | -11.33 | 24.87 | 332.90 | 72.68 | 21.99 | -11.03 | 24.60 | 333.37 |
| 31.00 | 73.21 | 30.03 | -8.60 | 31.24 | 344.03 | 74.16 | 29.18 | -8.48 | 30.39 | 343.79 |
| 32.00 | 74.17 | 26.46 | -0.66 | 26.47 | 358.56 | 74.69 | 27.00 | 0.56 | 27.00 | 1.19 |
| 33.00 | 64.07 | 6.33 | 2.48 | 6.80 | 21.43 | 63.24 | 5.78 | 1.66 | 6.01 | 15.98 |
| 34.00 | 69.96 | 32.46 | 33.04 | 46.32 | 45.51 | 68.92 | 33.78 | 34.25 | 48.10 | 45.40 |
| 35.00 | 68.23 | 35.22 | 37.55 | 51.48 | 46.83 | 67.47 | 36.12 | 37.18 | 51.84 | 45.83 |
| 36.00 | 62.48 | 42.73 | 49.93 | 65.72 | 49.45 | 61.81 | 43.79 | 49.51 | 66.10 | 48.51 |
| 37.00 | 64.53 | 18.88 | 37.15 | 41.67 | 63.07 | 57.47 | 16.94 | 29.11 | 33.68 | 59.80 |
| 38.00 | 68.38 | 5.08 | 15.36 | 16.18 | 71.70 | 68.15 | 4.77 | 15.66 | 16.37 | 73.06 |
| 39.00 | 64.38 | 4.25 | 14.12 | 14.75 | 73.25 | 63.64 | 4.62 | 12.96 | 13.76 | 70.40 |
| 40.00 | 64.65 | 3.19 | 11.14 | 11.59 | 74.01 | 64.57 | 2.65 | 11.13 | 11.44 | 76.61 |
| 41.00 | 64.51 | 5.67 | 28.56 | 29.12 | 78.78 | 63.49 | 6.06 | 29.02 | 29.65 | 78.20 |
| 42.00 | 64.89 | 2.24 | 12.36 | 12.56 | 79.74 | 64.03 | 1.80 | 13.63 | 13.75 | 82.50 |
| 43.00 | 66.41 | 2.48 | 14.38 | 14.59 | 80.21 | 65.87 | 2.48 | 14.35 | 14.56 | 80.21 |
| 44.00 | 64.21 | 0.42 | 13.34 | 13.35 | 88.19 | 63.74 | 0.38 | 12.43 | 12.43 | 88.27 |
| 45.00 | 64.56 | 0.19 | 12.46 | 12.46 | 89.14 | 64.21 | 0.32 | 13.17 | 13.17 | 88.59 |
| 46.00 | 62.00 | -5.22 | 2.98 | 6.01 | 150.30 | 61.31 | -5.73 | 2.22 | 6.15 | 158.86 |
| 47.00 | 61.99 | -5.44 | 2.50 | 5.98 | 155.31 | 63.37 | -4.97 | 2.45 | 5.54 | 153.78 |
| 48.00 | 61.34 | -5.52 | 2.12 | 5.91 | 158.96 | 61.90 | -5.19 | 2.62 | 5.81 | 153.19 |

| | | | | | | | | | | |
|---|---|---|---|---|---|---|---|---|---|---|
| 49.00 | 63.92 | -27.96 | -24.39 | 37.11 | 221.10 | 64.72 | -29.60 | -23.79 | 37.97 | 218.79 |
| 50.00 | 62.62 | -21.19 | -29.56 | 36.37 | 234.36 | 62.85 | -22.16 | -29.65 | 37.01 | 233.22 |
| 51.00 | 60.39 | -4.58 | -17.10 | 17.71 | 255.01 | 60.46 | -4.43 | -17.70 | 18.24 | 255.94 |
| 52.00 | 66.89 | 3.30 | -13.90 | 14.29 | 283.36 | 66.48 | 4.06 | -14.38 | 14.95 | 285.77 |
| 53.00 | 69.49 | 5.29 | -21.19 | 21.84 | 284.03 | 69.05 | 4.74 | -19.90 | 20.46 | 283.40 |
| 54.00 | 69.49 | 5.37 | -21.19 | 21.85 | 284.21 | 69.01 | 4.80 | -19.89 | 20.46 | 283.58 |
| 55.00 | 57.64 | 53.23 | 7.48 | 53.76 | 8.00 | 56.26 | 52.56 | 6.62 | 52.97 | 7.18 |
| 56.00 | 56.72 | 28.23 | 4.10 | 28.53 | 8.27 | 55.23 | 29.01 | 2.82 | 29.14 | 5.55 |
| 57.00 | 53.60 | 39.63 | 6.99 | 40.24 | 10.00 | 54.23 | 38.89 | 6.73 | 39.47 | 9.81 |
| 58.00 | 59.61 | 10.94 | 3.31 | 11.43 | 16.84 | 59.65 | 11.34 | 3.48 | 11.86 | 17.07 |
| 59.00 | 59.99 | 31.75 | 36.06 | 48.05 | 48.64 | 59.76 | 32.03 | 38.61 | 50.17 | 50.32 |
| 60.00 | 57.92 | 26.00 | 38.34 | 46.33 | 55.86 | 61.58 | 31.46 | 43.66 | 53.81 | 54.23 |
| 61.00 | 52.65 | 5.50 | 9.29 | 10.80 | 59.35 | 52.29 | 4.69 | 8.64 | 9.83 | 61.51 |
| 62.00 | 53.89 | 3.95 | 8.67 | 9.52 | 65.52 | 52.24 | 2.99 | 7.56 | 8.13 | 68.45 |
| 63.00 | 53.66 | 13.80 | 31.80 | 34.66 | 66.53 | 52.11 | 13.52 | 30.31 | 33.18 | 65.96 |
| 64.00 | 55.62 | 5.94 | 15.47 | 16.57 | 68.98 | 55.18 | 6.23 | 14.86 | 16.11 | 67.26 |
| 65.00 | 54.88 | 7.17 | 20.87 | 22.06 | 71.04 | 55.84 | 7.43 | 20.22 | 21.55 | 69.82 |
| 66.00 | 51.44 | 0.26 | 10.97 | 10.97 | 88.63 | 50.12 | -0.24 | 10.70 | 10.70 | 91.29 |
| 67.00 | 53.69 | -0.20 | 18.97 | 18.97 | 90.60 | 52.45 | 0.10 | 19.45 | 19.45 | 89.71 |
| 68.00 | 51.72 | -2.82 | 8.73 | 9.17 | 107.88 | 51.48 | -2.07 | 8.45 | 8.70 | 103.77 |
| 69.00 | 56.75 | -17.66 | 34.08 | 38.38 | 117.39 | 55.70 | -17.17 | 35.37 | 39.31 | 115.89 |
| 70.00 | 58.12 | -14.13 | 13.83 | 19.77 | 135.63 | 57.27 | -11.24 | 12.13 | 16.54 | 132.81 |
| 71.00 | 57.25 | -18.32 | 7.87 | 19.94 | 156.74 | 56.28 | -18.59 | 8.12 | 20.28 | 156.40 |
| 72.00 | 58.33 | -25.88 | -0.51 | 25.89 | 181.13 | 56.07 | -25.55 | -0.29 | 25.55 | 180.64 |
| 73.00 | 56.61 | -25.34 | -8.68 | 26.79 | 198.90 | 56.37 | -25.72 | -7.21 | 26.71 | 195.65 |
| 74.00 | 53.48 | -20.43 | -8.26 | 22.04 | 202.02 | 51.25 | -20.58 | -8.65 | 22.33 | 202.81 |
| 75.00 | 54.60 | -13.75 | -13.87 | 19.53 | 225.26 | 55.78 | -16.88 | -17.85 | 24.57 | 226.61 |
| 76.00 | 56.39 | -21.38 | -32.88 | 39.22 | 236.96 | 55.82 | -23.18 | -30.00 | 37.91 | 232.30 |
| 77.00 | 52.62 | 18.58 | -2.42 | 18.74 | 352.59 | 52.13 | 17.88 | -1.78 | 17.97 | 354.30 |
| 78.00 | 51.97 | 18.12 | -1.53 | 18.19 | 355.16 | 53.30 | 18.61 | -2.28 | 18.75 | 353.03 |
| 79.00 | 52.73 | 53.49 | -4.46 | 53.67 | 355.23 | 50.74 | 55.25 | -3.67 | 55.37 | 356.20 |
| 80.00 | 48.73 | 22.33 | 1.56 | 22.39 | 4.00 | 48.91 | 23.24 | 0.53 | 23.25 | 1.29 |
| 81.00 | 41.18 | 55.76 | 13.68 | 57.42 | 13.79 | 40.18 | 53.19 | 11.95 | 54.51 | 12.66 |
| 82.00 | 47.08 | 49.79 | 17.54 | 52.79 | 19.40 | 48.16 | 49.21 | 16.30 | 51.84 | 18.32 |
| 83.00 | 49.63 | 51.57 | 44.31 | 68.00 | 40.67 | 50.05 | 50.83 | 44.62 | 67.63 | 41.28 |
| 84.00 | 44.28 | 4.04 | 4.61 | 6.13 | 48.76 | 44.55 | 4.39 | 4.25 | 6.11 | 44.09 |
| 85.00 | 48.82 | 6.00 | 7.65 | 9.72 | 51.91 | 48.60 | 6.24 | 5.96 | 8.63 | 43.70 |
| 86.00 | 50.49 | 4.43 | 8.20 | 9.32 | 61.64 | 51.52 | 4.08 | 7.65 | 8.67 | 61.96 |
| 87.00 | 45.53 | 5.51 | 11.84 | 13.06 | 65.04 | 43.79 | 6.19 | 11.78 | 13.31 | 62.29 |
| 88.00 | 50.57 | 6.21 | 16.22 | 17.36 | 69.06 | 51.36 | 6.37 | 16.25 | 17.45 | 68.58 |
| 89.00 | 45.50 | 6.22 | 16.45 | 17.59 | 69.27 | 48.17 | 6.69 | 17.94 | 19.14 | 69.53 |
| 90.00 | 45.85 | -9.21 | 2.23 | 9.48 | 166.41 | 46.34 | -8.83 | 2.00 | 9.05 | 167.26 |
| 91.00 | 44.88 | -36.09 | 3.91 | 36.30 | 173.82 | 43.56 | -35.93 | 4.91 | 36.26 | 172.22 |
| 92.00 | 47.16 | -10.31 | -2.15 | 10.53 | 191.75 | 46.64 | -10.46 | -2.97 | 10.87 | 195.85 |
| 93.00 | 47.53 | -1.93 | -1.53 | 2.47 | 218.39 | 46.90 | -1.59 | -2.19 | 2.71 | 233.92 |
| 94.00 | 41.12 | -2.68 | -5.22 | 5.87 | 242.86 | 39.35 | -2.66 | -5.54 | 6.15 | 244.32 |
| 95.00 | 50.23 | -4.53 | -35.14 | 35.43 | 262.65 | 47.95 | -4.39 | -36.40 | 36.66 | 263.13 |
| 96.00 | 41.69 | 11.12 | -9.99 | 14.95 | 318.07 | 42.43 | 10.68 | -10.10 | 14.71 | 316.60 |
| 97.00 | 35.35 | 24.74 | 0.32 | 24.74 | 0.75 | 34.12 | 22.92 | -3.00 | 23.12 | 352.53 |
| 98.00 | 33.64 | 51.22 | 7.03 | 51.70 | 7.82 | 32.05 | 48.74 | 6.90 | 49.22 | 8.06 |
| 99.00 | 33.02 | 50.35 | 7.90 | 50.96 | 8.92 | 32.03 | 48.61 | 6.96 | 49.11 | 8.15 |

| | | | | | | | | | | |
|---|---|---|---|---|---|---|---|---|---|---|
| 100.00 | 36.27 | 37.48 | 11.14 | 39.10 | 16.55 | 36.63 | 37.36 | 8.30 | 38.28 | 12.53 |
| 101.00 | 34.81 | 55.18 | 21.91 | 59.37 | 21.65 | 34.45 | 54.25 | 23.77 | 59.23 | 23.66 |
| 102.00 | 38.32 | 53.25 | 28.94 | 60.61 | 28.53 | 38.03 | 53.85 | 29.04 | 61.18 | 28.34 |
| 103.00 | 34.42 | 7.77 | 14.58 | 16.52 | 61.93 | 33.57 | 6.70 | 11.46 | 13.27 | 59.68 |
| 104.00 | 39.13 | 2.82 | 6.48 | 7.07 | 66.46 | 38.98 | 2.45 | 6.46 | 6.91 | 69.25 |
| 105.00 | 35.44 | 5.66 | 13.82 | 14.93 | 67.73 | 35.51 | 6.29 | 13.20 | 14.63 | 64.52 |
| 106.00 | 38.13 | -5.35 | 16.53 | 17.38 | 107.92 | 39.36 | -5.36 | 16.77 | 17.61 | 107.74 |
| 107.00 | 36.10 | -3.58 | -12.46 | 12.96 | 253.98 | 33.84 | -3.05 | -13.85 | 14.18 | 257.57 |
| 108.00 | 31.42 | -3.06 | -12.82 | 13.18 | 256.59 | 31.29 | -2.33 | -14.54 | 14.73 | 260.90 |
| 109.00 | 33.94 | -0.49 | -28.62 | 28.62 | 269.02 | 35.45 | -0.84 | -29.52 | 29.54 | 268.37 |
| 110.00 | 30.71 | 2.35 | -21.85 | 21.97 | 276.14 | 33.23 | 1.11 | -18.42 | 18.45 | 273.45 |
| 111.00 | 33.19 | 8.65 | -29.80 | 31.03 | 286.19 | 33.16 | 7.98 | -30.03 | 31.07 | 284.89 |
| 112.00 | 28.02 | 32.01 | 11.22 | 33.92 | 19.32 | 28.34 | 33.67 | 12.30 | 35.85 | 20.07 |
| 113.00 | 29.25 | 2.75 | 1.05 | 2.94 | 21.00 | 29.16 | 2.78 | 2.29 | 3.61 | 39.51 |
| 114.00 | 29.41 | 40.38 | 16.69 | 43.70 | 22.46 | 29.97 | 42.02 | 18.75 | 46.02 | 24.04 |
| 115.00 | 29.35 | 27.88 | 18.15 | 33.27 | 33.05 | 31.65 | 28.63 | 20.40 | 35.15 | 35.46 |
| 116.00 | 29.33 | -3.19 | -17.11 | 17.40 | 259.42 | 29.93 | -3.20 | -17.16 | 17.45 | 259.43 |
| 117.00 | 29.72 | 4.03 | -27.26 | 27.55 | 278.40 | 30.11 | 3.32 | -27.72 | 27.92 | 276.83 |

**Appendix F2 Reflectance values of data set 2**

| REF. | PAIR NUMBERS | | | | | | | | | | | | |
|---|---|---|---|---|---|---|---|---|---|---|---|---|---|
| nm | 1 | 2 | 3 | 4 | 5 | 6 | 7 | 8 | 9 | 10 | 11 | 12 | 13 |
| 400 | 44.26 | 33.11 | 26.50 | 42.76 | 36.48 | 37.24 | 31.21 | 35.03 | 13.96 | 15.51 | 40.83 | 33.89 | 12.74 |
| 410 | 44.28 | 33.53 | 25.70 | 42.34 | 36.10 | 36.59 | 30.64 | 34.51 | 12.52 | 13.71 | 40.59 | 33.46 | 11.39 |
| 420 | 43.88 | 33.37 | 25.47 | 41.71 | 35.48 | 35.87 | 30.01 | 33.84 | 11.64 | 12.60 | 40.12 | 32.89 | 10.52 |
| 430 | 43.50 | 33.27 | 25.79 | 41.30 | 35.03 | 35.47 | 29.79 | 33.45 | 11.38 | 12.36 | 39.78 | 32.71 | 10.30 |
| 440 | 43.15 | 33.23 | 26.34 | 41.16 | 34.86 | 35.39 | 29.86 | 33.35 | 11.60 | 12.72 | 39.68 | 32.77 | 10.56 |
| 450 | 43.22 | 33.28 | 27.33 | 41.44 | 35.11 | 35.75 | 30.43 | 33.67 | 12.48 | 13.89 | 39.98 | 33.21 | 11.39 |
| 460 | 43.63 | 33.36 | 28.58 | 42.42 | 35.97 | 36.96 | 31.73 | 34.65 | 14.35 | 16.36 | 40.91 | 33.88 | 13.03 |
| 470 | 44.12 | 33.43 | 29.87 | 43.61 | 37.06 | 38.39 | 33.17 | 35.84 | 16.91 | 19.88 | 42.06 | 34.81 | 15.32 |
| 480 | 44.32 | 33.54 | 31.24 | 44.81 | 38.17 | 40.02 | 34.74 | 37.14 | 20.58 | 25.04 | 43.25 | 36.17 | 18.61 |
| 490 | 44.36 | 33.72 | 32.45 | 45.91 | 39.13 | 41.62 | 36.27 | 38.33 | 24.39 | 30.30 | 44.39 | 37.78 | 21.79 |
| 500 | 44.36 | 34.14 | 33.88 | 47.26 | 40.34 | 43.64 | 38.17 | 39.81 | 29.27 | 36.38 | 45.80 | 40.23 | 25.24 |
| 510 | 44.13 | 34.56 | 35.29 | 48.40 | 41.36 | 45.64 | 39.67 | 41.17 | 35.24 | 43.01 | 47.03 | 43.47 | 28.91 |
| 520 | 43.77 | 35.89 | 36.52 | 49.08 | 41.85 | 47.18 | 40.82 | 42.10 | 42.43 | 50.22 | 47.85 | 47.82 | 33.29 |
| 530 | 43.38 | 37.55 | 37.67 | 49.37 | 42.07 | 48.11 | 41.87 | 42.55 | 50.03 | 57.11 | 48.05 | 52.64 | 38.37 |
| 540 | 43.44 | 38.77 | 39.01 | 49.65 | 42.20 | 48.86 | 42.30 | 42.91 | 57.42 | 62.98 | 48.06 | 57.55 | 44.01 |
| 550 | 43.67 | 40.20 | 40.15 | 49.84 | 42.25 | 49.27 | 42.04 | 43.06 | 63.12 | 66.70 | 48.02 | 61.22 | 49.00 |
| 560 | 44.17 | 43.63 | 41.10 | 50.02 | 42.25 | 49.55 | 42.03 | 43.17 | 67.46 | 68.82 | 47.56 | 63.62 | 53.00 |
| 570 | 45.03 | 50.41 | 42.34 | 50.30 | 42.36 | 49.89 | 43.67 | 43.32 | 69.15 | 68.63 | 47.17 | 63.80 | 54.32 |
| 580 | 47.90 | 58.43 | 44.88 | 51.78 | 43.55 | 51.40 | 46.18 | 44.49 | 69.07 | 67.80 | 47.34 | 62.88 | 53.77 |
| 590 | 52.24 | 64.58 | 48.39 | 54.05 | 45.45 | 53.63 | 48.06 | 46.38 | 68.59 | 66.45 | 48.02 | 61.43 | 52.38 |
| 600 | 56.02 | 67.41 | 51.26 | 55.82 | 46.91 | 55.35 | 48.77 | 47.81 | 67.81 | 65.32 | 48.48 | 60.10 | 50.98 |
| 610 | 58.00 | 67.92 | 52.64 | 56.41 | 47.30 | 55.94 | 48.75 | 48.22 | 66.93 | 64.29 | 48.50 | 58.86 | 49.67 |
| 620 | 58.71 | 67.64 | 53.01 | 56.42 | 47.21 | 55.98 | 48.17 | 48.18 | 65.75 | 62.98 | 48.11 | 57.46 | 48.18 |
| 630 | 59.26 | 66.93 | 53.40 | 56.62 | 47.35 | 56.18 | 48.29 | 48.32 | 64.65 | 61.78 | 48.22 | 56.23 | 46.81 |
| 640 | 60.58 | 66.49 | 54.83 | 57.86 | 48.68 | 57.39 | 49.06 | 49.74 | 63.82 | 60.92 | 49.38 | 55.62 | 45.97 |
| 650 | 63.53 | 66.82 | 58.05 | 60.95 | 51.95 | 60.46 | 52.15 | 53.02 | 64.20 | 61.31 | 52.50 | 56.13 | 46.37 |
| 660 | 67.52 | 67.45 | 62.44 | 65.20 | 56.75 | 64.71 | 56.98 | 57.69 | 65.97 | 63.11 | 57.05 | 57.78 | 48.15 |

| | | | | | | | | | | | | | |
|---|---|---|---|---|---|---|---|---|---|---|---|---|---|
| 670 | 72.03 | 68.53 | 67.55 | 70.14 | 62.66 | 69.65 | 63.17 | 63.26 | 69.18 | 66.46 | 62.63 | 60.81 | 51.51 |
| 680 | 76.08 | 70.99 | 72.25 | 74.66 | 68.28 | 74.17 | 69.22 | 68.57 | 73.22 | 70.73 | 68.10 | 65.14 | 56.26 |
| 690 | 78.87 | 74.38 | 75.45 | 77.78 | 72.32 | 77.26 | 73.68 | 72.39 | 76.84 | 74.68 | 72.20 | 69.87 | 61.53 |
| 700 | 81.24 | 79.12 | 78.31 | 80.52 | 76.13 | 79.96 | 77.84 | 75.96 | 81.04 | 79.48 | 76.13 | 76.29 | 69.36 |

| Ref | Pair numbers | | | | | | | | | | | | |
|---|---|---|---|---|---|---|---|---|---|---|---|---|---|
| nm | 14 | 15 | 16 | 17 | 18 | 19 | 20 | 21 | 22 | 23 | 24 | 25 | 26 |
| 400 | 26.40 | 27.29 | 28.49 | 44.67 | 12.29 | 37.23 | 37.23 | 47.57 | 56.52 | 49.12 | 53.19 | 58.42 | 61.36 |
| 410 | 25.51 | 26.46 | 27.70 | 44.29 | 10.55 | 35.53 | 35.53 | 49.21 | 57.49 | 54.19 | 55.60 | 61.49 | 63.70 |
| 420 | 24.69 | 25.62 | 26.95 | 43.68 | 9.49 | 34.17 | 34.17 | 49.68 | 57.81 | 57.26 | 56.70 | 63.29 | 64.83 |
| 430 | 24.29 | 25.22 | 26.59 | 43.39 | 9.32 | 33.87 | 33.87 | 50.24 | 57.85 | 59.68 | 57.21 | 63.93 | 65.27 |
| 440 | 24.30 | 25.19 | 26.66 | 43.28 | 9.79 | 34.30 | 34.30 | 51.51 | 57.72 | 61.94 | 56.91 | 63.83 | 64.98 |
| 450 | 24.77 | 25.63 | 27.24 | 43.63 | 11.04 | 35.74 | 35.74 | 53.40 | 57.83 | 62.89 | 56.41 | 63.04 | 64.23 |
| 460 | 26.07 | 26.91 | 28.76 | 44.83 | 13.90 | 38.72 | 38.72 | 56.49 | 58.32 | 63.39 | 55.73 | 61.93 | 63.03 |
| 470 | 27.69 | 28.52 | 30.69 | 46.28 | 18.97 | 42.75 | 42.75 | 60.41 | 58.76 | 63.54 | 54.79 | 60.46 | 61.32 |
| 480 | 29.79 | 30.65 | 33.19 | 47.97 | 28.13 | 48.07 | 48.07 | 64.53 | 58.93 | 62.89 | 53.38 | 58.49 | 58.87 |
| 490 | 32.03 | 32.96 | 35.92 | 49.64 | 39.08 | 52.58 | 52.58 | 67.14 | 58.98 | 61.98 | 51.95 | 56.62 | 56.80 |
| 500 | 35.09 | 36.21 | 39.73 | 51.84 | 51.23 | 56.08 | 56.08 | 67.75 | 58.93 | 60.56 | 50.48 | 54.70 | 54.75 |
| 510 | 38.65 | 40.06 | 44.30 | 53.94 | 58.97 | 58.01 | 58.01 | 66.89 | 58.36 | 58.38 | 48.73 | 52.54 | 52.31 |
| 520 | 41.99 | 43.85 | 48.72 | 55.61 | 59.86 | 59.05 | 59.05 | 65.71 | 57.26 | 56.07 | 46.95 | 50.55 | 50.38 |
| 530 | 44.59 | 46.73 | 52.00 | 56.26 | 57.47 | 58.98 | 58.98 | 64.14 | 55.34 | 53.12 | 44.89 | 48.29 | 48.70 |
| 540 | 46.33 | 48.33 | 53.64 | 56.19 | 53.44 | 58.23 | 58.23 | 61.60 | 53.05 | 49.54 | 42.83 | 46.15 | 47.18 |
| 550 | 47.09 | 48.66 | 53.74 | 55.68 | 49.11 | 56.78 | 56.78 | 58.41 | 50.93 | 45.72 | 41.11 | 44.41 | 45.70 |
| 560 | 47.33 | 48.22 | 53.26 | 54.61 | 44.42 | 55.02 | 55.02 | 54.88 | 48.49 | 41.59 | 39.15 | 42.42 | 44.27 |
| 570 | 47.33 | 46.90 | 51.51 | 53.07 | 40.36 | 52.88 | 52.88 | 52.03 | 45.68 | 37.99 | 36.91 | 40.17 | 43.12 |
| 580 | 47.55 | 45.58 | 49.53 | 51.71 | 36.79 | 50.49 | 50.49 | 49.01 | 43.07 | 34.77 | 34.88 | 38.15 | 42.19 |
| 590 | 48.32 | 44.74 | 48.12 | 50.92 | 33.10 | 48.23 | 48.23 | 44.84 | 41.10 | 31.50 | 33.54 | 36.77 | 41.48 |
| 600 | 48.81 | 44.23 | 47.34 | 50.48 | 29.12 | 46.44 | 46.44 | 38.92 | 39.81 | 27.73 | 32.75 | 35.93 | 40.97 |
| 610 | 48.84 | 43.71 | 46.68 | 50.00 | 27.03 | 44.93 | 44.93 | 35.84 | 38.80 | 25.57 | 32.06 | 35.20 | 40.38 |
| 620 | 48.54 | 43.04 | 45.77 | 49.32 | 26.25 | 43.37 | 43.37 | 35.16 | 37.69 | 24.74 | 31.40 | 34.43 | 39.58 |
| 630 | 48.60 | 43.11 | 45.85 | 49.41 | 25.44 | 42.01 | 42.01 | 34.91 | 37.14 | 24.12 | 31.46 | 34.59 | 39.68 |
| 640 | 49.86 | 44.38 | 46.64 | 50.64 | 24.61 | 41.31 | 41.31 | 34.13 | 37.25 | 23.46 | 32.73 | 35.36 | 40.47 |
| 650 | 53.08 | 47.68 | 49.75 | 53.86 | 22.82 | 41.82 | 41.82 | 31.63 | 38.73 | 22.32 | 35.85 | 38.06 | 43.58 |
| 660 | 57.74 | 52.53 | 54.67 | 58.48 | 18.89 | 43.67 | 43.67 | 25.32 | 41.89 | 18.93 | 40.57 | 42.25 | 48.56 |
| 670 | 63.47 | 58.62 | 61.07 | 64.09 | 15.81 | 47.17 | 47.17 | 19.93 | 46.90 | 15.81 | 46.71 | 47.92 | 55.23 |
| 680 | 68.93 | 64.59 | 67.36 | 69.45 | 15.73 | 52.15 | 52.15 | 19.54 | 52.93 | 16.10 | 52.95 | 54.00 | 62.03 |
| 690 | 72.92 | 69.13 | 72.07 | 73.34 | 19.54 | 57.96 | 57.96 | 24.25 | 58.84 | 20.68 | 57.98 | 59.20 | 67.50 |
| 700 | 76.56 | 73.53 | 76.51 | 77.00 | 29.76 | 66.98 | 66.98 | 35.88 | 66.54 | 31.75 | 63.31 | 65.09 | 72.90 |

| Ref. | Pair numbers | | | | | | | | | | | | |
|---|---|---|---|---|---|---|---|---|---|---|---|---|---|
| nm | 27 | 28 | 29 | 30 | 31 | 32 | 33 | 34 | 35 | 36 | 37 | 38 | 39 |
| 400 | 68.97 | 66.13 | 59.14 | 56.00 | 55.50 | 47.60 | 29.60 | 18.15 | 15.41 | 7.83 | 11.89 | 27.60 | 24.55 |
| 410 | 70.67 | 67.78 | 60.90 | 58.71 | 57.94 | 48.07 | 29.43 | 17.59 | 14.76 | 7.40 | 11.25 | 26.94 | 24.01 |
| 420 | 71.77 | 68.88 | 61.57 | 60.05 | 59.27 | 48.11 | 29.51 | 17.08 | 14.22 | 7.10 | 10.79 | 26.19 | 23.41 |
| 430 | 72.45 | 69.61 | 61.40 | 60.19 | 59.73 | 48.30 | 29.87 | 16.96 | 14.04 | 7.05 | 10.57 | 25.75 | 23.00 |
| 440 | 72.52 | 69.75 | 60.48 | 59.13 | 59.23 | 48.41 | 30.23 | 17.02 | 14.07 | 7.09 | 10.53 | 25.61 | 22.88 |
| 450 | 72.41 | 69.66 | 59.19 | 56.98 | 57.57 | 48.53 | 30.80 | 17.30 | 14.47 | 7.29 | 10.78 | 25.91 | 23.12 |
| 460 | 71.25 | 68.48 | 57.86 | 54.24 | 54.75 | 48.10 | 31.28 | 17.61 | 15.21 | 7.52 | 11.43 | 26.92 | 23.86 |
| 470 | 69.14 | 66.25 | 56.39 | 51.33 | 51.40 | 46.78 | 31.65 | 17.98 | 16.04 | 7.83 | 12.27 | 28.16 | 24.84 |
| 480 | 65.94 | 62.88 | 54.18 | 47.74 | 47.30 | 44.44 | 31.66 | 18.48 | 17.04 | 8.29 | 13.40 | 29.60 | 25.96 |

| | | | | | | | | | | | | | |
|---|---|---|---|---|---|---|---|---|---|---|---|---|---|
| 490 | 63.11 | 60.04 | 51.98 | 44.70 | 44.03 | 42.51 | 31.49 | 19.06 | 18.05 | 8.74 | 14.55 | 30.98 | 26.99 |
| 500 | 60.49 | 57.31 | 49.89 | 41.97 | 41.18 | 40.63 | 31.17 | 19.87 | 19.14 | 9.48 | 16.11 | 32.74 | 28.30 |
| 510 | 57.34 | 54.13 | 47.80 | 39.42 | 38.38 | 38.12 | 30.73 | 20.93 | 20.19 | 10.50 | 17.91 | 34.50 | 29.62 |
| 520 | 54.93 | 51.74 | 46.09 | 37.56 | 36.48 | 36.59 | 30.17 | 22.63 | 21.54 | 12.11 | 19.47 | 35.77 | 30.47 |
| 530 | 53.34 | 50.18 | 44.74 | 36.42 | 35.68 | 36.35 | 29.79 | 24.77 | 23.01 | 14.24 | 20.81 | 36.57 | 30.99 |
| 540 | 52.27 | 49.20 | 44.40 | 36.23 | 35.41 | 36.23 | 29.77 | 26.59 | 23.69 | 16.30 | 22.04 | 37.28 | 31.45 |
| 550 | 51.03 | 48.08 | 44.37 | 36.30 | 35.46 | 35.78 | 29.82 | 28.38 | 24.57 | 18.32 | 22.92 | 37.64 | 31.67 |
| 560 | 50.32 | 47.53 | 44.45 | 36.62 | 35.86 | 36.34 | 29.97 | 32.11 | 27.73 | 22.09 | 23.64 | 37.84 | 31.90 |
| 570 | 51.03 | 48.42 | 45.31 | 38.63 | 38.97 | 41.02 | 30.30 | 39.95 | 35.63 | 29.76 | 25.03 | 38.40 | 32.22 |
| 580 | 52.86 | 50.59 | 48.09 | 43.32 | 45.51 | 50.21 | 31.85 | 51.26 | 47.55 | 41.09 | 28.30 | 40.28 | 33.76 |
| 590 | 54.35 | 52.57 | 52.26 | 50.59 | 55.57 | 62.15 | 34.12 | 63.56 | 61.25 | 54.35 | 33.43 | 42.98 | 36.09 |
| 600 | 55.64 | 54.31 | 55.87 | 58.15 | 66.86 | 72.69 | 35.89 | 73.06 | 72.78 | 66.19 | 38.50 | 45.09 | 37.90 |
| 610 | 57.13 | 55.94 | 57.69 | 63.38 | 76.03 | 78.96 | 36.53 | 78.51 | 79.74 | 74.20 | 41.71 | 45.84 | 38.52 |
| 620 | 57.77 | 56.67 | 58.28 | 66.46 | 82.72 | 82.35 | 36.69 | 81.75 | 83.87 | 79.50 | 43.41 | 45.97 | 38.61 |
| 630 | 56.68 | 55.68 | 58.76 | 67.81 | 85.66 | 83.39 | 36.90 | 83.01 | 85.24 | 81.89 | 44.26 | 46.12 | 38.78 |
| 640 | 55.13 | 54.33 | 60.06 | 69.31 | 87.11 | 83.98 | 38.32 | 83.53 | 85.88 | 83.18 | 45.89 | 47.52 | 40.03 |
| 650 | 56.49 | 55.79 | 63.04 | 71.92 | 87.74 | 84.76 | 41.53 | 83.94 | 86.18 | 84.11 | 49.17 | 50.86 | 43.11 |
| 660 | 61.85 | 61.10 | 67.09 | 75.08 | 87.99 | 85.63 | 46.35 | 84.15 | 86.35 | 84.60 | 53.85 | 55.71 | 47.79 |
| 670 | 69.95 | 69.09 | 71.70 | 78.43 | 88.08 | 86.34 | 52.58 | 84.24 | 86.36 | 84.92 | 59.70 | 61.68 | 53.88 |
| 680 | 77.39 | 76.50 | 75.82 | 81.27 | 88.17 | 86.87 | 58.87 | 84.33 | 86.37 | 85.18 | 65.45 | 67.42 | 60.05 |
| 690 | 81.96 | 81.19 | 78.63 | 83.14 | 88.23 | 87.17 | 63.85 | 84.33 | 86.27 | 85.27 | 69.81 | 71.59 | 64.90 |
| 700 | 85.21 | 84.60 | 81.03 | 84.70 | 88.30 | 87.39 | 68.93 | 84.32 | 86.18 | 85.30 | 74.04 | 75.49 | 69.85 |

| Ref. | Pair numbers | | | | | | | | | | | | |
|---|---|---|---|---|---|---|---|---|---|---|---|---|---|
| nm | 40 | 41 | 42 | 43 | 44 | 45 | 46 | 47 | 48 | 49 | 50 | 51 | 52 |
| 400 | 26.53 | 15.84 | 24.41 | 25.82 | 24.84 | 24.78 | 27.90 | 30.23 | 28.40 | 32.39 | 32.05 | 40.58 | 48.06 |
| 410 | 26.02 | 15.17 | 23.82 | 25.16 | 24.22 | 24.16 | 27.74 | 30.12 | 28.29 | 38.68 | 38.41 | 42.55 | 50.04 |
| 420 | 25.36 | 14.58 | 23.16 | 24.46 | 23.55 | 23.48 | 27.37 | 29.70 | 27.92 | 43.05 | 43.87 | 43.40 | 50.90 |
| 430 | 24.93 | 14.30 | 22.76 | 24.09 | 23.15 | 23.10 | 27.12 | 29.44 | 27.62 | 47.30 | 49.96 | 43.68 | 50.86 |
| 440 | 24.82 | 14.26 | 22.66 | 24.03 | 23.07 | 23.05 | 27.09 | 29.33 | 27.53 | 52.26 | 56.94 | 43.26 | 50.05 |
| 450 | 25.12 | 14.58 | 22.95 | 24.34 | 23.36 | 23.37 | 27.42 | 29.59 | 27.80 | 55.52 | 60.91 | 42.60 | 48.94 |
| 460 | 25.97 | 15.47 | 23.89 | 25.36 | 24.33 | 24.36 | 28.19 | 30.32 | 28.52 | 58.12 | 62.33 | 41.76 | 47.65 |
| 470 | 27.03 | 16.64 | 25.02 | 26.57 | 25.47 | 25.55 | 29.08 | 31.20 | 29.40 | 60.72 | 62.57 | 40.70 | 46.26 |
| 480 | 28.20 | 18.21 | 26.36 | 27.99 | 26.81 | 26.95 | 29.98 | 32.12 | 30.33 | 61.20 | 60.17 | 39.19 | 44.21 |
| 490 | 29.27 | 19.88 | 27.61 | 29.34 | 28.05 | 28.28 | 30.80 | 32.89 | 31.10 | 59.93 | 56.79 | 37.73 | 42.18 |
| 500 | 30.56 | 22.25 | 29.18 | 31.00 | 29.61 | 29.92 | 31.67 | 33.78 | 32.03 | 57.34 | 52.64 | 36.18 | 40.22 |
| 510 | 31.80 | 25.16 | 30.80 | 32.67 | 31.16 | 31.57 | 32.28 | 34.43 | 32.71 | 53.52 | 48.03 | 34.52 | 38.31 |
| 520 | 32.49 | 27.97 | 31.89 | 33.83 | 32.20 | 32.70 | 32.34 | 34.56 | 32.83 | 49.03 | 43.58 | 32.83 | 36.55 |
| 530 | 32.81 | 30.37 | 32.52 | 34.49 | 32.70 | 33.28 | 32.07 | 34.34 | 32.61 | 44.04 | 38.94 | 31.05 | 35.07 |
| 540 | 33.05 | 32.24 | 32.93 | 35.03 | 32.97 | 33.59 | 31.42 | 33.77 | 32.02 | 38.68 | 34.21 | 29.41 | 34.19 |
| 550 | 33.12 | 33.37 | 33.04 | 35.16 | 32.98 | 33.62 | 30.62 | 33.01 | 31.28 | 33.38 | 29.87 | 28.01 | 33.61 |
| 560 | 33.14 | 34.03 | 33.05 | 35.29 | 32.77 | 33.47 | 29.50 | 31.95 | 30.20 | 27.85 | 25.55 | 26.44 | 32.89 |
| 570 | 33.24 | 34.72 | 33.07 | 35.45 | 32.73 | 33.42 | 28.23 | 30.76 | 29.01 | 23.46 | 22.05 | 24.72 | 32.60 |
| 580 | 34.36 | 36.39 | 33.95 | 36.59 | 33.14 | 33.83 | 27.34 | 29.95 | 28.22 | 20.01 | 19.10 | 23.27 | 32.90 |
| 590 | 36.18 | 38.76 | 35.47 | 38.40 | 34.25 | 34.95 | 26.97 | 29.69 | 27.97 | 16.65 | 16.17 | 22.33 | 33.83 |
| 600 | 37.56 | 40.59 | 36.58 | 39.78 | 35.09 | 35.79 | 26.68 | 29.44 | 27.72 | 13.19 | 13.20 | 21.75 | 34.51 |
| 610 | 37.91 | 41.19 | 36.80 | 40.15 | 35.16 | 35.87 | 26.28 | 29.06 | 27.33 | 11.47 | 11.78 | 21.21 | 34.47 |
| 620 | 37.85 | 41.28 | 36.79 | 40.10 | 35.06 | 35.78 | 25.81 | 28.59 | 26.85 | 10.78 | 11.32 | 20.69 | 34.28 |
| 630 | 37.99 | 41.41 | 36.96 | 40.28 | 35.20 | 35.90 | 25.91 | 28.66 | 26.89 | 10.43 | 11.01 | 20.71 | 34.32 |
| 640 | 39.33 | 42.78 | 38.27 | 41.59 | 36.48 | 37.16 | 27.10 | 29.87 | 28.08 | 10.08 | 10.73 | 21.73 | 35.60 |
| 650 | 42.64 | 45.91 | 41.54 | 44.85 | 39.71 | 40.37 | 30.08 | 32.92 | 31.10 | 9.07 | 9.63 | 24.29 | 38.77 |
| 660 | 47.61 | 50.65 | 46.44 | 49.73 | 44.55 | 45.23 | 34.67 | 37.58 | 35.81 | 6.49 | 7.11 | 28.40 | 43.64 |

| | | | | | | | | | | | | | |
|---|---|---|---|---|---|---|---|---|---|---|---|---|---|
| 670 | 54.02 | 56.68 | 52.76 | 55.89 | 50.86 | 51.49 | 40.81 | 43.77 | 42.07 | 4.94 | 5.41 | 33.98 | 50.08 |
| 680 | 60.40 | 62.69 | 59.11 | 62.01 | 57.27 | 57.85 | 47.18 | 50.11 | 48.50 | 5.00 | 5.42 | 39.99 | 56.59 |
| 690 | 65.35 | 67.30 | 64.11 | 66.71 | 62.43 | 62.91 | 52.48 | 55.32 | 53.78 | 7.19 | 7.68 | 45.31 | 61.78 |
| 700 | 70.34 | 71.87 | 69.16 | 71.33 | 67.69 | 68.06 | 58.20 | 60.87 | 59.44 | 13.74 | 14.36 | 51.31 | 67.18 |

| Ref. | Pair numbers | | | | | | | | | | | | |
|---|---|---|---|---|---|---|---|---|---|---|---|---|---|
| nm | 53 | 54 | 55 | 56 | 57 | 58 | 59 | 60 | 61 | 62 | 63 | 64 | 65 |
| 400 | 49.75 | 49.75 | 21.93 | 23.11 | 20.24 | 26.58 | 9.97 | 9.29 | 16.65 | 17.15 | 8.29 | 16.12 | 14.33 |
| 410 | 53.05 | 52.93 | 22.71 | 23.37 | 20.48 | 26.46 | 9.39 | 8.76 | 16.27 | 16.78 | 7.84 | 15.62 | 13.72 |
| 420 | 55.99 | 55.95 | 23.29 | 23.18 | 20.33 | 26.03 | 8.95 | 8.31 | 15.81 | 16.31 | 7.48 | 15.05 | 13.16 |
| 430 | 58.85 | 58.76 | 23.54 | 22.78 | 19.92 | 25.62 | 8.72 | 8.14 | 15.56 | 16.04 | 7.33 | 14.76 | 12.87 |
| 440 | 60.87 | 60.82 | 23.39 | 22.21 | 19.38 | 25.29 | 8.68 | 8.09 | 15.44 | 15.90 | 7.33 | 14.67 | 12.77 |
| 450 | 61.25 | 61.17 | 22.30 | 21.78 | 18.91 | 25.30 | 8.93 | 8.33 | 15.63 | 16.08 | 7.56 | 14.91 | 13.04 |
| 460 | 59.65 | 59.55 | 20.24 | 21.43 | 18.52 | 25.52 | 9.55 | 8.90 | 16.20 | 16.61 | 8.10 | 15.57 | 13.75 |
| 470 | 56.84 | 56.72 | 17.74 | 21.00 | 18.05 | 25.79 | 10.37 | 9.68 | 16.87 | 17.29 | 8.82 | 16.42 | 14.66 |
| 480 | 52.85 | 52.73 | 15.13 | 20.22 | 17.21 | 25.86 | 11.48 | 10.81 | 17.57 | 18.00 | 9.83 | 17.42 | 15.83 |
| 490 | 49.55 | 49.44 | 13.30 | 19.25 | 16.23 | 25.77 | 12.61 | 12.03 | 18.12 | 18.55 | 10.86 | 18.31 | 16.95 |
| 500 | 46.35 | 46.22 | 11.51 | 18.28 | 15.21 | 25.55 | 14.16 | 13.83 | 18.75 | 19.17 | 12.33 | 19.41 | 18.42 |
| 510 | 42.77 | 42.68 | 10.01 | 17.32 | 14.27 | 25.28 | 15.97 | 16.14 | 19.24 | 19.70 | 14.09 | 20.53 | 19.99 |
| 520 | 40.19 | 40.11 | 9.55 | 16.39 | 13.37 | 24.75 | 17.51 | 18.46 | 19.36 | 19.82 | 15.68 | 21.17 | 21.11 |
| 530 | 38.47 | 38.39 | 9.44 | 15.89 | 12.90 | 24.38 | 18.86 | 20.66 | 19.42 | 19.86 | 17.08 | 21.58 | 21.94 |
| 540 | 36.89 | 36.80 | 9.41 | 15.96 | 12.97 | 24.40 | 20.25 | 22.69 | 19.45 | 19.83 | 18.33 | 22.02 | 22.68 |
| 550 | 35.24 | 35.19 | 9.63 | 16.16 | 13.24 | 24.49 | 21.34 | 24.20 | 19.44 | 19.73 | 19.13 | 22.18 | 23.05 |
| 560 | 34.40 | 34.33 | 11.39 | 16.50 | 13.70 | 24.67 | 22.29 | 25.48 | 19.44 | 19.59 | 19.71 | 22.39 | 23.29 |
| 570 | 34.73 | 34.72 | 16.99 | 17.88 | 15.10 | 25.47 | 24.30 | 27.60 | 19.58 | 19.57 | 20.76 | 22.75 | 23.84 |
| 580 | 35.70 | 35.67 | 26.89 | 21.60 | 19.10 | 27.95 | 29.09 | 32.30 | 20.67 | 20.38 | 23.20 | 24.33 | 25.66 |
| 590 | 36.25 | 36.23 | 40.20 | 28.29 | 26.89 | 31.75 | 37.66 | 40.58 | 22.43 | 21.77 | 26.79 | 26.72 | 28.37 |
| 600 | 36.68 | 36.67 | 54.10 | 36.61 | 37.75 | 35.06 | 48.72 | 51.34 | 23.82 | 22.81 | 29.94 | 28.58 | 30.59 |
| 610 | 37.07 | 37.06 | 65.30 | 43.79 | 49.25 | 36.73 | 59.15 | 61.88 | 24.26 | 22.99 | 31.55 | 29.22 | 31.45 |
| 620 | 37.24 | 37.22 | 73.51 | 49.11 | 59.79 | 37.31 | 67.66 | 70.74 | 24.37 | 23.03 | 32.19 | 29.38 | 31.74 |
| 630 | 37.31 | 37.28 | 77.35 | 51.77 | 66.57 | 37.74 | 72.26 | 75.74 | 24.52 | 23.18 | 32.75 | 29.53 | 31.94 |
| 640 | 37.56 | 37.55 | 79.51 | 54.26 | 71.11 | 39.25 | 75.18 | 78.96 | 25.85 | 24.40 | 34.29 | 30.91 | 33.32 |
| 650 | 39.60 | 39.57 | 81.16 | 57.83 | 74.77 | 42.55 | 77.78 | 81.42 | 28.82 | 27.35 | 37.60 | 34.03 | 36.52 |
| 660 | 43.76 | 43.70 | 82.54 | 62.46 | 77.83 | 47.44 | 80.02 | 83.40 | 33.44 | 31.98 | 42.49 | 38.83 | 41.40 |
| 670 | 50.27 | 50.19 | 83.64 | 67.77 | 80.45 | 53.73 | 81.97 | 84.98 | 39.62 | 38.21 | 48.85 | 45.16 | 47.79 |
| 680 | 57.85 | 57.76 | 84.48 | 72.69 | 82.36 | 59.99 | 83.38 | 86.08 | 46.12 | 44.73 | 55.28 | 51.66 | 54.36 |
| 690 | 65.02 | 64.88 | 84.87 | 76.18 | 83.49 | 64.83 | 84.15 | 86.57 | 51.62 | 50.24 | 60.41 | 56.99 | 59.63 |
| 700 | 73.33 | 73.19 | 85.13 | 79.32 | 84.16 | 69.68 | 84.48 | 86.86 | 57.56 | 56.26 | 65.70 | 62.58 | 65.05 |

| Ref. | Pair numbers | | | | | | | | | | | | |
|---|---|---|---|---|---|---|---|---|---|---|---|---|---|
| nm | 66 | 67 | 68 | 69 | 70 | 71 | 72 | 73 | 74 | 75 | 76 | 77 | 78 |
| 400 | 14.14 | 10.52 | 16.09 | 3.93 | 17.85 | 19.41 | 16.66 | 26.51 | 23.01 | 25.15 | 29.30 | 22.62 | 23.98 |
| 410 | 13.69 | 10.05 | 15.70 | 3.90 | 17.52 | 18.82 | 18.02 | 27.06 | 23.22 | 29.43 | 34.47 | 22.85 | 24.30 |
| 420 | 13.21 | 10.06 | 15.18 | 4.03 | 17.11 | 18.28 | 18.38 | 26.77 | 23.13 | 31.94 | 38.31 | 22.63 | 24.11 |
| 430 | 12.93 | 10.25 | 14.90 | 4.44 | 17.03 | 18.05 | 18.70 | 26.70 | 23.11 | 34.10 | 41.76 | 22.21 | 23.68 |
| 440 | 12.84 | 10.70 | 14.78 | 5.17 | 17.23 | 18.07 | 19.76 | 26.82 | 23.10 | 36.35 | 45.23 | 21.67 | 23.11 |
| 450 | 13.07 | 11.40 | 14.98 | 6.50 | 17.82 | 18.51 | 21.74 | 27.53 | 23.44 | 37.10 | 47.34 | 21.28 | 22.72 |
| 460 | 13.67 | 12.29 | 15.58 | 8.76 | 18.71 | 19.61 | 25.20 | 28.85 | 24.31 | 37.14 | 48.71 | 21.06 | 22.43 |
| 470 | 14.43 | 13.19 | 16.35 | 11.76 | 19.70 | 20.97 | 29.77 | 30.55 | 25.25 | 36.70 | 49.43 | 20.71 | 22.01 |

| | | | | | | | | | | | | | |
|---|---|---|---|---|---|---|---|---|---|---|---|---|---|
| 480 | 15.36 | 14.29 | 17.25 | 15.59 | 20.97 | 22.72 | 34.45 | 32.69 | 26.28 | 35.40 | 48.68 | 20.09 | 21.27 |
| 490 | 16.18 | 15.33 | 18.07 | 18.96 | 22.17 | 24.57 | 36.51 | 34.41 | 27.18 | 34.18 | 46.67 | 19.25 | 20.31 |
| 500 | 17.19 | 16.60 | 19.06 | 22.38 | 23.65 | 26.88 | 35.95 | 35.61 | 27.98 | 32.68 | 43.42 | 18.37 | 19.33 |
| 510 | 18.23 | 18.00 | 20.05 | 25.58 | 25.38 | 29.27 | 33.48 | 35.61 | 28.02 | 31.05 | 39.25 | 17.51 | 18.37 |
| 520 | 18.68 | 19.25 | 20.43 | 27.76 | 27.24 | 30.71 | 30.85 | 34.74 | 27.35 | 30.04 | 34.83 | 16.59 | 17.34 |
| 530 | 18.91 | 20.38 | 20.62 | 28.75 | 28.85 | 30.86 | 28.97 | 32.47 | 25.51 | 29.03 | 30.23 | 16.02 | 16.74 |
| 540 | 18.95 | 21.41 | 20.53 | 28.64 | 29.45 | 29.64 | 27.43 | 29.37 | 22.95 | 27.29 | 25.76 | 15.95 | 16.67 |
| 550 | 18.85 | 21.94 | 20.25 | 27.83 | 29.26 | 27.78 | 25.09 | 26.08 | 20.53 | 24.97 | 21.87 | 16.03 | 16.75 |
| 560 | 18.46 | 22.15 | 19.72 | 26.42 | 28.40 | 25.49 | 22.36 | 22.50 | 18.06 | 22.64 | 18.08 | 16.24 | 16.97 |
| 570 | 18.27 | 22.11 | 19.24 | 24.44 | 26.87 | 22.89 | 20.67 | 19.36 | 15.64 | 20.79 | 14.94 | 17.11 | 17.93 |
| 580 | 18.44 | 22.17 | 19.26 | 22.52 | 24.95 | 20.44 | 19.68 | 16.89 | 13.46 | 18.78 | 12.41 | 19.76 | 20.83 |
| 590 | 19.18 | 22.42 | 19.54 | 21.17 | 23.13 | 18.58 | 17.83 | 14.52 | 11.84 | 15.98 | 10.27 | 24.10 | 25.51 |
| 600 | 19.67 | 22.59 | 19.76 | 20.41 | 21.74 | 17.35 | 14.45 | 12.42 | 10.80 | 12.37 | 8.46 | 28.31 | 29.99 |
| 610 | 19.68 | 22.52 | 19.70 | 19.81 | 20.63 | 16.45 | 12.61 | 11.39 | 10.10 | 10.57 | 7.50 | 30.78 | 32.57 |
| 620 | 19.58 | 22.33 | 19.50 | 19.14 | 19.53 | 15.58 | 12.15 | 10.73 | 9.45 | 10.10 | 6.97 | 32.01 | 33.75 |
| 630 | 19.63 | 22.44 | 19.53 | 19.18 | 18.53 | 14.86 | 11.90 | 10.55 | 8.83 | 9.86 | 6.55 | 32.61 | 34.37 |
| 640 | 20.77 | 23.63 | 20.62 | 19.81 | 18.01 | 14.76 | 11.43 | 10.37 | 8.58 | 9.47 | 6.26 | 34.06 | 35.95 |
| 650 | 23.55 | 26.50 | 23.33 | 22.35 | 18.28 | 15.20 | 10.12 | 9.69 | 8.68 | 8.37 | 5.79 | 37.11 | 39.27 |
| 660 | 28.06 | 31.01 | 27.68 | 26.75 | 19.63 | 17.09 | 7.05 | 7.97 | 9.66 | 5.86 | 4.98 | 41.66 | 44.30 |
| 670 | 34.27 | 37.12 | 33.66 | 33.16 | 22.51 | 20.72 | 4.88 | 8.08 | 12.01 | 4.13 | 4.56 | 47.62 | 50.75 |
| 680 | 40.82 | 43.56 | 40.06 | 40.19 | 26.82 | 25.75 | 4.79 | 10.83 | 15.65 | 4.09 | 4.94 | 53.79 | 57.28 |
| 690 | 46.46 | 49.14 | 45.64 | 46.54 | 32.39 | 31.64 | 6.96 | 16.70 | 20.46 | 5.96 | 6.90 | 58.90 | 62.40 |
| 700 | 52.71 | 55.22 | 51.88 | 53.69 | 41.84 | 40.58 | 13.66 | 25.02 | 28.37 | 11.82 | 12.56 | 64.32 | 67.63 |

| Ref. | Pair numbers | | | | | | | | | | | | |
|---|---|---|---|---|---|---|---|---|---|---|---|---|---|
| nm | 79 | 80 | 81 | 82 | 83 | 84 | 85 | 86 | 87 | 88 | 89 | 90 | 91 |
| 400 | 22.23 | 18.60 | 8.10 | 11.07 | 4.18 | 13.03 | 15.17 | 16.33 | 9.87 | 12.84 | 10.22 | 14.69 | 8.16 |
| 410 | 23.19 | 18.77 | 8.18 | 10.89 | 4.01 | 12.79 | 14.88 | 15.94 | 9.55 | 12.30 | 9.82 | 14.42 | 8.28 |
| 420 | 23.92 | 18.57 | 8.28 | 10.71 | 3.88 | 12.46 | 14.49 | 15.59 | 9.22 | 11.80 | 9.42 | 14.09 | 8.53 |
| 430 | 24.33 | 18.21 | 8.39 | 10.70 | 3.86 | 12.24 | 14.24 | 15.43 | 9.02 | 11.56 | 9.22 | 13.90 | 8.85 |
| 440 | 24.42 | 17.71 | 8.47 | 10.74 | 3.87 | 12.11 | 14.08 | 15.42 | 8.93 | 11.50 | 9.17 | 13.84 | 9.37 |
| 450 | 23.59 | 17.38 | 8.45 | 10.88 | 3.99 | 12.23 | 14.25 | 15.70 | 9.09 | 11.74 | 9.35 | 14.07 | 10.18 |
| 460 | 20.78 | 17.17 | 7.91 | 10.89 | 4.16 | 12.51 | 14.59 | 16.21 | 9.42 | 12.36 | 9.84 | 14.66 | 11.57 |
| 470 | 17.44 | 16.85 | 6.91 | 10.44 | 4.37 | 12.91 | 15.09 | 16.69 | 9.92 | 13.14 | 10.46 | 15.34 | 13.62 |
| 480 | 13.96 | 16.24 | 5.72 | 9.65 | 4.62 | 13.27 | 15.53 | 17.14 | 10.49 | 14.08 | 11.28 | 16.13 | 16.90 |
| 490 | 11.72 | 15.42 | 4.92 | 8.92 | 4.83 | 13.47 | 15.80 | 17.47 | 10.97 | 14.95 | 12.06 | 16.81 | 20.22 |
| 500 | 9.97 | 14.60 | 4.29 | 8.21 | 5.10 | 13.68 | 16.07 | 17.74 | 11.58 | 16.04 | 13.09 | 17.57 | 22.91 |
| 510 | 8.38 | 13.81 | 3.66 | 7.27 | 5.32 | 13.78 | 16.23 | 17.94 | 12.15 | 17.13 | 14.22 | 18.18 | 23.79 |
| 520 | 7.50 | 12.98 | 3.41 | 6.75 | 5.72 | 13.66 | 16.15 | 18.22 | 12.45 | 17.80 | 15.04 | 18.22 | 22.77 |
| 530 | 7.33 | 12.53 | 3.33 | 6.67 | 6.17 | 13.54 | 16.07 | 18.42 | 12.69 | 18.23 | 15.67 | 18.00 | 20.48 |
| 540 | 7.22 | 12.54 | 3.31 | 6.63 | 6.49 | 13.43 | 16.01 | 18.38 | 12.88 | 18.63 | 16.21 | 17.38 | 17.50 |
| 550 | 7.24 | 12.66 | 3.33 | 6.62 | 6.91 | 13.34 | 15.97 | 18.33 | 12.96 | 18.79 | 16.43 | 16.55 | 14.66 |
| 560 | 7.47 | 13.07 | 3.44 | 6.74 | 8.36 | 13.25 | 15.97 | 19.21 | 13.04 | 18.98 | 16.67 | 15.47 | 11.89 |
| 570 | 9.71 | 13.93 | 4.29 | 8.91 | 12.95 | 13.28 | 16.15 | 21.08 | 13.22 | 19.29 | 16.97 | 14.25 | 9.62 |
| 580 | 15.20 | 16.83 | 7.09 | 14.63 | 21.63 | 14.03 | 17.30 | 22.45 | 14.27 | 20.71 | 18.24 | 13.29 | 7.82 |
| 590 | 24.88 | 21.87 | 13.75 | 25.03 | 33.83 | 15.30 | 19.16 | 22.72 | 15.89 | 22.86 | 20.16 | 12.76 | 6.30 |
| 600 | 37.78 | 27.25 | 24.64 | 38.23 | 46.73 | 16.25 | 20.63 | 22.65 | 17.18 | 24.61 | 21.70 | 12.41 | 5.22 |
| 610 | 52.02 | 30.86 | 37.05 | 50.31 | 57.03 | 16.48 | 21.09 | 22.28 | 17.58 | 25.24 | 22.23 | 12.08 | 4.73 |
| 620 | 65.98 | 32.86 | 48.66 | 59.53 | 64.29 | 16.58 | 21.22 | 21.72 | 17.66 | 25.43 | 22.39 | 11.81 | 4.42 |
| 630 | 75.97 | 33.77 | 55.74 | 63.78 | 67.42 | 16.72 | 21.40 | 21.53 | 17.77 | 25.59 | 22.59 | 11.80 | 4.14 |

| | | | | | | | | | | | | | |
|---|---|---|---|---|---|---|---|---|---|---|---|---|---|
| 640 | 82.10 | 35.43 | 60.18 | 66.43 | 69.36 | 17.72 | 22.76 | 21.83 | 18.74 | 26.91 | 23.74 | 12.66 | 3.89 |
| 650 | 85.03 | 38.75 | 64.19 | 69.46 | 71.73 | 20.13 | 25.75 | 23.88 | 21.12 | 29.90 | 26.42 | 14.86 | 3.53 |
| 660 | 86.46 | 43.68 | 68.57 | 73.02 | 74.56 | 23.99 | 30.38 | 27.67 | 24.91 | 34.58 | 30.56 | 18.62 | 3.33 |
| 670 | 86.92 | 50.05 | 73.22 | 76.75 | 77.59 | 29.31 | 36.57 | 33.30 | 30.08 | 40.83 | 36.10 | 24.04 | 3.39 |
| 680 | 87.20 | 56.47 | 77.26 | 79.86 | 80.18 | 35.04 | 42.97 | 39.65 | 35.52 | 47.39 | 41.97 | 30.02 | 4.20 |
| 690 | 87.32 | 61.59 | 79.89 | 81.74 | 81.85 | 40.15 | 48.37 | 45.49 | 40.17 | 52.88 | 46.98 | 35.46 | 6.24 |
| 700 | 87.40 | 66.75 | 82.04 | 83.22 | 83.01 | 46.01 | 54.19 | 52.21 | 45.41 | 58.77 | 52.59 | 41.65 | 10.38 |

| Ref. | Pair numbers | | | | | | | | | | | | |
|---|---|---|---|---|---|---|---|---|---|---|---|---|---|
| nm | 92 | 93 | 94 | 95 | 96 | 97 | 98 | 99 | 100 | 101 | 102 | 103 | 104 |
| 400 | 16.97 | 17.34 | 13.22 | 32.90 | 17.82 | 9.52 | 5.56 | 5.53 | 8.47 | 3.31 | 3.43 | 5.23 | 8.99 |
| 410 | 16.90 | 17.26 | 13.27 | 36.29 | 18.19 | 9.45 | 6.00 | 5.98 | 8.34 | 3.35 | 3.35 | 4.99 | 8.74 |
| 420 | 16.62 | 16.96 | 13.06 | 39.85 | 18.27 | 9.36 | 6.36 | 6.33 | 8.15 | 3.36 | 3.29 | 4.82 | 8.43 |
| 430 | 16.46 | 16.68 | 12.88 | 42.15 | 18.23 | 9.34 | 6.61 | 6.58 | 7.96 | 3.40 | 3.29 | 4.74 | 8.25 |
| 440 | 16.38 | 16.51 | 12.68 | 42.66 | 18.02 | 9.34 | 6.71 | 6.68 | 7.64 | 3.42 | 3.30 | 4.70 | 8.14 |
| 450 | 16.58 | 16.63 | 12.71 | 41.83 | 17.73 | 9.36 | 6.51 | 6.47 | 7.27 | 3.37 | 3.34 | 4.81 | 8.27 |
| 460 | 17.12 | 16.92 | 12.86 | 40.14 | 17.12 | 9.20 | 5.30 | 5.28 | 6.83 | 3.21 | 3.37 | 5.02 | 8.54 |
| 470 | 17.71 | 17.30 | 13.02 | 37.92 | 16.14 | 8.71 | 4.05 | 4.04 | 6.23 | 2.89 | 3.33 | 5.33 | 8.96 |
| 480 | 18.33 | 17.55 | 13.09 | 34.97 | 14.87 | 7.85 | 3.08 | 3.09 | 5.57 | 2.55 | 3.22 | 5.70 | 9.41 |
| 490 | 18.80 | 17.65 | 13.05 | 32.10 | 13.84 | 7.15 | 2.64 | 2.65 | 5.10 | 2.37 | 3.12 | 5.99 | 9.72 |
| 500 | 19.27 | 17.66 | 12.89 | 28.69 | 12.63 | 6.46 | 2.35 | 2.37 | 4.67 | 2.23 | 2.99 | 6.41 | 10.13 |
| 510 | 19.49 | 17.60 | 12.65 | 25.15 | 11.52 | 5.68 | 2.17 | 2.19 | 4.27 | 2.12 | 2.85 | 6.74 | 10.40 |
| 520 | 19.33 | 17.13 | 12.16 | 22.04 | 11.03 | 5.23 | 2.09 | 2.11 | 4.08 | 2.09 | 2.76 | 6.94 | 10.47 |
| 530 | 18.65 | 16.57 | 11.59 | 19.06 | 10.79 | 5.10 | 2.10 | 2.11 | 4.08 | 2.12 | 2.76 | 7.09 | 10.48 |
| 540 | 17.67 | 16.11 | 11.11 | 16.08 | 10.43 | 5.01 | 2.13 | 2.14 | 4.18 | 2.15 | 2.79 | 7.22 | 10.42 |
| 550 | 16.60 | 15.67 | 10.65 | 13.76 | 10.45 | 4.97 | 2.19 | 2.19 | 4.30 | 2.21 | 2.84 | 7.27 | 10.31 |
| 560 | 15.30 | 15.01 | 10.01 | 12.09 | 11.00 | 5.05 | 2.28 | 2.28 | 4.51 | 2.30 | 2.92 | 7.30 | 10.12 |
| 570 | 13.85 | 14.51 | 9.50 | 10.81 | 12.74 | 6.01 | 2.56 | 2.56 | 5.75 | 2.47 | 3.46 | 7.38 | 10.09 |
| 580 | 12.64 | 14.46 | 9.28 | 9.39 | 14.27 | 8.35 | 3.34 | 3.34 | 8.86 | 3.22 | 5.38 | 8.03 | 10.43 |
| 590 | 11.88 | 14.65 | 9.26 | 8.13 | 14.81 | 11.50 | 6.30 | 6.27 | 14.36 | 6.00 | 10.57 | 9.14 | 11.24 |
| 600 | 11.45 | 14.83 | 9.27 | 7.87 | 14.84 | 14.01 | 13.23 | 13.19 | 20.70 | 13.15 | 20.32 | 10.07 | 11.84 |
| 610 | 11.06 | 14.75 | 9.15 | 7.97 | 14.59 | 15.17 | 23.11 | 23.03 | 25.33 | 25.02 | 33.20 | 10.40 | 11.89 |
| 620 | 10.76 | 14.62 | 9.01 | 8.10 | 14.26 | 15.62 | 33.03 | 32.93 | 28.19 | 39.47 | 47.09 | 10.51 | 11.88 |
| 630 | 10.73 | 14.67 | 9.02 | 7.76 | 14.06 | 15.94 | 38.85 | 38.76 | 29.42 | 53.67 | 58.33 | 10.67 | 11.95 |
| 640 | 11.54 | 15.66 | 9.73 | 7.26 | 14.34 | 17.11 | 42.27 | 42.17 | 31.03 | 65.42 | 66.12 | 11.52 | 12.84 |
| 650 | 13.65 | 18.13 | 11.59 | 7.74 | 16.05 | 19.62 | 45.58 | 45.51 | 34.01 | 73.43 | 71.23 | 13.61 | 15.08 |
| 660 | 17.28 | 22.24 | 14.89 | 10.33 | 19.41 | 23.65 | 50.04 | 50.02 | 38.46 | 78.16 | 74.97 | 17.16 | 18.94 |
| 670 | 22.59 | 28.04 | 19.86 | 16.42 | 24.64 | 29.16 | 55.86 | 55.86 | 44.36 | 80.79 | 78.00 | 22.35 | 24.52 |
| 680 | 28.46 | 34.33 | 25.48 | 24.70 | 30.66 | 35.08 | 61.85 | 61.87 | 50.52 | 82.20 | 80.32 | 28.12 | 30.57 |
| 690 | 33.82 | 39.91 | 30.70 | 33.69 | 36.40 | 40.32 | 66.57 | 66.62 | 55.71 | 82.72 | 81.64 | 33.32 | 36.00 |
| 700 | 39.91 | 46.16 | 36.77 | 45.07 | 43.15 | 46.27 | 71.40 | 71.45 | 61.30 | 83.11 | 82.65 | 39.25 | 42.12 |

| Ref. | Pair numbers | | | | | | | | | | | | |
|---|---|---|---|---|---|---|---|---|---|---|---|---|---|
| nm | 105 | 106 | 107 | 108 | 109 | 110 | 111 | 112 | 113 | 114 | 115 | 116 | 117 |
| 400 | 5.43 | 5.31 | 12.28 | 11.07 | 19.19 | 13.58 | 17.88 | 3.57 | 4.98 | 2.91 | 3.01 | 10.94 | 14.58 |
| 410 | 5.23 | 5.05 | 12.84 | 11.60 | 21.63 | 14.47 | 20.52 | 3.44 | 4.90 | 2.85 | 2.86 | 11.59 | 16.47 |
| 420 | 5.08 | 5.05 | 13.00 | 11.76 | 22.91 | 14.85 | 22.13 | 3.37 | 4.88 | 2.84 | 2.81 | 11.86 | 17.48 |
| 430 | 5.00 | 5.17 | 12.94 | 11.67 | 23.11 | 14.90 | 22.25 | 3.35 | 4.98 | 2.85 | 2.81 | 11.87 | 17.69 |
| 440 | 4.97 | 5.40 | 12.72 | 11.41 | 22.70 | 14.62 | 21.67 | 3.35 | 5.16 | 2.85 | 2.80 | 11.64 | 17.24 |
| 450 | 5.11 | 5.77 | 12.56 | 11.24 | 21.79 | 14.25 | 20.23 | 3.37 | 5.41 | 2.85 | 2.86 | 11.43 | 16.35 |

| | | | | | | | | | | | | | |
|---|---|---|---|---|---|---|---|---|---|---|---|---|---|
| 460 | 5.35 | 6.17 | 12.45 | 11.10 | 20.46 | 13.74 | 18.28 | 3.37 | 5.60 | 2.83 | 2.96 | 11.21 | 15.12 |
| 470 | 5.70 | 6.68 | 12.21 | 10.82 | 18.88 | 13.10 | 16.34 | 3.27 | 5.74 | 2.70 | 3.07 | 10.83 | 13.77 |
| 480 | 6.14 | 7.33 | 11.82 | 10.40 | 17.04 | 12.23 | 14.17 | 3.12 | 5.81 | 2.54 | 3.19 | 10.32 | 12.21 |
| 490 | 6.50 | 7.99 | 11.35 | 9.91 | 15.49 | 11.31 | 12.33 | 3.00 | 5.82 | 2.42 | 3.26 | 9.74 | 10.84 |
| 500 | 7.02 | 8.88 | 10.78 | 9.35 | 13.91 | 10.38 | 10.69 | 2.86 | 5.79 | 2.31 | 3.36 | 9.09 | 9.54 |
| 510 | 7.48 | 9.92 | 10.16 | 8.74 | 12.39 | 9.47 | 9.32 | 2.71 | 5.71 | 2.20 | 3.39 | 8.41 | 8.37 |
| 520 | 7.81 | 10.96 | 9.41 | 8.02 | 10.99 | 8.59 | 8.18 | 2.60 | 5.62 | 2.17 | 3.46 | 7.65 | 7.36 |
| 530 | 8.05 | 11.93 | 8.68 | 7.35 | 9.71 | 7.84 | 7.29 | 2.58 | 5.62 | 2.19 | 3.59 | 6.91 | 6.50 |
| 540 | 8.24 | 12.62 | 8.04 | 6.81 | 8.59 | 7.31 | 6.73 | 2.59 | 5.60 | 2.23 | 3.71 | 6.28 | 5.85 |
| 550 | 8.32 | 12.75 | 7.53 | 6.35 | 7.67 | 6.91 | 6.35 | 2.62 | 5.53 | 2.28 | 3.79 | 5.75 | 5.36 |
| 560 | 8.36 | 12.65 | 6.89 | 5.79 | 6.73 | 6.40 | 5.87 | 2.65 | 5.49 | 2.37 | 3.95 | 5.16 | 4.81 |
| 570 | 8.45 | 11.92 | 6.31 | 5.31 | 5.82 | 5.98 | 5.49 | 2.81 | 5.61 | 2.54 | 4.84 | 4.63 | 4.35 |
| 580 | 9.10 | 11.08 | 5.92 | 4.98 | 5.11 | 5.76 | 5.32 | 3.61 | 6.00 | 3.31 | 7.23 | 4.22 | 3.98 |
| 590 | 10.22 | 10.52 | 5.74 | 4.84 | 4.68 | 5.70 | 5.30 | 5.98 | 6.33 | 5.85 | 11.22 | 4.01 | 3.81 |
| 600 | 11.18 | 10.11 | 5.63 | 4.74 | 4.44 | 5.66 | 5.31 | 10.58 | 6.43 | 11.66 | 15.23 | 3.88 | 3.69 |
| 610 | 11.53 | 9.77 | 5.50 | 4.63 | 4.28 | 5.58 | 5.26 | 15.85 | 6.36 | 19.75 | 17.60 | 3.77 | 3.61 |
| 620 | 11.67 | 9.52 | 5.39 | 4.54 | 4.16 | 5.51 | 5.20 | 20.09 | 6.26 | 27.67 | 18.77 | 3.70 | 3.54 |
| 630 | 11.87 | 9.50 | 5.40 | 4.61 | 4.16 | 5.55 | 5.22 | 22.05 | 6.28 | 32.05 | 19.40 | 3.74 | 3.60 |
| 640 | 12.79 | 10.26 | 5.89 | 4.95 | 4.37 | 6.05 | 5.68 | 23.94 | 6.83 | 34.65 | 20.75 | 3.98 | 3.84 |
| 650 | 14.97 | 12.14 | 7.11 | 6.01 | 5.18 | 7.32 | 6.84 | 26.98 | 8.23 | 37.56 | 23.49 | 4.75 | 4.57 |
| 660 | 18.60 | 15.45 | 9.49 | 8.11 | 6.96 | 9.66 | 9.09 | 31.54 | 10.86 | 41.75 | 27.71 | 6.37 | 6.15 |
| 670 | 23.77 | 20.30 | 13.30 | 11.68 | 10.24 | 13.37 | 12.75 | 37.64 | 14.98 | 47.50 | 33.29 | 9.26 | 9.01 |
| 680 | 29.37 | 25.70 | 17.89 | 16.10 | 14.66 | 17.79 | 17.16 | 44.05 | 19.79 | 53.74 | 39.15 | 13.04 | 12.78 |
| 690 | 34.39 | 30.63 | 22.43 | 20.63 | 19.53 | 22.10 | 21.56 | 49.49 | 24.39 | 59.00 | 44.07 | 17.13 | 16.91 |
| 700 | 40.01 | 36.25 | 27.89 | 26.14 | 25.87 | 27.26 | 26.89 | 55.39 | 29.84 | 64.69 | 49.50 | 22.28 | 22.13 |

**Appendix G Visual assessment results for data set 1**

| pair no | Assessor 1 % Hue | Assessor 2 % Hue | Assessor 1 %D | Assessor 2 %D | Assessor 1 %B | Assessor 2 %B |
|---|---|---|---|---|---|---|
| 1 | 0.6Y | 0.5R | -0.4 | -0.5 | 0 | 0 |
| 2 | 0 | 0.8Y | -0.8 | -0.2 | -0.2 | 0 |
| 3 | 0.2Y | 1Y | -0.8 | 0 | 0 | 0 |
| 4 | 0 | 0.4R | -0.9 | -0.4 | -0.3 | -0.2 |
| 5 | 0 | 0 | -1 | -0.5 | 0 | 0.5 |
| 6 | 0.5Y | 0.4R | 0.5 | 0.1 | 0 | 0.5 |
| 7 | 0.5B | 0.1R | 0 | 0.1 | -0.5 | 0.8 |
| 8 | 0.6G | 1Y | -0.4 | 0 | 0 | 0 |
| 9 | 0.1Y | 0.1Y | 0 | 0.8 | -0.9 | 0.1 |
| 10 | 0.5R/B | 0.5B/R | -0.5 | 0 | 0 | 0.5 |
| 11 | 0.5R | 0.1R | 0 | 0 | 0.5 | 0.9 |
| 12 | 0.5B | 0.3B | -0.5 | -0.2 | 0 | -0.5 |
| 13 | 0.2B | 0.4R | -0.8 | -0.2 | 0 | 0.4 |
| 14 | 0.2R | 0.5R/Y | -0.8 | 0 | 0 | 0.5 |
| 15 | 0.5R | 0.5R | -0.5 | 0.1 | 0 | 0.4 |
| 16 | 1R | 0.5R | 0 | -0.5 | 0 | 0 |
| 17 | 1G | 0.6G | 0 | -0.1 | 0 | 0.3 |
| 18 | 1B | 0 | 0 | 0.6 | 0 | -0.4 |
| 19 | 0 | 0.8Y | -0.7 | 0 | -0.3 | -0.2 |
| 20 | 0 | 0 | -1 | 0.5 | 0 | 0.5 |
| 21 | 0 | 0.1Y | -1 | -0.9 | 0 | 0 |
| 22 | 0.8B | 0.8R | -0.2 | 0 | 0 | 0.2 |
| 23 | 1B | 0 | 0 | 0.6 | 0 | 0.4 |
| 24 | 0 | 0.2G | -1 | 0.6 | 0 | 0.2 |
| 25 | 0.3G | 0.3Y/B | -0.7 | -0.4 | 0 | 0.3 |
| 26 | 0 | 0.3Y | -1 | -0.5 | 0 | 0.2 |
| 27 | 0.5R | 0.5R | -0.5 | 0 | 0 | 0.5 |
| 28 | 0.2Y | 0 | -0.8 | -0.8 | 0 | -0.2 |
| 29 | 0.33G | 1Y | -0.33 | 0 | 0.33 | 0 |
| 30 | 0.5B | 0.5B | -0.5 | -0.5 | 0 | 0 |
| 31 | 0.5R | 1R | 0 | 0 | 0.5 | 0 |
| 32 | 0.5B | 0 | 0.5 | 0.8 | 0 | 0.2 |
| 33 | 0 | 0.3B | 0.5 | 0.2 | -0.5 | -0.5 |
| 34 | 0 | 0.8B | 1 | 0 | 0 | 0.2 |
| 35 | 0.5B | 0 | 0 | 0 | -0.5 | 1 |
| 36 | 0.5B | 0.3B | -0.5 | 0 | 0 | 0.7 |
| 37 | 0.5B | 0.8B | 0 | 0 | -0.5 | -0.2 |
| 38 | 0 | 1B | 0 | 0 | -1 | 0 |
| 39 | 0 | 0.1B | -0.5 | -0.8 | -0.5 | -0.1 |
| 40 | 0.4Y | 0.4Y | 0.6 | 0.2 | 0 | -0.4 |
| 41 | 1Y | 0.4Y | 0 | -0.1 | 0 | -0.5 |
| 42 | 0.7Y | 0.6R | 0 | 0 | 0.3 | 0.4 |
| 43 | 1Y | 0 | 0 | -1 | 0 | 0 |
| 44 | 1R | 0.2B | 0 | 0 | 0 | 0.8 |
| 45 | 1B | 0.1B | -0.6 | -0.8 | 0 | -0.1 |
| 46 | 0.33B | 0 | -0.33 | 0 | -0.33 | -1 |
| 47 | 1B | 0.9B | 0 | 0 | 0 | 0.1 |
| 48 | 0.5B | 0.3B | 0 | 0 | -0.5 | -0.7 |
| 49 | 0 | 0 | 0 | 0 | -1 | 0 |

**Appendix H Reflectance data of the seven dyed pairs used to study the behaviour of the WSF algorithm (iterative and linear) for batches possessing identical L* C* h values but different %R values**

| | PAIR 1 | | PAIR 2 | | PAIR 3 | | PAIR 4 | | PAIR 5 | | PAIR 6 | | PAIR 7 | |
|---|---|---|---|---|---|---|---|---|---|---|---|---|---|---|
| | **Batch 1** | **Batch 2** | **Batch 1** | **Batch 2** | **Batch 1** | **Batch 2** | **Batch 1** | **Batch 2** | **Batch 1** | **Batch 2** | **Batch 1** | **Batch 2** | **Batch 1** | **Batch 2** |
| nm | % R | % R | % R | % R | % R | % R | % R | % R | % R | % R | % R | % R | % R | % R |
| 400 | 4.9 | 4.33 | 2.76 | 2.12 | 11.5 | 14.15 | 16.7 | 16.85 | 3.1 | 5.5 | 1.4 | 1.5 | 6.2 | 6.5 |
| 410 | 5.7 | 5.04 | 2.99 | 2.48 | 11.8 | 14.55 | 16.9 | 17.25 | 3.15 | 5.5 | 1.67 | 1.75 | 6.7 | 7 |
| 420 | 6.6 | 5.84 | 3.31 | 2.56 | 12 | 14.85 | 17.9 | 18.25 | 3.3 | 5.65 | 1.85 | 2 | 7.25 | 7.7 |
| 430 | 7.3 | 6.43 | 3.71 | 3.06 | 12.9 | 15 | 18.9 | 18.75 | 3.8 | 5.85 | 2.05 | 2.3 | 8 | 8.3 |
| 440 | 7.7 | 7.02 | 4.25 | 3.57 | 14.3 | 15.2 | 20 | 20.05 | 5 | 5.9 | 2.4 | 2.5 | 8.5 | 8.75 |
| 450 | 8.05 | 7.73 | 4.9 | 4.4 | 15.89 | 15.6 | 22 | 21.55 | 6.1 | 6 | 2.9 | 2.8 | 8.8 | 8.85 |
| 460 | 8.25 | 8.47 | 5.42 | 5.25 | 17.93 | 16.85 | 25 | 24.15 | 6.3 | 5.5 | 3.39 | 3.45 | 8.9 | 8.7 |
| 470 | 8.15 | 8.97 | 5.6 | 6.28 | 19.94 | 18.1 | 28.3 | 28.05 | 6.3 | 5 | 4.71 | 4.3 | 8.75 | 8.1 |
| 480 | 7.9 | 9.04 | 5.43 | 6.81 | 21.55 | 19.8 | 31.5 | 33 | 6.4 | 4.4 | 6.25 | 6.2 | 8.1 | 7.6 |
| 490 | 7.65 | 8.56 | 4.99 | 6.8 | 22.36 | 21.9 | 34.7 | 36.5 | 6.4 | 4 | 7.4 | 7.3 | 6 | 6.76 |
| 500 | 6.95 | 7.79 | 4.56 | 6.4 | 22.51 | 23.4 | 37 | 38.1 | 6.3 | 3.8 | 7.82 | 8.1 | 5.02 | 5.83 |
| 510 | 6.25 | 6.96 | 4.29 | 5.6 | 22.47 | 24.1 | 37.5 | 38.6 | 5.9 | 3.6 | 7.67 | 8.3 | 4.25 | 4.4 |
| 520 | 5.92 | 6.3 | 4.18 | 4.9 | 22.64 | 24.8 | 37.4 | 38.1 | 5.4 | 3.5 | 7.2 | 7.95 | 3.62 | 3.5 |
| 530 | 5.72 | 5.86 | 4.17 | 4.7 | 22.93 | 24.2 | 36.9 | 37.65 | 4.4 | 3.4 | 7 | 7.45 | 3.12 | 2.95 |
| 540 | 5.8 | 5.56 | 4.41 | 4.4 | 23.04 | 24 | 36 | 36.9 | 3.9 | 3.5 | 6.94 | 6.5 | 2.71 | 2.55 |
| 550 | 5.91 | 5.41 | 5.18 | 4.7 | 23.44 | 23.7 | 34.6 | 35 | 2.8 | 3.8 | 7.04 | 6.4 | 2.39 | 2.35 |
| 560 | 6.3 | 5.45 | 6.56 | 5.3 | 24.86 | 23.99 | 32.7 | 32 | 2.2 | 4.51 | 7.49 | 7 | 2.18 | 2.15 |
| 570 | 6.45 | 5.67 | 7.94 | 6.25 | 25.95 | 24 | 30.5 | 28.9 | 1.96 | 5 | 8.34 | 8 | 2.03 | 2.05 |
| 580 | 6.1 | 5.81 | 8.79 | 7.3 | 26.26 | 24.65 | 27.6 | 24.8 | 2 | 5.3 | 9.31 | 9.3 | 1.89 | 1.92 |
| 590 | 5.5 | 5.71 | 9.13 | 8.76 | 25.8 | 24.4 | 23.9 | 21.62 | 2.3 | 5.5 | 9.96 | 10.1 | 1.77 | 1.75 |
| 600 | 5.13 | 5.52 | 9.18 | 9.49 | 24.9 | 22.85 | 20.7 | 19.79 | 2.7 | 5.5 | 10.2 | 10.5 | 1.69 | 1.7 |
| 610 | 4.95 | 5.44 | 9.12 | 9.89 | 23.89 | 20.7 | 17.5 | 17.96 | 3.5 | 5.4 | 10.4 | 10.8 | 1.68 | 1.65 |
| 620 | 4.9 | 5.49 | 9.02 | 10.06 | 23.53 | 21 | 14.6 | 15.83 | 5 | 5.4 | 10.6 | 10.8 | 1.65 | 1.7 |
| 630 | 4.77 | 5.42 | 8.92 | 10.1 | 23.44 | 22 | 12.1 | 14.2 | 8 | 5.3 | 10.5 | 11 | 1.65 | 1.7 |
| 640 | 4.8 | 5.21 | 8.96 | 10.8 | 23.5 | 26 | 10.7 | 13.75 | 13.7 | 5.3 | 10.7 | 10.9 | 1.62 | 1.72 |
| 650 | 5.25 | 5.13 | 9.37 | 11.3 | 23.79 | 35 | 10.1 | 15.95 | 22.0 | 5.3 | 11 | 11 | 1.65 | 1.7 |
| 660 | 5.7 | 5.49 | 10.3 | 11.8 | 24.65 | 47 | 13 | 19.55 | 32.0 | 5.3 | 11.7 | 11.2 | 1.63 | 1.7 |
| 670 | 6.8 | 6.55 | 11.7 | 14 | 26 | 60 | 17.7 | 24.55 | 41.9 | 5.3 | 13 | 11.7 | 1.75 | 1.9 |
| 680 | 8.2 | 8.67 | 13.8 | 17 | 28 | 69 | 25.5 | 33.55 | 51.2 | 5.3 | 16.1 | 13.8 | 1.9 | 2.3 |
| 690 | 10.1 | 11.9 | 16.7 | 23 | 30.9 | 76 | 34.5 | 43.55 | 59.2 | 5.3 | 21.1 | 18.5 | 2.5 | 2.91 |
| 700 | 13.4 | 16.57 | 20.7 | 30 | 35 | 81 | 47 | 51.5 | 67.3 | 5.3 | 27.7 | 25 | 3.5 | 4.59 |